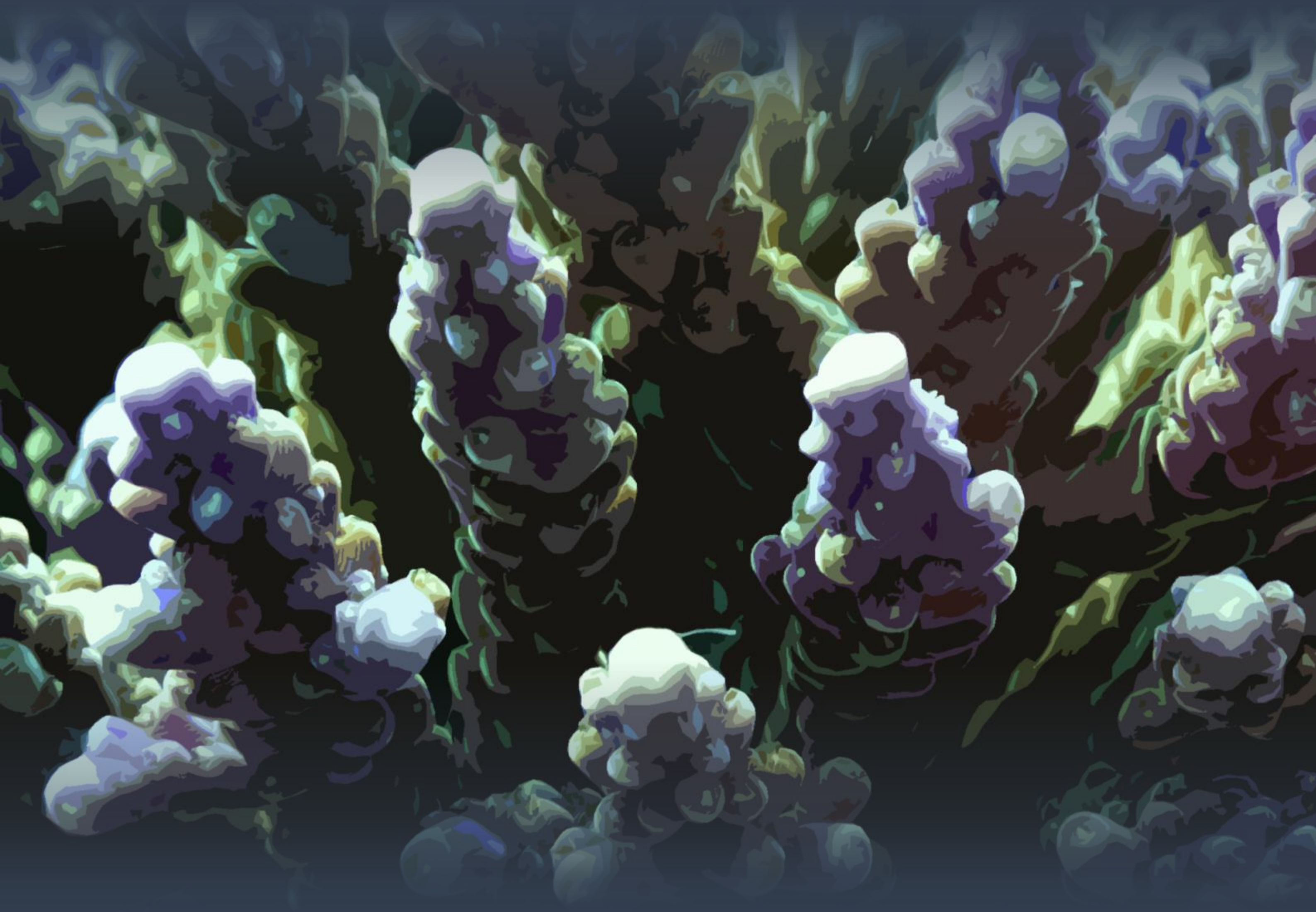

Coral community demographics: The variation between tropical and subtropical assemblages

James Cant

University of Leeds

Nov 2021

Front page: Subtropical *Acropora* spp. colony in the Solitary Islands Marine Park (Australia)

Photo: James Cant

Coral community demographics: The variation between tropical and subtropical assemblages

James Cant

Submitted in accordance with the requirements for the degree of Doctor of Philosophy.

The University of Leeds

School of Biology

November 2021

Supervisors: Assoc. Prof. Maria Beger

Assoc. Prof. Roberto Salguero-Gómez

Prof. William Kunin

Assessment committee: Assoc. Prof. Christopher Hassall (University of Leeds)

Dr Steven Sait (University of Leeds)

Prof. Cristina Linares (University of Barcelona)

The candidate confirms that the work submitted is their own, except where work which has formed part of jointly authored publications has been included. The contribution of the candidate and the other authors to this work has been explicitly indicated below. The candidate confirms that appropriate credit has been given within the thesis where reference has been made to the work of others.

1. Section 1.1 of the Introduction is under development for publication as a jointly authored research perspective in Coral Reefs as follows:
   Transient demographic approaches can drastically expand the toolbox of coral reef science. **Cant J.,** Salguero-Gómez R., Beger M.
   A preprint of this work is also available on BioRxiv at
   https://doi.org/10.1101/2021.04.08.438926.
   In this work I was responsible for generating and developing all ideas for the manuscript, conducting the literature review analysis, and led the writing of the manuscript.
   The contribution of the other authors was to provide constructive feedback to help refine the research ideas and develop the subsequent manuscript.

2. The work presented in Chapter 1 of this thesis is part of a jointly authored manuscript being developed for publication as a primary research article as follows:
   Evolutionary processes, not environmental drivers, determine demographic resilience. **Cant J.,** Capdevila P., Beger M., Salguero-Gómez R.
   In this manuscript I was responsible for generating and developing the research ideas and extracted extensive abiotic and demographic records from the CHELSA, and COM(P)ADRE databanks. I also developed and implemented all analyses and led the writing of the manuscript.
   The other authors contributed to refining the research ideas and analytical approaches. They also provided constructive comments and feedbacks on successive manuscript drafts.

3. The work presented in Chapter 2 of this thesis has appeared in jointly authored publication as follows:
   The projected degradation of subtropical coral assemblages by recurrent thermal stress. **Cant J.,** Salguero-Gómez R., Kim S. W., Sims C. A., Sommer B., Brooks M., Malcolm H. A., Pandolfi J. M., Beger M. (2021) *Journal of Animal Ecology*. 90(8) 233-247.

In this publication I was responsible for developing the research ideas, collecting demographic field data, extracting climate forecasts, implementing all analyses/model simulations, and led the writing of the final manuscript.
The other authors contributed through the development of the initial research concept, providing all necessary research permits, and assisting in the collection and processing of field data. These authors also assisted with the development of modelling approaches and contributed ideas and comments during final manuscript write-up.

4. The work presented in Chapter 3 of this thesis is part of a jointly authored manuscript being developed for publication as a primary research article as follows: *Transient amplification enhances the persistence of tropicalising coral populations in marginal high latitude environments*. **Cant J.,** Cook K., Reimer J. D., Mezaki T., Nakamura M., O'Flaherty C., Salguero-Gómez R., Beger M.
A preprint of this work is also available on BioRxiv at https://doi.org/10.1101/2021.04.23.441133.
Across this work I was responsible for generating/developing all research ideas and setting up and implementing all field surveys. I also conducted all research analyses and led the writing of the final manuscript.
The other authors contributed ideas and constructive feedback during the development of the research questions, provided logistical support during field surveys, helped to refine research analyses, and provided feedback on successive manuscript drafts. M. Nakamura also provided further field data regarding the settlement of coral larvae which was collected as part of an earlier research publication. Appropriate reference has been made to the original source of this additional data within the Chapter.

5. The work presented in Chapter 4 of this thesis is part of a jointly authored manuscript being developed for publication as a primary research article as follows: *Coral assemblages at higher latitudes favour short-term potential over long-term performance*. **Cant J.,** Reimer J. D., Sommer B., Cook K., Kim S. W., Sims C. A., Mezaki T., O'Flaherty C., Brooks M., Malcolm H. A., Pandolfi J. M., Salguero-Gómez R., Beger M.
A preprint of this work is also available on BioRxiv at https://doi.org/10.1101/2021.09.29.462350.

Across this manuscript I was responsible for generating and developing the research ideas, collecting demographic field data, implementing all analyses and model simulations, and led the writing of the final manuscript.
The other authors contributed through feedback during the development of research ideas, the provision of necessary research permits and research funding, and assisting in the collection and processing of field data. These authors also assisted with the subsequent development of modelling approaches and contributed ideas and comments during final manuscript write-up.

Acknowledgements

I would first and foremost like thank my primary supervisor Maria Beger for her support and guidance throughout my PhD. Before enrolling on this PhD, Maria invited me to assist on field work that would eventually form the core focus of my own research. This gave me the opportunity to make the project my own, and with hindsight, reduced the impact of the COVID-19 lockdown on the quality of my PhD, for which I am truly grateful. I also owe equal thanks to my co-supervisor Rob Salguero-Gómez, who has continually made regular time to coach me through the complexities of demographic modelling. I would also like to say thank you to William Kunin for the advice he has offered during my PhD to help me approach my research from a broader ecological perspective.

The research presented in this thesis is the result of contributions from a team of people including Brigitte Sommer, James Riemer, Katie Cook, Sun Kim, Carrie Sims, John Pandolfi, Takuma Mezaki, Clio O'Flaherty, Maxime Brooks, Hamish Malcolm, and Masako Nakamura. My own contributions, fully and explicitly indicated in the thesis, have been to generate and develop the research ideas across each chapter, collect field data, implement analytical approaches, and lead manuscript write-up. Meanwhile the other members of this team have contributed data, feedback, field assistance, research funding and research permits for which I am hugely grateful. Equally, I would like to thank the Natural Environment Research Council, who have supported my PhD through the Spheres DTP. I also thank the Royal Geographical Society and the Priestley International Centre for Climate for their additional financial support.

Finally, none of this would have been possible without Rhian Stephens who has supported and put up with me, throughout my PhD journey.

Abstract

Climate change is exposing coral reefs worldwide to increasingly recurrent disturbances. However, with current knowledge of coral population dynamics focused on long-term (*i.e.*, asymptotic) characteristics, our capacity to forecast the resilience of coral communities, specifically, their resistance and recovery following disturbances, is restricted. Recurrent disturbances ensure that populations never achieve a stable equilibrium and will thus never attain their asymptotic trajectories. Instead, it is imperative that we quantify the performance of coral populations within non-stationary environments using their transient (*i.e.*, short-term) dynamics, and evaluate the determinants of variation across these transient dynamics as conditions change. Here, I utilise state-structured demographic approaches and transient demographic theory to explore the association between abiotic variation and measures of demographic resilience. I illustrate how patterns in demographic resilience across animal and plant populations do not correlate with gradients in their exposure to abiotic variability, and thus recent experience of variable environments does not guarantee resilience to future climate variability. Next, I explore these insights in the context of resistance and recovery in coral populations to enhance understanding of coral community resilience. Using an Integral Projection Model framework, I show how, despite enduring more variable seasonal climates, subtropical coral communities remain vulnerable to future recurrent thermal stress. I also demonstrate how spatial variation in the transient dynamics of acroporid coral populations in southern Japan underpins the establishment of populations at higher latitudes. Finally, to further explore the mechanisms facilitating the establishment of subtropical coral populations, I evaluate spatial patterns in the impact of environmental variability on the long-term performance and transient dynamics of coral populations across coral taxa. Overall, this research represents a crucial step in quantifying the transient dynamics of coral populations, an approach which requires greater commitment if we are to anticipate the future resilience, viability, and condition of global coral communities.

Contents

List of tables and illustrative materials

Introduction

Disturbances are a natural part of all ecological systems and, by influencing resource availability and the structural composition of natural populations, play a fundamental role in the assembly of biological communities (Connell 1978; Pickett & White 1985; Turner 2010). However, climate change and human activity are exposing ecosystems worldwide to historically novel variability, changing the frequency, intensity and severity of local disturbance regimes (Turner 2010; Thornton *et al.* 2014). Across terrestrial and marine environments localised warming is increasing the frequency of heat stress events, droughts, and heavy rainfall, whilst processes such as urbanisation, deforestation and overfishing diminish resource and habitat availability (Easterling *et al.* 2000a; Wilson *et al.* 2008; Hughes *et al.* 2018a). Subsequently, the future management of global biodiversity requires assessments into the performance and viability of natural populations that consider their tolerance and responses to repeated disturbances (Park 2019).

Alongside tropical rainforests, coral reefs represent a posterchild for the impacts of climate change and anthropogenic pressure on the functioning of natural ecosystems and the economies they uphold (França *et al.* 2020). Despite covering less than 300,000 km (0.1%) of the Earth's surface, coral reefs sustain a substantial proportion of marine biodiversity, and carry considerable economic value (Costanza & Folke 1997; Spalding *et al.* 2001; Cinner 2014). Valued at US$ 375 billion per annum, coral reef ecosystems provide employment and subsistence opportunities for coral reef fishers (Teh *et al.* 2013), and reduce coastal flooding and storm damage (Ferrario *et al.* 2014); a provision which, in the US alone, is estimated to prevent US$ 1.8 billion worth of damage each year (Reguero *et al.* 2021). Equally, coral reefs support a large and rapidly expanding tourism industry providing further employment opportunities and helping to redistribute global wealth (Spalding *et al.* 2017). Indeed, coral reefs directly sustain the nutritional, economic, and cultural needs of more than 500 million people globally (Moberg & Folke 1999; Hoegh-Guldberg *et al.* 2019). However, despite their economic and intrinsic importance, or perhaps because of it, the ongoing vulnerability of coral reef ecosystems cannot be overstated, with coral ecosystems worldwide threatened by human exploitation and changing climate regimes (Riegl *et al.* 2009; Bruno & Valdivia 2016).

Historical evidence illustrates a long association between human activity and declines in global coral coverage (Pandolfi *et al.* 2003). However, the rate and extent of coral reef degradation has accelerated in recent decades, such that pristine examples of coral reef habitat no longer exist (Hughes *et al.* 2003, 2010). Coral communities are susceptible to a range of natural and human-induced disturbances including storm damage, zoonotic disease, sedimentation, and overfishing (Nyström *et al.* 2000). Yet, by far the greatest threat to the persistence of coral reef environments is the increase in ocean temperatures driven by global climate change (Hoegh-Guldberg *et al.* 2007). Coral bleaching, arising from a breakdown in the relationship between corals and their zooxanthellae algal symbionts following thermal stress, is rapidly becoming an increasingly common phenomenon (Hoegh-Guldberg 2011). Following initial observations of large-scale bleaching in the 1980's, recurrent thermal stress events have increased in both frequency and severity resulting in mass coral mortality events and the restructuring of global reef ecosystems (Hoegh-Guldberg *et al.* 2007; Hughes *et al.* 2018a, b; Sully *et al.* 2019). This warming of shallow ocean waters is expected to exacerbate existing stressors and to soon exceed the thermal tolerances of many coral species, rendering many tropical regions inhospitable (Hoegh-Guldberg *et al.* 2007; Descombes *et al.* 2015). Already, 36% of the worlds reefs are considered in a critical state or beyond their threshold for recovery, with the most impacted reefs having experienced an 80-90% decline in coral cover since the late 1970s (Gardner *et al.* 2003; Côté *et al.* 2005; Wilkinson 2008).

Corresponding with this bleak outlook for global coral reefs, there have been numerous calls for an increased commitment towards evaluating and predicting the resilience of coral communities (Hughes *et al.* 2010; Pandolfi *et al.* 2011; Lam *et al.* 2020). Climate change is challenging ecologists to develop frameworks to forecast where and how environmental change will impact species, populations, and ecosystems (Wolkovich *et al.* 2014). Predicting the dynamics of biological systems exposed to changing environments is fundamental for anticipating their vulnerability, and designing effective conservation strategies (Petchey *et al.* 2015). To forecast the future condition and dynamics of coral communities, we require an understanding of the mechanisms driving the varied responses of coral populations to environmental stressors (Hughes *et al.* 2010; Pandolfi *et al.* 2011). However, many reef monitoring programs, and assessments into the response of coral communities following disturbance, typically rely on correlative assessments of coral cover (see Selig & Bruno 2010; Ateweberhan *et al.* 2011; De'Ath *et al.* 2012; Johns *et al.* 2014), therefore masking the true implications of environmental change (Edmunds *et al.* 2014; Madin & Madin 2015). Consequently, our limited knowledge of the mechanisms underpinning the resilience, or lack of it, in global coral assemblages has restricted our capacity for recognising and preventing the collapse of many coral reef ecosystems (Bellwood *et al.* 2004).

1.1. Expanding the toolbox of coral reef science.

The work presented in the following section comprises a jointly authored research perspective currently under development for publication in Coral Reefs and is available as a preprint article on BioRxiv at https://doi.org/10.1101/2021.04.08.438926.

Coral populations are sensitive to a range of biotic and abiotic pressures (Riegl 2020), many of which will be exacerbated by future climatic change and human exploitation (Wolff *et al.* 2018; Riegl & Glynn 2020). The future resilience of coral populations subsequently comprises their capacity for enduring, and recovering from, this increased disturbance (Holling 1973). Accordingly, a resilience-orientated focus is becoming commonplace in reef management (Mcleod *et al.* 2019; McLeod *et al.* 2021), although this requires the ability for anticipating the responses of coral populations to varying biotic and abiotic regimes (Lam *et al.* 2020). Appropriately, state-structured demographic models are being increasingly utilised for quantifying the mechanisms supporting or preventing the persistence and revival of disturbed coral communities (e.g. Kayal *et al.* 2018; Cant *et al.* 2021). Indeed, understanding how patterns in the survival, size, and reproduction of individual colonies influences population-level characteristics is paramount for effectively managing conservation resources (Riegl *et al.* 2018; Pisapia *et al.* 2020). However, the contemporary application of state-structured demographic approaches to ascertain the viability of coral populations does not reflect our need to evaluate their resilience.

Structured population approaches examine how variation at the level of individuals translates to population-level attributes (Caswell 2001). The state of individuals (typically their size, age, or developmental stage [Caswell 2001]) arbitrates their survival and reproduction, which in turn shape the responses of their populations to local biotic and abiotic conditions (Benton *et al.* 2006). Within natural populations, the diversity of individual-level characteristics can be expressed through the state-structured vital rates of survival, progression (growth & development), retrogression (shrinkage [Salguero-Gómez and Casper 2010] & rejuvenation [Salguero-Gómez *et al.* 2013]), and reproduction (Metcalf & Pavard 2007). Patterns across these vital rates, and their response to changing population structures, subsequently underpin the characteristics of populations and define their capacity for tolerating various environments (Boyce *et al.* 2006; Ehrlén *et al.* 2016). Equally, combined with an explicit consideration for the interaction between multiple populations, structured population analyses also facilitate the exploration of community recovery (Kayal *et al.* 2018) and coexistence (Adler *et al.* 2010). Evaluating the vital rates and structure of numerous populations, and their association with abiotic regimes, has thus proven instrumental in calculating the extinction risk of highly threatened populations (Mace *et al.* 2008), and the management, and conservation of natural communities (Morris & Doak 2002; Jongejans *et al.* 2008).

With many coral communities facing imminent reassembly and population collapse, the demand for an improved understanding of coral population dynamics has never been greater (Edmunds & Riegl 2020). Although limited, the application of demographic theory within coral research is not a novel concept (Edmunds *et al.* 2014). Veritably, there is a growing appreciation for how the size structure of coral populations influences their dynamics and endurance, with recent appeals for demographic approaches to be concentrated towards gauging the resilience of coral communities (Dietzel *et al.* 2020; Pisapia *et al.* 2020; Cant *et al.* 2021; Lachs *et al.* 2021). However, prevailing knowledge of coral population dynamics centres around isolated patterns in colony survival, changes in size, or recruitment, and long-term (*asymptotic*) population characteristics. Quantifying the asymptotic characteristics of various populations presents a valuable comparative tool for exploring abiotic tolerances (Beissinger & Westphal 1998). Yet, to achieve their asymptotic dynamics, populations typically require stable conditions, which seldom occur naturally, and are becoming increasingly unlikely given current climate projections (Hastings *et al.* 2018; Francis *et al.* 2021). Consequently, a focus towards exploring the asymptotic characteristics of populations limits our appreciation of their dynamics within natural environments (Ezard *et al.* 2010), and will inhibit our capacity to accurately predict the future condition of global coral assemblages.

Cyclic abiotic and biotic disturbances (e.g. seasonality in temperature or resource availability) ensure that natural environments rarely exist at a stable equilibrium (Williams *et al.* 2011). The perpetual instability generated by regular disturbances ensures that natural populations rarely attain their asymptotic trajectories (Hastings 2001; Hastings *et al.* 2018). Instead, the short-term or *transient* characteristics of populations, which reflect their dynamics within non-equilibrate environments, play a fundamental role in the assembly of biological communities (Hastings 2004). With the transient dynamics of populations defining their performance following disturbance, these characteristics also represent quantifiable measures of population resilience (Capdevila *et al.* 2020). Globally, coral communities are being exposed to increasingly recurrent disturbance events (Hughes *et al.* 2018a), with various species shifting their distributions poleward or establishing populations within marginal habitats (Beger *et al.* 2014; Camp *et al.* 2018; Vergés *et al.* 2019). Here, we discuss why enhancing our capacity for anticipating the future resilience of coral communities requires an understanding of the transient dynamics in their constituent populations.

1.1.1. Transient versus asymptotic population dynamics.

Population dynamics characterise and define the trajectories of populations according to the individual-level allocation of resources towards survival, changes in size (or the state of interest), and reproduction (Box 1). Any population can be structured according to the distribution of its individuals across some state variable, be that age, size, developmental stage, or a combination. The transition of individuals across state classes is, in turn, mediated by selection gradients that emerge from the state-specific patterns of survival and reproduction (Groenendael *et al.* 1988; van Tienderen 2000). In state-structured demography, patterns across these multiple vital rates can subsequently be condensed into a population projection matrix ($\boldsymbol{A}$), with each matrix element (a_{ij}) expressing the expected transition of individuals into state class i from state class j during the time interval t to $t+1$, or the per-capita a/sexual contributions of state j individuals into state class i during that same interval (Caswell 2001). This population matrix can then be used to project the size of a population (N, number of individuals) over time, using the change in its state structure ($\mathbf{n}$):

$$N_{t+1} = \sum \mathbf{n}_{t+1} = \sum \boldsymbol{A}\mathbf{n}_t. \tag{1.1}$$

Within a stable environment, the state structure of a population is expected to converge towards an equilibrium state (Caswell 2001). At equilibrium, the size of a population is then expected to change at a constant rate over time, termed its asymptotic population growth rate (λ, Caswell 2001). The value of λ, for any state-structured population, is equal to the dominant eigenvalue of its corresponding population matrix $\boldsymbol{A}$. Estimates of λ represent the proportional change in the size of populations over time and exist on a non-negative scale reflecting population growth ($\lambda > 1$), decline ($\lambda < 1$), or stasis ($\lambda = 1$).

Box 1: Scaling from individuals to communities.

Following individual corals over time facilitates the calculation of vital rate patterns relating to colony survival, size, and reproduction, and how they govern the characteristics of populations and their wider community interactions (Fig. I). As corals mature and grow, they experience changes in their resource demands, with the capacity of corals for continually meeting these changing demands subsequently influencing their ability to maintain their somatic condition and tolerate local biotic and abiotic stressors (Hughes 1984). The repeated survey of individual colonies allows for documenting how the size of individuals regulates their survival, development, and reproductive contribution over time, and how this is shaped by changing environmental conditions. Condensing these temporal observations from across multiple tagged colonies then allows population ecologists to explore how individual-level vital rates underpin the dynamics of populations.

Crucially, state-structured demographic approaches enable the quantification of the relationship between abiotic conditions and population-level characteristics. Such an understanding is necessary if ecologists are to accurately predict the impact of recurrent disturbances and simulate populations under varying climate scenarios. Similarly, by understanding interactions across the dynamics of various co-occurring populations, and their differential responses to changing conditions, ecologists can better understand the mechanisms driving coexistence (Adler *et al.* 2010), and predict the transition of coral communities amidst changing climatic conditions (Hughes 1996; Kayal *et al.* 2018; Cant *et al.* 2021). Indeed, although more time consuming, demographic approaches transcend the correlative techniques previously used for evaluating the viability of coral populations and communities, and for predicting their resilience to future climatic stressors (Edmunds *et al.* 2014; Edmunds & Riegl 2020).

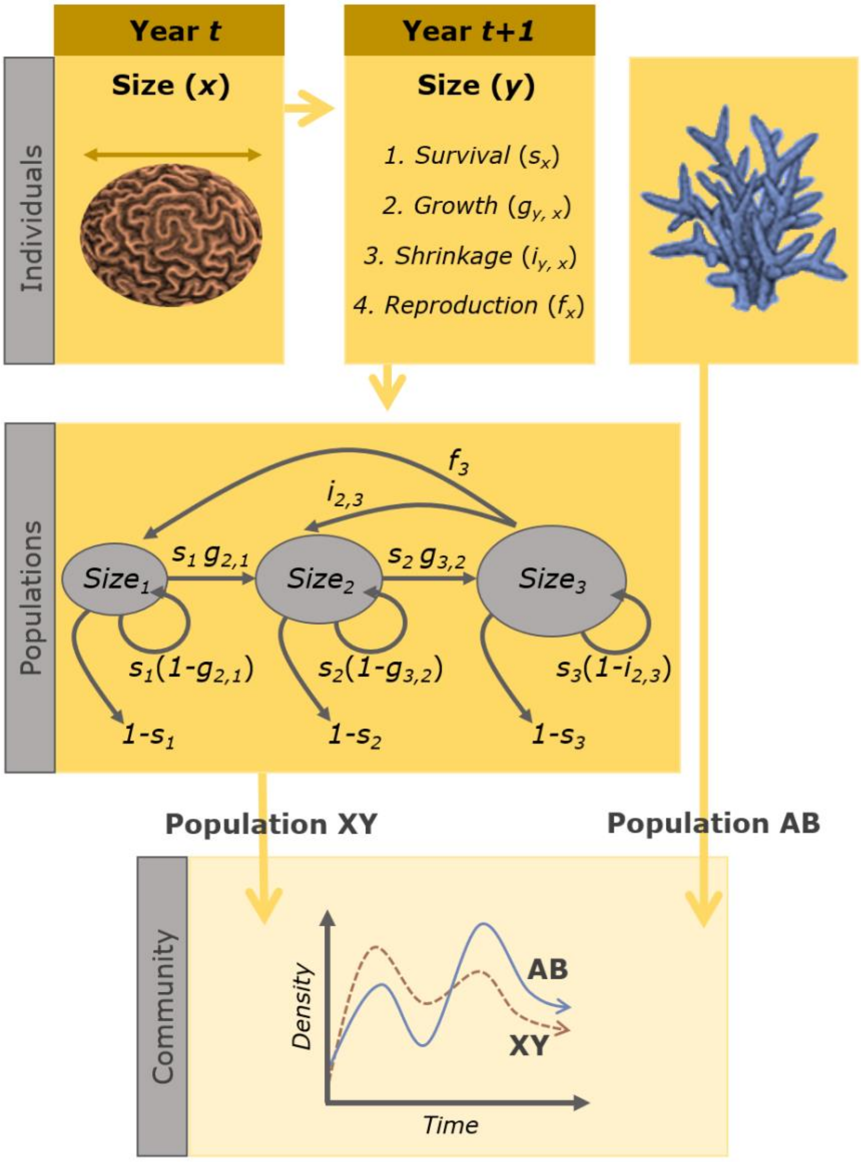

Figure I. Records of survival, size, and reproductive output, collected from tagged coral colonies over time, can be used to enhance predictions of population trajectories and community reassembly under future climate scenarios. Here, subscript notation is used to reflect how the changing state of individuals corresponds with changes in individual-level characteristics. In this schematic the state of individuals refers to colony size and thus the growth (g) of individuals between size x and y is expressed as g_{yx}.

Crucially, though, with populations rarely exposed to stable conditions or equilibria, deterministic estimates of λ are unlikely to represent a true reflection of a population's trajectory (Boyce 1992; Beissinger & Westphal 1998). To achieve their asymptotic growth rate populations require a stable population structure, at which their vital rate patterns will maintain a consistent distribution of individuals across state classes over time (Caswell 2001). Yet, for their stable structure to manifest, populations typically require time in a constant environment to allow the state distribution of individuals to convergence towards equilibrium, without displacement by local disturbances (Fig 1.1; Bierzychudek 1999). Additionally, the vital rate patterns used in constructing population projection matrices are themselves not consistent, and contingent on the environmental conditions in which they are observed (Benton & Grant 1996; Boyce *et al.* 2006). Equally, as populations change in size their dynamics are subject to density–dependant processes that regulate their trajectories within shared environments (Engen *et al.* 1998; Lande *et al.* 2003). Thus the dynamics of populations can be expected to vary over time as environmental conditions change (Tuljapurkar & Orzack 1980; Tuljapurkar 1989).

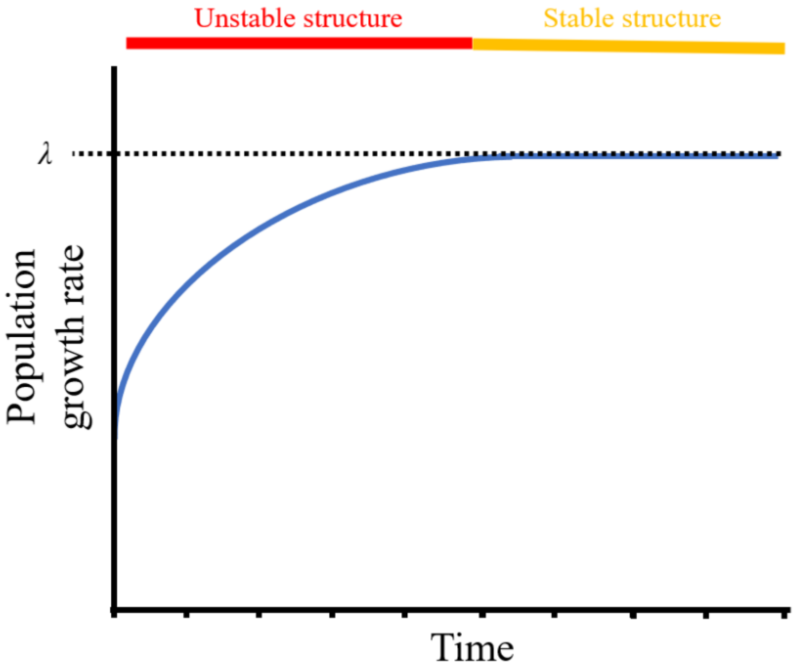

Figure 1.1. At stationary equilibrium, populations are expected to change size at a constant rate, termed their asymptotic growth rate (λ). However, to display

asymptotic characteristics, populations need a stable state structure and so require time at equilibrium to enable the development of this stable structure. In the absence of a stable state structure, populations will display varying growth rates as they converge towards asymptotic expectations, even within equilibrate environments. Note that, although in this schematic the populations growth rate is increasing towards its asymptotic trajectory, estimates of λ can also reflect asymptotic decline.

Recurrent perturbations prevent populations from acquiring, or preserving, a stable state structure (Bierzychudek 1999; Williams *et al.* 2011). Instead, environments persist within a non-equilibrate condition maintaining populations within a transient state during which their trajectories can radically differ from asymptotic expectations (Stott *et al.* 2010, 2011; Hastings *et al.* 2018). Accordingly, anticipating the future condition and endurance of populations requires an awareness for their transient characteristics (Box 2; Ezard *et al.* 2010). Moreover, with the transient characteristics of populations reflecting their response to disturbance and instability, they represent quantifiable measures of population resilience (Capdevila *et al.* 2020). Transient shifts in the state structure of populations can elevate (*amplification*) or diminish (*attenuation*) their growth rates relative to asymptotic projections (Townley *et al*. 2007). Equally, for populations existing in a transient state, there is a natural tendency for their state structure to converge towards a stable structure (Caswell 2001). Intuitively, with population resilience comprised of the attributes of *resistance* (the ability to withstand disturbances), *compensation* (the ability to benefit from disturbances) and *recovery* (the speed and ability to reattain stability), the transient characteristics of populations resemble these features of resilience (Hodgson *et al.* 2015; Capdevila *et al.* 2020).

Evaluating the transient characteristics of populations, and therefore their demographic resilience, is possible through the calculation of transient measures readily accessible from population projection matrices (Box 2; see Stott *et al.* [2011] for a detailed review). Briefly, measures of *reactivity* ($\overline{\rho}$) and *first-timestep attenuation* ($\underline{\rho}$) reflect the initial behaviour in a population’s growth rate following a perturbation, with the *damping ratio* (ρ) describing the rate at which a population is expected to reacquire a stable state structure (Caswell 2001; Stott *et al.* 2011).

Box 2: Measuring transient population characteristics.

Within natural environments, abiotic and biotic perturbations generate constant shifts within the state structure of populations ensuring they persist within a transient state, rather than converging towards equilibrium (Hastings *et al.* 2018). Within this transient state, the growth rate of populations can differ dramatically from their asymptotic trajectories, with populations undergoing *amplification* (increases in growth rate) or *attenuation* (declines in growth rate), which can subsequently influence the viability of a population in the longer-term (Fig. II). Accordingly, it is necessary to explore the transient characteristics of populations to gain insights into their responses to disturbance, and therefore better understand their resilience (Ezard *et al.* 2010; Capdevila *et al.* 2020). Evaluating the transient dynamics of populations is made possible through the calculation of transient indices from population projection matrices (Stott *et al.* 2011). These measures include population *reactivity* ($\overline{\rho}$) and *first-timestep attenuation* ($\underline{\rho}$) which describe the increase or decline in a populations growth rate within one time interval of a perturbation, relative to λ (Stott *et al.* 2011). Equally, the measures of *maximal amplification* ($\overline{\rho}_{max}$) and *maximal attenuation* ($\underline{\rho}_{max}$) can be used to evaluate the maximum amplification or attenuation expected in the growth rate of populations, relative to λ (Townley *et al.* 2007; Townley & Hodgson 2008).

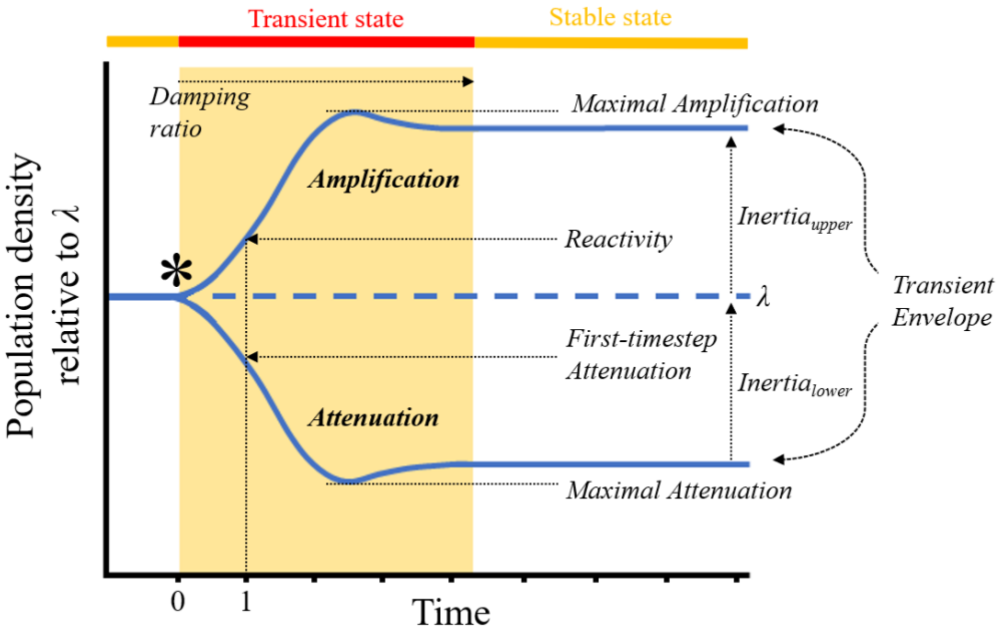

Figure II. Various measures exist for quantifying the transient characteristics of populations, and how the short-term responses of populations following a disturbance (*) will modify their trajectories relative to asymptotic expectations.

The *damping ratio* (ρ) of a population defines the rate at which at population will converge back to a stable equilibrium following a perturbation to its stable structure (Caswell 2001). Finally, *upper* & *lower population inertia* ($Inertia_{upper}$ & $Inertia_{lower}$ respectively) can be used to explore the extent to which the transient characteristics of populations influence their long-term trajectories, also known as a populations *transient envelope* (*TE*) (Koons *et al.* 2005; Stott *et al.* 2011).

Alternatively, estimates of *maximal amplification* ($\overline{\rho}_{max}$), *maximal attenuation* ($\underline{\rho}_{max}$), and *population inertia* ($Inertia_x$) illustrate the magnitude by which the growth rate of a population can be expected to fluctuate, and the influence of this short-term variation on the population's long-term trajectory (Koons *et al.* 2005; Townley *et al.* 2007; Stott *et al.* 2011). Furthermore, with population projection matrices providing a link between each transient characteristic and a population's vital rates, sensitivity analyses can be applied to evaluate the mechanistic drivers underlying the short-term characteristics of populations (Stott 2016; Caswell 2019). Overall, transient demographic approaches present an effective tool for explicitly evaluating the resilience of natural populations (Capdevila *et al.* 2020), and have proven instrumental in our understanding of the establishment of populations within novel and variable environments (Iles *et al.* 2016; McDonald *et al.* 2016, 2017; Jelbert *et al.* 2019).

1.1.2. Coral population dynamics: Current knowledge.

To examine the advancement of state-structured population approaches within coral research, we conducted a review of the relevant ecological literature. Specifically, we searched for the term coral* AND demograph* across the titles, abstracts, and keywords of research literature within the SCOPUS database. We applied our search across all indexed peer-reviewed journals published between 1960 and 2020, inclusive. This search initially returned 781 studies, from which we retained all studies that explicitly measured or quantified state-structured patterns in the survival, size transitions (including shrinkage via partial mortality or fission), and/or reproduction (e.g., fecundity) of coral colonies. We also retained studies measuring larval settlement rates, as the recruitment of early life stage individuals is a key demographic aspect within coral communities (Adjeroud *et al.* 2017). Following this refinement, we retained a total of 145 studies (~19% of our original search), which we then categorised according to whether they involved the presentation of (i) asymptotic dynamics/simulations, (ii) transient characteristics, or (iii) an assessment of vital rate patterns only.

Following the seminal work of Hughes and Jackson (1980), the application of state-structured demographic assessments has increased within coral research, with a particularly rapid growth in popularity since 2007 (Fig. 1.2). However, much of this research (97%) has focused on either exploring the asymptotic dynamics of coral populations (34%; 50 studies) or solely evaluating patterns across one or more of the vital rates of survival, changes in size, or reproduction (63%; 91 studies). Presently, the majority of knowledge regarding the dynamics of coral populations centres around their long-term trajectories. Thus, our current understanding regarding the dynamics of coral populations assumes that these populations will experience the stable environments necessary for achieving optimum population structures.

A limited amount of previous research has considered the unpredictable nature of natural environments when evaluating the future trajectories of coral populations. Our search identified nine studies that either included estimates of stochastic population growth (λ_s; Lewontin and Cohen 1969) or explicitly parameterised the density-dependant regulation of vital rates within their population models (Fig. 1.2; see Linares *et al.* 2007; Linares and Doak 2010; Hernandez-Pacheco *et al.* 2011; Vardi *et al.* 2012; Bramanti *et al.* 2015; Mercado-Molina *et al.* 2015; Kayal *et al.* 2018; Montero-Serra *et al.* 2019). Estimates of λ_s describe the average periodic change in the size of a population over a series of successive time intervals (Engen & Saether 1998). As such, this metric of population performance provides a more accurate consideration of vital rate and environmental variation when evaluating future population trajectories, compared to deterministic λ. However, with estimates of λ_s often derived using a series of population sizes estimated over numerous time intervals or with initial inconsistent estimates of population size omitted, λ_s is still fundamentally a long-term measure of population viability (Ellner & Rees 2007). Consequently, this measure still neglects the short-term characteristics of populations,

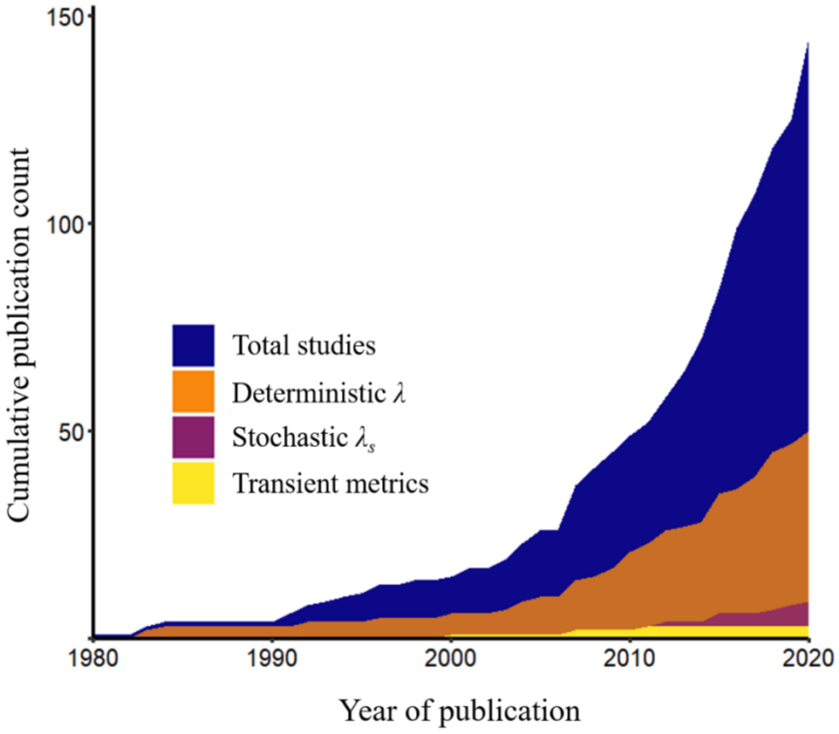

Figure 1.2. The cumulative number of studies that explicitly explore the state-structured demographics of coral populations as identified by our search for the term coral* AND demograph* across the peer-reviewed literature within the SCOPUS database. The colour scale differentiates between studies that focus on only investigating patterns in colony survival, growth, and/or reproduction, and those that utilised estimates of either deterministic population growth (λ), stochastic asymptotic characteristics (λ_s), or transient population characteristics, to evaluate the dynamics of coral populations.

and thus, our capacity to fully anticipate the future dynamics of coral populations remains restricted.

Whilst state-structured demographic approaches are being adopted within coral research, our review of the literature demonstrates how prominently the assumption of stable equilibria dominates our understanding of coral population dynamics. Subsequently, we lack the understanding necessary for accurately projecting the future reassembly and persistence of coral communities under increasingly recurrent disturbance regimes. Only three of the 145 studies in our literature search calculated measures of the transient characteristics of coral populations (Fig. 1.2; see Hughes and Tanner 2000; Linares *et al.* 2007; Bruno *et al.* 2011). Alongside asymptotic population characteristics, these studies estimated population damping ratios to outline the rate at which their focal populations would converge back to a stable state structure following a perturbation. Yet, the damping ratio represents a dimensionless, mathematical property of population projection matrices, and alone is of limited use to population managers seeking to predict the short term responses of populations to disturbance (Stott *et al.* 2011). Forecasting the resilience of coral populations is essential for the future conservation of various reef communities (Roche *et al.* 2018; Lam *et al.* 2020). We have illustrated here, however, that current approaches used in coral population ecology to evaluate population growth rates do not constitute measures of population resilience. Our understanding of coral population dynamics needs to be further expanded in order to meet our need for quantifying the resilience, and responses, of coral communities to increasingly frequent disturbances.

1.1.3. Transient dynamics and the resilience of coral communities.

Exploring the transient characteristics of coral populations will enhance our understanding regarding the future diversity, condition, and resilience, of coral communities. The frequency of widespread thermal stress events is increasing across global coral communities, and soon expected to exceed the recovery time required by most coral species (Hughes *et al.* 2018a; Sully *et al.* 2019). Presently, considerable value is placed on classifying coral species according to their morphological and functional traits, with the subsequent categorisation of coral taxa offering proxies for the vulnerability of various coral communities to said recurrent stress events (Darling *et al.* 2012, 2019). Quantifying the relative affinities of different coral populations for demographic recovery presents the opportunity for justifying these assumptions; helping to distinguish the species and populations most vulnerable and or resilient to projected recurrent disturbance regimes.

Intuitively, the amplification and attenuation characteristics of populations simultaneously reflect their stability following a disturbance. However, recognising the differential attributes of compensation and resistance in different populations is important for managing the future condition of biological communities (Capdevila *et al.* 2020). Assessments of coral communities following repeated disturbances have demonstrated divergent shifts in species compositions (Adjeroud *et al.* 2009; Pratchett *et al.* 2011, 2020). With knowledge of the capacity for various coral populations to undergo demographic amplification or for avoiding demographic attenuation, we can begin to forecast and anticipate the reassembly of coral communities, thereby improving the effectiveness of adaptive reef management. Alternatively, a disturbance does not necessarily imply a negative impact, merely a change to a system (Pickett & White 1985). Disturbances to the structure of populations can be brought about by the cessation of a continuous pressure, changes in resource availability, or establishment within a novel environment. The transient characteristics of populations offer insights into their invasive potential (Iles *et al.* 2016), with the ability of natural populations for undergoing demographic compensation underpinning their capacity for exploiting changes within their local environments (Jelbert *et al.* 2019). Accordingly, comprehending and quantifying demographic compensation within coral populations will aid predicting the winners and losers in reef communities targeted by conservation initiatives, restoration strategies, or climate induced range shifts. Assessing coral reef community resilience within such a framework requires an increased focus on the temporal nature of resilience, a view that would transcend current approaches of conducting single reef assessments to determine resilience (Maynard *et al.* 2015; McLeod *et al.* 2021).

Complexities in the modelling approaches used to explore the dynamics of natural populations have resulted in these techniques remaining largely overlooked within coral research (Edmunds *et al.* 2014). Indeed, parametrising the demographic models needed to quantify population characteristics requires considerable amounts of data (Ellner *et al.* 2002). Although, despite the data demanding nature of state-structured demographic models, the collection of the necessary data regarding the survival, transitions in size, fragmentation, and recruitment, of individual coral colonies is possible alongside current reef monitoring efforts (Edmunds & Riegl 2020). Furthermore, new techniques for analysing the demographic characteristics of populations structured by a continuous state variable like size (Integral Projection Models [IPMs; Easterling et al. 2000]) have reduced the data demands of demographic assessments (Ramula *et al.* 2009). As a result, IPM frameworks are growing in popularity throughout coral research (e.g. Bruno et al. 2011; Madin et al. 2012; Zychaluk et al. 2012; Elahi et al. 2016; Kayal et al. 2018; Precoda et al. 2018; Scavo

Lord et al. 2020; Cant et al. 2021; Carlot et al. 2021). Finally, studying the dynamics, particularly the transient characteristics, of coral populations is made increasingly accessible by the development of demographic analysis packages such as *popdemo* (Stott *et al.* 2012).

It is not our intention to dismiss previous efforts to evaluate the dynamics of coral populations using asymptotic characteristics. Changes in individual vital rates can of course have critical repercussions on the dynamics of populations (e.g. Bellier *et al.* 2018), and asymptotic characteristics provide valuable insights for the management of threatened populations (e.g. Johnson *et al.* 2010). However, as we have illustrated here, the asymptotic characteristics of populations do not represent indicators of population resilience. Here, we advocate for a greater commitment towards investigating the transient dynamics of coral populations that more accurately reflect their dynamics within natural environments (Ezard *et al.* 2010; Stott *et al.* 2011; Capdevila *et al.* 2020). With changing climatic regimes and increased anthropogenic interference exposing global reef ecosystems to increasingly frequent disturbances (Hoegh-Guldberg *et al.* 2017), evaluating the transient dynamics of coral populations, and their mechanistic drivers, will provide a new effective lens on coral reef resilience.

1.2. Thesis aims and objectives.

The overarching objective of this thesis is to explore patterns in demographic resilience, with a particular focus on how variation in the dynamics of coral communities between tropical and subtropical assemblages mediates the establishment and performance of coral populations at higher latitudes. Forecasting the response of natural communities to changing climate regimes requires an explicit understanding for how abiotic drivers regulate the dynamics of their constituent populations (Merow *et al.* 2017). Many future climate predictions represent no-analogue scenarios in comparison to current local climate regimes (Williams *et al.* 2007). However, investigating the characteristics and dynamics of marginalised populations that inhabit supposedly suboptimal conditions, can provide vital insights into the capacity for populations to endure future environmental stress (Rastrick *et al.* 2018). Accordingly, by exploring the characteristics of subtropical coral populations and, crucially, how they differ from those of tropical populations, we can begin to decipher the mechanisms underpinning coral community persistence (Camp *et al.* 2018).

More specifically, the research within this thesis aimed to investigate spatial patterns in the demographic resilience of coral populations, and how these correspond with trends in abiotic variation. Compared to tropical coral reefs, subtropical coral communities experience enhanced abiotic variation, cooler seasonal temperatures, and reduced photosynthetic radiation (Yamano *et al.* 2012; Sommer *et al.* 2014, 2017; Muir *et al.* 2015). Despite these apparent constraints, subtropical coral communities continue to thrive and are considered among potential avenues for conserving future coral biodiversity (Hughes *et al.* 2010; Beger *et al.* 2011). State-structured demographic approaches permit the calculation of various measures of population performance and resilience (Crone *et al.* 2011; Capdevila *et al.* 2020), yet, these approaches remain neglected within coral research (Edmunds & Riegl 2020). Adopting state-structured demographic modelling techniques, the research presented throughout this thesis aims to enhance our capacity to predict the winners and losers within coral communities following future climate shifts. Subsequently, this work will help enable us to better forecast changes in coral species compositions and manage shifting and deteriorating coral communities.

This thesis consists of four research chapters, each building on the previous, to advance understanding of spatial patterns in demographic resilience, particularly exploring the association between abiotic variation and demographic resilience and how this influences the dynamics of coral populations across a tropical-subtropical gradient (Fig. 1.3). Accordingly, Chapter 1 discusses comparative research into broad spatial patterns in demographic resilience across a range of taxa and populations. Using Matrix Population Models (MPMs) extracted from the COMPADRE and COMADRE databases (Salguero-Gómez *et al.* 2015, 2016) and the application of transient demographic theory (Caswell 2001; Stott *et al.* 2010, 2011), this chapter investigates the association between exposure to abiotic variability and the capacity for populations to resist, or recover from, further disturbances. Consequently, this chapter asks whether past experience of enhanced variability infers a greater capacity for tolerating future climatic variability. Chapter 2 then presents research quantifying variation in the response of subtropical coral taxa towards thermal stress and simulating their future viability using an Integral Projection Model (IPM) framework.

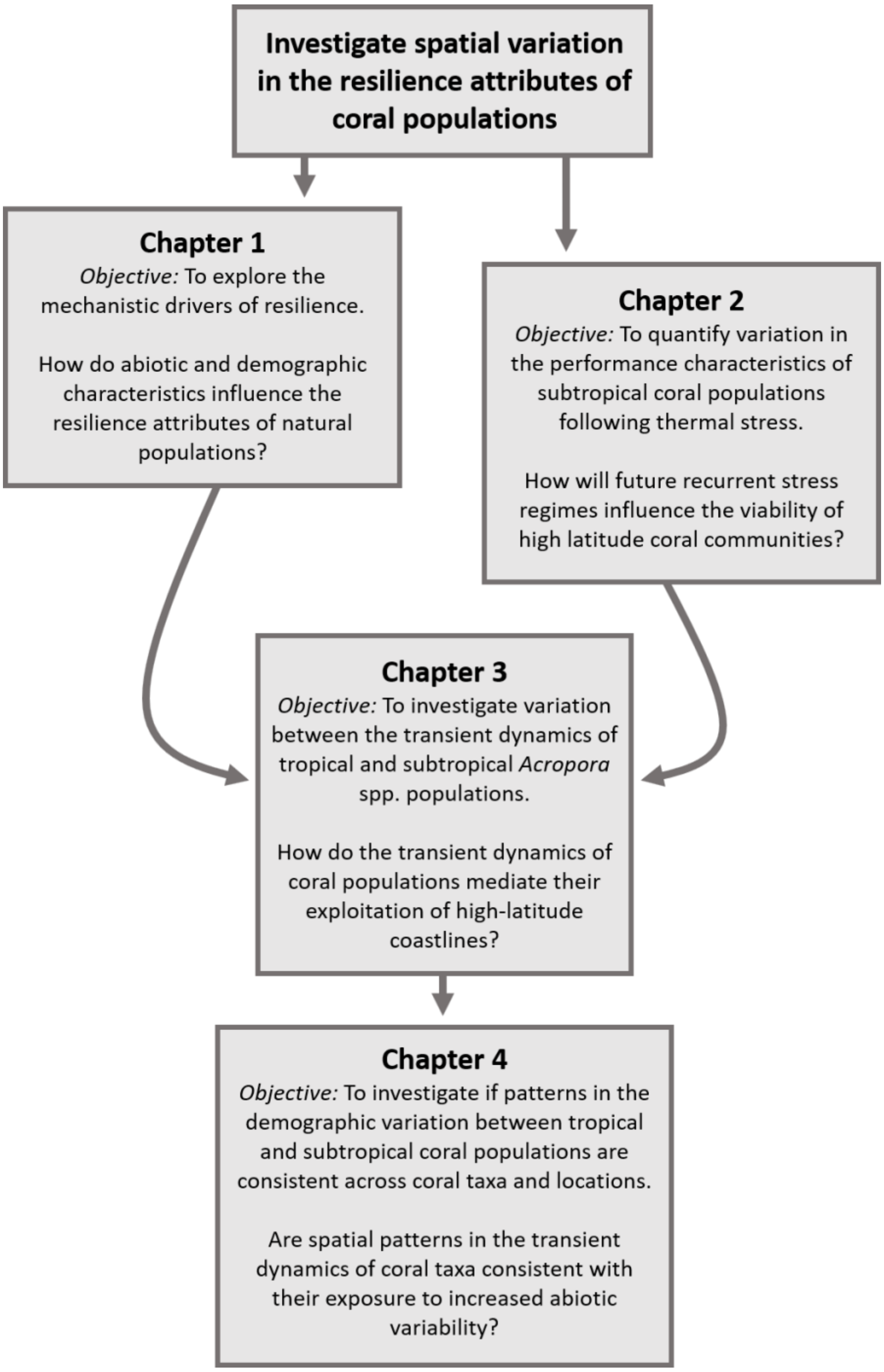

Figure 1.3. Schematic diagram reflecting the evolution of the research presented in this thesis. The primary aim of this thesis was to explore how the demographic performance and resilience of coral communities varies between tropical and subtropical assemblages. This aim is then divided into four research chapters focused on developing understanding of transient dynamics and demographic resilience in coral populations.

Data regarding the survival, growth, and recruitment patterns of individual colonies were collected from subtropical corals tagged in the Solitary Islands Marine Park (SIMP), Australia, both during and after the 2015/16 global bleaching event. These data were then used to parametrise IPMs investigating how the performance of different coral populations was affected during the stress event, and the demographic mechanisms supporting any subsequent recovery. Combined with future temperature projections, these IPMs were then used to project the dynamics of the different populations under varying recurrent thermal stress cycles to evaluate their vulnerability to different forecasted climate scenarios.

Chapter 3 represents a detailed exploration of the transient dynamics of hard coral populations. Transient demographic theory has been instrumental in our understanding of invasive populations, revealing the key processes facilitating the exploitation of non-native environments (Iles *et al.* 2016; Jelbert *et al.* 2019). Focusing on *Acropora* spp. populations in southern Japan, the research presented in Chapter 3 evaluates how variation between the transient dynamics of tropical and subtropical coral populations mediates the establishment of coral populations at higher latitudes. Finally, combining data collected across demographic surveys conducted in Japan and Australia between 2017 and 2019, Chapter 4 evaluates whether the patterns observed in the transient dynamics of *Acropora* spp. presented in Chapter 3 are consistent across coral taxa along tropical and subtropical transitional zones. Consequently, this final chapter explores the association between the transient dynamics, and therefore resilience, of coral populations and their exposure to increased abiotic variability, and how this link can be used to inform the future management of coral reef environments. This thesis then concludes with a discussion illustrating how this work will help to enhance our understanding of coral community dynamics, before highlighting key areas of research that require continued attention.

As climate change and anthropogenic disturbances place natural environments under increasing pressure, managing the future viability of biological communities requires an improved understanding of the resilience of various populations towards repeated disturbances. This notion is particularly true in the context of global coral reef environments which carry considerable biological and economic value and yet, without a detailed understanding of resilience in coral communities, many contemporary reef conservation efforts are likely to prove ineffective (Kleypas *et al.*

2021). Consequently, this thesis represents a key step in evaluating the mechanistic drivers of resilience in coral populations; providing insights into the capacity of coral populations for enduring climatic variability and thereby enhancing our ability to forecast the future resilience, viability, and condition of global coral communities.

1.3. References

Adjeroud, M., Kayal, M. & Penin, L. (2017). Importance of recruitment processes in the dynamics and resilience of coral reef assemblages. In: *Marine Animal Forests: The Ecology of Benthic Biodiversity Hotspots* (eds. Rossi, S., Bramanti, L., Gori, A. & Orejas, C.). Springer International Publishing, Cham, pp. 549–569.

Adjeroud, M., Michonneau, F., Edmunds, P.J., Chancerelle, Y., de Loma, T.L., Penin, L., *et al.* (2009). Recurrent disturbances, recovery trajectories, and resilience of coral assemblages on a South Central Pacific reef. *Coral Reefs*, 28, 775–780.

Adler, P.B., Ellner, S.P. & Levine, J.M. (2010). Coexistence of perennial plants: An embarrassment of niches. *Ecol. Lett.*, 13, 1019–1029.

Ateweberhan, M., McClanahan, T.R., Graham, N.A.J. & Sheppard, C.R.C. (2011). Episodic heterogeneous decline and recovery of coral cover in the Indian Ocean. *Coral Reefs*, 30, 739–752.

Beger, M., Babcock, R., Booth, D.J., Bucher, D., Condie, S.A., Creese, B., *et al.* (2011). Research challenges to improve the management and conservation of subtropical reefs to tackle climate change threats: (Findings of a workshop conducted in Coffs Harbour, Australia on 13 September 2010). *Ecol. Manag. Restor.*, 12, 1–4.

Beger, M., Sommer, B., Harrison, P.L., Smith, S.D.A. & Pandolfi, J.M. (2014). Conserving potential coral reef refuges at high latitudes. *Divers. Distrib.*, 20, 1–13.

Beissinger, S.R. & Westphal, M.I. (1998). On the use of demographic models of population viability in endangered species management. *J. Wildl. Manage.*, 62, 821–841.

Bellier, E., Kéry, M. & Schaub, M. (2018). Relationships between vital rates and ecological traits in an avian community. *J. Anim. Ecol.*, 87, 1172–1181.

Bellwood, D.R., Hughes, T.P., Folke, C. & Nyström, M. (2004). Confronting the coral reef crisis. *Nature*, 429, 827–833.

Benton, T.G. & Grant, A. (1996). How to keep fit in the real world: Elasticity analyses and selection pressures on life histories in a variable environment. *Am. Nat.*, 147, 115–139.

Benton, T.G., Plaistow, S.J. & Coulson, T.N. (2006). Complex population dynamics and complex causation: Devils, details and demography. *Proc. R. Soc. B Biol. Sci.*, 273, 1173–1181.

Bierzychudek, P. (1999). Looking backwards: Assessing the projections of a transition matrix model. *Ecol. Appl.*, 9, 1278–1287.

Boyce, M.S. (1992). Population viability analysis. *Annu. Rev. Ecol. Syst.*, 23, 481–506.

Boyce, M.S., Haridas, C. V., Lee, C.T., Boggs, C.L., Bruna, E.M., Coulson, T., *et al.* (2006). Demography in an increasingly variable world. *Trends Ecol. Evol.*, 21, 141–148

Bramanti, L., Iannelli, M., Fan, T.Y. & Edmunds, P.J. (2015). Using demographic models to project the effects of climate change on scleractinian corals: Pocillopora damicornis as a case study. *Coral Reefs*, 34, 505–515.

Bruno, J.F., Ellner, S.P., Vu, I., Kim, K. & Harvell, C.D. (2011). Impacts of aspergillosis on sea fan coral demography: modeling a moving target. *Ecol. Monogr.*, 81, 123–139.

Bruno, J.F. & Valdivia, A. (2016). Coral reef degradation is not correlated with local human population density. *Sci. Rep.*, 6, 1–8.

Camp, E.F., Schoepf, V., Mumby, P.J., Hardtke, L.A., Rodolfo-Metalpa, R., Smith, D.J., *et al.* (2018). The future of coral reefs subject to rapid climate change: Lessons from natural extreme environments. *Front. Mar. Sci.*, 5, 1–21.

Cant, J., Salguero-Gómez, R., Kim, S.W., Sims, C.A., Sommer, B., Brooks, M., *et* *al.* (2021). The projected degradation of subtropical coral assemblages by recurrent thermal stress. *J. Anim. Ecol.*, 90, 233–247.

Capdevila, P., Stott, I., Beger, M. & Salguero-Gómez, R. (2020). Towards a comparative framework of demographic resilience. *Trends Ecol. Evol.*, 35, 776–786.

Carlot, J., Kayal, M., Lenihan, H.S., Brandl, S.J., Casey, J.M., Adjeroud, M., *et al.* (2021). Juvenile corals underpin coral reef carbonate production after disturbance. *Glob. Chang. Biol.*, 1–10.

Caswell, H. (2001). *Matrix population models: Construction, analysis and interpretation*. 2nd Edition. Oxford University Press Inc.

Caswell, H. (2019). *Sensitivity Analysis: Matrix Methods in Demography and Ecology*. Springer, Cham.

Cinner, J. (2014). Coral reef livelihoods. *Curr. Opin. Environ. Sustain.*, 7, 65–71.

Connell, J.H. (1978). Diversity of tropical rainforests and coral reefs. *Science*, 99, 1304–1310.

Costanza, R. & Folke, C. (1997). Valuing ecosystem services with efficiency, fairness, and sustainability as goals. In: *Nature's services: Societal dependence on natural ecosystems* (ed. Daily, G.C.). Island Press, Washington, pp. 49–68.

Côté, I.M., Gill, J.A., Gardner, T.A. & Watkinson, A.R. (2005). Measuring coral reef decline through meta-analyses. *Philos. Trans. R. Soc. B Biol. Sci.*, 360, 385–395.

Crone, E.E., Menges, E.S., Ellis, M.M., Bell, T., Bierzychudek, P., Ehrlén, J., *et al.* (2011). How do plant ecologists use matrix population models? *Ecol. Lett.*, 14, 1–8.

Darling, E.S., Alvarez-Filip, L., Oliver, T.A., Mcclanahan, T.R. & Côté, I.M. (2012). Evaluating life-history strategies of reef corals from species traits. *Ecol. Lett.*, 15, 1378–1386.

Darling, E.S., McClanahan, T.R., Maina, J., Gurney, G.G., Graham, N.A.J., Januchowski-Hartley, F., *et al.* (2019). Social–environmental drivers inform strategic management of coral reefs in the Anthropocene. *Nat. Ecol. Evol.*, 3, 1341–1350.

De'Ath, G., Fabricius, K.E., Sweatman, H. & Puotinen, M. (2012). The 27-year decline of coral cover on the Great Barrier Reef and its causes. *Proc. Natl. Acad. Sci. U. S. A.*, 109, 17995–17999.

Descombes, P., Wisz, M.S., Leprieur, F., Parravicini, V., Heine, C., Olsen, S.M., *et al.* (2015). Forecasted coral reef decline in marine biodiversity hotspots under climate change. *Glob. Chang. Biol.*, 21, 2479–2487.

Dietzel, A., Bode, M., Connolly, S.R. & Hughes, T.P. (2020). Long-term shifts in the colony size structure of coral populations along the Great Barrier Reef. *Proc. R. Soc. B Biol. Sci.*, 287, 1–9.

Easterling, D.R., Meehl, G.A., Parmesan, C., Changnon, S.A., Karl, T.R. & Mearns, L.O. (2000a). Climate Extremes: Observations, Modeling, and Impacts. *Science*, 289, 268–274.

Easterling, M.R., Ellner, S.P. & Dixon, P.M. (2000b). Size-specific sensitivity: applying a new structured population model. *Ecology*, 81, 694–708.

Edmunds, P.J., Burgess, S.C., Putnam, H.M., Baskett, M.L., Bramanti, L., Fabina, N.S., *et al.* (2014). Evaluating the causal basis of ecological success within the scleractinia: an integral projection model approach. *Mar. Biol.*, 161, 2719–2734.

Edmunds, P.J. & Riegl, B. (2020). Urgent need for coral demography in a world where corals are disappearing. *Mar. Ecol. Prog. Ser.*, 635, 233–242.

Ehrlén, J., Morris, W.F., von Euler, T. & Dahlgren, J.P. (2016). Advancing environmentally explicit structured population models of plants. *J. Ecol.*, 104, 292–305.

Elahi, R., Sebens, K.P. & De Leo, G.A. (2016). Ocean warming and the demography of declines in coral body size. *Mar. Ecol. Prog. Ser.*

Ellner, S.P., Fieberg, J., Ludwig, D. & Wilcox, C. (2002). Precision of population viability analysis. *Conserv. Biol.*, 16, 258–261.

Ellner, S.P. & Rees, M. (2007). Stochastic stable population growth in integral projection models: Theory and application. *J. Math. Biol.*, 54, 227–256.

Engen, S., Bakke, Ø. & Islam, A. (1998). Demographic and environmental stochasticity - Concepts and definitions. *Biometrics*, 54, 840–846.

Engen, S. & Saether, B. (1998). Stochastic population models: Some concepts, definitions and results. *Oikos*, 83, 345–352.

Ezard, T.H.G., Bullock, J.M., Dalgleish, H.J., Millon, A., Pelletier, F., Ozgul, A., *et al.* (2010). Matrix models for a changeable world: The importance of transient dynamics in population management. *J. Appl. Ecol.*, 47, 515–523.

Ferrario, F., Beck, M.W., Storlazzi, C.D., Micheli, F., Shepard, C.C. & Airoldi, L. (2014). The effectiveness of coral reefs for coastal hazard risk reduction and adaptation. *Nat. Commun.*, 5, 1–9.

França, F.M., Benkwitt, C.E., Peralta, G., Robinson, J.P.W., Graham, N.A.J., Tylianakis, J.M., *et al.* (2020). Climatic and local stressor interactions threaten tropical forests and coral reefs. *Philos. Trans. R. Soc. B Biol. Sci.*, 375, 1–10.

Francis, T.B., Abbott, K.C., Cuddington, K., Gellner, G., Hastings, A., Lai, Y.C., *et al.* (2021). Management implications of long transients in ecological systems. *Nat. Ecol. Evol.*, 5, 285–294.

Gardner, T.A., Côté, I.M., Gill, J.A., Grant, A. & Watkinson, A.R. (2003). Long-term region-wide declines in Caribbean corals. *Science*, 301, 958–960.

Groenendael, J. van, Kroon, H. de & Caswell, H. (1988). Projection matrices in population biology. *Trends Ecol. Evol.*, 3, 264–269.

Hastings, A. (2001). Transient dynamics and persistence of ecological systems. *Ecol. Lett.*, 4, 215–220.

Hastings, A. (2004). Transients: The key to long-term ecological understanding? *Trends Ecol. Evol.*, 19, 39–45.

Hastings, A., Abbott, K.C., Cuddington, K., Francis, T., Gellner, G., Lai, Y.C., *et al.* (2018). Transient phenomena in ecology. *Science*, 361, 1–9.

Hernandez-Pacheco, R., Hernandez-Delgado, E.A. & Sabat, A.M. (2011).

Demographics of bleaching in a major Caribbean reef-building coral: Montastraea annularis. *Ecosphere*, 2, 1–13.

Hodgson, D., McDonald, J.L. & Hosken, D.J. (2015). What do you mean, “resilient”? *Trends Ecol. Evol.*, 30, 503–506.

Hoegh-Guldberg, O. (2011). The impact of climate change on coral reef ecosystems. In: *Coral Reefs: An Ecosystem in Transition*. Springer Netherlands, pp. 391–403.

Hoegh-Guldberg, O., Mumby, P.J., Hooten, A.J., Steneck, R.S., Greenfield, P., Gomez, E., *et al.* (2007). Coral reefs under rapid climate change and ocean acidification. *Science*, 318, 1737–1742.

Hoegh-Guldberg, O., Pendleton, L. & Kaup, A. (2019). People and the changing nature of coral reefs. *Reg. Stud. Mar. Sci.*, 30, 2–20.

Hoegh-Guldberg, O., Poloczanska, E.S., Skirving, W. & Dove, S. (2017). Coral reef ecosystems under climate change and ocean acidification. *Front. Mar. Sci.*, 4, 1–20.

Holling, C.S. (1973). Resilience and stability of ecological systems. *Annu. Rev. Ecol. Syst.*, 4, 1–23.

Hughes, T.P. (1984). Population Dynamics Based on Individual Size Rather than Age: A General Model with a Reef Coral Example. *Am. Nat.*, 123, 778–795.

Hughes, T.P. (1996). Demographic Approaches to Community Dynamics: A Coral Reef Example. *Ecology*, 77, 2256–2260.

Hughes, T.P., Anderson, K.D., Connolly, S.R., Heron, S.F., Kerry, J.T., Lough, J.M., *et al.* (2018a). Spatial and temporal patterns of mass bleaching of corals in the Anthropocene. *Science*, 359, 80–83.

Hughes, T.P., Baird, A.H., Bellwood, D.R., Card, M., Connolly, S.R., Folke, C., *et al.* (2003). Climate change, human impacts, and the resilience of coral reefs. *Science*, 301, 929–933.

Hughes, T.P., Graham, N.A.J., Jackson, J.B.C., Mumby, P.J. & Steneck, R.S. (2010). Rising to the challenge of sustaining coral reef resilience. *Trends Ecol.*

Evol., 25, 633–642.

Hughes, T.P. & Jackson, J.B.C. (1980). Do corals lie about their age? Some demographic consequences of partial mortality, fission, and fusion. *Science*, 209, 713–715.

Hughes, T.P., Kerry, J.T., Baird, A.H., Connolly, S.R., Dietzel, A., Eakin, C.M., *et al.* (2018b). Global warming transforms coral reef assemblages. *Nature*, 556, 492–496.

Hughes, T.P. & Tanner, J.E. (2000). Recruitment Failure, Life Histories, and Long-Term Decline of Caribbean Corals. *Ecology*, 81, 2250–2263.

Iles, D.T., Salguero-Gómez, R., Adler, P.B. & Koons, D.N. (2016). Linking transient dynamics and life history to biological invasion success. *J. Ecol.*, 104, 399–408.

Jelbert, K., Buss, D., McDonald, J., Townley, S., Franco, M., Stott, I., *et al.* (2019). Demographic amplification is a predictor of invasiveness among plants. *Nat. Commun.*, 10, 1–6.

Johns, K.A., Osborne, K.O. & Logan, M. (2014). Contrasting rates of coral recovery and reassembly in coral communities on the Great Barrier Reef. *Coral Reefs*, 33, 553–563.

Johnson, H.E., Mills, L.S. & Stephenson, T.R. (2010). Population-specific vital rate contributions influence management of an endangered ungulate. *Ecol. Appl.*, 20, 1753–1765.

Jongejans, E., Skarpaas, O. & Shea, K. (2008). Dispersal, demography and spatial population models for conservation and control management. *Perspect. Plant Ecol. Evol. Syst.*, 9, 153–170.

Kayal, M., Lenihan, H.S., Brooks, A.J., Holbrook, S.J., Schmitt, R.J. & Kendall, B.E. (2018). Predicting coral community recovery using multi-species population dynamics models. *Ecol. Lett.*, 22, 605–615.

Kleypas, J., Allemand, D., Anthony, K., Baker, A.C., Beck, M.W., Hale, L.Z., *et al.* (2021). Designing a blueprint for coral reef survival. *Biol. Conserv.*, 257, 1–7.

Koons, D.N., Grand, J.B., Zinner, B. & Rockwell, R.F. (2005). Transient population dynamics: Relations to life history and initial population state. *Ecol. Modell.*, 185, 283–297.

Lachs, L., Sommer, B., Cant, J., Hodge, J.M., Pandolfi, J.M. & Beger, M. (2021). Linking population size structure, heat stress and bleaching responses in a subtropical endemic coral. *Coral Reefs*, 40, 770–790.

Lam, V.Y.Y., Doropoulos, C., Bozec, Y.M. & Mumby, P.J. (2020). Resilience concepts and their application to coral reefs. *Front. Ecol. Evol.*, 8, 1–14.

Lande, R., Engen, S. & Sther, B.E. (2003). *Stochastic population dynamics in ecology and conservation*. Oxford University Press, Oxford.

Lewontin, R.C. & Cohen, D. (1969). On population growth in a randomly varying environment. *Proc. Natl. Acad. Sci.*, 62, 1056–1060.

Linares, C. & Doak, D.F. (2010). Forecasting the combined effects of disparate disturbances on the persistence of long-lived gorgonians: A case study of Paramuricea clavata. *Mar. Ecol. Prog. Ser.*, 402, 59–68.

Linares, C., Doak, D.F., Coma, R., Diaz, D. & Zabala, M. (2007). Life history and viability of a long-lived marine invertebrate: The octocoral Paramuricea clavata. *Ecology*, 88, 918–928.

Mace, G.M., Collar, N.J., Gaston, K.J., Hilton-Taylor, C., Akçakaya, H.R., Leader-Williams, N., *et al.* (2008). Quantification of extinction risk: IUCN's system for classifying threatened species. *Conserv. Biol.*, 22, 1424–1442.

Madin, J.S., Hughes, T.P. & Connolly, S.R. (2012). Calcification, Storm Damage and Population Resilience of Tabular Corals under Climate Change. *PLoS One*, 7, 1–10.

Madin, J.S. & Madin, E.M.P. (2015). The full extent of the global coral reef crisis. *Conserv. Biol.*, 29, 1724–1726.

Maynard, J.A., McKagan, S., Raymundo, L., Johnson, S., Ahmadia, G.N., Johnston, L., *et al.* (2015). Assessing relative resilience potential of coral reefs to inform management. *Biol. Conserv.*, 192, 109–119.

McDonald, J.L., Franco, M., Townley, S., Ezard, T.H.G., Jelbert, K. & Hodgson, D.J. (2017). Divergent demographic strategies of plants in variable environments. *Nat. Ecol. Evol.*, 1, 1–6.

McDonald, J.L., Stott, I., Townley, S. & Hodgson, D.J. (2016). Transients drive the demographic dynamics of plant populations in variable environments. *J. Ecol.*, 104, 306–314.

Mcleod, E., Anthony, K.R.N., Mumby, P.J., Maynard, J., Beeden, R., Graham, N.A.J., *et al.* (2019). The future of resilience-based management in coral reef ecosystems. *J. Environ. Manage.*, 233, 291–301.

McLeod, E., Shaver, E.C., Beger, M., Koss, J. & Grimsditch, G. (2021). Using resilience assessments to inform the management and conservation of coral reef ecosystems. *J. Environ. Manage.*, 277, 1–8.

Mercado-Molina, A.E., Ruiz-Diaz, C.P., Pérez, M.E., Rodríguez-Barreras, R. & Sabat, A.M. (2015). Demography of the threatened coral Acropora cervicornis: implications for its management and conservation. *Coral Reefs*, 34, 1113–1124.

Merow, C., Bois, S.T., Allen, J.M., Xie, Y. & Silander, J.A. (2017). Climate change both facilitates and inhibits invasive plant ranges in New England. *Proc. Natl. Acad. Sci.*, 114, 1–9.

Metcalf, C.J.E. & Pavard, S. (2007). Why evolutionary biologists should be demographers. *Trends Ecol. Evol.*, 22, 205–212.

Moberg, F. & Folke, C. (1999). Ecological goods and services of coral reef ecosystems. *Ecol. Econ.*, 29, 215–233.

Montero-Serra, I., Garrabou, J., Doak, D.F., Ledoux, J.B. & Linares, C. (2019). Marine protected areas enhance structural complexity but do not buffer the consequences of ocean warming for an overexploited precious coral. *J. Appl. Ecol.*, 56, 1063–1074.

Morris, W.F. & Doak, D.F. (2002). *Quantitative conservation biology: Theory and practice of population viability analysis*. Sinauer Associates, Inc.

Muir, P., Wallace, C.., Done, T. & Aguirre, J.D. (2015). Limited scope for latitudinal extension of reef corals. *Science*, 348, 1135–1138.

Nyström, M., Folke, C. & Moberg, F. (2000). Coral reef disturbance and resilience in a human-dominated environment. *Trends Ecol. Evol.*, 15, 413–417.

Pandolfi, J.M., Bradbury, R.H., Sala, E., Hughes, T.P., Bjorndal, K.A., Cooke, R.G., *et al.* (2003). Global trajectories of the long-term decline of coral reef ecosystems. *Science*, 301, 955–958.

Pandolfi, J.M., Connolly, S.R., Marshall, D.J. & Cohen, A.L. (2011). Projecting coral reef futures under global warming and ocean acidification. *Science (80-.).*, 333, 418–422.

Park, J.S. (2019). Cyclical environments drive variation in life-history strategies: A general theory of cyclical phenology. *Proc. R. Soc. B Biol. Sci.*, 286, 1–9.

Petchey, O.L., Pontarp, M., Massie, T.M., Kéfi, S., Ozgul, A., Weilenmann, M., *et al.* (2015). The ecological forecast horizon, and examples of its uses and determinants. *Ecol. Lett.*, 18, 597–611.

Pickett, S.T.A. & White, P.S. (1985). *The ecology of natural disturbance and patch dynamics*. Academic Press Inc., San Diego, California.

Pisapia, C., Edmunds, P.J., Moeller, H. V., Riegl, B.M., McWilliam, M., Wells, C.D., *et al.* (2020). Projected shifts in coral size structure in the Anthropocene. In: *Advances in Marine Biology*. Academic Press, pp. 31–60.

Pratchett, M.S., McWilliam, M.J. & Riegl, B. (2020). Contrasting shifts in coral assemblages with increasing disturbances. *Coral Reefs*, 39, 783–793.

Pratchett, M.S., Trapon, M., Berumen, M.L. & Chong-Seng, K. (2011). Recent disturbances augment community shifts in coral assemblages in Moorea, French Polynesia. *Coral Reefs*, 30, 183–193.

Precoda, K., Baird, A.H., Madsen, A., Mizerek, T., Sommer, B., Su, S.N., *et al.* (2018). How does a widespread reef coral maintain a population in an isolated environment? *Mar. Ecol. Prog. Ser.*, 594, 85–94.

Ramula, S., Rees, M. & Buckley, Y.M. (2009). Integral projection models perform better for small demographic data sets than matrix population models: A case study of two perennial herbs. *J. Appl. Ecol.*, 46, 1048–1053.

Rastrick, S.S.P., Graham, H., Azetsu-Scott, K., Calosi, P., Chierici, M., Fransson, A., *et al.* (2018). Using natural analogues to investigate the effects of climate change and ocean acidification on Northern ecosystems. *ICES J. Mar. Sci.*, 75, 2299–2311.

Reguero, B.G., Storlazzi, C.D., Gibbs, A.E., Shope, J.B., Cole, A.D., Cumming, K.A., *et al.* (2021). The value of US coral reefs for flood risk reduction. *Nat. Sustain.*, 1–11.

Riegl, B., Bruckner, A., Coles, S.L., Renaud, P. & Dodge, R.E. (2009). Coral reefs: Threats and conservation in an era of global change. *Ann. N. Y. Acad. Sci.*, 1162, 136–186.

Riegl, B., Johnston, M., Purkis, S., Howells, E., Burt, J., Steiner, S.C.C., *et al.* (2018). Population collapse dynamics in Acropora downingi, an Arabian/Persian Gulf ecosystem-engineering coral, linked to rising temperature. *Glob. Chang. Biol.*, 24, 2447–2462.

Riegl, B.M. (2020). The population dynamics of the coral reef crisis—Prologue. In: *Population Dynamics of the Reef Crisis*, Advances in Marine Biology (ed. Riegl, B.M.). Academic Press, pp. xxxvii–xi.

Riegl, B.M. & Glynn, P.W. (2020). Population dynamics of the reef crisis: Consequences of the growing human population. *Adv. Mar. Biol.*, 87, 1–30.

Roche, R.C., Williams, G.J. & Turner, J.R. (2018). Towards developing a mechanistic understanding of coral reef resilience to thermal stress across multiple scales. *Curr. Clim. Chang. Reports*, 4, 51–64.

Salguero-Gómez, R. & Casper, B.B. (2010). Keeping plant shrinkage in the demographic loop. *J. Ecol.*, 98, 312–323.

Salguero-Gómez, R., Jones, O.R., Archer, C.R., Bein, C., de Buhr, H., Farack, C., *et al.* (2016). COMADRE: A global data base of animal demography. *J. Anim. Ecol.*, 85, 371–384.

Salguero-Gómez, R., Jones, O.R., Archer, C.R., Buckley, Y.M., Che-Castaldo, J., Caswell, H., *et al.* (2015). The COMPADRE Plant Matrix Database: An open online repository for plant demography. *J. Ecol.*, 103, 202–218.

Salguero-Gómez, R., Shefferson, R.P. & Hutchings, M.J. (2013). Plants do not count... or do they? New perspectives on the universality of senescence. *J. Ecol.*, 101, 545–554.

Scavo Lord, K., Lesneski, K.C., Bengtsson, Z.A., Kuhn, K.M., Madin, J., Cheung, B., *et al.* (2020). Multi-Year viability of a reef coral population living on mangrove roots suggests an important role for mangroves in the broader habitat mosaic of corals. *Front. Mar. Sci.*, 7, 1–16.

Selig, E.R. & Bruno, J.F. (2010). A global analysis of the effectiveness of marine protected areas in preventing coral loss. *PLoS One*, 5, 1–7.

Sommer, B., Harrison, P.L., Beger, M. & Pandolfi, J.M. (2014). Trait-mediated environmental filtering drives assembly at biogeographic transition zones. *Ecology*, 95, 1000–1009.

Sommer, B., Sampayo, E.M., Beger, M., Harrison, P.L., Babcock, R.C. & Pandolfi, J.M. (2017). Local and regional controls of phylogenetic structure at the high-latitude range limits of corals. *Proc. R. Soc. Biol. Sci. Ser. B*, 284, 1–13.

Spalding, M., Burke, L., Wood, S.A., Ashpole, J., Hutchison, J. & zu Ermgassen, P. (2017). Mapping the global value and distribution of coral reef tourism. *Mar. Policy*, 82, 104–113.

Spalding, M.D., Corinna, R. & Green, E.P. (2001). *World Atlas of Coral Reefs*. University of California Press.

Stott, I. (2016). Perturbation analysis of transient population dynamics using matrix projection models. *Methods Ecol. Evol.*, 7, 666–678.

Stott, I., Franco, M., Carslake, D., Townley, S. & Hodgson, D. (2010). Boom or bust? A comparative analysis of transient population dynamics in plants. *J. Ecol.*, 98, 302–311.

Stott, I., Hodgson, D.J. & Townley, S. (2012). Popdemo: An R package for population demography using projection matrix analysis. *Methods Ecol. Evol.*, 3, 797–802.

Stott, I., Townley, S. & Hodgson, D. (2011). A framework for studying transient dynamics of population projection matrix models. *Ecol. Lett.*, 14, 959–970.

Sully, S., Burkepile, D.E., Donovan, M.K., Hodgson, G. & van Woesik, R. (2019). A global analysis of coral bleaching over the past two decades. *Nat. Commun.*, 10, 1–5.

Teh, L.S.L., Teh, L.C.L. & Sumaila, U.R. (2013). A global estimate of the number of coral reef fishers. *PLoS One*, 8, 1–10.

Thornton, P.K., Ericksen, P.J., Herrero, M. & Challinor, A.J. (2014). Climate variability and vulnerability to climate change: A review. *Glob. Chang. Biol.*, 20, 3313–3328.

van Tienderen, P.H. (2000). Elasticities and the link between demographic and evolutionary dynamics. *Ecology*, 81, 666–679.

Townley, S., Carslake, D., Kellie-Smith, O., Mccarthy, D. & Hodgson, D. (2007). Predicting transient amplification in perturbed ecological systems. *J. Appl. Ecol.*, 44.

Townley, S. & Hodgson, D.J. (2008). Erratum et addendum: Transient amplification and attenuation in stage-structured population dynamics. *J. Appl. Ecol.*, 45, 1836–1839.

Tuljapurkar, S. (1989). An uncertain life: Demography in random environments. *Theor. Popul. Biol.*, 35, 227–294.

Tuljapurkar, S.D. & Orzack, S.H. (1980). Population dynamics in variable environments I. Long-run growth rates and extinction. *Theor. Popul. Biol.*, 18, 314–342.

Turner, M.G. (2010). Disturbance and landscape dynamics in a changing world. *Ecology*, 91, 1–17.

Vardi, T., Williams, D.E. & Sandin, S.A. (2012). Population dynamics of threatened elkhorn coral in the northern Florida Keys, USA. *Endanger. Species Res.*, 19, 157–169.

Vergés, A., McCosker, E., Mayer-Pinto, M., Coleman, M.A., Wernberg, T., Ainsworth, T., *et al.* (2019). Tropicalisation of temperate reefs: Implications for ecosystem functions and management actions. *Funct. Ecol.*, 1–14.

Wilkinson, C. (2008). *Status of coral reefs of the world: 2008*. Townsville, Australia.

Williams, J.L., Ellis, M.M., Bricker, M.C., Brodie, J.F. & Parsons, E.W. (2011). Distance to stable stage distribution in plant populations and implications for near-term population projections. *J. Ecol.*, 99, 1171–1178.

Williams, J.W., Jackson, S.T., Kutzbach, J.E. & Schneider, S.H. (2007). Projected distributions of novel and disappearing climates by 2100 AD. *Proc. Natl. Acad. Sci.*, 104, 5738–5742.

Wilson, S.K., Fisher, R., Pratchett, M.S., Graham, N.A.J., Dulvy, N.K., Turner, R.A., *et al.* (2008). Exploitation and habitat degradation as agents of change within coral reef fish communities. *Glob. Chang. Biol.*, 14, 2796–2809.

Wolff, N.H., Mumby, P.J., Devlin, M. & Anthony, K.R.N. (2018). Vulnerability of the Great Barrier Reef to climate change and local pressures. *Glob. Chang. Biol.*, 24, 1978–1991.

Wolkovich, E.M., Cook, B.I., McLauchlan, K.K. & Davies, T.J. (2014). Temporal ecology in the Anthropocene. *Ecol. Lett.*, 17, 1365–1379.

Yamano, H., Sugihara, K., Watanabe, T., Shimamura, M. & Hyeong, K. (2012). Coral reefs at 34°N, Japan: Exploring the end of environmental gradients. *Geology*, 40, 835–838.

Zychaluk, K., Bruno, J.F., Clancy, D., McClanahan, T.R. & Spencer, M. (2012). Data-driven models for regional coral-reef dynamics. *Ecol. Lett.*, 15, 151–158.

Chapter 1

Evolutionary processes, not environmental drivers, determine demographic resilience

James Cant[1, *], Pol Capdevila[2,3], Maria Beger[1,4], and Roberto Salguero-Gómez[2, 4, 5]

1. School of Biology, Faculty of Biological Sciences, University of Leeds, Leeds, LS2 9JT United Kingdom.
2. Department of Zoology, University of Oxford, Oxford, 11a Mansfield Rd, OX1 3SZ United Kingdom.
3. School of Biological Sciences, University of Bristol, 24 Tyndall Ave, BS8 1TQ, Bristol, UK.
4. Centre for Biodiversity and Conservation Science, School of Biological Sciences, University of Queensland, Brisbane, QLD, 4072 Australia.
5. Max Planck Institute for Demographic Research, Konrad Zuße Straße 1, 18057 Rostock, Germany.

In preparation for Nature Ecology & Evolution

Evolutionary processes, not environmental drivers, determine demographic resilience

2.1. Abstract

Our capacity to forecast the persistence of natural populations despite climatic change is impeded by our limited understanding for how environmental stochasticity shapes the resilience of natural populations to disturbances. Here, we explore variation across different dimensions of resilience in 2,242 populations of 369 terrestrial and aquatic animal and plant species from diverse climate regimes. We hypothesised that the mechanisms shaping the ability for populations to resist, recover, and, occasionally, benefit from disturbances are defined by local environmental regimes. Unexpectedly, however, recent-past climatic disturbance regimes do not correlate with the short-term dynamics of natural populations. Instead, our analyses reveal a strong evolutionary component to population resilience, and the key role played by individual survival and development patterns in shaping population responses to disturbance. We conclude that recent exposure to environmental stochasticity does not guarantee the resilience of populations to the future intensification of abiotic disturbances. Rather, the capacity for populations to endure future climatic change is determined by their evolutionary history.

2.2. Introduction

Identifying the determinants of population resilience is of paramount importance in conservation biology (Standish *et al.* 2014; Angeler & Allen 2016). Resilience comprises the capacity for systems to resist and recover from disturbances (Holling 1973), factors that push systems away from their stationary equilibrium. In reality though, resilience is beset by the often conflicting attributes of stability, exposure, resistance, persistence, recovery, and robustness (Donohue *et al.* 2013, 2016; Hodgson *et al.* 2015; Ingrisch & Bahn 2018). Complex interactions between the dynamics of populations and the biotic and abiotic features of their local environments then serve to further obscure the mechanistic drivers underpinning their resilience attributes

(Benton *et al.* 2006; Paniw *et al.* 2021). Predicting the resilience of ecological systems, therefore, remains controversial (Standish *et al.* 2014) and challenging (Kéfi *et al.* 2019). Yet, with climate change disrupting seasonal abiotic patterns and exposing populations worldwide to unprecedented environmental stochasticity (Thornton *et al.* 2014; Paniw *et al.* 2019; Cordes *et al.* 2020), forecasting the future performance and viability of natural populations requires an explicit consideration for the drivers mediating their resilience to repeated disturbances (Park 2019).

The response of populations following disturbances can be explored through their short-term (*i.e.*, transient) dynamics (Ezard *et al.* 2010). In stable environments, the long-term performance of a population is reflected in its long-term (*i.e.*, asymptotic) dynamics (Caswell 2001). Within unstable environments, however, disturbances regularly perturb the structure of populations, forcing them into a transient phase during which their dynamics can vary considerably from their stable asymptotic trajectories (Hastings 2004; Koons *et al.* 2005; Fig. 2.1). The exact duration and form of this transient phase depends on the form of disturbance, as well as a populations' resilience attributes of recovery and demographic stability. Here, *recovery* constitutes the time taken for populations to converge back to a stationary equilibrium following disturbance, whilst demographic stability encompasses two further attributes: (1) *resistance*, the ability to oppose change following a disturbance by avoiding declines/attenuation in population size, and (2) *compensation*, the extent to which a population expands following a disturbance through increases/amplification in population size (Hodgson *et al.* 2015; Capdevila *et al.* 2020b). Quantifying these transient dynamics provides insight into the inherent ability for populations to be displaced (or not) from their stable state, and the time then needed for reobtaining an equilibrate structure (Koons *et al.* 2005; Stott *et al.* 2011). Thus, transient dynamics present an ideal framework for evaluating the resilience of populations to repeated disturbances (Stott *et al.* 2011; Capdevila *et al.* 2020b). Indeed, transient characteristics have recently been found to promote the persistence of populations within variable, and suboptimal, environments (Ellis & Crone 2013; McDonald *et al.* 2016). Yet, for this understanding to inform future resilience-based management, we require a deeper understanding for the drivers of the transient responses of populations within stochastic environments (Francis *et al.* 2021).

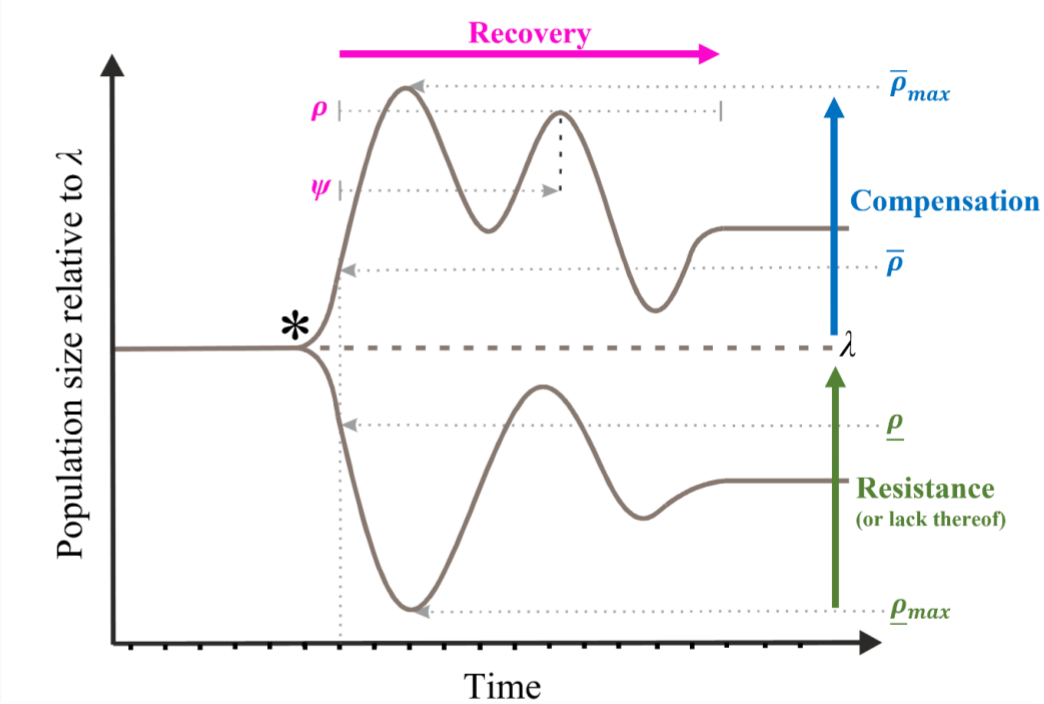

Figure 2.1. Within variable environments the dynamics of populations can vary considerably from long-term (*i.e.*, asymptotic) expectations. Under stable conditions, populations display asymptotic growth trajectories whereby the size of a population changes at a constant rate (λ). However, following a disturbance (*), populations enter a transient state during which their growth rate can change unexpectedly from asymptotic expectations. The development of transient demographic theory offers the opportunity for quantifying these short-term dynamics of populations, thus unlocking the potential for comparative studies exploring patterns in demographic resilience. Transient increases in population size (*compensation*) can be evaluated using metrics of population reactivity ($\overline{\rho}$; increase in growth size within one time step following perturbation) and maximal amplification ($\overline{\rho}_{max}$; maximum increase in size during transient period). Equally, the magnitude of transient declines in population size (*resistance*), can be assessed using the metrics of first-step attenuation ($\underline{\rho}$; decrease in size within one time step following perturbation) and maximal attenuation ($\underline{\rho}_{max}$; maximum decrease in size during transient period). Finally, the damping ratio (ρ; rate of convergence back to stability), and period of oscillation (ψ; time between corresponding phases of the largest oscillatory cycle in

population size) of populations offer insights into their capacity to *recover* back to a stable equilibrium.

Climate drivers shape population performance (Compagnoni *et al.* 2021). It is logical, therefore, that the current ability of individuals for responding to disturbances has been shaped by disturbance regimes they have experienced in the past (Boyd *et al.* 2016; Walker 2020). Indeed, coral individuals inhabiting coastal lagoons that experience daily variability in thermal regimes, display fewer symptoms of thermal shock when exposed to heat stress in comparison with individuals from more stable environments (Oliver & Palumbi 2011). Natural selection acts upon the inheritable traits of individuals, imposing selection pressures that, over time, result in evolutionary change (Lande & Arnold 1983). Thus, exploring patterns in trait variation can offer insights into how selection pressures define population characteristics (Horvitz *et al.* 2018). For instance, it is now well known that individuals operate under a strong trade-off that regulates investments in survival vs. reproduction to maximise the long-term performance of their population (Stearns 1989, 1992). Research into these trade-offs has shown how life-history traits (*i.e.,* key events along the life cycle of an organism such as age at maturity) can be effectively coordinated along two key axes of variation: the fast-slow continuum (Promislow & Harvey 1990; Stearns 1992), and the reproductive parity continuum (Gaillard *et al.* 1989; Salguero-Gómez *et al.* 2016b; Rüger *et al.* 2018). Together, these two continua reflect how life-history variation is constrained by respective trade-offs between survival and somatic development (*i.e.,* growth), and semelparous (*i.e.,* one reproductive episode) and iteroparous (*i.e.,* multiple reproductive cycles) reproductive schedules (Stearns 1983, 1989, 1992; Gaillard *et al.* 1989; Salguero-Gómez *et al.* 2016b; Paniw *et al.* 2018; Healy *et al.* 2019).

Within stochastic environments, recurrent disturbances reshape optimum population characteristics by modifying the existing trade-off profiles between the fitness components of individuals (Park 2019). The vital rates of survival, progression (e.g. growth, development), retrogression (e.g. shrinkage [Salguero-Gómez & Casper 2010], rejuvenation [Salguero-Gómez *et al.* 2013]), and reproduction describe how fitness trade-offs at the individual-level translate into population characteristics (van

Tienderen 1995; Metcalf & Pavard 2007). How these vital rates manifest across life cycles then underpins not only the long-term performance of populations (Groenendael *et al.* 1988; Caswell 2001), but also their transient dynamics (Fox & Gurevitch 2000; Caswell 2001). Subsequently, vital rates provide an explicit link between individual-level fitness and population characteristics (van Tienderen 2000), such as their attributes of recovery, resistance, and compensation. Therefore, by examining the sources of variation in resilience attributes across gradients in environmental stochasticity, we can investigate the determinants mediating population resilience.

To evaluate drivers of population resilience, we calculate the resilience attributes of recovery, resistance, and compensation in 2,242 natural populations, across 61 animal, 305 plant, and 3 algae species using the COMPADRE (Salguero-Gómez *et al.* 2015) and COMADRE (Salguero-Gómez *et al.* 2016a) databases (Appendix 1.1 & 1.2; Table S1.1 & Fig. S1.1). We explore how patterns within these resilience attributes correspond with the relative exposure of populations to environmental stochasticity across a 50-year period. Specifically, with frequently perturbed populations often displaced further from their stable state (Hastings *et al.* 2018), we hypothesise that exposure to a higher frequency in stochastic oscillations will select for enhanced recovery. By contrast, we anticipate that broader spectra in environmental conditions will select for transient responses maximising demographic stability (*i.e.*, resistance and compensation). We also expect that these potential effects of environmental stochasticity on the resilience attributes of populations will manifest through the underlying fitness components of their individuals (Metcalf & Pavard 2007). Concurrently, we also apply sensitivity analyses to assess how environmental stochasticity mediates trade-offs between survival, development, and reproduction to determine the resilience attributes of populations (van Tienderen 2000). Overall, we provide a detailed insight into the determinants of population resilience that will inform predictions into the future continuity of biodiversity.

2.3. Methods

2.3.1. Demographic data extraction & transient indices

To evaluate the selection pressures on the resilience attributes of natural populations, we extracted Matrix Population Models (MPMs) from the open-source COMPADRE

Plant Matrix Database (v. 5.0.1; Salguero-Gómez *et al.* 2015) and COMADRE Animal Matrix Database (v. 3.0.1; Salguero-Gómez *et al.* 2016a). MPMs are discrete time, structured population models where the lifecycle is categorised into discrete state classes (*i.e.*, age, size, and/or developmental stages [Caswell 2001]). Combined, COMPADRE and COMADRE contain over 12,000 MPMs from more than 1,100 animal and plant species. However, here we only retained MPMs satisfying the following six criteria to test our hypotheses: (1) MPMs reflecting the demographic characteristics of individual populations recorded across a single time period (*individual* MPMs). We did, however, select MPMs consisting of demographic information averaged across multiple populations and/or time periods (*mean* MPMs), for populations for which no individual matrices were available (330 populations after applying the additional criteria below); (2) MPMs based on annual surveys to ensure all subsequent metrics obtained reflected identical units of time, thus allowing for their comparability; (3) MPMs representing wild, un-manipulated populations, to guarantee investigating the selection pressures underpinning the resilience of natural populations and the possibility to link their dynamics to their local environmental regimes; (4) MPMs comprised of three or more life stages, as lower dimension MPMs typically lack the necessary resolution for estimating vital rates (Salguero-Gómez & Plotkin 2010) and transient dynamics (Tenhumberg *et al.* 2009); (5) MPMs from populations with known latitude and longitude information to allow us to link their demographic properties to local environmental regimes; and finally (6) MPMs describing full life cycles (e.g., no missing data on survival, progression, retrogression, and reproduction) to ensure the correct calculation of vital rates and transient metrics. Following these criteria, we retained 3,890 MPMs corresponding with 3,204 populations across 441 plant species, 665 populations across 113 animal species, and 21 populations across six algae species (Appendix 1.1; Table S1.1).

We further refined our list of MPMs according to their transient, asymptotic, and species-specific properties. All MPMs were tested for irreducibility (*i.e.*, all life cycle stages are either directly, or indirectly connected to one another), ergodicity (*i.e.*, asymptotic dynamics are independent of the initial population structure), and primitivity (*i.e.*, MPMs consist of non-negative elements [Caswell 2001]). A total of 1,203 reducible, imprimitive, and/or non-ergodic MPMs were excluded from further analyses on the basis that they represent untenable life-cycles that defy logical biological processes (Stott *et al.* 2010). MPMs with population growth rates $\lambda > 2$, indicating that the population is projected to increase two-fold or more every year, were also rejected as they represent unlikely realisations of population performance in our experience. Equally, MPMs from highly migratory (e.g., > 1,000 km) species were discarded, since their vital rate schedules are unlikely to be mostly shaped by the environment in which they were measured. We also note here that, across our initial population sample, the vital rate of clonality (κ) was rare, with only 140 populations across 37 plant species, and two populations from one animal species (*Amphimedon compressa* [Mercado-Molina *et al.* 2011]) explicitly exhibiting this demographic process. Thus, to focus our analyses on common demographic currencies, we excluded all populations exhibiting clonality. Overall, our strict selection criteria resulted in a final sample of 2,242 MPMs, corresponding with 369 species: 402 populations from 61 animal species, 1,830 populations from 305 plant species, and 10 populations from three species of algae (Appendix 1.1; Table S1.1).

For each retained MPM, we calculated six transient metrics quantifying each population's potential for demographic recovery (damping ratio, ρ & period of oscillation, ψ), resistance (first-timestep attenuation, $\underline{\rho}$ & and maximal attenuation, $\underline{\rho}_{max}$), and compensation (reactivity, $\bar{\rho}$ & maximal amplification, $\bar{\rho}_{max}$) following a disturbance (Capdevila *et al.* 2020b; Fig. 2.1). Firstly, with estimates of transient dynamics known to be contingent on the reproductive strategies of populations, it was necessary to convert all post-reproductive matrices into a pre-reproductive format by adjusting patterns of reproduction to include a measure of adult survival (Jelbert *et al.* 2019). All MPMs were then standardised to separate their transient and asymptotic properties by dividing each matrix element by the MPM's dominant eigenvalue, λ (Caswell 2001; Koons *et al.* 2005). Following standardisation, estimates of the aforementioned transient metrics were obtained using the *R* package '*popdemo*' (Stott *et al.* 2012), except the period of oscillation (ψ), which was calculated using the subdominant eigenvalue (λ_2) of each MPM (Caswell 2001)

$$\psi = \frac{2\pi}{\theta_2} \qquad \text{Where: } \theta_2 = \tan^{-1}\left(\frac{I(\lambda_2)}{R(\lambda_2)}\right). \tag{2.1}$$

To explore how the fitness components of individuals mediate the selection gradients placed on demographic resilience by environmental stochasticity, we calculated the sensitivity of each transient metric towards the vital rates of survival

(σ), progression (γ), retrogression (τ), and fecundity (φ). For each MPM, we first estimated all vital rate sensitivities from their element-level constituents. Individual elements a_{ij} within the MPM $\boldsymbol{A}$ typically describe combinations of multiple vital rates (Franco & Silvertown 2004). Subsequently, calculating the sensitivity of each transient metric (s_x) with respect to underlying vital rates requires the decomposition of element-level sensitivities into their vital rate components (Franco & Silvertown 2004). Briefly, this decomposition requires the estimation of stage-specific survival probabilities (σ_j) for each MPM. These estimates of σ_j are then used to determine the proportion of each matrix element a_{ij} corresponding with survival (σ), progression (γ), retrogression (τ), and fecundity (φ; Franco & Silvertown 2004). Accordingly, we initially calculated the sensitivity of each transient metric at the matrix element-level (s_{ij}). The sensitivities of the damping ratio (ρ) and period of oscillation (ψ) were determined as follows, using the real (R) and imaginary (I) components of the element-level sensitivity matrices of the dominant (s_{ij}^1) and subdominant (s_{ij}^2) eigenvalues (Caswell 2001),

$$s_{\rho_{ij}} = \frac{1}{|\lambda_2|}\left(s_{ij}^1 - \frac{\rho}{|\lambda_2|}\left[R\left(s_{ij}^2\right) + I\left(s_{ij}^2\right)\right]\right) \tag{2.2}$$

$$s_{\psi_{ij}} = \frac{-2\pi}{\theta_2|\lambda_2|^2}\left(I\left(s_{ij}^2\right) - R\left(s_{ij}^2\right)\right). \tag{2.3}$$

The sensitivities of reactivity, amplification, and attenuation (s_{ij}) with respect to element a_{ij} were then estimated as the magnitude of change (δ) in each transient metric (x) following a small change (here 0.01) in a_{ij} (Morris & Doak 2002).

$$s_{ij} = \frac{\delta x}{\delta a_{ij}} = \frac{x_{Perturbed} - x_{Original}}{a_{ij}^{Perturbed} - a_{ij}^{Original}} \tag{2.4}$$

The distributions of each transient metric and its corresponding vital rate sensitivities were checked prior to subsequent regression analyses. Across each distribution, outliers, defined as values outside the 95% confidence intervals of the distribution, were omitted. Each distribution was then checked for normality and transformed if necessary. For each transient metric, power transformations (y^x) were used to achieve approximate normality using the Box-Cox transformation functions of the R package '*caret*'(Kuhn 2020) to estimate x. The distributions of damping ratio, period of oscillation, reactivity, and maximal amplification raised negative x values, and so their transformations took the form $1/y^{|x|}$. Inverse and log transformations were also necessary for several of the vital rate sensitivity variables (See Table S1.2 for further details).

2.3.2. Phylogenetic correction

Evaluating the selection pressures exerted on attributes of demographic resilience across multiple species requires an explicit consideration for how traits are expected to covary due to ancestral relationships (Freckleton *et al.* 2002; Freckleton 2009; Revell 2010). To account for such relationships in our analyses, we constructed a population-within-species level phylogenetic tree using taxonomic data extracted from the Open tree of Life (OTL; Hinchliff *et al.* 2015; Appendix 1.4). Our approach here also allowed us to accommodate studies that included multiple, separate populations for the same species (*see below*). Firstly, the scientific names of each species associated with our extracted MPMs were checked against current taxonomy records using the *R* package '*taxize*' (Chamberlain *et al.* 2020). Next, we extracted information regarding the taxonomic classification and phylogeny of each species from the OTL database with the *R* package '*rotl*' (Michonneau *et al.* 2016). Subsequently, using the '*ape*' (Paradis & Schliep 2018) and *'phytools'* packages (Revell 2012), this phylogenetic information was used to construct a species-level phylogenetic tree corresponding with the 369 unique species within our MPM list.

Beyond accounting for phylogenetic signals in trait variance-covariance across our population sample, it was necessary to ensure that our phylogenetic tree reflected the influence of spatial signals in the development of traits within species. Thus, we expanded our phylogenetic tree by adding branch tips to incorporate multiple population entries per species (*sensu* Freckleton & Jetz 2009), generating a population-level tree comprising our full sample of 2,242 populations (Appendix 1.4). Finally, we calculated the branch lengths for our phylogenetic tree using the function *compute.brlen* in the *R* package '*ape*' (Paradis & Schliep 2018). These branch lengths were estimated using Grafen's arbitrary branch lengths (Grafen 1989), assuming a Brownian motion model with the variance between species directly proportional to time since divergence (Revell *et al.* 2008). Importantly, we constrained branch lengths between populations of the same species to approximately zero (0.0000001) under the assumption of negligible phylogenetic distance between species replicate populations.

2.3.3. Quantifying environmental stochasticity

To investigate the role of environmental selection pressures on the compensation, resistance, and recovery attributes of resilience in natural populations, we used a pPLS regression exploring the association between transient characteristics and metrics of environmental stochasticity. We quantified the magnitude and frequency of environmental variation to which each population was exposed using the GPS location information extracted with each MPM from COMPADRE & COMADRE (Appendix 1.5). Since temperature and precipitation rates are universal drivers of biological community assembly across terrestrial environments (Howard *et al.* 2020), we selected data describing temporal trends in thermal and precipitation regimes as a measure of the environmental stochasticity experienced by each population. Crucially, however, with precipitation not directly influencing marine environments (although see Haapkylä *et al.* 2011), we excluded marine populations (29 populations from six animal species, and 10 populations from three algal species) from this portion of our analyses.

We quantified environmental variance through the metrics of autocorrelation, abiotic range, and frequency spectrum using long-term temperature and precipitation records sourced from the CHELSA climate database (Karger *et al.* 2017). For each population, we extracted monthly records of maximum and minimum temperatures (°C) and mean precipitation rates (kg m^{-2}) corresponding with the specific time period during which the population was surveyed as detailed in COMPADRE and COMADRE, plus an additional 50 years prior to the onset of censusing to account for environmental legacy effects (Evers *et al.* 2021). We condensed maximum and minimum temperature readings into monthly estimates of mean temperatures and thermal range. Next, as a gauge of disturbance magnitude (m), we estimated the mean thermal range experienced by each population across their associated temporal records. We then arranged our monthly mean temperature and precipitation estimates into time series depicting the temporal environmental regimes to which each population was exposed. Using the '*colorednoise*' package (Pilowsky 2019), we calculated the autocorrelation of each temperature (a_T) and precipitation (a_P) time series as a measure of environmental predictability (Ruokolainen *et al.* 2009).

The colour of environmental variation is depicted on a red to blue colour scale, from lower to higher frequencies, respectively (Ruokolainen *et al.* 2009). The frequency spectrum of a time series is expressed by its spectral exponent (β), which is calculated as the negative slope of the linear regression between the log spectral density and log frequency of the time series (Vasseur & Yodzis 2004). We calculated the frequency spectrum of each precipitation (β_P) and temperature (β_T) time series as an indicator of the colour of environmental variation experienced by each population (Vasseur & Yodzis 2004). The spectral exponent for each time series was estimated using the spectrum function from the *R* package '*stats'* (*R* Core Team 2019).

2.3.4. Partial Least Squares Regression

We utilised a phylogenetically corrected Partial Least Squares regression (pPLS) framework to test our hypothesis that the resistance, recovery, and compensatory attributes of natural populations correspond with gradients in environmental stochasticity and evaluate how this is mediated by fitness investments. Using a pPLS, we evaluated the relationship between estimates of transient dynamics, and both associated environmental stochasticity regimes and their vital rate sensitivities. The pPLS technique is considered a more powerful comparative tool than other available multivariate regression methods (Carrascal *et al.* 2009), as it simultaneously condenses the variation among numerous predictors whilst maximising the variance explained among response variables. Subsequently, we investigated the selection pressures on the compensation, resistance, and recovery attributes of natural populations, and therefore the capacity for environmental legacies, and vital rate characteristics, to serve as predictors of resilience attributes.

We first applied a phylogenetically corrected Pearson's correlation test and pPLS to analyse the correlation between environmental stochasticity and transient demographic characteristics. This approach enabled us to test for covariation between the transient characteristics of populations and gradients in their exposure to environmental stochasticity. pPLS tests were carried out for each transient measure with the predictor variable set comprised of our five metrics of environmental stochasticity. From each test, we then extracted component scores and loadings, which describe the arrangement of the environmental predictor variables within a multivariate space. We also obtained the percentage variance (*%var*) among the predictors explained by each regression component and the proportion of variance in the transient response variable explained by each component (r^2) to estimate the strength of any association between environmental stochasticity and the transient dynamics of our population sample.

Finally, phylogenetically corrected correlation tests and pPLS analyses were used to examine for patterns between each transient characteristics and its associated vital rate sensitivities. Again, test coefficients (r), component scores, loadings, *%var*, and r^2 values were calculated to quantify the influence of the fitness components of survival, progression, retrogression, and reproduction towards the transient characteristics of natural populations. All pPLS analyses were conducted using the *'pls' R* package (Mevik *et al.* 2019), with modifications included to ensure our analyses accounted for any evolutionary covariance between the sensitivity patterns and transient characteristics of different populations (Revell 2009, 2012; Adams & Felice 2014; Appendix 1.6).

We carried out all pPLS analyses using only complete entries, omitting populations missing estimates for any one variable. However, to provide further clarity regarding any patterns we observed between the transient characteristics of populations and their environmental legacies and vital-rate sensitivities we repeated each analysis twice. During these repeated tests, we first evaluated whether considering the life expectancies of populations influenced any observed patterns (Appendix 1.8). Within a given time period, long-lived species will likely experience fewer generations than shorter-lived species diminishing the relative impact of existing selection pressures on their trait characteristics (Robert *et al.* 2004). Thus, it was necessary to ensure that the inclusion of long-lived species within our population sample did not limit our capacity for exploring environmental selection pressures. We categorised each population within our sample as either long- or short-lived according to their associated mean life expectancy (η_e) calculated from each extracted MPM using the *R* package '*IPMpack*' (Metcalf *et al.* 2013). Next, we repeated our pPLS analyses using only 'short-lived' populations for which $\eta_e \leq 10$ years (n = 1606 populations). This threshold was selected as a balance between maximising the number of generations experienced by populations during the 50-year time series used in calculating environmental legacies and maximising our sample size.

We also repeated our initial analyses with all missing demographic measurements estimated using phylogenetic imputation (Appendix 1.7). We calculated the phylogenetic signal (Pagel's λ [Pagel 1999]) of each transient and sensitivity variable using the *phylosig* function from the '*phytools*' package (Revell 2012). Pagel's λ exists on the scale $0 < \lambda > 1$, with 0 indicating traits have evolved independently of phylogeny, and 1 representing a high phylogenetic signal (Pagel 1999). For any variable exhibiting a strong phylogenetic signal (*i.e.*, Pagel's $\lambda \geq 0.65$), we then imputed all missing values assuming a Brownian motion evolutionary model, before repeating our pPLS analyses.

2.4. Results and Discussion

Frequently, it is assumed that the periodic exposure of systems to disturbance will promote their resilience towards future disturbances (Boyd *et al.* 2016; Rivest *et al.* 2017; Walker 2020). However, we found no evidence that past exposure to environmental stochasticity predicts population resilience. Using phylogenetically corrected partial least squares regression, we explored the relationship between the demographic resilience attributes of natural populations, as defined by their transient dynamics (Fig. 2.1), and their exposure to environmental stochasticity. Indeed, variation across measures of the demographic resilience attributes of recovery, resistance, and compensation does not correspond with patterns in the exposure of populations to environmental stochasticity during the 50-years prior to demographic assessment (Fig. 2.2). Accordingly, this finding suggests that contemporary exposure to varying degrees of environmental stochasticity neither limits nor guarantees the resilience of populations towards future recurrent disturbances.

Instead, we illustrate how the resilience attributes of the examined natural populations are determined by selection pressures acting on their long-term performance. The sensitivities of the transient dynamics across our population sample to underlying vital rates (e.g., survival, reproduction) reveal that the resilience attributes of populations are constrained by the relative energetic investments of their individuals (Fig. 2.3). Estimating the phylogenetic signal within the transient dynamics of our population sample, we further illustrate how patterns in demographic resilience, particularly resistance and compensation, are distinctly coordinated by evolutionary history (Table 2.2). Yet, with attributes of resilience, therefore,

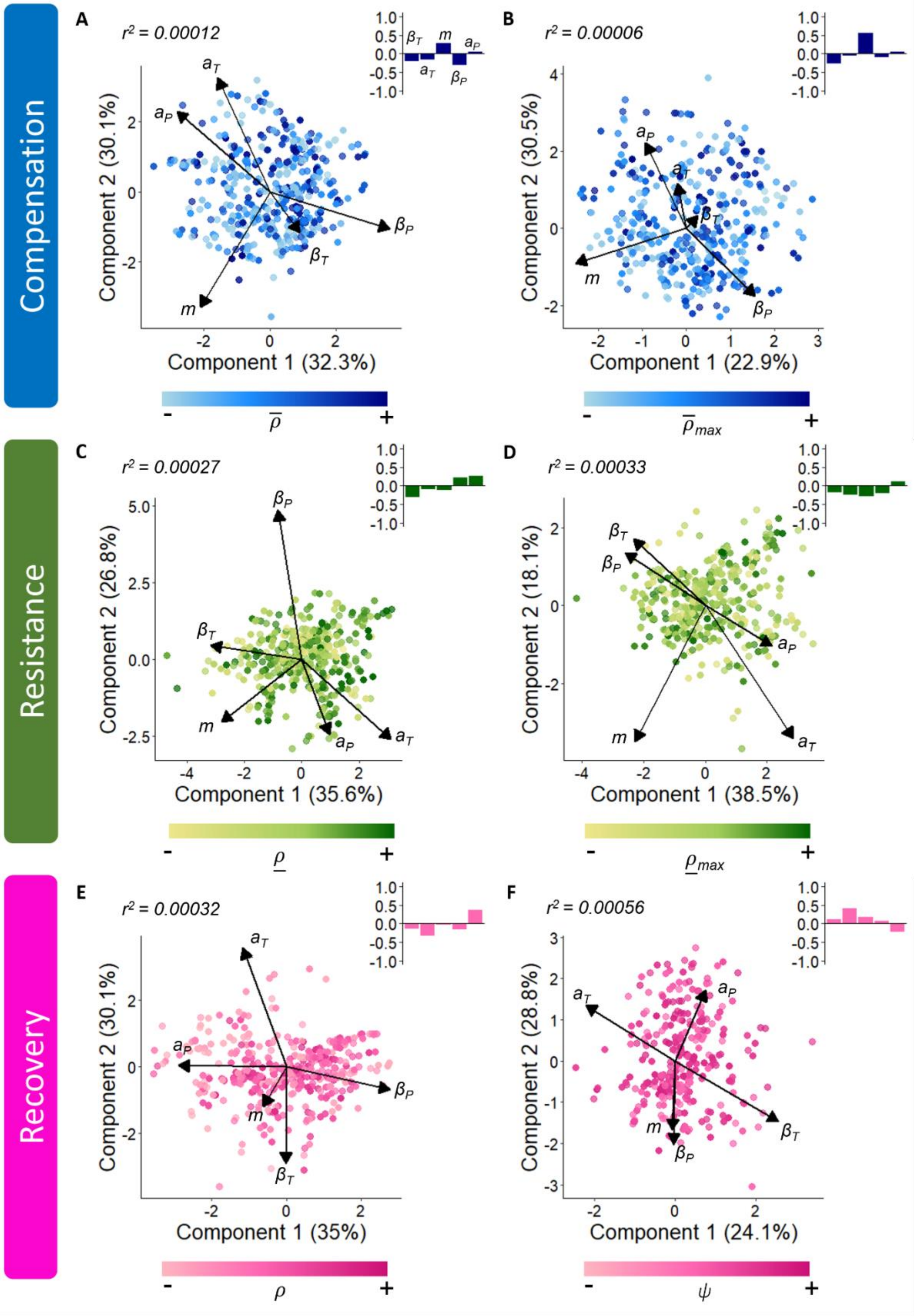
Compensation
Resistance
Recovery
A
$r^2 = 0.00012$
β_T
a_T
m
β_P
a_P
Component 2 (30.1%)
Component 1 (32.3%)
$\overline{\rho}$
B
$r^2 = 0.00006$
Component 2 (30.5%)
Component 1 (22.9%)
$\overline{\rho}_{max}$
C
$r^2 = 0.00027$
Component 2 (26.8%)
Component 1 (35.6%)
$\underline{\rho}$
D
$r^2 = 0.00033$
Component 2 (18.1%)
Component 1 (38.5%)
$\underline{\rho}_{max}$
E
$r^2 = 0.00032$
Component 2 (30.1%)
Component 1 (35%)
ρ
F
$r^2 = 0.00056$
Component 2 (28.8%)
Component 1 (24.1%)
ψ
-
+
1.0
0.5
0.0
-0.5
-1.0

Figure 2.2. Variation across measures of the demographic resilience attributes of compensation (blue), resistance (green), and recovery (pink) does not correspond with patterns in the exposure of populations to environmental stochasticity. Scores and loadings of a phylogenetically-weighted Partial Least Squares regression analysis exploring the correlation between patterns in the variation of the six transient metrics of **(A)** reactivity ($\bar{\rho}$), **(B)** maximal amplification ($\bar{\rho}_{max}$), **(C)** first-step attenuation ($\underline{\rho}$), **(D)** maximal attenuation ($\underline{\rho}_{max}$), **(E)** damping ratio (ρ), and **(F)** period of oscillation (ψ), and the five metrics of environmental stochasticity: temperature frequency spectrum (β_T), temperature autocorrelation (a_T), thermal range/magnitude (m), precipitation frequency spectrum (β_P), and precipitation autocorrelation (a_P). Colour gradation reflects the relative magnitude of each transient metric recorded from each population, with darker shades indicating higher estimates. Associated bar plots are the standardised regression coefficients (b) highlighting the relative weighting of each abiotic variable in the overall capacity of each model to explain variation within each transient metric (r^2).

developing irrespective of a populations' recent exposure to environmental variability, these characteristics of resilience may undermine the capacity for many populations to endure future increases in environmental stochasticity.

2.4.1. Limited environmental regulation of demographic resilience

None of our measures of environmental stochasticity consistently predicted patterns across population resilience (Fig. 2.2), a finding that was insensitive to phylogenetic imputation (Fig. S1.4), and population longevity (Fig. S1.6). We used six transient metrics to quantify the attributes of compensation (reactivity, $\bar{\rho}$ & maximal amplification, $\bar{\rho}_{max}$), resistance (first-step attenuation, $\underline{\rho}$ & maximal attenuation, $\underline{\rho}_{max}$), and recovery (damping ratio, ρ & period of oscillation, ψ) in populations following disturbance (Caswell 2001; Stott *et al.* 2011; Capdevila *et al.* 2020b; Fig. 2.1). Next, we calculated the exposure of populations to environmental stochasticity using measures of mean thermal range [m], and the spectral frequency and autocorrelation of temperature [β_T & a_T] and precipitation [β_P & a_P] regimes during the 50 years preceding each study. To evaluate the selection pressures placed on the resilience attributes of populations by environmental stochasticity, we then performed a pPLS exploring the coordination between our demographic and abiotic variables. Overall, we report little association between the six transient metrics and our measures of environmental stochasticity (r^2 <0.001; Fig. 2.2). This limited association between demographic resilience and environmental stochasticity is further reflected in a phylogenetically corrected Pearson's test of correlation between each transient metric and estimates of the frequency and magnitude of environmental stochasticity ($|r| < 0.015$; Table 2.1).

Table 2.1. Patterns across the resilience attributes of compensation (blue), resistance (green), and recovery (pink) of natural populations do not correlate with their relative exposure to environmental stochasticity. Using a phylogenetically-corrected Pearson's test of correlation, we explored the association between transient metrics of demographic compensation (reactivity, $\bar{\rho}$ & maximal amplification, $\bar{\rho}_{max}$), resistance (first-timestep attenuation, $\underline{\rho}$ & and maximal attenuation, $\underline{\rho}_{max}$), and recovery (damping ratio, ρ & period of oscillation, ψ) and five metrics of environmental stochasticity: temperature frequency spectrum (β_T), temperature autocorrelation (a_T), thermal range (m), precipitation frequency spectrum (β_P), and precipitation autocorrelation (a_P). Correlation displayed using Pearson's correlation coefficient (r).

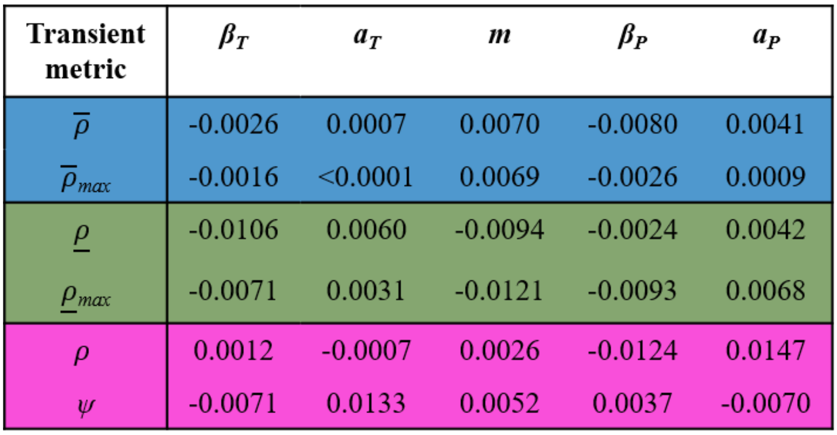

Transient metric	β_T	a_T	m	β_P	a_P
$\bar{\rho}$	-0.0026	0.0007	0.0070	-0.0080	0.0041
$\bar{\rho}_{max}$	-0.0016	<0.0001	0.0069	-0.0026	0.0009
$\underline{\rho}$	-0.0106	0.0060	-0.0094	-0.0024	0.0042
$\underline{\rho}_{max}$	-0.0071	0.0031	-0.0121	-0.0093	0.0068
ρ	0.0012	-0.0007	0.0026	-0.0124	0.0147
ψ	-0.0071	0.0133	0.0052	0.0037	-0.0070

Our findings, here, warn that past exposure to environmental stochasticity does not ensure the continued resilience of populations to increasingly frequent disturbances. Increased exposure to disturbances can filter out vulnerable individuals,

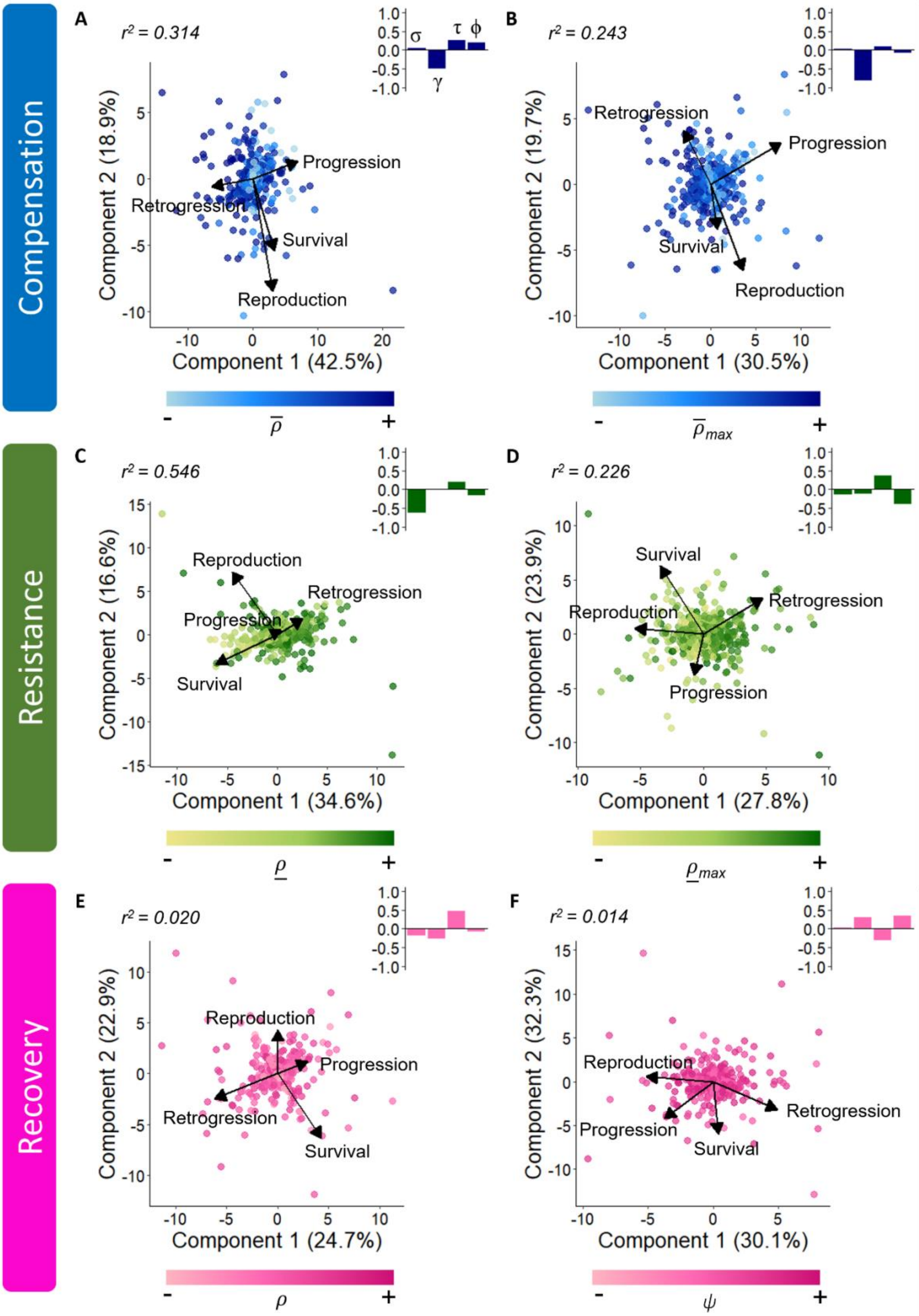
Compensation
Resistance
Recovery
A
$r^2 = 0.314$
σ
γ
τ
ϕ
1.0
0.5
0.0
-0.5
-1.0
Progression
Retrogression
Survival
Reproduction
Component 2 (18.9%)
Component 1 (42.5%)
$\bar{\rho}$
-
+
B
$r^2 = 0.243$
Retrogression
Progression
Survival
Reproduction
Component 2 (19.7%)
Component 1 (30.5%)
$\bar{\rho}_{max}$
C
$r^2 = 0.546$
Reproduction
Retrogression
Progression
Survival
Component 2 (16.6%)
Component 1 (34.6%)
$\underline{\rho}$
D
$r^2 = 0.226$
Survival
Reproduction
Retrogression
Progression
Component 2 (23.9%)
Component 1 (27.8%)
$\underline{\rho}_{max}$
E
$r^2 = 0.020$
Reproduction
Progression
Retrogression
Survival
Component 2 (22.9%)
Component 1 (24.7%)
ρ
F
$r^2 = 0.014$
Reproduction
Retrogression
Progression
Survival
Component 2 (32.3%)
Component 1 (30.1%)
ψ

Figure 2.3. The resilience attributes of compensation (blue), resistance (green), and recovery (pink) in natural populations are determined by the relative energetic investments of their individuals. Scores and loadings of a phylogenetically weighted Partial Least Squares regression analysis exploring the sensitivity patterns of the six transient metrics of **(A)** reactivity ($\bar{\rho}$), **(B)** maximal amplification ($\bar{\rho}_{max}$), **(C)** first-step attenuation ($\underline{\rho}$), **(D)** maximal attenuation ($\underline{\rho}_{max}$), **(E)** damping ratio (ρ), and **(F)** period of oscillation (ψ), towards the vital rates of survival (σ), progression (γ), retrogression (τ), and reproduction (ϕ). Colour gradation reflects the magnitude of each transient metric estimated for each population, with darker shades indicating higher estimates. Associated bar plots are the standardised regression coefficients (b) highlighting the relative weighting of each vital rate in the overall capacity of each model to explain variation within each transient metric (r^2).

thereby cultivating populations capable of successfully navigating further disturbances (Betts *et al.* 2019). Populations and ecosystems in variable environments, or those having overcome past extreme disturbance events, are often regarded as refuges and considered more resilient to future climatic stress (Camp *et al.* 2018; Darling & Côté 2018). Simultaneously, however, frequent and repeated disturbances can quickly exceed the recovery potential of populations, diminishing their resilience over time and pushing them towards ecological tipping points (Oliveras & Malhi 2016; van de Leemput *et al.* 2018). These contradictory observations of the localised influence of stochasticity regimes on the resilience of populations agree with our broader findings that local environmental stochasticity does not directly influence population resilience.

Caution is necessary when interpreting our findings regarding the selection pressures maintained by environmental stochasticity. Our exploration into the environmental drivers of demographic resilience focuses only on terrestrial populations. Marine species typically inhabit conditions close to their physiological limits, making them sensitive to abiotic shifts (Paniw *et al.* 2018; Blowes *et al.* 2019). Conversely, physiological adaptations such as thermoregulation, and the ability to seek out tolerable microclimates, affords terrestrial populations with broader abiotic margins thus reducing their susceptibility to environmental stochasticity (Blowes *et al.* 2019). More crucially, however, quantifying abiotic exposure is contingent on the time-scale under consideration, with shorter timeseries providing lower resolution (Gilljam *et al.* 2019).

Table 2.2. A strong phylogenetic signal exists across the resilience attributes of compensation (blue), resistance (green), and recovery (pink) in natural populations. However, whilst a strong signal is also evident across the vital rate sensitivities of measures of compensation and resistance, there is a negligible signal across the vital rate sensitivities of measures of demographic recovery. To quantify the strength of statistical non-independence in the resilience attributes of natural populations due to common ancestry, we estimated the phylogenetic signal (Pagel's λ[65]) across our transient metrics of demographic compensation (reactivity, $\bar{\rho}$ & maximal amplification, $\bar{\rho}_{max}$), resistance (first-timestep attenuation, $\underline{\rho}$ & and maximal attenuation, $\underline{\rho}_{max}$), and recovery (damping ratio, ρ & period of oscillation, ψ), as well as their sensitivities to the vital rates of survival (σ), progression (γ), retrogression (τ), and reproduction (ϕ). Pagel's λ[65] ranges between 0, indicating that traits have evolved independently of phylogeny, and 1, representing a high phylogenetic signal. Colour gradation highlights the relative strength of the phylogenetic signal across each transient metric and its vital rate sensitivities, with darker shades representing stronger signals.

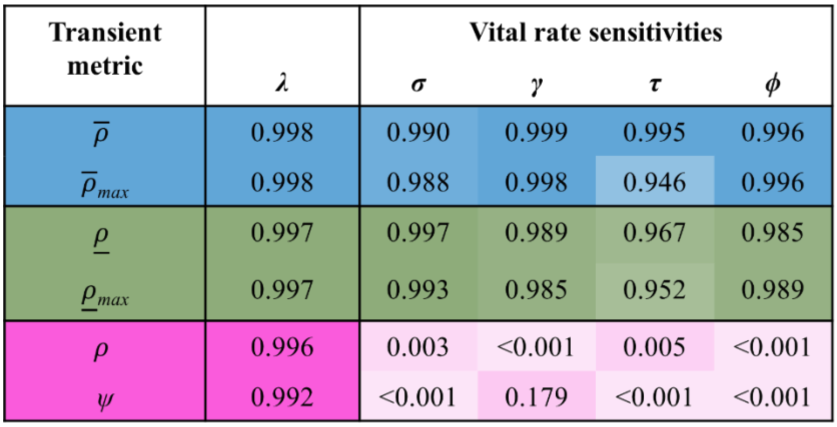

Transient metric		**Vital rate sensitivities**			
	λ	σ	γ	τ	ϕ
$\bar{\rho}$	0.998	0.990	0.999	0.995	0.996
$\bar{\rho}_{max}$	0.998	0.988	0.998	0.946	0.996
$\underline{\rho}$	0.997	0.997	0.989	0.967	0.985
$\underline{\rho}_{max}$	0.997	0.993	0.985	0.952	0.989
ρ	0.996	0.003	<0.001	0.005	<0.001
ψ	0.992	<0.001	0.179	<0.001	<0.001

Using abiotic records covering the 50 years prior to demographic census, we illustrate how recent-past exposure to environmental stochasticity does not predict demographic resilience. Yet, it is entirely plausible that deeper-time environmental stochasticity regimes offer greater predictive potential. Whilst environmental stochasticity is known to influence population dynamics (Lande *et al.* 2003), its observable effects on population characteristics can remain negligible until compounded by external factors such as changing habitat configurations (Fraterrigo *et al.* 2009). Any direct impacts of stochasticity on the resilience attributes of natural populations may, therefore, become detectable overtime. Accordingly, our appreciation for the abiotic determinants of resilience would likely benefit from an understanding for the historical climate legacies of populations, although sourcing climatic records at the necessary temporal and spatial resolution presents a considerable challenge (Kwiatkowski *et al.* 2014; Dixon *et al.* 2021). Meanwhile, the challenges associated with evaluating the historical climate legacies of populations ensure that the susceptibility of species to future climatic change is often inferred from their contemporary abiotic exposure (Foden *et al.* 2019). Thus, it is still worthwhile to highlight the limitations for using the recent exposure of populations to environmental stochasticity in predicting their resilience to future climatic change.

2.4.2. Indirect selection and population resilience

The responses of populations towards climatic drivers are often the consequence of covariation across numerous demographic properties compelled by interactions between biotic and abiotic drivers (Benton *et al.* 2006; Urban *et al.* 2016). To investigate how investment patterns across the fitness components of individuals underpin the resilience of their populations, we calculated the sensitivities of our six transient metrics towards each of the vital rates of survival (σ), progression (γ), retrogression (τ), and fecundity (φ). These vital rate sensitivities reflect how much each transient metric changes following an infinitesimally small change in each vital rate (de Kroon *et al.* 1986, 2000; Caswell 2001). Thus, these sensitivities highlight how investments into any one vital rate influences a populations' capacity to compensate, resist, or recover following disturbances, providing a measure of the absolute importance of each vital rate in shaping demographic resilience. We focused on sensitivities here, rather than elasticities (proportional sensitivities (de Kroon *et al.* 2000)), as they provide a closer representation of selection gradients (van Tienderen 2000).

Overall, selection gradients across the fitness investments of individuals display greater predictive capacity for the resilience attributes of populations than environmental stochasticity, particularly compensation and resistance (Fig. 2.3). Crucially, these findings are insensitive to phylogenetic imputation (Appendix 1.7; Fig. S1.5), and correspond with a strong phylogenetic signal (*i.e.*, Pagels $\lambda > 0.94$) detected across the transient metrics of reactivity, maximal amplification, first-timestep attenuation, maximal attenuation, and their vital rate sensitivities (Table 2.2). A phylogenetic signal reflects the proportion of variation in a trait that can be explained using evolutionary history, and represents the extent to which evolution refines the expression of population traits (Pagel 1999; Freckleton *et al.* 2002). That the resilience attributes of populations have evolved regardless of whether or not populations need to endure frequent disturbances is indicative of indirect selection. Indirect selection occurs when selective forces operate simultaneously on multiple trait characteristics (Lande 1979; Lande & Arnold 1983; Conner 2001). In the event that population characteristics are contingent on similar underlying mechanisms, directional selection can promote covariance across a combination of trait characteristics (Lande & Arnold 1983). Accordingly, non-adaptive and maladaptive trait characteristics can appear contrary to expected selection pressures due to responses driven by selective forces acting upon other trait characteristics (Lande 1979).

We observe that demographic compensation displays a strong sensitivity towards individual-level growth and development patterns. Reactivity and maximal amplification are negatively correlated with the vital rate of progression (Fig. 2.3A & B), such that faster development at the individual-level corresponds with reduced reactivity (r: σ = -0.11, γ = -0.49, τ = 0.39, ϕ = -0.04) and maximal amplification (r: σ = -0.02, γ = -0.49, τ = -0.13, ϕ = -0.14). Populations of fast growing individuals typically exhibit shorter generation times, enabling them to possess the high turnover rates needed to rapidly colonise new environments (Gaillard *et al.* 2005). However, the development of fast-growth strategies also suggests a need to escape vulnerable early life stages (Arendt 1997), and can make populations vulnerable to periodic climatic disturbances (Ouédraogo *et al.* 2013). Alternatively, reactivity is positively associated with retrogressive strategies (r = 0.39), although this remains a secondary influence compared with investments into progression (Fig. 2.3A). Retrogressive strategies, such as vegetative dormancy, facilitate the propagation of plant populations following fire and storm disturbances (Miller & Chesson 2009). Similarly, following physical disturbances, the on-growth of colony fragments has been demonstrated to replenish the density of coral populations faster than sexual recruitment (Connell 1997).

Meanwhile, populations demonstrating greater survival investments exhibit enhanced short-term resistance, whilst long-term resistance is less influenced by any one vital rate (Fig. 2.3C & D). High investment into the survival of individuals enables populations to tolerate temporal variation in resource availability by prioritising the persistence of the most viable individuals (Gaillard & Yoccoz 2003). The transient metrics of first-timestep attenuation, and maximal attenuation describe the inclination for populations to decline in size following a disturbance, and thus present inverse measures of demographic resistance (Stott *et al.* 2011; Capdevila *et al.* 2020b). Estimates of first-timestep attenuation strongly correlate with survival investments, with enhanced survival diminishing population attenuation (r: $\sigma = -0.70$, $\gamma = -0.07$, $\tau = 0.28$, $\phi = -0.39$). Although, patterns in the maximal attenuation characteristics of populations do not align with any one vital rate in particular (r: $\sigma = -0.17$, $\gamma = -0.07$, $\tau = 0.31$, $\phi = -0.34$; Fig 2.3D), suggesting less of an influence of survival on long-term resistance.

A small association between demographic resistance and both retrogression and reproductive investments also persists for both first-timestep attenuation and maximal attenuation (Fig 2.3C & D). With retrogression associated with enhanced demographic compensation (Fig 2.3A), it is perhaps unsurprising that this component would serve to reduce overall demographic stability. However, that demographic resistance can be enhanced in populations placing an emphasis on reproduction contradicts conventional understanding of the fast-slow continuum of life histories (Stearns 1989, 1992). Traditionally, a strong selection gradient between maintaining body condition *vs.* reproductive investment was presumed to restrict high reproductive outputs to 'fast' species (Stearns 1992). However, our findings support views that the continuum exists as two separate axes, with a secondary axis, the reproductive parity continuum, allowing for higher reproductive output in species also associated with low mortality (Franco & Silvertown 1996; Salguero-Gómez *et al.* 2016b; Rüger *et al.* 2018; Capdevila *et al.* 2020a). Although energetically expensive, combining survival and reproduction does not situate species within an unsustainable region on the fast-slow continuum (Law 1979). Rather, this scenario reflects the shift of individuals along the continuum as they develop. Our population sample included numerous coral and tree species, many of whom exhibit high individual survival, yet also display high reproductive outputs to counteract elevated mortality during early life stages (Lorimer *et al.* 2001; Vermeij & Sandin 2008; Capdevila *et al.* 2020a). Subsequently, simultaneous investments into both survival and reproduction can be associated with resistant populations.

Patterns in the resilience attributes of compensation and resistance aligned with investments into the fitness components of somatic development and survival, and are therefore consistent with the selection pressures imposed on the coordination of life-history strategies along the fast-slow continuum (Stearns 1989, 1992; Salguero-Gómez *et al.* 2016b; Healy *et al.* 2019). However, we show no evidence for demographic selection pressures on attributes of recovery (r, ρ: $\sigma = -0.06$, $\gamma = -0.06$, $\tau = 0.11$, $\phi = -0.01$; ψ: $\sigma = < 0.01$, $\gamma = 0.06$, $\tau = -\ 0.08$, $\phi = 0.08$; Fig. 2.3E & F) nor evidence of a strong phylogenetic influence on the vital rate sensitivities of our recovery metrics (damping ratio & period of oscillation; Table 2.2). Previous work has reported a trade-off between stability and recovery (Hillebrand & Kunze 2020); although we argue that this result depends on how recovery is being defined. If the enhanced population growth associated with population amplification following a disturbance is defined as a measure of recovery (Jelbert *et al.* 2019), then our reported gradient between the attributes of compensation and resistance would represent a trade-off between recovery and resistance. However, from a demographic perspective distinguishing between the characteristics of compensation, resistance, and recovery, is important for the development of effective management and conservation strategies (Capdevila *et al.* 2020b). Accordingly, in this context demographic recovery describes the transition back to a stable equilibrium (Hodgson *et al.* 2015), thereby reinforcing our original interpretation.

2.5. Conclusions

Although, resilience is a complex concept, intervening and reversing global declines in biodiversity require an understanding for the drivers underpinning the resilience of populations and their communities to future climate shifts (Standish *et al.* 2014;

Angeler & Allen 2016; Kéfi *et al.* 2019; Francis *et al.* 2021). Impacting upon the periodicity of phenological drivers, and reducing the return times between severe disturbance events, climate change is exposing natural populations to increased environmental stochasticity (Thornton *et al.* 2014; Paniw *et al.* 2019; Cordes *et al.* 2020). Consequently, many natural communities face regime shifts or imminent collapse and, if we are to avoid the ensuing catastrophic loss of biodiversity and natural resources, forecasting the resilience and response of populations to future disturbances is imperative (Standish *et al.* 2014; Angeler & Allen 2016). Here we have presented a comprehensive assessment into the role environmental stochasticity plays in determining the resilience attributes of populations, a crucial insight needed for the future management of biological communities.

Considerable emphasis is often placed upon using the past exposure of populations to varying levels of environmental stochasticity as a predictor for their future resilience potential (Darling & Côté 2018; Willis *et al.* 2018; Walker 2020). Our results show that this assumption is inappropriate and, therefore, its application may lead to undesirable outcomes from biodiversity predictions and management. Alternatively, it appears that selective forces, acting on other adaptive population characteristics, have indirectly refined the compensation, resistance, and recovery attributes of natural populations. Selection pressures constrain how individuals allocate finite resources across survival, somatic development, and reproduction, thus mediating the capacity for populations to exploit and prevail within their local environments (Lande & Arnold 1983; Stearns 1989). Over time, these selective forces have moulded the demographic resilience attributes of populations, which govern their capacity to resist and recover from disturbances (Hodgson *et al.* 2015; Capdevila *et al.* 2020b). Consequently, the resilience of populations, and their communities, is rooted in their evolutionary history and not their recent environmental legacies.

2.6. References

Adams, D.C. & Felice, R.N. (2014). Assessing trait covariation and morphological integration on phylogenies using evolutionary covariance matrices. *PLoS One*, 9.

Angeler, D.G. & Allen, C.R. (2016). Quantifying resilience. *J. Appl. Ecol.*, 53, 617–624.

Arendt, J.D. (1997). Adaptive intrinsic growth rates: An integration across taxa. *Q. Rev. Biol.*, 72, 149–177.

Benton, T.G., Plaistow, S.J. & Coulson, T.N. (2006). Complex population dynamics and complex causation: Devils, details and demography. *Proc. R. Soc. B Biol. Sci.*, 273, 1173–1181.

Betts, M.G., Wolf, C., Pfeifer, M., Banks-Leite, C., Arroyo-Rodríguez, V., Bandini Ribeiro, D., *et al.* (2019). Extinction filters mediate the global effects of habitat fragmentation on animals. *Science*, 366, 1236–1239.

Blowes, S.A., Supp, S.R., Antão, L.H., Bates, A., Bruelheide, H., Chase, J.M., *et al.* (2019). The geography of biodiversity change in marine and terrestrial assemblages. *Science*, 366, 339–345.

Boyd, P.W., Cornwall, C.E., Davison, A., Doney, S.C., Fourquez, M., Hurd, C.L., *et al.* (2016). Biological responses to environmental heterogeneity under future ocean conditions. *Glob. Chang. Biol.*, 22, 2633–2650.

Camp, E.F., Schoepf, V., Mumby, P.J., Hardtke, L.A., Rodolfo-Metalpa, R., Smith, D.J., *et al.* (2018). The future of coral reefs subject to rapid climate change: Lessons from natural extreme environments. *Front. Mar. Sci.*, 5, 1–21.

Capdevila, P., Beger, M., Blomberg, S.P., Hereu, B., Linares, C. & Salguero-Gómez, R. (2020a). Longevity, body dimension and reproductive mode drive differences in aquatic versus terrestrial life history strategies. *Funct. Ecol.*, 00, 1–13.

Capdevila, P., Stott, I., Beger, M. & Salguero-Gómez, R. (2020b). Towards a comparative framework of demographic resilience. *Trends Ecol. Evol.*, 35, 776–786.

Carrascal, L.M., Galván, I. & Gordo, O. (2009). Partial least squares regression as an alternative to current regression methods used in ecology. *Oikos*, 118, 681–690.

Caswell, H. (2001). *Matrix population models: Construction, analysis and interpretation*. 2nd Edition. Oxford University Press Inc.

Chamberlain, S., Szoecs, E., Foster, Z., Arendsee, Z., Boettiger, C., Ram, K., *et al.* (2020). taxize: Taxonomic information from around the web.

Compagnoni, A., Levin, S., Childs, D.Z., Harpole, S., Paniw, M., Römer, G., *et al.* (2021). Herbaceous perennial plants with short generation time have stronger responses to climate anomalies than those with longer generation time. *Nat. Commun.*, 12, 1–8.

Connell, J.H. (1997). Disturbance and recovery of coral assemblages. *Coral Reefs*, 16, 101–113.

Conner, J.K. (2001). How strong is natural selection? *Trends Ecol. Evol.*, 16, 215–217.

Cordes, L.S., Blumstein, D.T., Armitage, K.B., CaraDonna, P.J., Childs, D.Z., Gerber, B.D., *et al.* (2020). Contrasting effects of climate change on seasonal survival of a hibernating mammal. *Proc. Natl. Acad. Sci. U. S. A.*, 117, 18119–18126.

Darling, E.S. & Côté, I.M. (2018). Seeking resilience in marine ecosystems. *Science*, 359, 986–987.

Dixon, A.M., Forster, P.M. & Beger, M. (2021). Coral conservation requires ecological climate-change vulnerability assessments. *Front. Ecol. Environ.*, 19, 243–250.

Donohue, I., Hillebrand, H., Montoya, J.M., Petchey, O.L., Pimm, S.L., Fowler, M.S., *et al.* (2016). Navigating the complexity of ecological stability. *Ecol. Lett.*, 19, 1172–1185.

Donohue, I., Petchey, O.L., Montoya, J.M., Jackson, A.L., Mcnally, L., Viana, M., *et al.* (2013). On the dimensionality of ecological stability. *Ecol. Lett.*, 16, 421–429.

Ellis, M.M. & Crone, E.E. (2013). The role of transient dynamics in stochastic population growth for nine perennial plants. *Ecology*, 94, 1681–1686.

Evers, S., Knight, T., Inouye, D., Miller, T., Salguero-Gómez, R., Iler, A., *et al.* (2021). Lagged and dormant-season climate better predict plant vital rates than climate during the growing season. *Glob. Chang. Biol.*, 27, 1927–1941.

Ezard, T.H.G., Bullock, J.M., Dalgleish, H.J., Millon, A., Pelletier, F., Ozgul, A., *et al.* (2010). Matrix models for a changeable world: The importance of transient dynamics in population management. *J. Appl. Ecol.*, 47, 515–523.

Foden, W.B., Young, B.E., Akçakaya, H.R., Garcia, R.A., Hoffmann, A.A., Stein, B.A., *et al.* (2019). Climate change vulnerability assessment of species. *Wiley Interdiscip. Rev. Clim. Chang.*, 10, 1–36.

Fox, G.A. & Gurevitch, J. (2000). Population Numbers Count: Tools for Near-Term Demographic Analysis. *Am. Nat.*, 156, 242–256.

Francis, T.B., Abbott, K.C., Cuddington, K., Gellner, G., Hastings, A., Lai, Y.C., *et al.* (2021). Management implications of long transients in ecological systems. *Nat. Ecol. Evol.*, 5, 285–294.

Franco, M. & Silvertown, J. (1996). Life history variation in plants: an exploration of the fast-slow continuum hypothesis. *Philos. Trans. R. Soc. B*, 351, 1341–1348.

Franco, M. & Silvertown, J. (2004). A comparative demography of plants based upon elasticities of vital rates. *Ecology*, 85, 531–538.

Fraterrigo, J.M., Pearson, S.M. & Turner, M.G. (2009). Joint effects of habitat configuration and temporal stochasticity on population dynamics. *Landsc. Ecol.*, 24, 863–877.

Freckleton, R.P. (2009). The seven deadly sins of comparative analysis. *J. Evol. Biol.*, 22, 1367–1375.

Freckleton, R.P., Harvey, P.H. & Pagel, M. (2002). Phylogenetic analysis and comparative data: A test and review of evidence. *Am. Nat.*, 160, 712–726.

Freckleton, R.P. & Jetz, W. (2009). Space versus phylogeny: Disentangling phylogenetic and spatial signals in comparative data. *Proc. R. Soc. B Biol. Sci.*, 276, 21–30.

Gaillard, J. & Yoccoz, N.G. (2003). Temporal variation in survival of mammals: A case of environmental canalization? *Ecology*, 84, 3294–3306.

Gaillard, J., Yoccoz, N.G., Lebreton, J., Bonenfant, C., Devillard, S., Loison, A., *et al.* (2005). Generation Time: A reliable metric to measure life-history variation among mammalian populations. *Am. Nat.*, 166, 119–123.

Gaillard, J.M., Pontier, D., Allainé, D., Lebreton, J.D. & Trouvilliez, J. (1989). An analysis of demographic tactics in birds and mammals. *Okios*, 56, 59–76.

Gilljam, D., Knape, J., Lindén, A., Mugabo, M., Sait, S.M. & Fowler, M.S. (2019). The colour of environmental fluctuations associated with terrestrial animal population dynamics. *Glob. Ecol. Biogeogr.*, 28, 118–130.

Grafen, A. (1989). The phylogenetic regression. *Philos. Trans. R. Soc. London. Ser. B. Biol. Sci.*, 326, 119–157.

Groenendael, J. van, Kroon, H. de & Caswell, H. (1988). Projection matrices in population biology. *Trends Ecol. Evol.*, 3, 264–269.

Haapkylä, J., Unsworth, R.K.F., Flavell, M., Bourne, D.G., Schaffelke, B. & Willis, B.L. (2011). Seasonal rainfall and runoff promote coral disease on an inshore reef. *PLoS One*, 6.

Hastings, A. (2004). Transients: The key to long-term ecological understanding? *Trends Ecol. Evol.*, 19, 39–45.

Hastings, A., Abbott, K.C., Cuddington, K., Francis, T., Gellner, G., Lai, Y.C., *et al.* (2018). Transient phenomena in ecology. *Science*, 361, 1–9.

Healy, K., Ezard, T.H.G., Jones, O.R., Salguero-Gómez, R. & Buckley, Y.M. (2019). Animal life history is shaped by the pace of life and the distribution of age-specific mortality and reproduction. *Nat. Ecol. Evol.*, 3, 1217–1224.

Hillebrand, H. & Kunze, C. (2020). Meta-analysis on pulse disturbances reveals differences in functional and compositional recovery across ecosystems. *Ecol. Lett.*, 23, 575–585.

Hinchliff, C.E., Smith, S.A., Allman, J.F., Burleigh, J.G., Chaudhary, R., Coghill, L.M., *et al.* (2015). Synthesis of phylogeny and taxonomy into a comprehensive tree of life. *Proc. Natl. Acad. Sci.*, 112, 12764–12769.

Hodgson, D., McDonald, J.L. & Hosken, D.J. (2015). What do you mean, “resilient”? *Trends Ecol. Evol.*, 30, 503–506.

Holling, C.S. (1973). Resilience and stability of ecological systems. *Annu. Rev. Ecol. Syst.*, 4, 1–23.

Horvitz, C.C., Denslow, J.S., Johnson, T., Gaoue, O. & Uowolo, A. (2018). Unexplained variability among spatial replicates in transient elasticity: implications for evolutionary ecology and management of invasive species. *Popul. Ecol.*, 60, 61–75.

Howard, C., Flather, C.H. & Stephens, P.A. (2020). A global assessment of the drivers of threatened terrestrial species richness. *Nat. Commun.*, 11, 1–10.

Ingrisch, J. & Bahn, M. (2018). Towards a comparable quantification of resilience. *Trends Ecol. Evol.*, 33, 251–259.

Jelbert, K., Buss, D., McDonald, J., Townley, S., Franco, M., Stott, I., *et al.* (2019). Demographic amplification is a predictor of invasiveness among plants. *Nat. Commun.*, 10, 1–6.

Karger, D.N., Conrad, O., Böhner, J., Kawohl, T., Kreft, H., Soria-Auza, R.W., *et al.* (2017). Climatologies at high resolution for the earth's land surface areas. *Sci. Data*, 4, 1–20.

Kéfi, S., Domínguez-García, V., Donohue, I., Fontaine, C., Thébault, E. & Dakos, V. (2019). Advancing our understanding of ecological stability. *Ecol. Lett.*, 22, 1349–1356.

Koons, D.N., Grand, J.B., Zinner, B. & Rockwell, R.F. (2005). Transient population dynamics: Relations to life history and initial population state. *Ecol. Modell.*, 185, 283–297.

de Kroon, H., van Groenendael, J. & Ehrlén, J. (2000). Elasticities: a review of methods and model limitations. *Ecology*, 81, 607–618.

de Kroon, H., Plaisier, A., van Groenendael, J., Caswell, H., Thomas, S.C., Wallach, R., *et al.* (1986). Elasticity: the relative contribution of demographic parameters to population growth rate. *Ecology*, 67, 1427–1431.

Kuhn, M. (2020). caret: Classification and regression training.

Kwiatkowski, L., Halloran, P.R., Mumby, P.J. & Stephenson, D.B. (2014). What spatial scales are believable for climate model projections of sea surface temperature? *Clim. Dyn.*, 43, 1483–1496.

Lande, R. (1979). Quantitative genetic analysis of multivariate evolution, applied to brain:body size allometry. *Evolution*, 33, 402–416.

Lande, R. & Arnold, S.J. (1983). The measurement of selection on correlated characters. *Evolution*, 37, 1210–1226.

Lande, R., Engen, S. & Sther, B.E. (2003). *Stochastic population dynamics in ecology and conservation*. Oxford University Press, Oxford.

Law, R. (1979). Optimal life histories under age-specific predation. *Am. Nat.*, 114, 399–417.

van de Leemput, I.A., Dakos, V., Scheffer, M. & van Nes, E.H. (2018). Slow Recovery from local disturbances as an indicator for loss of ecosystem resilience. *Ecosystems*, 21, 141–152.

Lorimer, C.G., Dahir, S.E. & Nordheim, E. V. (2001). Tree mortality rates and longevity in mature and old-growth hemlock-hardwood forests. *J. Ecol.*, 89, 960–971.

McDonald, J.L., Stott, I., Townley, S. & Hodgson, D.J. (2016). Transients drive the demographic dynamics of plant populations in variable environments. *J. Ecol.*, 104, 306–314.

Mercado-Molina, A.E., Sabat, A.M. & Yoshioka, P.M. (2011). Demography of the demosponge Amphimedon compressa: Evaluation of the importance of sexual versus asexual recruitment to its population dynamics. *J. Exp. Mar. Bio. Ecol.*, 407, 355–362.

Metcalf, C.J.E., McMahon, S.M., Salguero-Gómez, R. & Jongejans, E. (2013). IPMpack: An R package for integral projection models. *Methods Ecol. Evol.*, 4, 195–200.

Metcalf, C.J.E. & Pavard, S. (2007). Why evolutionary biologists should be demographers. *Trends Ecol. Evol.*, 22, 205–212.

Mevik, B., Wehrens, R. & Hovde Liland, K. (2019). pls: Partial least squares and principal components regression.

Michonneau, F., Brown, J. & Winter, D. (2016). rotl: An R package to interact with the Open Tree of Life data. *Methods Ecol. Evol.*, 7, 1–17.

Miller, A.D. & Chesson, P. (2009). Coexistence in disturbance-prone communities: How a resistance-resilience trade-off generates coexistence via the storage effect. *Am. Nat.*, 173, 30–43.

Morris, W.F. & Doak, D.F. (2002). *Quantitative conservation biology: Theory and practice of population viability analysis*. Sinauer Associates, Inc.

Oliver, T.A. & Palumbi, S.R. (2011). Do fluctuating temperature environments elevate coral thermal tolerance? *Coral Reefs*, 30, 429–440.

Oliveras, I. & Malhi, Y. (2016). Many shades of green: The dynamic tropical forest–savannah transition zones. *Philos. Trans. R. Soc. B Biol. Sci.*, 371, 1–15.

Ouédraogo, D.Y., Mortier, F., Gourlet-Fleury, S., Freycon, V. & Picard, N. (2013). Slow-growing species cope best with drought: Evidence from long-term measurements in a tropical semi-deciduous moist forest of Central Africa. *J. Ecol.*, 101, 1459–1470.

Pagel, M. (1999). Inferring the historical patterns of biological evolution. *Nature*, 401, 877–884.

Paniw, M., de la Riva, E.G. & Lloret, F. (2021). Demographic traits improve predictions of spatiotemporal changes in community resilience to drought. *J. Ecol.*, 00, 1–13.

Paniw, M., Maag, N., Cozzi, G., Clutton-Brock, T. & Ozgul, A. (2019). Life history responses of meerkats to seasonal changes in extreme environments. *Science*, 363, 631–635.

Paniw, M., Ozgul, A. & Salguero-Gómez, R. (2018). Interactive life-history traits predict sensitivity of plants and animals to temporal autocorrelation. *Ecol. Lett.*, 21, 275–286.

Paradis, E. & Schliep, K. (2018). ape 5.0: an environment for modern phylogenetics and evolutionary analyses in R. *Bioinformatics*, 35.

Park, J.S. (2019). Cyclical environments drive variation in life-history strategies: A general theory of cyclical phenology. *Proc. R. Soc. B Biol. Sci.*, 286, 1–9.

Pilowsky, J. (2019). colorednoise: Simulate temporally autocorrelated populations.

Promislow, D.E.L. & Harvey, P.H. (1990). Living fast and dying young: A comparative analysis of life-history variation among mammals. *J. Zool.*, 220, 417–437.

R Core Team. (2019). R: A language and environment for statistical computing.

Revell, L.J. (2009). Size-correction and principal components for interspecific comparative studies. *Evolution*, 63, 3258–3268.

Revell, L.J. (2010). Phylogenetic signal and linear regression on species data. *Methods Ecol. Evol.*, 1, 319–329.

Revell, L.J. (2012). phytools: An R package for phylogenetic comparative biology (and other things). *Methods Ecol. Evol.*, 3, 217–223.

Revell, L.J., Harmon, L.J. & Collar, D.C. (2008). Phylogenetic signal, evolutionary process, and rate. *Syst. Biol.*, 57, 591–601.

Rivest, E.B., Comeau, S. & Cornwall, C.E. (2017). The role of natural variability in shaping the response of coral reef organisms to climate change. *Curr. Clim. Chang. Reports*, 3, 271–281.

Robert, A., Sarrazin, F., Couvet, D. & Legendre, S. (2004). Releasing adults versus young in reintroductions: Interactions between demography and genetics. *Conserv. Biol.*, 18, 1078–1087.

Rüger, N., Comita, L.S., Condit, R., Purves, D., Rosenbaum, B., Visser, M.D., *et al.* (2018). Beyond the fast–slow continuum: demographic dimensions structuring a tropical tree community. *Ecol. Lett.*, 21, 1075–1084.

Ruokolainen, L., Lindén, A., Kaitala, V. & Fowler, M.S. (2009). Ecological and evolutionary dynamics under coloured environmental variation. *Trends Ecol. Evol.*, 24, 555–563.

Salguero-Gómez, R. & Casper, B.B. (2010). Keeping plant shrinkage in the demographic loop. *J. Ecol.*, 98, 312–323.

Salguero-Gómez, R., Jones, O.R., Archer, C.R., Bein, C., de Buhr, H., Farack, C., *et al.* (2016a). COMADRE: A global data base of animal demography. *J. Anim.*

Ecol., 85, 371–384.

Salguero-Gómez, R., Jones, O.R., Archer, C.R., Buckley, Y.M., Che-Castaldo, J., Caswell, H., *et al.* (2015). The COMPADRE Plant Matrix Database: An open online repository for plant demography. *J. Ecol.*, 103, 202–218.

Salguero-Gómez, R., Jones, O.R., Jongejans, E., Blomberg, S.P., Hodgson, D.J., Mbeau-Ache, C., *et al.* (2016b). Fast–slow continuum and reproductive strategies structure plant life-history variation worldwide. *Proc. Natl. Acad. Sci.*, 113, 220–235.

Salguero-Gómez, R. & Plotkin, J.B. (2010). Matrix dimensions bias demographic inferences: Implications for comparative plant demography. *Am. Nat.*, 176, 710–722.

Salguero-Gómez, R., Shefferson, R.P. & Hutchings, M.J. (2013). Plants do not count... or do they? New perspectives on the universality of senescence. *J. Ecol.*, 101, 545–554.

Standish, R.J., Hobbs, R.J., Mayfield, M.M., Bestelmeyer, B.T., Suding, K.N., Battaglia, L.L., *et al.* (2014). Resilience in ecology: Abstraction, distraction, or where the action is? *Biol. Conserv.*, 177, 43–51.

Stearns, S.C. (1983). The Influence of size and phylogeny on patterns of covariation among life-history traits in the mammals. *Okios*, 41, 173–187.

Stearns, S.C. (1989). Trade-Offs in Life-History Evolution. *Funct. Ecol.*, 3, 259–268.

Stearns, S.C. (1992). *The Evolution of Life Histories*. Oxford University Press, London.

Stott, I., Hodgson, D.J. & Townley, S. (2012). Popdemo: An R package for population demography using projection matrix analysis. *Methods Ecol. Evol.*, 3, 797–802.

Stott, I., Townley, S., Carslake, D. & Hodgson, D.J. (2010). On reducibility and ergodicity of population projection matrix models. *Methods Ecol. Evol.*, 1, 242–252.

Stott, I., Townley, S. & Hodgson, D. (2011). A framework for studying transient dynamics of population projection matrix models. *Ecol. Lett.*, 14, 959–970.

Tenhumberg, B., Tyre, A.J. & Rebarber, R. (2009). Model complexity affects transient population dynamics following a dispersal event: a case study with pea aphids. *Ecology*, 90, 1878–1890.

Thornton, P.K., Ericksen, P.J., Herrero, M. & Challinor, A.J. (2014). Climate variability and vulnerability to climate change: A review. *Glob. Chang. Biol.*, 20, 3313–3328.

van Tienderen, P.H. (1995). Life cycle trade-offs in matrix population models. *Ecology*, 76, 2482–2489.

van Tienderen, P.H. (2000). Elasticities and the link between demographic and evolutionary dynamics. *Ecology*, 81, 666–679.

Urban, M.C., Bocedi, G., Hendry, A.P., Mihoub, J.B., Pe'er, G., Singer, A., *et al.* (2016). Improving the forecast for biodiversity under climate change. *Science*, 353, 1113–1124.

Vasseur, D.A. & Yodzis, P. (2004). The color of environmental noise. *Ecology*, 85, 1146–1152.

Vermeij, M.J.A. & Sandin, S.A. (2008). Density-dependant settlement and mortality structure the earliest life phases of a coral population. *Ecology*, 89, 1994–2004.

Walker, B.H. (2020). Resilience: what it is and is not. *Ecol. Soc.*, 25, 1–3.

Willis, K.., Jeffers, E.S. & Tovar, C. (2018). What makes a terrestrial ecosystem resilient? *Science*, 359, 988–989.

Chapter 2

The projected degradation of subtropical coral assemblages by recurrent thermal stress

James Cant[1], Roberto Salguero-Gómez[2, 3, 4], Sun W. Kim[5], Carrie A. Sims[5], Brigitte Sommer[6], Maxime Brooks[1], Hamish Malcolm[7], John M. Pandolfi[5], and Maria Beger[1, 3]

1. School of Biology, Faculty of Biological Sciences, University of Leeds, Leeds, LS2 9JT United Kingdom.
2. Department of Zoology, University of Oxford, Oxford, 11a Mansfield Rd, OX1 3SZ United Kingdom.
3. Centre for Biodiversity and Conservation Science, School of Biological Sciences, University of Queensland, Brisbane, QLD, 4072 Australia.
4. Max Planck Institute for Demographic Research, Konrad Zuße Straße 1, 18057 Rostock, Germany.
5. Australian Research Council Centre of Excellence for Coral Reef Studies, School of Biological Sciences, The University of Queensland, Brisbane, QLD 4072, Australia.
6. School of Life and Environmental Science, University of Sydney, Camperdown, NSW 2006, Australia.
7. Fisheries Research, NSW Department of Primary Industries, Coffs Harbour, NSW 2450, Australia.

Published in the Journal of Animal Ecology

(2021) **90**, 233-247

The projected degradation of subtropical coral assemblages by recurrent thermal stress

3.1. Abstract

- Subtropical coral assemblages are threatened by similar extreme thermal stress events to their tropical counterparts. Yet, the mid- and long-term thermal stress responses of corals in subtropical environments remain largely unquantified, limiting our capacity to predict their future viability.
- The annual survival, growth, and recruitment of 311 individual corals within the Solitary Islands Marine Park (Australia) was recorded over a three-year period (2016 – 2018), including the 2015/16 thermal stress event. This data was used to parameterise Integral Projection Models quantifying the effect of thermal stress within a subtropical coral assemblage. Stochastic simulations were also applied to evaluate the implications of recurrent thermal stress scenarios predicted by four different Representative Concentration Pathways.
- We report differential shifts in population growth rates (λ) among coral populations during both stress and non-stress periods, confirming contrasting bleaching responses amongst taxa. However, even during non-stress periods, the observed dynamics for all taxa were unable to maintain current community composition, highlighting the need for external recruitment sources to support the community structure.
- Across all coral taxa, projected stochastic growth rates (λ_s) were found to be lowest under higher emissions scenarios. Correspondingly, predicted increases in recurrent thermal stress regimes may accelerate the loss of coral coverage, species diversity, and structural complexity within subtropical regions.
- We suggest that these trends are primarily due to the susceptibility of subtropical specialists and endemic species, such as *Pocillopora aliciae,* to thermal stress. Similarly, the viability of many tropical coral populations at higher latitudes is highly dependent on the persistence of up-current tropical systems. As such, the inherent dynamics of subtropical coral populations appear unable to support their future persistence under unprecedented thermal disturbance scenarios.

3.2. Introduction

Climate change and anthropogenic disturbance are reshaping the structure of biological communities and modifying the global distribution of abiotic regimes (Pecl *et al.* 2017; Newman 2019). These disturbances are exposing many organisms to increasingly novel environments to which they are often not adapted (Hoffmann & Sgró 2011). In coral reef ecosystems, shifts from natural reef systems towards alternative degraded states are becoming commonplace (Hughes *et al.* 2003; Pandolfi *et al.* 2003; Graham *et al.* 2014). Despite comprehensive evidence of climate stress impacting reefs (Hughes *et al.* 2018b, 2019), we lack the mechanistic understanding to predict how changing environments will affect global coral population dynamics (Edmunds & Riegl 2020). Thus, it is crucial we define the link between environmental conditions and population performance, and identify drivers enhancing the resilience of corals to future environmental shifts (Benton *et al.* 2006; Darling & Côté 2018).

State-based demographic modelling allows for examining whether, which, and how the characteristics of individuals reflect on the viability and condition of natural populations (Caswell, 2001; Lefkovitch, 1965). These demographic approaches can therefore quantify the resilience of natural populations following environmental disturbance (Ellner *et al.* 2016; Kayal *et al.* 2018). In the 1980s, state-based demographic tools were first used to investigate the relationship between coral size and demographic characteristics, and thereby the varying population-level contributions of individual colonies (see Hughes 1984; Hughes & Connell, 1987). Demographic approaches applied to corals have since served to identify trends in vital-rates that underpin localised population trajectories (Hughes & Tanner 2000; Precoda *et al.* 2018; Riegl *et al.* 2018). However, few coral studies use these models to project the future impacts of changing environmental regimes on the viability of coral populations (Edmunds & Riegl 2020; but see Kayal *et al.* 2018). Without simulations that embrace the heterogeneity of coral assemblages, assessments of the future status of global coral populations will lack realism (Madin *et al.* 2012; Edmunds *et al.* 2014).

Local environmental regimes, together with physiological limitations, enforce trade-offs within an individual's vital-rate characteristics of survival, growth, and reproduction (Stearns 1992). Thus, environmental filtering influences the relative abundance of local populations based on differential abiotic tolerances and increases the prevalence of characteristics best suited to local conditions (Gallego-Fernández & Martínez 2011). However, demographic characteristics can undergo various adjustments (Pfister 1998; Jongejans *et al.* 2010), and the extent to which organisms can modify their vital-rate trade-offs defines the capacity of different populations to exploit new environments and respond to varying conditions (Benton *et al.* 2006; Tuljapurkar *et al.* 2009).

Extensive subtropical coral assemblages can be found at latitudes far beyond the typical range of coral reef development (>23.5°; Harriott & Smith 2000; Beger *et al.* 2014). At higher latitudes, enhanced seasonality, broader spectra in abiotic conditions, a high frequency of storm events, and reduced light availability exposes corals to stronger environmental filtering than their tropical counterparts (Beger *et al.* 2014; Sommer *et al.* 2014, 2017, 2018; Muir *et al.* 2015; Mizerek *et al.* 2016). Subtropical assemblages, therefore, represent ideal systems for quantifying the mechanistic link between coral dynamics and ecological performance (Kleypas *et al.* 1999; Mizerek *et al.* 2016; Camp *et al.* 2018). Yet, with the impacts of thermal stress becoming increasingly apparent within subtropical communities (Celliers & Schleyer 2002; Harrison *et al.* 2011; Abdo *et al.* 2012; Goyen *et al.* 2019; Kim *et al.* 2019), how does the ability of subtropical corals to tolerate natural variability influence their capacity to withstand increasingly frequent acute disturbances?

Many studies have assessed the response of tropical coral assemblages to thermal stress (e.g., Adjeroud *et al.* 2018; Hughes *et al.* 2018b; Kayal *et al.* 2018; Hughes *et al.* 2019). However, there exist multiple fundamental differences between the dynamics of tropical and subtropical coral species (Baird *et al.* 2009; Woolsey *et al.* 2015). Presently, the genus-specific collapse and recovery responses of subtropical corals and their drivers, following thermal stress events, remain largely unknown (Kim *et al.* 2019). This limited perspective regarding the future viability and condition of subtropical coral communities around the globe is hindering our capacity to predict their future and manage them effectively.

Here, we utilised Integral Projection models (IPMs; Easterling *et al.* 2000) and stochastic simulations to examine the impact of recurrent thermal stress on subtropical coral assemblages, providing insight into the potential future trajectories of subtropical coral assemblages. IPMs provide a robust framework for incorporating individual heterogeneity into population-level assessments and projections (Merow *et al.* 2014). As such, IPMs are ideal for quantifying and simulating population responses to varying environments and gaining insight into the viability of natural populations faced with changing climates (Ellner *et al*. 2016; Kayal *et al*. 2018). Thermal stress is expected to reduce the size and condition of different populations, whereas non-stress conditions may allow for recovery and population growth (see Adjeroud *et al*. 2018). We therefore also conducted stochastic projections to investigate the effects of future thermal stress patterns, predicted by the different Representative Concentration pathways (RCPs), on the long-term condition of a subtropical coral assemblage.

3.3. Methods

3.3.1. Field site description and census design

The Solitary Islands Marine Park (SIMP; -30.3°, 153.143°; Fig. 3.1a) is located off the coast of New South Wales, Australia. The SIMP consists of rocky coastal islands and shallow benthic communities characterised by a relatively high cover (up to 50%) of scleractinian corals (Dalton & Roff 2013). During the 2015/16 global bleaching event, extensive bleaching occurred throughout subtropical eastern Australia (Kim *et al.* 2019). Within the SIMP, the extent of bleaching was comparable to that of the Great Barrier Reef (Hughes *et al*. 2017).

In April 2016, during the 2015/16 bleaching period, we set up 31 permanent coral plots across four islands within the SIMP (Fig. 3.1a). Each plot consisted of a numbered tag fixed into an area of bare reef substrate, surrounded by coral colonies (Fig. 3.1b). At each location, plots were placed haphazardly in the coral habitat, at depths between 8-11 metres to capture the diversity and spatial arrangement of this subtropical coral assemblage. Photographs were used to identify corals within each plot and capture their initial size and position. During these primary surveys, plots were classified as either offshore or inshore depending on location. We initially surveyed 149 individual coral colonies, belonging to 24 species. We revisited all tagged colonies in October 2016, and again in August 2017, recording their survival, size, and fragmentation, to capture the dynamics of this community during and after a bleaching event (Fig. 3.1b & c). During surveys in August 2017, new plots and corals were added to replace those lost due to storms and mortality (Appendix 2.1), which

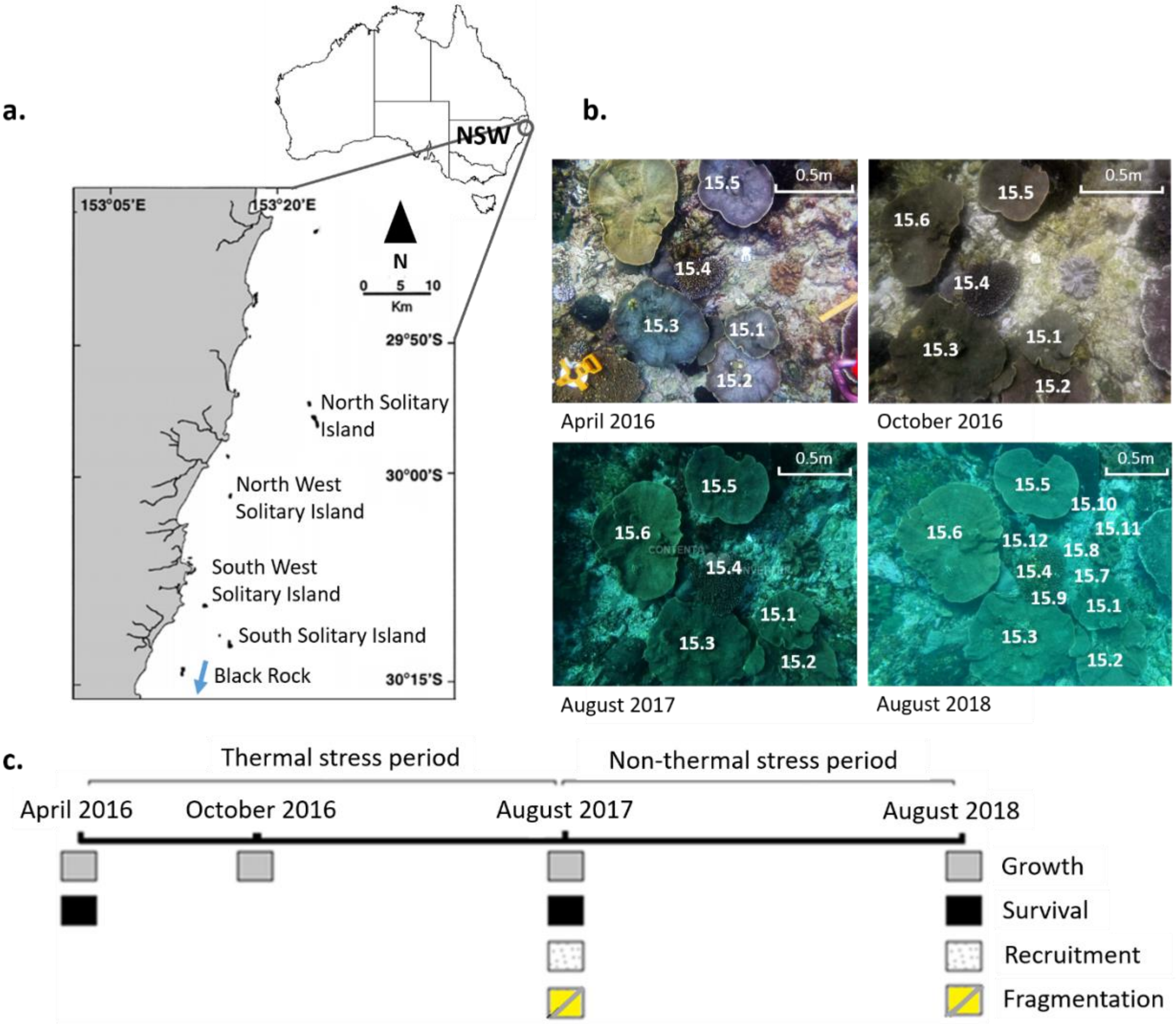

Figure 3.1. (a) The Solitary Islands Marine Park (SIMP) in New South Wales (NSW), Australia, showing the location of North Solitary Island, North West Solitary Island, South Solitary Island and South West Solitary Island, with Black Rock at South West Rocks (SWR) located to the south. **(b)** The general layout of a permanent coral plot with tagged colonies (numbered) arranged around a numbered tag, and the process of resurveying plots with new colonies added to track recruitment and to supplement the loss of tagged colonies. **(c)** Census schedule showing the frequency at which the different demographic variables of survival, growth, fragmentation and recruitment were measured, allowing for the construction of models comparing the dynamics of the population between thermal stress and non-stress periods.

increased the number of tagged colonies to 311 and included the setup of additional plots at Black Rock, to the south of the SIMP (Fig. 3.1a). During August/September 2018, the survival, size, and fragmentation of all tagged colonies were re-measured, on this occasion reflecting dynamics during a non-stress period (Fig. 3.1c).

3.3.2. Demographic measurements

During each census, demographic information was collected from each individual colony. We recorded the size of each colony using top-down photographs including a mm scale bar to minimise measurement error. Colony sizes were then measured as the visible horizontal surface area (z, see equation 3.1; cm^2), using the area calculation function in ImageJ (Schneider *et al.* 2012). Colony growth (γ) was then defined as the difference in size between successive surveys. Prior to use in analyses, the size data collected in April 2016 required 'advancing' by four months. This adjustment was necessary to standardise an inconsistency in the census intervals between April 2016 – August 2017 (16 months) and August 2017 – August/September 2018 (~12 months). To correct for this mismatch, a grouped mean monthly growth rate of tagged corals was calculated for the 16-month period between April 2016 and August 2017 (Appendix 2.2). We then used this monthly growth rate to estimate the size of each coral in August 2016 given their size in April 2016. Carrying out the size adjustment in this way ensured that all further analyses represented annual intervals and accounted for any seasonal variation in colony growth. Finally, colony size data were log transformed.

Colony survival (σ) and fragmentation (κ) were measured as the presence/absence of each colony and whether fragmentation had occurred, respectively. As with growth, the survival and fragmentation probabilities recorded for the period between April 2016 and August 2017 required adjusting to account for mismatches in census timings. This adjustment was carried out during model construction (see *Demographic model construction*). In the event of fragmentation, colony fragments were measured and included as new individuals, but marked as a product of colony fragmentation, with the largest fragment retaining the parent colony's identity.

Finally, during each of the 2017 and 2018 surveys, the size of new recruits within the tagged plot areas was recorded to capture a measure of recruitment (Fig.

3.1c). Here, we assumed that all new recruits were produced during the census interval in which they were observed. The fecundity (φ) of tagged colonies was not directly measured as part of the field surveys. Instead, a relationship between colony size and fecundity was obtained using data collected from tropical corals by Hall & Hughes (1996) sourced from the Coral Trait Database (Madin *et al*. 2016; see Appendix 2.3). This relationship described an exponential association between fecundity and colony size and allowed us to estimate the fecundity of our tagged colonies based on their size. We defined fecundity as combined egg & teste density (Hall & Hughes 1996), so per capita larval density (φ) was estimated to be half a colony's fecundity (Appendix 2.3).

Our methods for measuring recruitment and colony fecundity involved making several key assumptions regarding the reproductive biology of scleractinian corals. Firstly, we assume that recruits are produced during the annual phase in which they are observed. Yet, with coral recruits only discernible at a size that may reflect a longer growth period than the frequency of our surveys (~4cm^2), this may not be the case. Secondly, we are assuming a relationship between larval output and colony size measured in tropical corals can be applied to subtropical assemblages. The formulation of this fecundity-size relationship also involves the grouping of gonochoristic and hermaphroditic taxa and uses larval density (combined density of eggs & testes/mm^3) as a measure of colony fecundity. Thirdly, including fecundity in our demographic assessments in this way implies the assumption that we are dealing with a closed system; this is despite both local and external recruitment processes occurring within the SIMP (Harriott & Banks 1995; Harriott 1998). However, these assumptions were addressed through the inclusion of a recruit settlement factor (ψ) in our demographic models (see *Demographic model construction*). This settlement factor operates as a ratio that weights all reproductive functions by the actual number of observed recruits for each taxon/coral group. Subsequently, fecundity enabled us to include a link between adult and recruit dynamics, with the settlement factor then translating larval density estimates into a taxon-specific measure of 'the number of individuals surviving to an observable size in a subtropical setting'.

3.3.3. Demographic model construction

We used Integral Projection Models (IPMs) to evaluate the impact of thermal stress on the dynamics of different coral populations within the SIMP and to assess the future implications of different disturbance scenarios. IPMs bypass the need to artificially force continuous state variables (e.g. size) into discrete classes, a requirement in size-based matrix population models (Easterling *et al.* 2000). IPMs are therefore well suited for populations structured by continuous state variables where small state transitions can result in large changes in demographic characteristics (Burgess 2011).

With many unresolved taxonomic inconsistencies occurring throughout the Scleractinia, the identification of coral species can be problematic (Fukami *et al.* 2004), particularly without voucher specimens. Consequently, coral studies tend to focus on higher taxonomic levels (Darling *et al.* 2019). Compared to species identity, functional traits provide a superior capacity for understanding patterns and processes at the community- or assemblage-level, and the implications of changing abiotic conditions (McGill *et al.* 2006). Coral colony morphology strongly correlates with demographic characteristics and dictates how individuals interact with their environment, underpinning their success and vulnerability to varying abiotic conditions (Álvarez-Noriega *et al.* 2016; Zawada *et al.* 2019). Thus, to evaluate the dynamics of the coral assemblage in the SIMP, we pooled tagged colonies based on distinct morphological characteristics to construct separate IPMs for four coral groups reflecting the structural diversity of subtropical coral communities. Whilst we recognise these morphological clusters do not resemble true ‘populations’, we will henceforth refer to them as such, to aid clarity when discussing the outputs of our IPMs in a demographic context.

The four morphological coral groups we used accounted for approximately 90% of our tagged sample (88% of corals tagged in April 2016, and 90.5% of colonies surveyed in August 2017). Three of these groups comprised the three most common coral taxa found within the SIMP: *Acropora* spp., *Turbinaria* spp., and *Pocillopora aliciae*. For our fourth group (henceforth “Encrusting”) we pooled corals exhibiting sub-massive/encrusting growth forms from multiple genera (*Acanthastrea*, *Astrea*, *Dipsastraea*, *Goniopora*, *Micromussa*, *Montipora*, and *Paragoniastrea*). The coral species found within the SIMP belonging to these encrusting genera exhibit cosmopolitan distributions and are found across 41-74% of global coral habitats (Veron *et al.* 2016). Therefore, although this final coral cluster represents a diverse range of species, it does not reflect contrasting abiotic tolerances.

The remaining ~10% of our tagged sample consisted of *Porites heronensis* and *Stylophora pistillata* colonies. During the 2015/16 thermal stress event, we lost 85% of our tagged *P. heronensis* colonies through mortality. With low survival unrepresentative of its closest morphological group (Encrusting), including *P. heronensis* would unreasonably skew patterns for the ‘Encrusting’ group; therefore, this species was excluded from this group. Equally, despite both belonging to the *Pocilloporidae* and sharing similar morphological traits, *S. pistillata* could not be grouped with *P. aliciae*. *Stylophora pistillata* is a characteristic tropical species, with the Solitary Islands located close to the southern extent of this species’ geographical range (Veron *et al.* 2016). *Pocillopora aliciae* is instead a subtropical endemic (Schmidt-Roach *et al.* 2013), and therefore grouping these two coral species together would mask the differences underlying their contrasting distributions. Hence colonies of both *P. heronensis* and *S. pistillata* were excluded from further analyses.

An IPM (equation 3.1) describes changes in the structure and size of a population n over discrete time periods (time t to $t+1$). This model is defined by the IPM kernel K, which in this study was formulated from three sub-kernels P, H, and F (equation 3.2). The sub-kernel P outlines the probabilities of non-fragmenting corals surviving and retaining or changing their size (from z to z'). H combines the likelihood of corals undergoing fragmentation, and the eventual quantity, and size, of any fragments produced. F is the recruitment contribution of established individuals at time $t+1$. L and U are then the minimum and maximum size over which these properties of survival, growth, fragmentation, and reproduction were modelled, and are typically 10% above and below actual observed size boundaries (Merow *et al.* 2014)

$$n(z', t+1) = \int_L^U K(z', z) n(z, t) \Delta z \tag{3.1}$$

$$K(z', z) = P(z', z) + H(z', z) + F(z', z). \tag{3.2}$$

Here, we incorporated a discrete size class representing the dynamics of the largest colonies into our IPMs (Fig. 3.2). This was done to overcome statistical challenges in model convergence of vital rates due to the limited sample size for colonies at the large end of the size spectrum (*Acropora*: $z > 665\text{cm}^2$; *Turbinaria*: $z > 330\text{cm}^2$; *Pocillopora*: $z > 244\text{cm}^2$; Encrusting: $z > 706\text{cm}^2$; see Appendix 2.4 for details on how this size threshold was imposed for the continuous and discrete parts of the IPM, and for assessments of model sensitivity to threshold positioning). Correspondingly, additional vital rates were incorporated into our IPM sub-kernels to include between-stage transitions (Fig. 3.2).

In our models, sub-kernel *P* contains the size-based probability of survival (σ_1), and colony growth (γ) from size *z* to size z', for non-fragmenting colonies within the continuous stage class (equation 3.3). Sub-kernel *P* then also describes the size-based probability of colonies surviving and progressing into the discrete (large) size class (δ), and the survival of large discrete-size colonies (σ_2) (equation 3.3). Lastly, sub-kernel *P* also outlines colony shrinkage from the large discrete size class into the continuous size class (ρ), as well as the size distribution of corals produced by this retrogression (S_2) (equation 3.3). Sub-kernel *H* consists of the probability of fragmentation (κ_1), and the number (τ_1), and size of any fragments (f_1) produced by colonies in the continuous class (equation 3.4). These rates are combined with the likelihood of fragmentation within the discrete class (κ_2), and the quantity (τ_2), and size (f_2), of any fragments produced (equation 3.4). Sub-kernel *F* contains the per capita larvae density production by colonies in both the continuous (φ_1) and discrete stages (φ_2) (equation 3.5). These demographic processes are combined with a factor that converts larval density into a number of successfully settling recruits (ψ), and the size distribution of surviving recruits (C_1) (neither of which are dependent on the size class of the parent colony) (equation 3.5). Lastly, with data collection occurring post-breeding, colony survival is also built into both sub-kernels *H* and *F*.

$$P(z',z) = \begin{cases} (1-\ \delta(z))((1-\kappa_1(z))\ \sigma_1(z)\ \gamma(z',z)) \\ \delta(z)\ \sigma_1(z) \\ (1-\rho)(1-\kappa_2)\sigma_2 \\ \rho\ \sigma_2\ S_2(z') \end{cases} \tag{3.3}$$

$$H(z',z) = \begin{cases} (1-\ \delta(z))(\kappa_1(z)\sigma_1(z)\ \tau_1(z)\ f_1(z')) \\ \kappa_2\ \sigma_2\ \tau_2\ f_2(z') \end{cases} \tag{3.4}$$

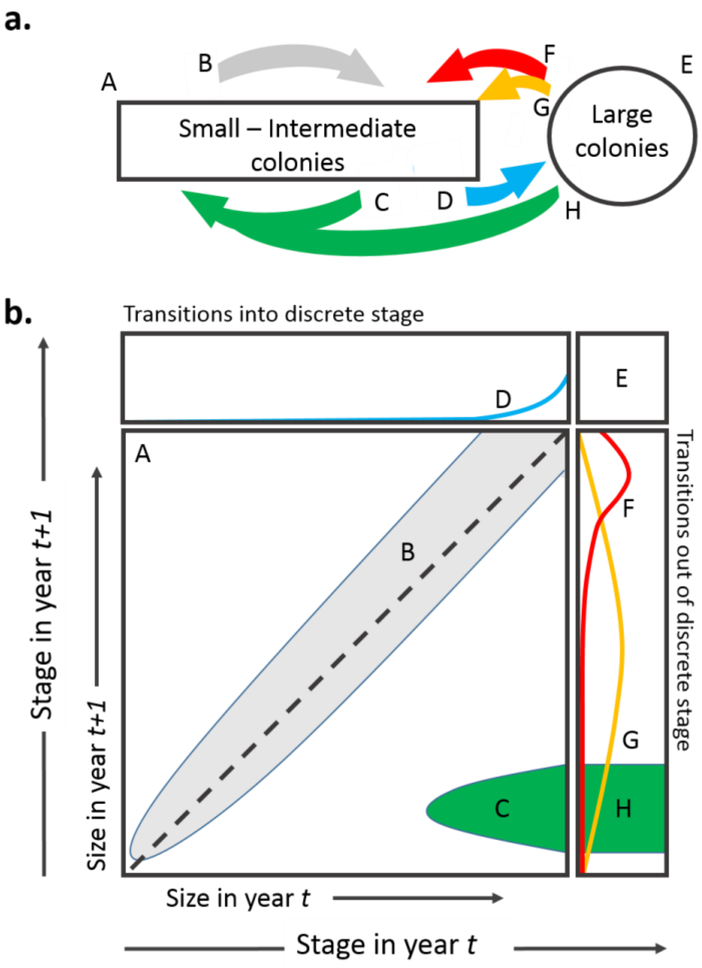

Figure 3.2. **(a)** Diagram depicting the coral life cycle structure used in this study, containing both a continuous (A) and a discrete (E) size class. **(b)** The representation of this life cycle in a two stage IPM format. Here the demographic characteristics of the life cycle are represented by the growth (B) and reproduction (C) of individuals within the continuous size class, the progression of individuals from the continuous class into the discrete stage (D), the survival of discrete stage individuals (E), and the retrogression (F), fragmentation (G) and reproduction (H) of discrete stage individuals back into the continuous class. The dashed line represents null growth within the continuous class. The threshold size between continuous and discrete size classes in each model was calculated as the point of intersection between bleaching and non-bleaching growth trends for each species. This two-stage format ensured the accurate representation of large colony dynamics.

$$F(z',z) = \begin{cases} \big(1- \delta(z)\big)\big(\sigma_1(z)\, \varphi_1(z)\psi\, C_1(z')\big) \\ \sigma_2\, \varphi_2\, \psi\, C_1(z') \end{cases}. \tag{3.5}$$

Given the low density of the coral assemblages within the SIMP (Appendix 2.4, Fig S2.6), all vital rates were modelled as density independent. Growth (γ) was analysed as the relationship between size *z* at time *t* and size at time *t+1*. The variance in growth was then fitted as a function of size at time *t*, using a gamma distribution to allow for a quadratic relationship whilst ensuring variance remained positive. Survival (σ_1) and fragmentation (κ_1) were both modelled as a function of colony size using logistic regressions. For the period between April 2016 and August 2017, these probabilities were also multiplied by the exponent *1.333* to ensure they were adjusted to represent transitions during a 12-month interval rather than the observed 16 months. The number of eggs produced was determined using a non-linear least squares regression, which allowed for an exponential relationship with colony size. Fragment size and quantity were modelled as a linear function of initial colony size, with the variance in fragment size modelled as a function of initial colony size using a gamma distribution. Recruit size distributions were also calculated, though kept independent of parent colony size as parental lineage could not be determined for each recruit. We then determined the recruit settlement factor (ψ), using the estimated density of larvae produced per colony (φ) and the total number of observed recruits (*R*)

$$\psi = \frac{\sum \varphi(z)}{R}. \tag{3.6}$$

All vital rate analyses were conducted with time as a fixed effect to allow us to separate models for both thermal stress and non-stress periods; this ensured we could empirically measure the effects of thermal stress and forecast the future implications of recurrent stress events. Then, to ensure that all analyses accounted for similarities resulting from random nesting in the data, island identity, island location (Inshore or Offshore; see Appendix 2.1), bleached state, and colony ID were also included as random effects in vital rate regressions. AIC scores were used to determine the most appropriate model structures.

3.3.4. Population growth rates and Life Table Response Experiments

To quantify the effect of thermal stress on the coral assemblage within the SIMP, we calculated the growth rate (λ) for each of our constructed IPMs. Values of λ exist on a scale of 0 to 2, with $\lambda < 1$ reflecting decline and $\lambda > 1$ representing growth. We obtained estimates of the variance in λ by repeating jack-knife resampling 1000 times, each time omitting 5% of our sample without replacement. One-way Life Table Response Experiment analyses (LTREs; Caswell 1989) were then used to quantify the vital-rate drivers behind any differences in λ observed between bleached and non-bleached models. For LTRE analysis, the non-stress state was set as the control group. Our LTRE analysis therefore defined λ during thermal stress as approximately equal to the sum of its corresponding value during non-stress, plus the relative contributions (α) of any changes in the different vital-rate regression parameters used to construct our IPMs

$$\lambda_{bleaching} \approx \lambda_{non-bleaching} + \alpha^{(parameter^1)} + \alpha^{(parameter^2)} \ldots + \alpha^{(parameter^i)}. \tag{3.7}$$

To determine α for each parameter, we first constructed an IPM equal to the mean of our associated bleaching and non-bleaching models $\boldsymbol{K}^{(\cdot\cdot)}$. The parameter-level sensitivities (S) of $\boldsymbol{K}^{(\cdot\cdot)}$ were then calculated (equation 3.8), using the stepwise change in λ for the mean model ($\Delta\lambda_k$) following small perturbations to each parameter (Δi). Multiplying these sensitivities of mean model $\boldsymbol{K}^{(\cdot\cdot)}$ by the observed differences in each parameter (i) between associated bleaching and non-bleaching models then returned the parameter-level contributions

$$S = \frac{\Delta\lambda_k}{\Delta i} \tag{3.8}$$

$$\alpha = S\left(i_{bleaching} - i_{non-bleaching}\right). \tag{3.9}$$

3.3.5. Model projections and bleaching simulations

Stochastic projections were used to evaluate the long-term viability of our subtropical coral assemblages given the dynamics observed during regular and thermal stress periods. The value of λ calculated from an IPM refers to asymptotic growth trends (Caswell 2001) and assumes environments are constant. Thus, λ is unlikely to reflect the true dynamics of systems exposed to varying environments (Ellner *et al.* 2016). For each of our coral groups, we therefore also calculated λ_s (equation 3.10). This variable is a stochastic measure of growth rate accounting for the transient nature of natural environments (Ellner *et al.* 2016), with N_t the total population size at time t, and equal to $\sum n_t$

$$\log(\lambda s) = E[\log\left(\frac{N_{t+1}}{N_t}\right)]. \tag{3.10}$$

We used sea surface temperature (SST) data from an ensemble of CMIP5 climate models (Appendix 2.5) to simulate future temperature trajectories for the Solitary Islands region. The model ensemble we used was selected to ensure our future SST estimates were comparable with projections used in other studies simulating future thermal stress responses in corals (see van Hooidonk *et al.* 2014). Corresponding with Liu *et al.* (2003), we used these simulations to determine Degree Heating Week (DHW) projections for the period 2018 to 2100 under each of the four different IPCC RCP scenarios (2.6, 4.5, 6.0 and 8.5; Appendix 2.5; IPCC, 2014). Typically, estimating DHWs only involves mean weekly SSTs that exceed the mean monthly maximum (MMM) by a threshold of 1°C (Liu *et al.* 2003). However, following the work of Kim *et al.* (2019), we removed the 1°C threshold, as this alternative approach captures the impact of low-level thermal stress found to affect subtropical corals (see also van Hooidonk & Huber 2009). Binomial regression analysis was then used to determine the annual likelihood of DHWs ≥ 4, from which we constructed a series of future annual thermal stress probabilities for each RCP scenario.

For each of our coral groups, we used these thermal stress simulations to investigate the relative impact of recurrent thermal stress regimes of varying intensities on the future condition of their population. Colony size distributions recorded in August 2018 for each population were set as the initial size distributions (n_0) for each projection. Then, using the corresponding IPMs, we projected each population to the end of the century to determine their future n_t distributions

$$n_{t+1} = \boldsymbol{K} n_t. \tag{3.11}$$

Here n_t is a probability distribution defining the size of individuals in the population at time t as a function of their size, and $\boldsymbol{K}$ is a discretised IPM matrix, with the number of iterations relating to the time frame over which the population is being assessed. During each annual iteration, the thermal stress probability associated with that step was used to determine whether the bleached or non-bleached IPM was selected. Following each iteration, the vector n_{t+1} was retained, allowing for a series of N_t values to be calculated and used in determining λ_s, and enabling us to record the temporal change in the coverage of each coral population. The coefficients of variance for all calculated metrics were also estimated, and a one-way ANOVA was used to test the effect of RCP scenario selection on the estimates of λ_s for each coral group.

3.4. Results

3.4.1. Population growth rates (λ) and LTRE analysis

The impact of thermal stress on population performance varied, with λ differing between non-stress and thermal stress periods across all four coral groups. Values of λ for both *Acropora* and *P. aliciae* reflected a state of population decline during the thermal stress period (λ <1; *Acropora*: $\lambda_{bleaching}$ = 0.8688, [95% CI: 0.8685, 0.8692]; *Pocillopora*: $\lambda_{bleaching}$ = 0.2989 [0.2980, 0.2998]). Despite a large increase in λ for *P. aliciae* during non-bleaching, both the *Acropora* and *P. aliciae* populations then remained in a state of decline throughout the non-stress period (*Acropora*: $\lambda_{non\text{-}bleaching}$ = 0.8767 [0.8752, 0.8782]; *Pocillopora*: $\lambda_{non\text{-}bleaching}$ = 0.8126 [0.8110, 0.8142]). In contrast, the *Turbinaria* group maintained relatively stable dynamics during the thermal stress period ($\lambda \approx 1$; $\lambda_{bleaching}$ = 0.9989 [0.9983, 0.9995]), though experienced a slight decline in population growth during the non-stress period ($\lambda_{non\text{-}bleaching}$ = 0.9859 [0.9857, 0.9862]). Lastly, the Encrusting group remained at equilibrium through-out both thermal stress and non-stress periods, showing marginal improvements during the non-stress phase ($\lambda_{bleaching}$ = 1.0002 [0.9998, 1.0007], $\lambda_{non\text{-}bleaching}$ = 1.0008 [1.0002, 1.0014]).

Our LTRE analysis provided an approximation as to the relative contribution changes in the processes of growth, survival and recruitment had on the observed differences in λ reported between the stress and non-stress periods. In the *Acropora* and *P. aliciae* populations, differences in λ between bleached and non-bleached periods involved changes in the parameters relating to survival (Fig. 3.3a & c). For *Acropora*, the survival of very large colonies (σ_2) was highest during thermal stress (Fig. 3.3a), however this corresponded with a decline in estimates of λ. This disparity indicates that improvements in large colony survival were unable to counteract the cumulative impacts of changes in the survival and growth dynamics of smaller colonies (Fig. 3.3a). In contrast, in *P. aliciae* the survival of both large colonies (σ_2), and those within the continuous size class (σ_1), were considerably lower during bleaching, prompting a large decline in λ (Fig. 3.3c). This LTRE analysis also shows that *P. aliciae* did not benefit from improvements in recruitment dynamics, despite

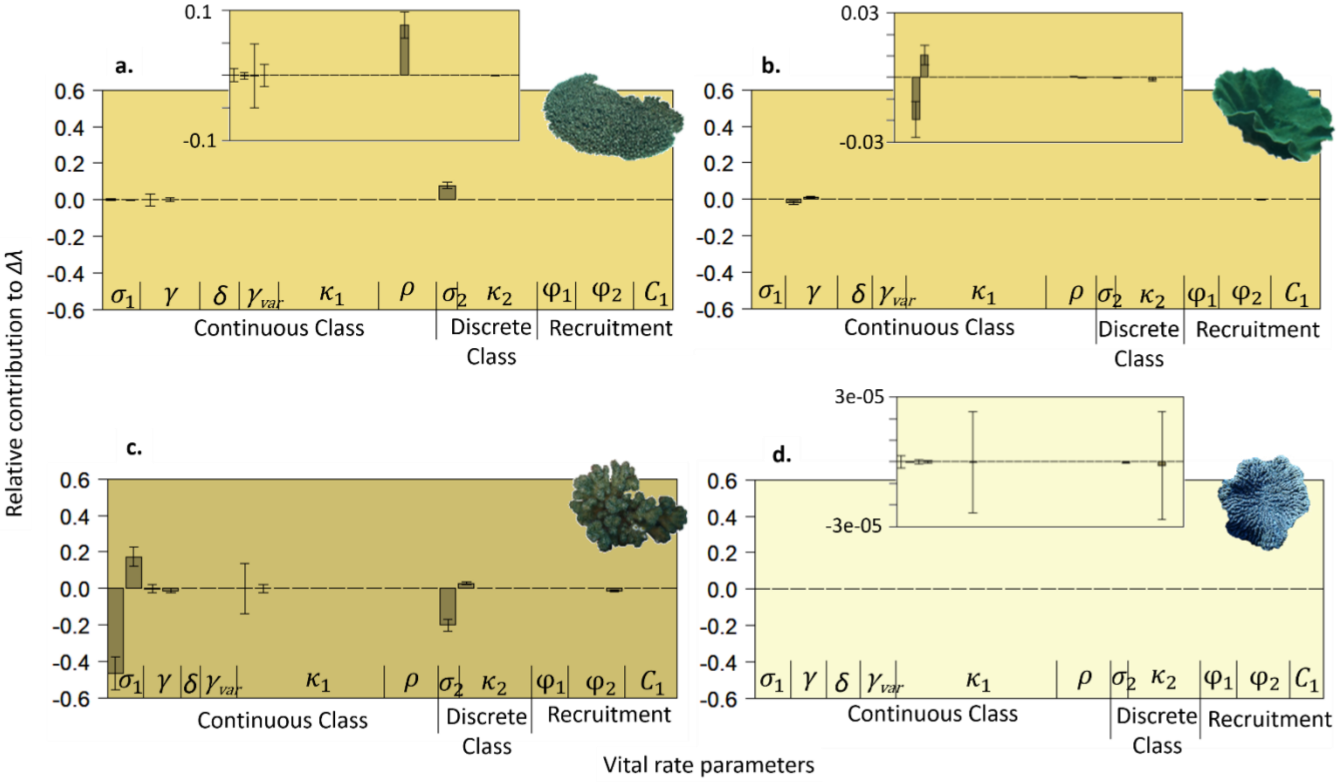

Figure 3.3. Life Table Response Experiment (LTRE) analysis showing the standardised parameter-level contributions of each vital-rate, towards the observed differences in population growth rates ($\Delta\lambda$) between bleaching and non-bleaching for the **(a)** *Acropora*, **(b)** *Turbinaria*, **(c)** *Pocillopora aliciae* and **(d)** Encrusting populations. Each parameter corresponds with a regression coefficient (left: intercept; right: slope) used in determining the size structured vital rates of survival (σ_1), growth (γ), growth variance (γ_{var}), fragmentation (κ_1), and recruitment within the continuous class, (ρ) progression into discrete class, and the survival (σ_2), fragmentation (κ_2), and recruitment of discrete class individuals. Inset panels highlight the contributions relative to each coral population. Panel colours reflect the absolute magnitude of $\Delta\lambda$, with darker shades representing greater dissimilarity between bleaching and non-bleaching dynamics.

an elevation in the number of *P. aliciae* recruits reported during the non-bleaching period (Table S2.2). Alternatively, the change in λ reported for the *Turbinaria* population, albeit small, appears to have been largely a result of changes in the growth (γ) dynamics of this population (Fig. 3.3b). Estimates of λ for the Encrusting population varied little between the stress and non-stress periods. This consistency in λ is reflected in the LTRE analysis, with vital-rate parameters for the Encrusting group remaining stable throughout both the stress and non-stress periods, at least compared to the scale of the changes observed in the other three coral groups (Fig. 3.3d).

3.4.2. Stochastic growth rate (λ_s) and community projections

Regional CMIP5 model projections indicate that the frequency of future thermal stress leading to bleaching responses will increase over time within SIMP, but that the exact prevalence of thermal stress will differ among the four RCP pathways (time: $p < 0.001$; RCP: $p < 0.001$; time * RCP: $p < 0.001$; Nagelkerke r^2: *0.593*. Appendix 2.5). Under RCP pathways 2.6, 4.5 and 6.0, future increases in the frequency of thermal stress events will be less severe than those predicted under RCP 8.5 (TukeyHSD: RCP 2.6 = 4.5 = 6.0 < 8.5). In both the 6.0 and 8.5 RCP scenarios, annual thermal stress events that are capable of inducing bleaching within the SIMP are expected before the end of the current century (Appendix 2.5: Fig. S2.7), although under both scenarios annual bleaching is not expected until after 2090. The RCP 4.5 scenario presents a more optimistic outlook with a maximum annual bleaching probability of 46% expected by the year 2100 within the SIMP. Unsurprisingly, RCP 2.6 offers the most encouraging future for the SIMP with thermally induced bleaching remaining low, and forecast once every 6.8 years by the end of the century.

RCP scenario selection was found to have a statistically significant effect on the stochastic growth rate of each coral group (ANOVA: *Acropora*: F = 6124, $p < 0.001$; *Turbinaria*: F = 4962, $p < 0.001$; *Pocillopora*: F = 29808, $p < 0.001$; Encrusting: F = 2738, $p < 0.001$). However, the relative impact of this effect differed among populations (Table 3.1). The greatest effect occurred in *P. aliciae*, with scenarios of heightened carbon emissions resulting in a severe reduction in λ_s (Table 3.1) (TukeysHSD: RCP 2.6 > 4.5 > 6.0 > 8.5). Similarly, for each of the other coral groups, scenario RCP 2.6 always resulted in larger λ_s values; however, higher emission scenarios resulted in only minimal declines, with the exact trend varying among populations (Table 3.1) (TukeysHSD: *Acropora* = RCP 2.6 > 4.5 > 6.0 < 8.5; *Turbinaria* = RCP 2.6 > 4.5 < 6.0 > 8.5; Encrusting = RCP 2.6 > 4.5 > 6.0 = 8.5). Across all populations, only *Turbinaria* was projected to exhibit positive population growth under any of the emissions scenarios (Table 3.1).

Table 3.1. The impact of the future thermal stress regimes predicted under each Representative Concentration Pathway scenario on the stochastic growth rates (λ_s) of each coral population. Variance displayed as 95% CI.

Population	RCP 2.6	RCP 4.5	RCP.6.0	RCP 8.5
Acropora	0.8725 [0.8727, 0.8722]	0.8636 [0.8637, 0.8634]	0.8604 [0.8604, 0.8603]	0.8632 [0.8633, 0.8632]
Turbinaria	1.0157 [1.0157, 1.0157]	1.0150 [1.0150, 1.0149]	1.0151 [1.0151, 1.0151]	1.0137 [1.0137, 1.0137]
Pocillopora aliciae	0.7212 [0.7230, 0.7193]	0.6395 [0.6415, 0.6376]	0.5243 [0.5254, 0.5232]	0.4123 [0.4133, 0.4113]
Encrusting	0.9863 [0.9866, 0.9860]	0.9804 [0.9807, 0.9802]	0.9759 [0.9759, 0.9758]	0.9758 [0.9759, 0.9758]

In comparison to projected population size, simulations of coral cover reveal a different future outlook for the diversity and condition of coral assemblages within the SIMP (Fig. 3.4). At present, coverage within our plots is primarily dominated by *Turbinaria* and Encrusting colonies, with *Acropora* and *P. aliciae* together contributing < 30% cover. Given the dynamics we observed across our tagged corals, coral cover within our plots is projected to decline to approximately half its current level, regardless of RCP scenario (Fig. 3.4a.i). Across all simulations this loss of coverage initially occurs very rapidly, driven by declines in all of our coral groups (Fig. 3.4a.ii - v). These declines result in the loss of *Acropora* and *P. aliciae* populations from the plots (Fig. 3.4). However, projected cover does eventually plateau as the cover of the *Turbinaria* and Encrusting groups achieves more stable levels (Fig. 3.4a). For the Encrusting group the stable coverage level remains uniform across RCP scenarios; yet for *Turbinaria* the threshold is highly dependent on the RCP scenario, with the higher emission scenarios of RCP 6.0 and 8.5 resulting in minimal coverage levels (Fig. 3.4). Ultimately, it is the variation in *Turbinaria* coverage that drives the projected variance in overall plot diversity and coverage under the different RCP scenarios (Fig. 3.4).

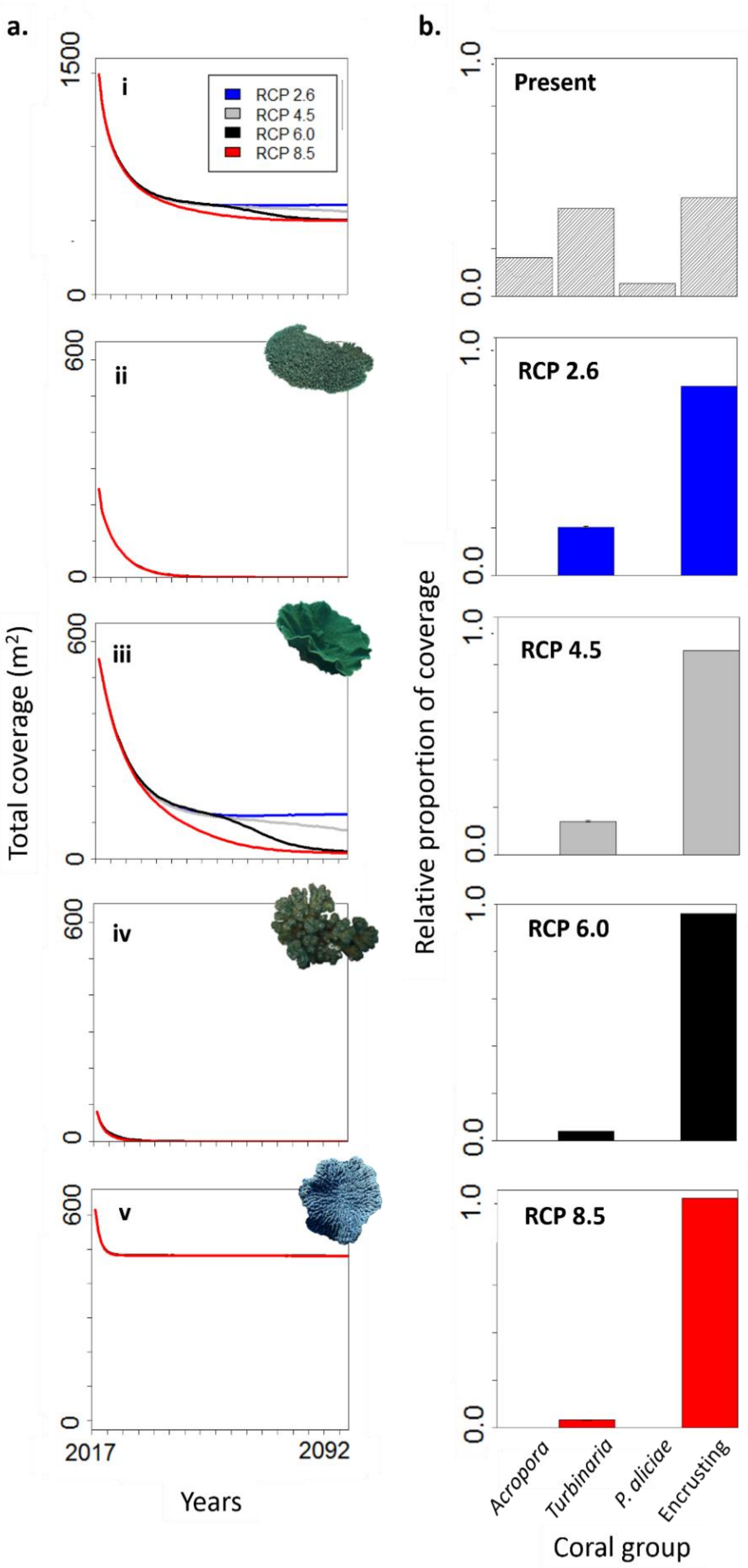
a.
b.
i
ii
iii
iv
v
RCP 2.6
RCP 4.5
RCP 6.0
RCP 8.5
1500
600
0
Total coverage (m^2)
2017
2092
Years
Present
RCP 2.6
RCP 4.5
RCP 6.0
RCP 8.5
1.0
0.0
Relative proportion of coverage
Acropora
Turbinaria
P. aliciae
Encrusting
Coral group

Figure 3.4. (a) Simulated trends in coral coverage within tagged plots under the different Representative Concentration Pathway scenarios showing **(i)** overall coverage, and the coverage of each separate population **(ii)** *Acropora*, **(iii)** *Turbinaria,* **(iv)** *Pocillopora aliciae,* and **(v)** Encrusting. **(b)** Comparison of the relative contribution towards overall coverage by each population between present coverage and projected coverage in 2100 under the four different Representative concentration pathway scenarios (RCP).

3.5. Discussion

Our capacity to manage global coral reef ecosystems in the face of rapidly changing climates relies on robust predictions of how environmental shifts influence the long-term viability of coral communities (Edmunds *et al.* 2014; Edmunds & Riegl 2020). Here, we show that within a subtropical assemblage, *Turbinaria* spp. and most corals displaying encrusting and massive morphologies possess enhanced resistance towards thermal stress events. In comparison, populations of *Acropora* spp. and *Pocillopora aliciae* are particularly sensitive to thermal stress. However, we illustrate that, regardless of this taxon-specific resistance, an increasing frequency of recurrent thermal stress events will reduce the coverage, complexity, diversity, and viability of subtropical coral assemblages.

3.5.1. Contrasting trajectories among coral groups

The contrasting responses of coral taxa to thermal stress needs to be considered in future ecosystem-level assessments and predictions for high-latitude coral communities. Indeed, *P. aliciae* is the least viable population within the Solitary Islands Marine Park (SIMP) due to a high susceptibility to thermal stress (Kim *et al.* 2019) and limited recovery during non-stress conditions. *Pocillopora aliciae* is a subtropical specialist, endemic to the east coast of Australia (Schmidt-Roach *et al.* 2013) between the Cook Island Aquatic Reserve (-28.1956, 153.5781; B. Sommer 2017, personal observation), and Sydney (-33.8688, 151.2093; Booth & Sears 2018). Corals adapted to a subtropical existence tolerate greater seasonal variance, and broader scales in abiotic measures than tropical assemblages (Camp *et al.* 2018; Sommer *et al.* 2018). However, the response of *P. aliciae* within the SIMP, following elevated temperature stress, illustrates that the enhanced stress tolerance expected of corals exposed to frequent abiotic variability (Oliver & Palumbi 2011) appears not to have benefitted this subtropical population. The accumulated thermal exposure experienced by corals in the SIMP during the 2015/2016 bleaching event exceeded the thermal tolerances of some subtropical corals (Kim *et al.* 2019); as such subtropical and other marginal species are highly vulnerable to future recurrent heat stress (Schoepf *et al.* 2015). Nevertheless, with *P. aliciae* exhibiting recent poleward range expansions (Booth & Sears 2018), our results may also reflect the reduced ability of this coral species to further alter its energetic trade-offs at the northern extent of its distribution (Sheth & Angert 2018).

Through our stochastic projections, the emerging models predict a reduction in the coverage of *Acropora* spp. within the SIMP. *Acropora* spp. typically constitute a large majority of the structural complexity in global reef environments (Nyström 2006). With *P. aliciae* also providing a considerable structural contribution (Harriott *et al.* 1994), a decline in the coverage of these corals will reduce benthic complexity within the Solitary Islands region where there is already a low diversity of branching coral species (Sommer *et al.* 2014). This loss of structural complexity will likely have cascading effects on the diversity of other taxa associated with these coral assemblages, and subsequently the overall resilience of the local ecosystem (Graham & Nash, 2013). However, this perspective assumes that other branching, more thermally tolerant tropical species will be unable to establish subtropical populations capable of fulfilling this structural role (Baird *et al.* 2012).

Thermal stress is not the only impact acting upon coral assemblages within the SIMP. The subtropical coastline of eastern Australia experiences frequent extratropical cyclones known as east coast lows (ECLs) (Harley *et al.* 2017). Therefore, it is not possible to fully attribute our projected reduction in *Acropora* spp. coverage to the consequences of thermal stress. During the 2015/16 thermal stress event, the observable symptoms of bleaching were minimal within the *Acropora* spp. assemblage of the SIMP (Kim *et al.* 2019). In June 2016, the coastline of NSW was subjected to a non-typical ECL system which produced uncharacteristic wave patterns and resulted in high levels of coastal erosion and coral damage (Mortlock *et al.* 2017). With their brittle, tabular structure highly susceptible to physical damage and abrasion, it is likely that this subtropical storm event contributed to the diminished survival of *Acropora* spp. reported in this study and must also be remembered when evaluating survival patterns across the other coral groups.

Corals exhibiting encrusting morphologies are forecasted to experience relative stability in terms of substrate coverage within the SIMP. The less complex morphologies of sub-massive and encrusting corals may provide them with a physiological advantage during thermal stress events (van Woesik *et al.* 2012), enhancing their viability under future recurrent thermal stress scenarios. However, *Porites heronensis*, which exhibits sub-massive and encrusting growth forms (Veron *et al.* 2016), was excluded from the Encrusting group for this analysis. The cause of this exclusion was the high mortality recorded for this species during the 2015/16 bleaching event, which was unrepresentative of the rest of the Encrusting group and prevented us modelling this species independently. Therefore, whilst relative stability is expected for the encrusting coral assemblage within the SIMP, the high level of bleaching vulnerability observed for *P. heronensis* does not follow this trend (Kim *et al.* 2019).

The subtropical *Turbinaria* spp. assemblage within the SIMP also appeared to display high resistance during the 2015/16 thermal stress event. *Turbinaria* spp. are known to possess a high tolerance threshold for a range of abiotic stressors (Sofonia & Anthony 2008; Morgan *et al.* 2017). Whilst *Turbinaria* spp. are capable of maintaining relatively stable population dynamics, our simulations indicate that extended, recurrent thermal disturbance will still elicit a decline in the coverage of this taxon. These contrasting trends suggest an accumulation of smaller sized colonies, which is a scenario often observed in coral communities following disturbance (Loya *et al.* 2001; Riegl & Purkis 2015). Akin to corals with reduced morphological complexity, increased rates of mass transfer in smaller colonies can enhance their survival during thermal stress events in comparison to larger conspecifics (Shenkar *et al.* 2005). Yet, a reduction in average colony size can also result in a decline in reproductive output (Álvarez-Noriega *et al.* 2016). Reef communities increasingly dominated by small and intermediately sized corals are therefore expected to display reduced recovery potential following future disturbances (Riegl & Purkis 2015; Pisapia *et al.* 2019).

3.5.2. Climate simulations for the Solitary Islands region

Relative to other subtropical communities, the Solitary Islands region may be afforded more time before bleaching becomes an annual occurrence. Under RCP 8.5 simulations, annual bleaching conditions in the subtropics could be expected from 2054 (van Hooidonk *et al.* 2014), whereas annual bleaching conditions under RCP 4.5 will occur ~25 years later (van Hooidonk *et al.* 2016). In contrast, our climate simulations suggest that under RCPs 4.5, 6.0 and 8.5 annual thermal stress events are not expected within the SIMP until much closer to the end of the 21st century (Appendix 2.5, Fig S2.7). Therefore, within the SIMP, corals may experience more buffered thermal regimes over the next century. This restrained warming of SSTs could provide corals in the SIMP with marginally more time to adapt to warming conditions. However, future shifts in the activity of destructive storms may offset this adaptive potential (Ji *et al.* 2015).

3.5.3. Recruitment limitation

The dynamics observed in our tagged coral populations, following the 2015/16 bleaching event, point to a future reduction in the coverage of coral assemblages within the SIMP, even under low emissions scenarios. The continued viability of subtropical coral assemblages is highly dependent on larval supply from lower latitudes (Beger *et al.* 2014), which supplements their existing genetic diversity and enhances their ability to recover from disturbance events (Noreen *et al.* 2009). Thus, evaluation of recruitment patterns is necessary when predicting trends in the future viability of subtropical corals.

Within the Solitary Islands region, recruitment at a scale large enough to support growing populations may be reliant on larval supply from the north (Harriott & Banks 1995; Sommer *et al.* 2014). Throughout our study, recruitment across all coral groups remained low, except in the endemic *P. aliciae* population. With larval supply in the subtropics often sporadic and asynchronous (Harrison 2011), our simulations could potentially be under-representing recruitment dynamics. However, the 2015/16 bleaching event caused a severe reduction in recruitment on the Great Barrier Reef (GBR) (Hughes *et al*. 2019). With the GBR a key contributor to the larval influx in eastern Australia’s subtropical coral assemblages (Noreen *et al.* 2009), it is unlikely the viability of coral populations in the SIMP will improve following future recurrent bleaching events of similar or greater magnitudes. Alternatively, with *P. aliciae* a known brooding species, new recruits typically settle close to their parent colony, enhancing colonisation potential whilst reducing dependency on external recruitment sources (Harriott & Banks 1995; Figueiredo *et al.* 2013; Schmidt-Roach *et al.* 2013).

Globally, coral populations have extended the poleward limits of their distributions into higher latitudes (Precht & Aronson 2004; Yamano *et al.* 2011; Baird *et al.* 2012). These expansions have occurred despite the presence of numerous abiotic restrictions, which limit the genetic and species diversity of the shifting assemblages, and reduce the continual supply of larvae to higher latitudes (Sommer *et al.* 2014; Nakabayashi *et al.* 2019). Coral species originating from the tropics are likely to be rarer in the subtropics and so more dependent on external sources of recruitment for maintaining viability, whereas for species with subtropical orientated distributions locally sourced larvae are likely more important in maintaining populations and genetic diversity (Ayre & Hughes 2000; Keith *et al.* 2015). It is important, therefore, to consider the role of local limitations on the larval stock dynamics within the SIMP when defining the observed trends in the viability of the local coral populations.

3.5.4. Environmental legacy effects

Some aspects of coral physiology, particularly those relating to the production of viable larvae, can require multiple years to recover from thermal stress (Hagedorn *et al.* 2016). Correspondingly, recovery of corals within the SIMP may have been incomplete during the collection of data reflecting population dynamics during a non-stress period. Our simulations would therefore be underestimating the viability of subtropical coral assemblages within the Solitary Island region. However, with the return times of thermal stress events decreasing, corals are unlikely to be afforded sufficient recovery time in the future (Hughes *et al.* 2018a).

Delayed effects can also apply to the negative impacts of thermal stress, as often the full extent of bleaching is not observed until well after the actual thermal stress event (McClanahan *et al.* 2009). Indeed, across each of the four coral groups we examined in this study, fragmentation was more readily observed during the non-stress phase (Appendix 2.4). Though, with the thermal stress period occurring first in our survey sequence, increasing colony fragmentation likely represents delayed partial mortality in response to the thermal stress, rather than a reaction to the conditions experienced during the non-stress period. Subsequently, the more resilient dynamics reported here for both the Encrusting and *Turbinaria* groups may not persist, over extended timeframes.

3.5.5. The caveats of an IPM framework

Whilst IPMs represent a powerful mathematical tool, the findings we present here must be considered in the context of the challenges encountered when implementing an IPM framework for a coral community. Our survey, conducted over two consecutive years, represents a comparatively restricted timeline. However, IPMs demand a data heavy approach which, coupled with the operational challenges facing the collection of long-term demographic data in coral communities, restricts the feasibility of this technique for use in assessments of scleractinian coral populations (Edmunds & Riegl 2020). To that extent, the temporal coverage of our work is comparable with previous efforts to construct IPM frameworks for coral populations using empirically derived data (Elahi *et al.* 2016; Kayal *et al.* 2018; Precoda *et al.* 2018; Scavo Lord *et al.* 2020). Additionally, in contrast to much of this previous work, we collected data for all vital rates simultaneously, thereby ensuring all estimates are subject to identical abiotic pressures. Although no model can completely satisfy the complexity of natural environments (Gertsev & Gertseva 2004), we need to understand the demographic characteristics of coral populations if we are to comprehend their responses, and viability, to future climate shifts (Edmunds *et al.* 2014). We have therefore endeavoured to ensure logistical obstacles have not hindered the efficacy, or pertinence of our study, whilst advocating for the expanded use of IPMs in coral research.

3.6. Conclusions

We have quantified the impact of thermal stress within a subtropical coral assemblage to evaluate the long-term viability of subtropical corals in the SIMP. The demographic approach we have applied transcends the purely correlative approaches previously used to evaluate the thermal stress responses of global coral assemblages (Edmunds & Riegl 2020). We demonstrate that despite prior exposure to variable abiotic environments, and a slow pace of thermal stress increase, subtropical coral assemblages will likely be subject to substantial degradation by future recurrent thermal stress events. In fact, the future reduction in complex morphologies that we forecast for the subtropical coral assemblage within the SIMP closely resembles observations in tropical reef communities (Loya *et al.* 2001); although poleward shifts in tropical coral species may temper this loss of complexity in the short term (Yamano *et al.* 2011; McIlroy *et al.* 2019).

Whilst there was considerable variation in the actual responses observed among different coral taxa, the overall expected loss of coverage, diversity and complexity in this subtropical region will hinder the functioning of the wider ecosystem that relies on this coral community (Graham & Nash 2013). Abiotic conditions within the SIMP may provide some buffering against the detrimental impacts of future warming. However, the susceptibility of subtropical specialist species to thermal stress (Kim *et al.* 2019), coupled with the high dependency on larval supply from tropical environments for many species with tropical origins (Sommer *et al.* 2014), is ultimately impeding the viability of subtropical coral assemblages. This vulnerability presents a challenge for the future management of these marginal environments and diminishes the potential for high-latitude locations to act as climate refugia for many coral species.

3.7. References

Abdo, D.A., Bellchambers, L.M. & Evans, S.N. (2012). Turning up the Heat: Increasing Temperature and Coral Bleaching at the High Latitude Coral Reefs of the Houtman Abrolhos Islands. *PLoS One*, 7, 1–11.

Adjeroud, M., Kayal, M., Iborra-Cantonnet, C., Vercelloni, J., Bosserelle, P., Liao, V., *et al.* (2018). Recovery of coral assemblages despite acute and recurrent disturbances on a South Central Pacific reef. *Sci. Rep.*, 8.

Álvarez-Noriega, M., Baird, A.H., Dornelas, M., Madin, J.S., Cumbo, V.R. & Connolly, S.R. (2016). Fecundity and the demographic strategies of coral morphologies. *Ecol. Soc. Am.*, 97, 3485–3493.

Ayre, D.J. & Hughes, T.P. (2000). Genotypic diversity and gene flow in brooding and spawning corals along the Great Barrier Reef, Australia. *Evolution*, 54, 1590–1605.

Baird, A.H., Birrel, C.L., Hughes, T.P., McDonald, A., Nojima, S., Page, C.. A., *et* *al.* (2009). Latitudinal variation in reproductive synchrony in Acropora assemblages: Japan vs. Australia. *Galaxea, J. Coral Reef Stud.*, 11, 101–108.

Baird, A.H., Sommer, B. & Madin, J.S. (2012). Pole-ward range expansion of Acropora spp. along the east coast of Australia. *Coral Reefs*, 31, 1063.

Beger, M., Sommer, B., Harrison, P.L., Smith, S.D.A. & Pandolfi, J.M. (2014). Conserving potential coral reef refuges at high latitudes. *Divers. Distrib.*, 20, 1–13.

Benton, T.G., Plaistow, S.J. & Coulson, T.N. (2006). Complex population dynamics and complex causation: Devils, details and demography. *Proc. R. Soc. B Biol. Sci.*, 273, 1173–1181.

Booth, D.J. & Sears, J. (2018). Coral expansion in Sydney and associated coral-reef fishes. *Coral Reefs*, 37, 995.

Burgess, H.R. (2011). Integral Projection Models and analysis of patch dynamics of the reef building coral Montastrea annularis. University of Exeter.

Camp, E.F., Schoepf, V., Mumby, P.J., Hardtke, L.A., Rodolfo-Metalpa, R., Smith, D.J., *et al.* (2018). The future of coral reefs subject to rapid climate change: Lessons from natural extreme environments. *Front. Mar. Sci.*, 5, 1–21.

Caswell, H. (1989). Analysis of Life Table Response Experiments I. Decomposition of effects on population growth rate. *Ecol. Modell.*, 46, 221–237.

Caswell, H. (2001). *Matrix population models: Construction, analysis and interpretation*. 2nd Edition. Oxford University Press Inc.

Celliers, L. & Schleyer, M.H. (2002). Coral bleaching on high-latitude marginal reefs at Sodwana Bay, South Africa. *Mar. Pollut. Bull.*, 44, 1380–1387.

Dalton, S.J. & Roff, G. (2013). Spatial and Temporal Patterns of Eastern Australia Subtropical Coral Communities. *PLoS One*, 8, 1–11.

Darling, E.S. & Côté, I.M. (2018). Seeking resilience in marine ecosystems. *Science.*, 359, 986–987.

Darling, E.S., McClanahan, T.R., Maina, J., Gurney, G.G., Graham, N.A.J., Januchowski-Hartley, F., *et al.* (2019). Social–environmental drivers inform strategic management of coral reefs in the Anthropocene. *Nat. Ecol. Evol.*, 3, 1341–1350.

Easterling, M.R., Ellner, S.P. & Dixon, P.M. (2000). Size-specific sensitivity: applying a new structured population model. *Ecology*, 81, 694–708.

Edmunds, P.J., Burgess, S.C., Putnam, H.M., Baskett, M.L., Bramanti, L., Fabina, N.S., *et al.* (2014). Evaluating the causal basis of ecological success within the scleractinia: an integral projection model approach. *Mar. Biol.*, 161, 2719–2734.

Edmunds, P.J. & Riegl, B. (2020). Urgent need for coral demography in a world where corals are disappearing. *Mar. Ecol. Prog. Ser.*, 635, 233–242.

Elahi, R., Sebens, K.P. & De Leo, G.A. (2016). Ocean warming and the demography of declines in coral body size. *Mar. Ecol. Prog. Ser.*, 560, 147–158.

Ellner, S.P., Childs, D.Z. & Rees, M. (2016). *Data-driven Modelling of Structured Populations*. Springer International Publishing, Switzerland.

Figueiredo, J., Baird, A.H. & Connolly, S.R. (2013). Synthesizing larval competence dynamics and reef-scale retention reveals a high potential for self-recruitment in corals. *Ecology*, 94, 650–659.

Fukami, H., Budd, A.F., Paulay, G., Solé -Cava, A., Chen, C.A., Iwao, K., *et al.* (2004). Conventional taxonomy obscures deep divergence between Pacific and Atlantic corals. *Nature*, 427, 829–832.

Gallego-Fernández, J.B. & Martínez, M.L. (2011). Environmental filtering and plant functional types on Mexican foredunes along the Gulf of Mexico. *Écoscience*, 18, 52–62.

Gertsev, V.I. & Gertseva, V.V. (2004). Classification of mathematical models in ecology. *Ecol. Modell.*, 178, 329–334.

Goyen, S., Camp, E.F., Fujise, L., Lloyd, A., Nitschke, M.R., LaJeunensse, T., *et al.* (2019). Mass coral bleaching of P. versipora in Sydney Harbour driven by the 2015–2016 heatwave. *Coral Reefs*, 38, 815–830.

Graham, N.A.J., Cinner, J.E., Norström, A.V. & Nyström, M. (2014). Coral reefs as novel ecosystems: embracing new futures. *Curr. Opin. Environ. Sustain.*, 7, 9–14.

Graham, N.A.J. & Nash, K.L. (2013). The importance of structural complexity in coral reef ecosystems. *Coral Reefs*, 32, 315–326.

Hagedorn, M., Carter, V.L., Lager, C., Camperio Ciani, J.F., Dygert, A.N., Schleiger, R.D., *et al.* (2016). Potential bleaching effects on coral reproduction. *Reprod. Fertil. Dev.*, 28, 1061–1071.

Hall, V.R. & Hughes, T.P. (1996). Reproductive strategies of modular organisms: Comparative studies of reef-building corals. *Ecology*, 77, 950–963.

Harley, M.D., Turner, I.L., Kinsela, M.A., Middleton, J.H., Mumford, P.J., Splinter, K.D., *et al.* (2017). Extreme coastal erosion enhanced by anomalous extratropical storm wave direction. *Sci. Rep.*, 7, 1–9.

Harriott, V.J. (1998). Growth of the staghorn coral Acropora formosa at Houtman Abrolhos, Western Australia. *Mar. Biol.*, 132, 319–325.

Harriott, V.J. & Banks, S.A. (1995). Recruitment of scleractinian corals in the Solitary Islands Marine Reserve, a high latitude coral-dominated community in Eastern Australia. *Mar. Ecol. Prog. Ser.*, 123, 155–161.

Harriott, V.J. & Smith, S.D.A. (2000). Coral population dynamics in a subtropical coral community, Solitary Islands Marine Park, Australia. In: *Proceedings 9th International Coral Reef Symposium*. pp. 1–9.

Harriott, V.J., Smith, S.D.A. & Harrison, P.L. (1994). Patterns of coral community structure of subtropical reefs in the Solitary Islands. *Mar. Ecol. Prog. Ser.*, 109, 67–76.

Harrison, P.L. (2011). Sexual reproduction of scleractinian corals. In: *Coral Reefs: An Ecosystem in Transition* (eds. Dubinsky, Z. & Stambler, N.). New York, U.S.A, pp. 59–85.

Harrison, P.L., Dalton, S.J. & Carroll, A.G. (2011). Extensive coral bleaching on the world’s southernmost coral reef at Lord Howe Island, Australia. *Coral Reefs*, 30, 775.

Hoffmann, A.A. & Sgró, C.M. (2011). Climate change and evolutionary adaptation. *Nature*, 470, 479–485.

van Hooidonk, R. & Huber, M. (2009). Quantifying the quality of coral bleaching predictions. *Coral Reefs*, 28, 579–587.

van Hooidonk, R., Maynard, J.A., Manzello, D. & Planes, S. (2014). Opposite latitudinal gradients in projected ocean acidification and bleaching impacts on coral reefs. *Glob. Chang. Biol.*, 20, 103–112.

van Hooidonk, R., Maynard, J.A., Tamelander, J., Gove, J., Ahmadia, G., Raymundo, L., *et al.* (2016). Local-scale projections of coral reef futures and implications of the Paris Agreement. *Sci. Rep.*, 6, 1–8.

Hughes, T.P. (1984). Population Dynamics Based on Individual Size Rather than Age: A General Model with a Reef Coral Example. *Am. Nat.*, 123, 778–795.

Hughes, T.P., Anderson, K.D., Connolly, S.R., Heron, S.F., Kerry, J.T., Lough, J.M., *et al.* (2018a). Spatial and temporal patterns of mass bleaching of corals in the Anthropocene. *Science (80-.).*, 359, 80–83.

Hughes, T.P., Baird, A.H., Bellwood, D.R., Card, M., Connolly, S.R., Folke, C., *et al.* (2003). Climate change, human impacts, and the resilience of coral reefs. *Science (80-.).*, 301, 929–933.

Hughes, T.P. & Connell, J.H. (1987). Population Dynamics Based on Size or Age? A Reef-Coral Analysis. *Am. Nat.*, 129, 818–829.

Hughes, T.P., Kerry, J.T., Álvarez-Noriega, M., Álvarez-Romero, J.G., Anderson, K.D., Baird, A.H., *et al.* (2017). Global warming and recurrent mass bleaching of corals. *Nature*, 543, 373–376.

Hughes, T.P., Kerry, J.T., Baird, A.H., Connolly, S.R., Chase, T.J., Dietzel, A., *et al.* (2019). Global warming impairs stock–recruitment dynamics of corals. *Nature*, 568, 387–390.

Hughes, T.P., Kerry, J.T., Baird, A.H., Connolly, S.R., Dietzel, A., Eakin, C.M., *et al.* (2018b). Global warming transforms coral reef assemblages. *Nature*, 556, 492–496.

Hughes, T.P. & Tanner, J.E. (2000). Recruitment Failure, Life Histories, and Long-Term Decline of Caribbean Corals. *Ecology*, 81, 2250–2263.

IPCC. (2014). *Climate Change 2014: Synthesis Report. Contribution of Working Groups I, II and III to the Fifth Assessment Report of the Intergovernmental Panel on Climate Change. [Core Writing Team, R.K. Pachauri and L.A. Meyer (eds.)]*. Geneva, Switzerland,.

Ji, F., Evans, J.P., Argueso, D., Fita, L. & Di Luca, A. (2015). Using large-scale diagnostic quantities to investigate change in East Coast Lows. *Clim. Dyn.*, 45, 2443–2453.

Jongejans, E., de Kroon, H., Tuljapurkar, S. & Shea, K. (2010). Plant populations track rather than buffer climate fluctuations. *Ecol. Lett.*, 13, 736–743.

Kayal, M., Lenihan, H.S., Brooks, A.J., Holbrook, S.J., Schmitt, R.J. & Kendall, B.E. (2018). Predicting coral community recovery using multi-species population dynamics models. *Ecol. Lett.*, 22, 605–615.

Keith, S.A., Woolsey, E.S., Madin, J.S., Byrne, M. & Baird, A.H. (2015). Differential establishment potential of species predicts a shift in coral assemblage structure across a biogeographic barrier. *Ecography*, 38, 1225–1234.

Kim, W.S., Sampayo, M.E., Sims A. C., Sommer, B., Gómez-Cabrera, M.C., Dalton, S.J., *et al.* (2019). Refugia under threat: Mass bleaching of coral assemblages in high-latitude eastern Australia. *Glob. Chang. Biol.*, 25, 3918–3931.

Kleypas, J.A., Mcmanusi, J.W. & Menez, L.A.B. (1999). Environmental limits to coral reef development: Where do we draw the line? *Am. Zool.*, 39, 146–15.

Lefkovitch, L.P. (1965). The Study of Population Growth in Organisms Grouped by Stages. *Biometrics*.

Liu, G., Strong, A. & Skirving, W. (2003). Remote Sensing of Sea Surface Temperatures During 2002 Barrier Reef Coral Bleaching. *Eos*, 84, 137–144.

Loya, Y., Sakai, K., Yamazato, K., Nakano, Y., Sambali, H. & van Woesik, R. (2001). Coral bleaching: the winners and the losers. *Ecol. Lett.*, 4, 122–131.

Madin, J.S., Anderson, K.D., Andreasen, M.H., Bridge, T.C., Cairns, S.D., Connolly, S.R., *et al.* (2016). The Coral Trait Database, a curated database of trait information for coral species from the global oceans. *Sci. Data*, 3, 1–21.

Madin, J.S., Hughes, T.P. & Connolly, S.R. (2012). Calcification, Storm Damage and Population Resilience of Tabular Corals under Climate Change. *PLoS One*, 7, 1–10.

McClanahan, T.R., Weil, E., Cortés, J., Baird, A.H. & Ateweberhan, M. (2009). Consequences of coral bleaching for sessile reef organisms. In: *Coral Bleaching* (eds. van Oppen, M.J.H. & Lough, J.M.). Springer-Verlag, Berlin, pp. 121–138.

McGill, B.J., Enquist, B.J., Weiher, E. & Westoby, M. (2006). Rebuilding community ecology from functional traits. *Trends Ecol. Evol.*, 21, 178–185.

McIlroy, S.E., Thompson, P.D., Yuan, F.L., Bonebrake, T.C. & Baker, D.M. (2019). Subtropical thermal variation supports persistence of corals but limits productivity of coral reefs. *Proc. R. Soc. B Biol. Sci.*, 286, 1–8.

Merow, C., Dahlgren, J.P., Metcalf, C.J.E., Childs, D.Z., Evans, M.E.K., Jongejans, E., *et al.* (2014). Advancing population ecology with integral projection models: A practical guide. *Methods Ecol. Evol.*, 5, 99–110.

Mizerek, T.L., Baird, A.H., Beaumont, L.J. & Madin, J.S. (2016). Environmental tolerance governs the presence of reef corals at latitudes beyond reef growth. *Glob. Ecol. Biogeogr.*, 25, 979–987.

Morgan, K.M., Perry, C.T., Johnson, J.A. & Smithers, S.G. (2017). Nearshore Turbid-Zone Corals Exhibit High Bleaching Tolerance on the Great Barrier Reef Following the 2016 Ocean Warming Event. *Front. Mar. Sci.*, 4, 1–13.

Mortlock, T.R., Goodwin, I.D., McAneney, J.K. & Roche, K. (2017). The June 2016 Australian East Coast Low: Importance of wave direction for coastal erosion assessment. *Water*, 9, 22.

Muir, P., Wallace, C.., Done, T. & Aguirre, J.D. (2015). Limited scope for latitudinal extension of reef corals. *Science*, 348, 1135–1138.

Nakabayashi, A., Yamakita, T., Nakamura, T., Aizawa, H., Kitano, Y.F., Iguchi, A., *et al.* (2019). The potential role of temperate Japanese regions as refugia for the coral Acropora hyacinthus in the face of climate change. *Sci. Rep.*, 9, 1–12.

Newman, E.A. (2019). Disturbance Ecology in the Anthropocene. *Front. Ecol. Evol.*, 7, 1–6.

Noreen, A.M.E., Harrison, P.L. & van Oppen, M.J.H. (2009). Genetic diversity and connectivity in a brooding reef coral at the limit of its distribution. *Proc. R. Soc. B Biol. Sci.*, 276, 3927–3935.

Nyström, M. (2006). Redundancy and Response Diversity of Functional Groups: Implications for the Resilience of Coral Reefs. *AMBIO A J. Hum. Environ.*, 35, 30–35.

Oliver, T.A. & Palumbi, S.R. (2011). Do fluctuating temperature environments elevate coral thermal tolerance? *Coral Reefs*, 30, 429–440.

Pandolfi, J.M., Bradbury, R.H., Sala, E., Hughes, T.P., Bjorndal, K.A., Cooke, R.G., *et al.* (2003). Global trajectories of the long-term decline of coral reef ecosystems. *Science*, 301, 955–958.

Pecl, G., Araujo, M.B., Bell, J.D., Blanchard, J. & Bonebrake, T.C. (2017). Biodiversity redistribution under climate change: Impacts on ecosystems and human well-being Publication Details. *Science*, 355, 1–9.

Pfister, C.A. (1998). Patterns of variance in stage-structured populations: Evolutionary predictions and ecological implications. *Proc. Natl. Acad. Sci.*, 95, 213–218.

Pisapia, C., Burn, D. & Pratchett, M.S. (2019). Changes in the population and community structure of corals during recent disturbances (February 2016-October 2017) on Maldivian coral reefs. *Sci. Rep.*, 9, 1–12.

Precht, W.F. & Aronson, R.B. (2004). Climate flickers and range shifts of reef corals. *Front Ecol Env.*, 2, 307–314.

Precoda, K., Baird, A.H., Madsen, A., Mizerek, T., Sommer, B., Su, S.N., *et al.* (2018). How does a widespread reef coral maintain a population in an isolated environment? *Mar. Ecol. Prog. Ser.*, 594, 85–94.

Riegl, B., Johnston, M., Purkis, S., Howells, E., Burt, J., Steiner, S.C.C., *et al.* (2018). Population collapse dynamics in Acropora downingi, an Arabian/Persian Gulf ecosystem-engineering coral, linked to rising temperature. *Glob. Chang. Biol.*, 24, 2447–2462.

Riegl, B. & Purkis, S. (2015). Coral population dynamics across consecutive mass mortality events. *Glob. Chang. Biol.*, 21, 3995–4005.

Scavo Lord, K., Lesneski, K.C., Bengtsson, Z.A., Kuhn, K.M., Madin, J., Cheung, B., *et al.* (2020). Multi-Year viability of a reef coral population living on mangrove roots suggests an important role for mangroves in the broader habitat mosaic of corals. *Front. Mar. Sci.*, 7, 1–16.

Schmidt-Roach, S., Miller, K.J. & Andreakis, N. (2013). Pocillopora aliciae: A new species of scleractinian coral (Scleractinia, Pocilloporidae) from subtropical Eastern Australia. *Zootaxa*, 3626, 576–582.

Schneider, C.A., Rasband, W.S. & Eliceiri, K.W. (2012). NIH Image to ImageJ: 25 years of image analysis. *Nat. Methods*, 9, 671–675.

Schoepf, V., Stat, M., Falter, J.L. & McCulloch, M.T. (2015). Limits to the thermal tolerance of corals adapted to a highly fluctuating, naturally extreme temperature environment. *Sci. Rep.*, 5, 1–14.

Shenkar, N., Fine, M. & Loya, Y. (2005). Size matters: bleaching dynamics of the coral Oculina patagonica. *Mar. Ecol. Prog. Ser.*, 294, 181–188.

Sheth, S.N. & Angert, A.L. (2018). Demographic compensation does not rescue populations at a trailing range edge. *Proc. Natl. Acad. Sci.*, 115, 2413–2418.

Sofonia, J.J. & Anthony, K.R.N. (2008). High-sediment tolerance in the reef coral Turbinaria mesenterina from the inner Great Barrier Reef lagoon (Australia). *Estuar. Coast. Shelf Sci.*, 78, 748–752.

Sommer, B., Beger, M., Harrison, P.L., Babcock, R.C. & Pandolfi, J.M. (2018). Differential response to abiotic stress controls species distributions at biogeographic transition zones. *Ecography*, 41, 478–490.

Sommer, B., Harrison, P.L., Beger, M. & Pandolfi, J.M. (2014). Trait-mediated environmental filtering drives assembly at biogeographic transition zones.

Ecology, 95, 1000–1009.

Sommer, B., Sampayo, E.M., Beger, M., Harrison, P.L., Babcock, R.C. & Pandolfi, J.M. (2017). Local and regional controls of phylogenetic structure at the high-latitude range limits of corals. *Proc. R. Soc. Biol. Sci. Ser. B*, 284, 1–13.

Stearns, S.C. (1992). *The Evolution of Life Histories*. Oxford University Press, London.

Tuljapurkar, S., Gaillard, J.M. & Coulson, T. (2009). From stochastic environments to life histories and back. *Philos. Trans. R. Soc. B*, 364, 1499–1509.

Veron, J.E.N., Stafford-Smith, M.G., Turak, E. & DeVantier, L.M. (2016). *Corals of the World*. Available at: http://www.coralsoftheworld.org/page/home/. Last accessed 12 November 2019.

van Woesik, R., Irikawa, A., Anzai, R. & Nakamura, T. (2012). Effects of coral colony morphologies on mass transfer and susceptibility to thermal stress. *Coral Reefs*, 31, 633–639.

Woolsey, E.S., Keith, S.A., Byrne, M., Schmidt-Roach, S. & Baird, A.H. (2015). Latitudinal variation in thermal tolerance thresholds of early life stages of corals. *Coral Reefs*, 34, 471–478.

Yamano, H., Sugihara, K. & Nomura, K. (2011). Rapid poleward range expansion of tropical reef corals in response to rising sea surface temperatures. *Geophys. Res. Lett.*, 38, 1–6.

Zawada, K.J.A., Madin, J.S., Baird, A.H., Bridge, T.C.L. & Dornelas, M. (2019). Morphological traits can track coral reef responses to the Anthropocene. *Funct. Ecol.*, 33, 962–975.

Chapter 3

Transient amplification enhances the persistence of tropicalising coral assemblages in marginal high latitude environments

James Cant[1], Katie Cook[1], James D. Reimer[2,3], Takuma Mezaki[4], Masako Nakamura[5], Cliodhna O'Flaherty[1], Roberto Salguero-Gómez[6,7,8], Maria Beger[1,7]

1. School of Biology, Faculty of Biological Sciences, University of Leeds, Leeds, LS2 9JT United Kingdom.
2. Molecular Invertebrate Systematics and Ecology Laboratory, Graduate School of Engineering and Science, University of the Ryukyus, Nishihara, Okinawa 903-0213, Japan.
3. Tropical Biosphere Research Centre, University of the Ryukyus, Nishihara, Okinawa 903-0213, Japan.
4. Kuroshio Biological Research Foundation, Nishidomari, Otsuki-cho, Kochi 788-0333, Japan.
5. School of Marine Science and Technology, Tokai University, Shimizu, Shizuoka 424-8610, Japan.
6. Department of Zoology, University of Oxford, Oxford, 11a Mansfield Rd, OX1 3SZ United Kingdom.
7. Centre for Biodiversity and Conservation Science, School of Biological Sciences, University of Queensland, Brisbane, QLD, 4072 Australia.
8. Max Planck Institute for Demographic Research, Konrad Zuße Straße 1, 18057 Rostock, Germany.

In preparation for Ecography and available as a preprint on BioRxiv at https://doi.org/10.1101/2021.04.23.441133.

Transient amplification enhances the persistence of tropicalising coral assemblages in marginal high latitude environments

4.1. Abstract

Predicting the viability of species exposed to increasing climatic stress requires an appreciation for the mechanisms underpinning the success or failure of marginal populations. Rather than traditional metrics of long-term population performance, here we illustrate that short-term (*i.e.*, transient) demographic characteristics, including measures of resistance, recovery, and compensation, are fundamental in the poleward range expansion of hard corals, facilitating the establishment of coral populations at higher latitudes. Through the annual census of tropical and subtropical *Acropora* spp. colonies in Japan between 2017-2019, we show how transient amplification (*i.e.*, short-term increases in population growth following disturbance) in a subtropical coral assemblage supports its persistence within unstable environmental conditions. The transient dynamics of both the tropical and subtropical assemblages were strongly influenced by their corresponding recruitment patterns. However, we demonstrate that variation in colony survival and fragmentation patterns between the two assemblages determines their relative capacities for transient amplification. This latitudinal variation in the transient dynamics of *Acropora* spp. assemblages emphasizes that coral populations can possess the demographic plasticity necessary for exploiting more variable, marginal conditions.

4.2. Introduction

The latitudinal diversity gradient, or poleward decline in biodiversity (von Humboldt 1808), is a fundamental macroecological pattern evident across all major taxa (Hillebrand 2004; Fine 2015). This pattern emerges partly due to increased climatic variation at higher latitudes (Willig *et al.* 2003; Archibald *et al.* 2010; Mannion *et al.* 2014). Increased environmental variation exerts a strong filter on the assembly of biological communities, selecting for species with broader ecological niches (Janzen 1967). Yet, corresponding with the changing global climate, many ecosystems face imminent reassembly as species distributions shift to track favourable conditions (Pecl *et al.* 2017; Williams & Blois 2018). Along shifting distributional boundaries, the endurance of populations depends on their ability to withstand abiotic fluctuations (Valladares *et al.* 2014). Across a given species' range, its populations are exposed to a series of environmental pressures giving rise to contrasting abilities between core and peripheral populations for tolerating abiotic variation (Angert 2009; Purves 2009). However, whilst the extent to which marginal populations can embrace environmental variation underpins the continued viability of numerous species, it is poorly understood how variation in the attributes that define the life cycles of species, such as longevity and age at reproduction, influences the persistence of populations along range boundaries (Valladares *et al.* 2014; Paniw *et al.* 2018; Healy *et al.* 2019).

Assessments of population viability typically explore long-term asymptotic dynamics, such as estimates of population growth rate (λ) (Beissinger & Westphal 1998; Crone *et al.* 2011; Selwood *et al.* 2015). However, evaluating the transient, or short-term, dynamics of natural populations is as important, if not more so, for anticipating the persistence of various species (Hastings 2001, 2004; McDonald *et al.* 2016). The transient dynamics of populations reflect their dynamics within unstable environments, describing how a population's trajectory can change in the short-term relative to its asymptotic growth rate (Stott *et al.* 2011; Table 4.1). Transient dynamics therefore provide a convenient means for quantifying population resilience, specifically, the ability of populations to resist and recover after disturbances (Capdevila *et al.* 2020). Driven by rapidly changing climate regimes and intense anthropogenic pressure, many ecosystems are at risk of bifurcation, *i.e.* the loss of an equilibrium state (*sensu* Poincaré 1885). Following a bifurcation, transient dynamics can provoke the increase (*amplification*) or decline (*attenuation*) of a population. Thus, understanding and predicting the transient dynamics of populations has become a priority for pest management and conservation (Ezard *et al.* 2010; Hodgson *et al.* 2015; Capdevila *et al.* 2020).

Global warming, together with strengthening poleward boundary currents, are driving the rapid tropicalisation of marine communities along tropical to temperate transition zones (Vergés *et al.* 2014; Kumagai *et al.* 2018). Consequently, tropical taxa, including many zooxanthellate hard coral species, are becoming increasingly prevalent in high-latitude subtropical environments (Denis *et al.* 2013; Vergés *et al.*

Table 4.1. Summary of the metrics used here to describe the transient (short-term) dynamics of tropical and subtropical *Acropora* spp. populations. Each metric is displayed alongside their corresponding disturbance response descriptor (resistance, compensation, and recovery) and demographic interpretation.

Transient measure	**Descriptor of population responses post disturbance**	**Demographic interpretation**
DAMPING RATIO (ρ)	*Recovery*	The rate at which a population converges back to equilibrium post disturbance
REACTIVITY ($\bar{\rho}$)	*Compensation*	Maximum population growth rate achieved in a single timestep post disturbance.
MAXIMAL AMPLIFICATION ($\bar{\rho}_{max}$)		Maximum rate of population growth achieved, assuming transient conditions are able to persist post disturbance.
FIRST-STEP ATTENUATION ($\underline{\rho}$)	*Resistance*	Minimum population growth rate achieved in a single timestep post-disturbance.
MAXIMAL ATTENUATION ($\underline{\rho}_{max}$)		Minimum rate of population growth achieved, assuming transient conditions are able to persist post disturbance.

2019). This establishment of coral populations along subtropical coastlines draws many similarities from the dynamics of invasive populations following their relocation, which, economic and ecological costs aside, represent the growth of small populations within novel environments (Iles *et al.* 2016). Particularly relevant in this context is evidence that the transient dynamics of plant populations are effective predictors of invasive potential (Iles *et al.* 2016). Indeed, populations possessing the capacity for rapid amplification following a perturbation (reflected here by the introduction of a novel environment) are more capable at exploiting new habitats (Jelbert *et al.* 2019). It can, therefore, be expected that the capacity of coral populations for establishing at higher latitudes may be dictated by their transient dynamics, rather than asymptotic population trajectories. Nevertheless, the transient dynamics of coral populations remain unexplored (Cant *et al.* 2021a).

Here, we explore if and how variation in the transient dynamics of coral assemblages is consistent with their exposure to abiotic variability. Specifically, we compare the relative stability (*attenuation* and *amplification;* see Table 4.1) and recovery attributes of tropical and subtropical *Acropora* spp. assemblages in southern Japan; a region considered an epicentre of tropicalisation (Vergés *et al.* 2014; Kumagai *et al.* 2018). Transient dynamics are thought to buffer the effects of environmental variability and are therefore accentuated in populations exposed to more frequent disturbances (Ellis & Crone 2013). Accordingly, we investigate whether coral assemblages at higher latitudes exhibit more pronounced transient dynamics than their tropical counterparts. Equally, the reproductive isolation associated with high-latitude coral assemblages ensures that they are typically supported by sporadic recruitment from up-current tropical reefs, with their endurance instead reliant on the dynamics of existing colonies (Cant *et al.* 2021b). Subsequently, we also conduct a transient Life Table Response Experiment (Koons *et al.* 2016) decomposing variation in the transient dynamics of tropical *vs.* subtropical *Acropora* spp. assemblages to test whether the transient dynamics of subtropical coral populations are indeed sustained by the dynamics of existing colonies.

4.3. Materials and Methods

4.3.1. Model parameterisation

To explore the influence of environmental variability on the transient dynamics of coral populations, we utilised an Integral Projection Model (IPM) framework (Easterling *et al.* 2000) to quantify the respective dynamics of *Acropora* spp. assemblages from a tropical and subtropical environment. An IPM describes how size-specific vital rates (e.g., survival, recruitment) observed at the individual-level translate into population characteristics:

$$n(z',t+1) = \int_{L}^{U} P(z',z) + F(z',z)\ n(z,t)\Delta z. \tag{4.1}$$

Here, the size (z; in this case, colony surface area, cm^2) structure, $n(z', t+1)$, of a population at time $t+1$ is a function of its structure at time t, $n(z, t)$, and the demographic patterns outlined by the sub-kernels P and F. P describes size-specific patterns relating to colony survival probability (σ), transitions in size (γ; growth, stasis, and shrinkage), the probability of fragmentation (κ), and the number and size of fragments produced (κ_n and κ_0, respectively):

$$P(z',z) = [1-\kappa(z)]\sigma(z)\gamma(z',z) + \kappa(z)\kappa_n(z)\kappa_0(z'). \tag{4.2}$$

F describes the recruitment of new, sexually produced individuals (C_1), which are the outcome of larval production per colony (colony fecundity, f_n). Crucially, we also included measures of larval settlement probability (ψ), and post-settlement survival probability (Ϯ), within our parameterisation of F:

$$F(z',z) = \psi\, f_n(z)\, \text{Ϯ}\, C_1(z'). \tag{4.3}$$

Incorporating larval settlement and post-settlement survival ensured that, with *Acropora* spp. assemblages influenced more by larval dispersal than local colony fecundity patterns (Hughes *et al.* 2000), recruitment within our models was determined by empirical settlement observations and not colony fecundity. The inclusion of fecundity instead enabled us to close the loop between adult and recruit colony dynamics, necessary for quantifying transient population characteristics (Caswell 2001). All size-specific vital rates reflect patterns estimated across a size range (Δz) equal to 10% above and below the maximum (U) and minimum (L)

observed sizes for the studied populations to avoid accidental eviction (Williams *et al.* 2012).

We empirically parameterised our IPMs through the annual census of tropical and subtropical *Acropora* spp. assemblages in southern Japan (Fig. 4.1). The *in situ* identification of *Acropora* colonies to species level is complicated by the widespread occurrence of morphologically cryptic subspecies and species hybridisation (Richards & Hobbs 2015; Richards *et al.* 2016). Thus, working at the genus-level we pooled data from across repeated surveys of tagged colonies in September 2017, August 2018, and August 2019 to quantify the regional dynamics of tropical and subtropical *Acropora* spp. assemblages. Although restricted, the temporal extent of our demographic assessment here, corresponds with timelines applied across previous work evaluating the performance characteristics of coral populations (e.g. Precoda *et al.* 2018; Shlesinger & van Woesik 2021) ensuring comparability between our findings and those of past research.

During our surveys we recorded region- and size-specific patterns in colony survival (σ), transitions in size (γ), and fragmentation (κ; Appendix 3.1). Colony survival represented the continued presence of tagged colonies over time and was modelled as a function of colony size at time t. Alternatively, transitions in colony size reflected the difference between colony surface areas recorded during successive annual surveys. In this context, transitions in colony size reflected both growth due to colony extension, and shrinkage following partial mortality (Madin *et al.* 2020), and was calculated using the relationship between colony size at time t and at time $t+1$. Next, using data pooled from both the tropical and subtropical assemblages, we modelled the probability of colony fragmentation as a function of colony size at time t. This approach was necessary due to the low frequency of annual fragmentation events (number of events reported, n_i^{κ}) observed within our tropical assemblage, although we weighted fragmentation probabilities according to the relative proportion of annual events recorded across the tropical and subtropical assemblages ($n_i^{\kappa}/n_{total}^{\kappa}$; see Appendix 3.1 for further details). We acknowledge that irrespective of the approach used, the likelihood of fragments dispersing away from our plots means that our estimates of fragmentation patterns are likely underestimates. Finally, we estimated patterns in fragment production (κ_n) and fragment size (κ_0) as a function of

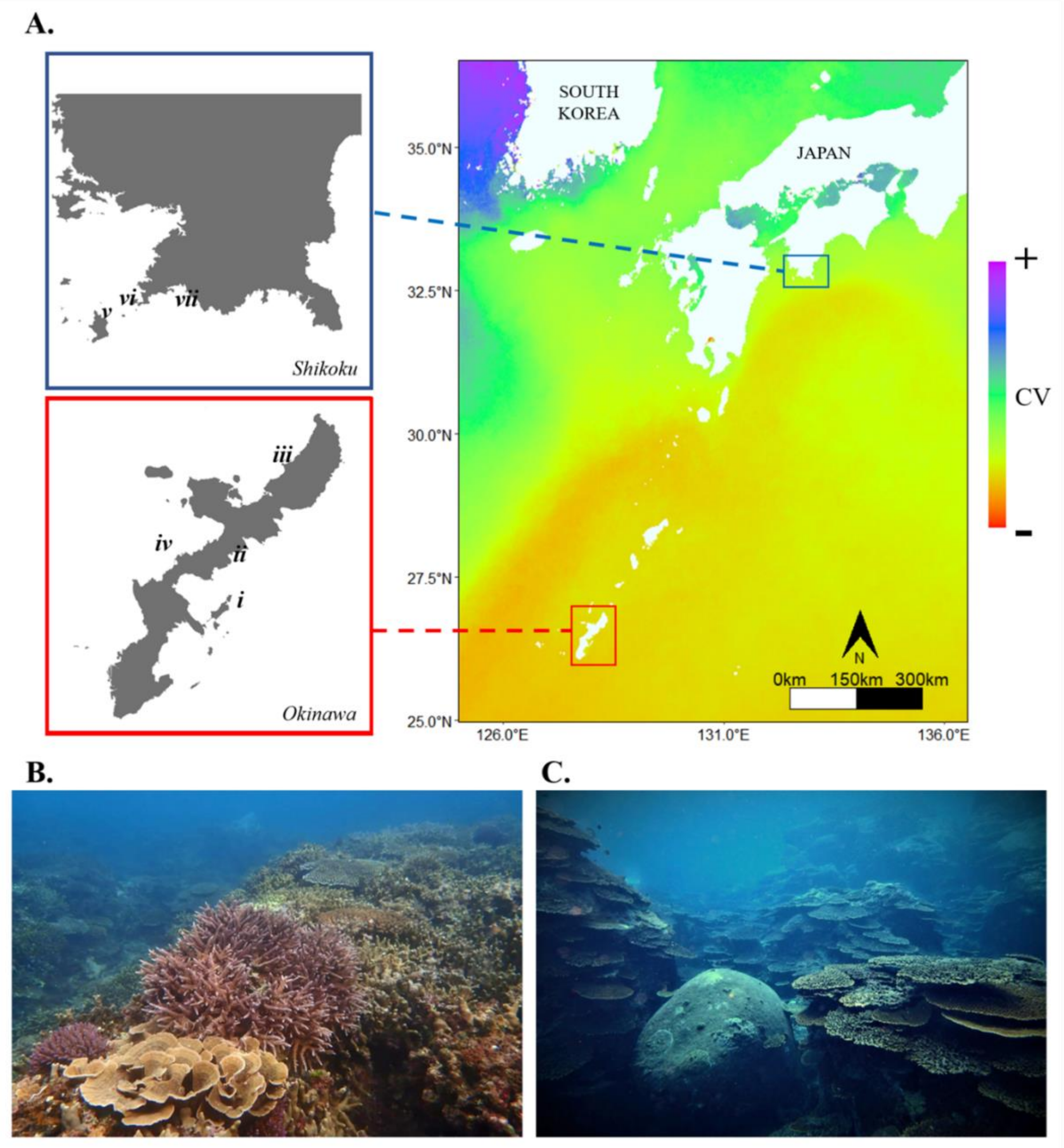

Figure 4.1. The locations of the surveyed tropical and subtropical *Acropora* spp. assemblages in Japan, separated by a distance of 990 km. **(A)** Mediated by the Kuroshio Current, the coastline of southern Japan aligns with a distinct gradient in environmental variability (coefficient of variation, CV) in monthly sea surface temperatures (SSTs) recorded during our sampling years between 2017 and 2019. We tagged individual *Acropora* spp. colonies at four locations within the tropical reef communities of Okinawa (Red): (i) Miyagi Channel, (ii) Oura Bay, (iii) Hentona, and (iv) Onna (only visited for deploying settlement tiles used to quantify recruitment patterns), and at three locations within the subtropical coral communities

of Kochi (Blue): (v) Okinoshima, (vi) Kashiwajima, and (vii) Nishidomari. Representative photographs of surveyed tropical and subtropical coral assemblages at **(B)** Hentona, Okinawa, and **(C)** Kashiwajima, Kochi. Photograph credits: K. Cook.

initial colony size, using the number and recorded size of all observed colony fragments.

In our IPMs, recruitment encompassed patterns in colony fecundity (f_n), and the probabilities of larval settlement (ψ) and post-settlement survival (henceforth recruit survival probability [Ƭ]). Although we did not directly measure colony fecundity due to the logistical challenges involved (Gilmour *et al.* 2016), we estimated annual larval output (volume of larvae produced, cm^3) as a function of colony size using a relationship reported for *Acropora* spp. on the Great Barrier Reef (Hall & Hughes 1996; Appendix 3.2). Additionally, we determined the probabilities of larval settlement and recruit survival, using larval counts made during prior tropical (2011-13; Nakamura *et al.* 2015) and subtropical (2016–18; Nakamura, *unpublished data*) settlement tile surveys in southern Japan (see Appendix 3.2 for further details). Combining the larval counts per unit area from these earlier surveys with our regional estimates of larval output and observed recruit densities enabled us to estimate ratios translating colony larval output from a measure of larval volume into expected counts of settling larvae (ψ; *sensu* Bramanti *et al.* 2015), and to define a series of post-settlement survival probabilities reflecting temporal trends in the survival of coral larvae between settlement and the point of observation within both a tropical and subtropical setting (Ƭ; Appendix 3.2). Finally, consistent with evidence that larval settlement and survival are coordinated by interactions between local biotic and abiotic drivers (Vermeij *et al.* 2009; Doropoulos *et al.* 2016), we modelled the size distribution (C_1) of tropical and subtropical recruits independently of parent colony size.

4.3.2. Quantifying transient dynamics

We used our IPMs to test our hypothesis of variation in the transient dynamics of tropical *vs.* subtropical coral populations. We focused on transient measures depicting the demographic resilience attributes described in Table 4.1: recovery (*damping ratio*

[ρ]), resistance (*first-step attenuation* [$\underline{\rho}$] & *maximal attenuation* [$\underline{\rho}_{max}$]), and compensation (*reactivity* [$\overline{\rho}$] & *maximal amplification* [$\overline{\rho}_{max}$]). To obtain estimates of variance in these transient metrics, we generated 1,000 variants of our tropical and subtropical IPMs using Jack-knife resampling; each time omitting 5% of our data without replacement whilst allowing the modelled probabilities of larval settlement (ψ) and recruit survival ($Ƭ$) to vary within observed limits. Next, we integrated the kernel of each model variant into a high-dimension matrix (200×200 cells) using the 'midpoint rule' (Ellner & Rees 2006; Zuidema *et al.* 2010), with the probability of individuals transitioning from one cell to the next estimated at the cell midpoint and multiplied by the cell width. In our case cell width corresponded with colony size increments of 0.716 cm^2 on the log-scale. Following this discretisation, we calculated the distribution (mean and variance) of each transient metric for the tropical and subtropical assemblages using the R package *popdemo* (Stott *et al.* 2012).

We calculated the amplification and attenuation characteristics of the tropical and subtropical assemblages as population structure-specific measures. Population structure-specific transient measures provide the predicted transient dynamics of a population given its current state distribution; as opposed to transient bounds which reflect the potential dynamics of a population irrespective of its state distribution (Stott *et al.* 2011). For these calculations, we derived the state distributions of both the tropical and subtropical *Acropora* spp. assemblages using the size distributions of tagged colonies recorded during our 2019 census. Across our Jack-knife model variants, some combinations of resampled vital rate schedules lacked the capacity for eliciting either amplification or attenuation in their corresponding population relative to asymptotic growth rates. We therefore present the percentage of model variants from which predictions of amplification and attenuation could be obtained as an additional indication of the transient potential of the tropical and subtropical *Acropora* spp. assemblages. Finally, to contextualise our estimates of transient dynamics against the long-term trends of each population, we calculated mean and variance estimates of their asymptotic growth rates (λ), with $\lambda < 1$ or > 1 reflecting negative or positive population growth (Caswell 2001).

4.3.3. Model decomposition

We tested our hypothesis that the transient dynamics of subtropical coral populations are sustained by the survival, transitions in size, and fragmentation patterns of existing colonies rather than patterns in recruitment using a transient Life Table Response Experiment (transient LTRE; Koons *et al.* 2016). The amplification characteristics of populations define their capacity to exploit and thrive within novel, variable environments (McDonald *et al.* 2016; Jelbert *et al.* 2019). Thus, we decomposed the vital rate influences of the relative maximal amplification characteristics ($\bar{\rho}_{\max}$) of the tropical *vs.* subtropical *Acropora* spp. assemblages. The transient dynamics of our focal coral assemblages (ξ) are contingent on three components: the size-specific vital rate patterns of established colonies (Θ), and the probabilities of larval settlement (ψ) and recruit survival (Ϯ). Variation in these components between the tropical and subtropical assemblages consequently drives any variation between their characteristics:

$$\xi^{(tropical)} = \xi\left[\Theta^{(1)},\ \psi^{(1)},\ \text{Ϯ}^{(1)}\right] \tag{4.4}$$

$$\xi^{(subtropical)} = \xi\left[\Theta^{(2)},\ \psi^{(2)},\ \text{Ϯ}^{(2)}\right]. \tag{4.5}$$

Within coral populations, rates of larval settlement and survival oscillate considerably over time (Davidson *et al.* 2019). Thus, we incorporated this variability into our IPMs by allowing the probabilities of larval settlement and recruit survival to fluctuate within observed boundaries, therefore introducing an element of within–assemblage variability to our models. Using the transient LTRE approach detailed below, we combined a traditional Life Table Response Experiment with a Kitagawa & Keyfitz decomposition (Kitagawa 1955; Keyfitz 1968; Caswell 2019). Briefly, this decomposition approach allowed us to account for within- assemblage variability when evaluating the vital rate mechanisms underlying the differences between the transient dynamics of the two assemblages (Maldonado-Chaparro *et al.* 2018; Layton-Matthews *et al.* 2021).

We first paired up tropical and subtropical model variants to evaluate the overall contributions (C) of the vital rate patterns of established colonies (Θ), larval settlement (ψ), and recruit survival (Ϯ), towards variation in $\bar{\rho}_{max}$ using a Kitagawa & Keyfitz decomposition. The overall contribution of each component was obtained by averaging the effect on $\overline{\rho}_{max}$ of substituting the tropical and subtropical form of the selected component against a fixed background of the other components (Caswell 2019):

$$
\begin{aligned}
C(\Theta) \approx \frac{1}{4}(&\overline{\rho}_{max}\left[\Theta^{(1)},\psi^{(1)},\dagger^{(1)}\right] - \overline{\rho}_{max}\left[\Theta^{(2)},\psi^{(1)},\dagger^{(1)}\right] \\
&+ \overline{\rho}_{max}\left[\Theta^{(1)},\psi^{(2)},\dagger^{(2)}\right] - \overline{\rho}_{max}\left[\Theta^{(2)},\psi^{(2)},\dagger^{(2)}\right] \\
&+ \overline{\rho}_{max}\left[\Theta^{(1)},\psi^{(1)},\dagger^{(2)}\right] - \overline{\rho}_{max}\left[\Theta^{(2)},\psi^{(1)},\dagger^{(2)}\right] \\
&+ \overline{\rho}_{max}\left[\Theta^{(1)},\psi^{(2)},\dagger^{(1)}\right] - \overline{\rho}_{max}\left[\Theta^{(2)},\psi^{(2)},\dagger^{(1)}\right]).
\end{aligned}
\tag{4.6}
$$

Across all decomposition analyses, we defined the tropical assemblage as our control model. Subsequently, positive contributions reflect greater influence towards the dynamics of the tropical assemblage, whereas negative contributions imply a greater importance towards the subtropical assemblage.

Next, we decomposed the separate contributions of the vital rates of survival, changes in size, and fragmentation, observed in established colonies, towards variation in $\overline{\rho}_{max}$. The contribution of each vital rate (C[θ_i]) corresponds with the change in that vital rate between paired tropical and subtropical models combined with the environmental-specific elasticity matrices of $\overline{\rho}_{max}$ (Caswell 2019):

$$
C(\theta_i) \approx \frac{1}{2}\left[\begin{matrix} \left(\left.\frac{\partial\overline{\rho}_{max}\left[\overline{\Theta},\ \psi^{(1)},\ \dagger^{(1)}\right]}{\partial\theta}\right|_{u=i}\right)\left({\theta_i}^{(1)} - {\theta_i}^{(2)}\right) + \\ \left(\left.\frac{\partial\overline{\rho}_{max}\left[\overline{\Theta},\ \psi^{(2)},\ \dagger^{(2)}\right]}{\partial\theta}\right|_{u=i}\right)\left({\theta_i}^{(1)} - {\theta_i}^{(2)}\right) \end{matrix}\right]. \tag{4.7}
$$

Here, the tropical- and subtropical-specific elasticity matrices of $\overline{\rho}_{max}$ ($\frac{\partial\overline{\rho}_{max}\left[\overline{\Theta},\ \psi^{i},\ \dagger^{i}\right]}{\partial\theta}$) were comprised of the proportional sensitivities (e_{ij}) of $\overline{\rho}_{max}$ towards the matrix elements (a_{ij}) of a discretised IPM kernel parameterised using the mean vital rates across our tropical and subtropical assemblages ($\overline{\Theta}$):

$$
e_{ij} = \frac{a_{ij}}{x}\frac{\partial x}{\partial a_{ij}} = \frac{a_{ij}}{x}\frac{\left(x^{Perturbed} - \mathrm{x}^{Original}\right)}{\left(a_{ij}^{Perturbed} - a_{ij}^{Original}\right)} \qquad \text{where } x = \overline{\rho}_{max}. \tag{4.8}
$$

4.4. Results

4.4.1. Trends in transient dynamics: Tropical vs. subtropical

The transient characteristics of the subtropical *Acropora* spp. assemblage were more pronounced than those of its tropical counterpart (Fig. 4.2). Of the two populations, the tropical *Acropora* spp. assemblage displayed the highest asymptotic growth rate (λ: Tropical = 0.916 [95% CI: 0.914, 0.918]; Subtropical = 0.655 [0.654, 0.655]). However, the subtropical assemblage is expected to exhibit a reactive ($\bar{\rho}$) transient response to perturbation, experiencing an increase in its growth rate relative to its asymptotic trajectory ($\bar{\rho}$: 1.033 [1.027, 1.039]). Although, across all Jack-knifed model variants, the subtropical variants presented more heterogenous responses to perturbations, than the tropical variants (Fig. 4.2A). Alternatively, post disturbance, the tropical assemblage was predisposed to experience attenuation ($\underline{p}$), resulting in a decline in its asymptotic growth rate ($\underline{p}$: 0.985 [0.983, 0.986]).

Notably, in comparison with the tropical assemblage, the transient dynamics of the subtropical assemblage demonstrated a superior capacity for maintaining elevated growth within unstable environments (Fig. 4.2B). Amplification was observed in 84.5% of subtropical model variants as opposed to in just 23.1% of tropical variants. Indeed, expected maximal amplification ($\bar{\rho}_{max}$) was also highest within the subtropical assemblage, and reflected a potential ~22% increase in population growth rate following a disturbance relative to asymptotic expectations ($\bar{\rho}_{max}$. Tropical = 1.019 [1.012, 1.026]; Subtropical = 1.228 [1.215, 1.241]). The tropical assemblage did, however, display a higher damping ratio (ρ) than the subtropical assemblage (ρ. Tropical = 1.638 [1.634, 1.641]; Subtropical = 1.429 [1.424, 1.433]), indicating a faster convergence rate to an equilibrium state. Yet, in this context, this disparity in convergence rate corresponds with the more prominent transient displacement observed in the subtropical model variants relative to their asymptotic characteristics (Fig. 4.2B). Conversely, maximal attenuation ($\underline{\rho}_{max}$) estimates for the tropical and subtropical assemblages suggest that, whilst attenuation was more readily observed within tropical model variants (observed in 96% and 40.3% of tropical and subtropical variants respectively), both assemblages are only expected to experience a <10% reduction in their growth rates relative to asymptotic

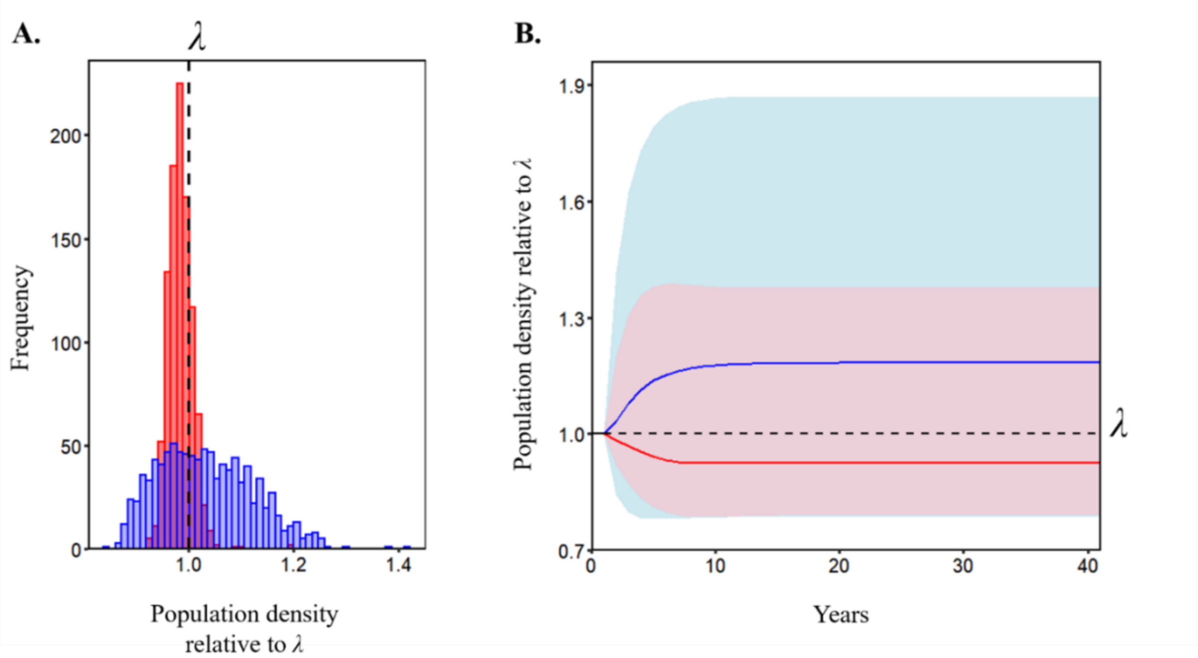

Figure 4.2. The subtropical *Acropora* spp. assemblage displays an enhanced capacity for demographic amplification compared to its tropical counterpart. We estimated measures of transient (short-term) dynamics describing the dynamics of the tropical (Red) and subtropical (Blue) *Acropora* spp. assemblages following disturbance across a series of Jack-knifed model variants. **(A)** The distribution of transient responses within one time–step of a perturbation, observed across the model variants. **(B)** Illustrates how the transient dynamics of the model variants manifest over 40 years post-disturbance modifying population trajectories relative to original asymptotic expectations. Solid lines represent the mean population trends with shaded areas reflecting the range of observed transient patterns for each population. Across both panels all transient responses in population size are displayed relative to each assemblage's corresponding asymptotic growth rate (*λ*, dashed line).

expectations should attenuation occur ($\underline{\rho}_{max}$. Tropical = 0.919 [0.916, 0.923]; Subtropical = 0.940 [0.935, 0.946]).

Considering the prevalence of uncertainties within coral taxonomy (Fukami *et al.* 2004), there is a precedence for assessments into the characteristics of coral populations to operate at higher taxonomic levels (Darling *et al.* 2019; Edmunds

2020). Thus, we present here a demographic assessment of *Acropora* spp. assemblages focused at the genus level. Interpretating our observed demographic variation therefore assumes a consistency in species configurations across our tropical and subtropical *Acropora* spp. assemblages. However, species records from both Okinawa and Kochi (see Nishihira & Veron [1995]; Veron *et al.* [2016]) indicate that there is considerable overlap in the composition of these tropical and subtropical *Acropora* spp. assemblages (Appendix 3.3). Equally, there is minimal variation in the morphological and functional traits of acroporid species associated with the coastal communities of Okinawa and Kochi (Appendix 3.3), reinforcing the validity of the demographic variation we describe here.

4.4.2. Transient LTRE decomposition

Despite clear evidence that recruitment patterns shape the transient dynamics of the tropical and subtropical *Acropora* spp. assemblages, the differential vital rate schedules of existing colonies are responsible for the variation observed between the amplification capacities of the two assemblages (Fig. 4.3). Patterns in larval settlement (ψ), recruit survival (*Ϯ*), and the vital rates of existing colonies (Θ) varied significantly in their contributions towards variation in the maximal amplification ($\bar{\rho}_{max}$) (ANOVA: $F_{2, 2997} = 29557$, $p < 0.001$; Tukey: $\psi > \Theta >$ *Ϯ*). Overall, larval settlement (ψ) and recruit survival (*Ϯ*) exerted the greatest influence on estimates of $\bar{\rho}_{max}$, although the influence of these two properties was not consistent across the tropical and subtropical assemblage (Fig. 4.3A). The amplification characteristics of the tropical assemblage were underpinned by patterns in larval settlement, whereas the corresponding characteristics in the subtropical assemblage were guided by patterns in recruit survival (see Appendix 3.2). Ultimately, these contrasting trends served to nullify the proportional contribution of recruitment dynamics towards variation in $\bar{\rho}_{max}$ between the tropical and subtropical populations.

Consequently, disparity in the dynamics of existing tropical and subtropical colonies, specifically their survival and fragmentation characteristics, underpinned the contrasting amplification capacities of their corresponding assemblages (Fig. 4.3B). Although variable, the relative contribution of colony survival towards variation in $\bar{\rho}_{max}$ decreased with increasing colony size, such that regional variation in the

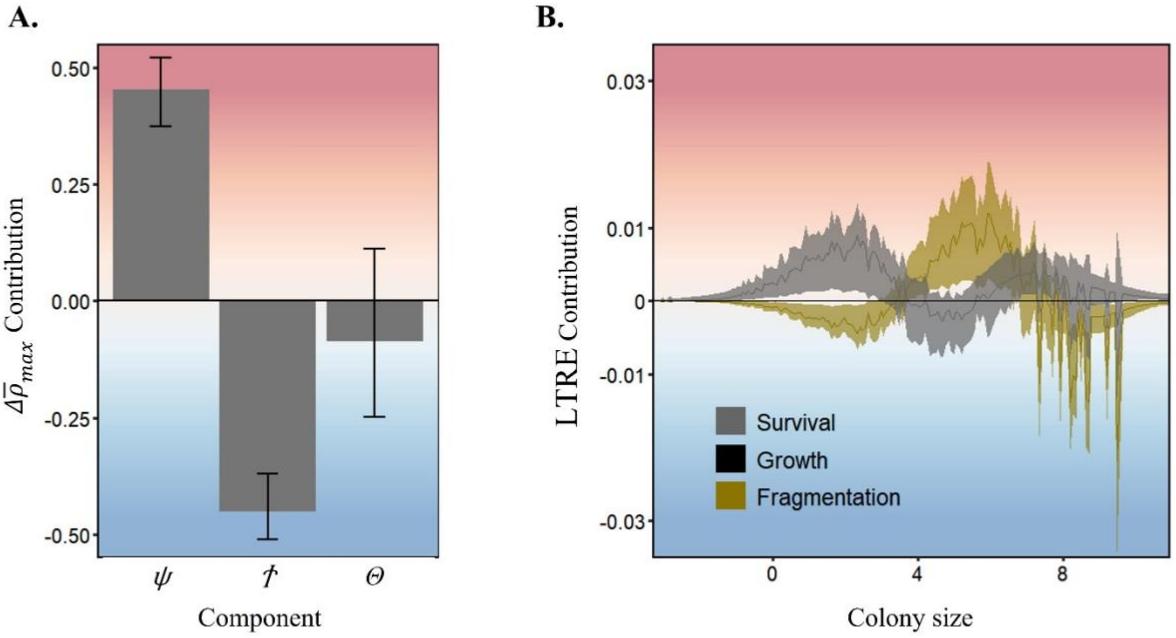

Figure 4.3. Size-specific patterns in colony survival and fragmentation underpin the varying amplification characteristics of the tropical and subtropical Acropora spp. assemblages. We used a transient Life Table Response Experiment to explore the vital rate contributions underpinning variation between the transient dynamics of tropical and subtropical *Acropora* spp. assemblages. **(A)** The proportional contribution of patterns in larval settlement (ψ), recruit survival (ϯ), and the vital rate schedules of existing colonies (Θ) towards differences in the maximal amplification characteristics between the two assemblages ($\Delta\bar{\rho}_{max}$). **(B)** The relative size-specific contributions of the vital rates of survival, growth, and fragmentation towards differences between the maximal amplification characteristics of the subtropical Acropora spp. assemblage compared with its tropical counterpart as a baseline. Solid lines represent mean contribution patterns. Across both panels, positive contributions reflect greater influence of a given vital rate towards the transient characteristic reported for the tropical assemblage (Red), whilst negative values reflect greater influence towards the subtropical assemblage (Blue). All error displayed represents the full range of observations observed across tropical and subtropical model variants.

survival patterns of colonies sized between 0.37 and 55 cm^2 (-1 to 4 cm^2 on the log scale) strongly influenced estimates of $\bar{\rho}_{max}$ (Fig 4.3B). Alternatively, the contribution of colony fragmentation towards variation in $\bar{\rho}_{max}$ increased with colony size, with the fragmentation patterns of large (>1097 cm^2, >7 cm^2 on the log scale) subtropical colonies serving to enhance the amplification capacity of their assemblage (Fig 4.3B). By contrast, the influence of colony growth characteristics on the transient amplification potential of either assemblage was negligible (Fig. 4.3B). Evidently, the enhanced amplification capacity of the subtropical coral assemblage is associated with the fragmentation characteristics of larger colonies. Meanwhile, the elevated survival of smaller tropical colonies, relative to subtropical colonies, serves to diminish the amplification potential of the tropical assemblage.

4.5. Discussion

Global climatic change is reassembling coral reef communities worldwide (Hughes *et al.* 2017, 2018). Accordingly, understanding the mechanisms underpinning the establishment and persistence of range-shifting coral species in subtropical and temperate locations is imperative for anticipating the future success or failure of global coral assemblages, and their continued provision of essential ecosystem services (Hoegh-Guldberg *et al.* 2017; Camp *et al.* 2018; Sommer *et al.* 2018). Comparing between the dynamics of tropical and subtropical *Acropora* spp. assemblages we reveal a higher asymptotic growth rate in the tropics. However, we illustrate that the expansion and endurance of a coral assemblage within a highly variable and comparatively stressful, subtropical environment corresponds with its superior capacity for amplified growth following disturbance compared to a down current tropical assemblage (Fig. 4.2). We also highlight how the transient dynamics of a subtropical *Acropora* spp. assemblage are contingent on the survival and fragmentation dynamics of existing colonies, highlighting key drivers underpinning the fitness of coral populations at higher latitudes. Recruitment had the largest overall effect on the dynamics of both the tropical and subtropical *Acropora* spp. assemblage. Yet, divergent larval settlement and recruit survival probabilities between the two assemblages ensures that the dynamics of existing colonies underpin the relative differences between their transient dynamics (Fig. 4.3). Overall, our findings here are consistent with insights from invasive populations whose transient demographic characteristics facilitate the colonisation of non-native environments (Iles *et al.* 2016;

Jelbert *et al.* 2019), evidencing mechanisms that shape the ability for coral species to shift their distributions into subtropical and temperate environments.

4.5.1. Transient versus asymptotic dynamics

Understanding within-species demographic variation across climatic gradients is essential for forecasting the success of populations at tracking favourable conditions and establishing themselves within novel environments (Merow *et al.* 2017). Our findings display an emergent latitudinal trade-off between the long-term viability and short-term exploitation potential of *Acropora* spp. assemblages in southern Japan. Similar divergent latitudinal patterns in stability and variability have been observed across various biological scales (Hillebrand *et al.* 2018; Antão *et al.* 2020), and are thought to underpin the vulnerability of lower-latitude populations to future climatic change (Barlow *et al.* 2018). Across tropical and subtropical *Acropora* spp. assemblages, asymptotic population growth was highest in the tropics, aligning with traditional expectations that population growth rates will decline towards species range boundaries as populations encounter increasingly demanding environments (Vucetich & Waite 2003). However, the strength and universal nature of this expectation is widely refuted (Sagarin & Gaines 2002; Sexton *et al.* 2009; Villellas *et al.* 2013). Instead, peripheral populations have been demonstrated to exhibit greater temporal variability in population growth rates (Villellas *et al.* 2013). Indeed, maximising transient amplification potential is considered a more beneficial strategy than prioritising long-term population growth for enhancing population persistence within unstable, marginal, environments (McDonald *et al.* 2016). Thus, whilst the tropical *Acropora* spp. assemblage appears more viable under stable conditions, the subtropical assemblage displays demographic strategies associated with the enhanced exploitation of more variable environments.

Peripheral populations inhabiting sub-optimal or more varied environments compared to core populations are becoming increasingly crucial for species persistence under climate change (Valladares *et al.* 2014). The mechanisms behind the long-term viability of coral populations at higher latitudes have long been disputed (Beger *et al.* 2014). At higher-latitudes coral populations are susceptible to bioerosion (Nozawa *et al.* 2008), thermal stress (Kim *et al.* 2019; Cant *et al.* 2021b), reproductive and genetic isolation (Thomas *et al.* 2017; Precoda *et al.* 2018; Nakabayashi *et al.*

2019), and are exposed to cooler, highly seasonal abiotic regimes, and reduced irradiance (Yamano *et al.* 2012; Muir *et al.* 2015; Sommer *et al.* 2017). However, legacies of exposure to variable environments affords populations with greater adaptive capacity, as abiotic variability cultivates and filters the traits necessary for the tolerance of further disturbances (Kroeker *et al.* 2020). In subtropical coral communities, the maintenance of diverse gene pools largely relies on their connectivity with up-current tropical reefs, a characteristic that is restricted in many of these systems (Noreen *et al.* 2009; Beger *et al.* 2014). However, sporadic larval supply into subtropical coral communities may benefit their adaptation to abiotic variability, preventing genetic swamping from tropical ecosystems that experience radically different selection pressures (Galipaud & Kokko 2020). However, as marginal populations become increasingly fragmented or isolated, their diminished genetic diversity inhibits their durability within variable environments (Pearson *et al.* 2009). Thus, although we have demonstrated that coral populations display the demographic plasticity necessary for exploiting more variable regimes, the continued success of high-latitude coral populations is likely contingent on continued support from core populations (Cant *et al.* 2021b).

4.5.2. Decomposing latitudinal contrasts within vital rate patterns

The size structure of coral populations has considerable repercussions on their dynamics and interactions within their wider reef communities (Dietzel *et al.* 2020; Pisapia *et al.* 2020). The heightened amplification characteristics we observed in the subtropical *Acropora* spp. assemblage were primarily supported by the survival and fragmentation patterns of larger individuals (Fig. 4.3). This pattern reflects our expectation that, with subtropical coral populations reliant on sporadic recruitment events, their endurance is conditional on the vital rates of existing colonies. Colony fragmentation is commonly observed within disturbed environments (Pisapia *et al.* 2019), and is a common trait amongst acroporid species enabling the rapid colonisation of available substrate (Roth *et al.* 2013). Indeed, the growth of colony remnants following fragmentation has been shown to support faster rates of recovery in coral cover than the growth of recruits and younger colonies of equal size (Connell 1997). Along tropicalising coastlines, colonisation through individual fragmentation could prove particularly effective, with rising temperatures and grazing tropical migrants reducing macroalgal competition (Vergés *et al.* 2016; Kumagai *et al.* 2018), and limited accretion reducing the density of existing coral communities (Kleypas *et al.* 1999). However, increased fragmentation also implies an accumulation of smaller sized colonies, and is attributed with the diminishing capacity for coral populations to persist during recurrent climatic disturbances (Riegl *et al.* 2012; Riegl & Purkis 2015; Pisapia *et al.* 2019).

It is not unusual for the dynamics of coral communities to revolve around the vital rates of the largest colonies (Dietzel *et al.* 2020), yet the reliance of subtropical *Acropora* spp. populations on the dynamics of larger individuals could render it sensitive to future climate shifts. In Japan, the frequency of severe typhoon storms is increasing (Hoshino *et al.* 2016). These storms are known to disproportionally impact upon the largest individuals within coral communities, particularly those with delicate tabular and branching structures such as *Acropora* spp. (Bries *et al.* 2004; Madin & Connolly 2006). During September 2018, Typhoon Jebi, possessing wind speeds upwards of 158km/h, made landfall along the southern coastline of Shikoku Island (Mori *et al.* 2019). This storm exerted considerable structural damage within the subtropical coral communities of Kochi (Cant, Cook & Reimer, 2019, *pers. obs.*), and is deemed responsible for a decline in mean colony size we observed within the subtropical *Acropora* spp. assemblage during 2019 (Appendix 3.1). The dominance of larger sized colonies in this subtropical assemblage (Appendix 3.1) suggests that this assemblage has successfully navigated past typhoon storms. However, with the intensity of future storms increasing (Hoshino *et al.* 2016), destructive events on the scale of Typhoon Jebi will become more frequent, possibly undermining the success of coral populations reliant on the characteristics of larger individuals.

Overall, differences between the transient dynamics of the tropical and subtropical *Acropora* spp. assemblages were underpinned by variation in the vital rate patterns of existing colonies. However, recruitment is a fundamental component in the dynamics and resilience of coral communities (Adjeroud *et al.* 2017). Accordingly, we observed that recruitment patterns actually exerted the largest absolute influence on the transient dynamics of the two populations, although this influence was masked by contrasting patterns in larval settlement and recruit survival (Fig. 4.3A). We observed that the settlement of *Acropora* spp. larvae was lower in the subtropics compared with the tropics. With abiotic barriers limiting the dispersal and survival of coral larvae at higher latitudes this pattern is to be expected (Nakabayashi *et al.* 2019), despite conflicting evidence of recent warming induced increases in the densities of settling subtropical larvae (Price *et al.* 2019). Intriguingly though, we report that the survival of coral larvae following successful settlement appeared highest in the subtropics. Whilst consistent with expected density dependant patterns in the survival of newly settled larvae (Cameron & Harrison 2020), our finding disagrees with previous reports of extremely high annual post-settlement larval mortality within a subtropical environment (Wilson & Harrison 2005). Seawater temperatures at the time of settlement influence the survival of coral larvae (Randall & Szmant 2009). Equally, acroporid corals are known to be highly sensitive to cold shock (short-term exposure to cold temperatures; Roth *et al.* 2012). Therefore, with our assessment of recruitment patterns reliant on settlement plates and plot surveys occurring during boreal summer months we acknowledge that our estimates of subtropical recruit survival may represent overestimates arising from the inclusion of individuals yet to experience the selective pressures of cooler subtropical seasons.

4.6. Conclusions

Understanding both the extent to which marginal populations can embrace environmental variation, and the mechanisms that underpin the success or failure of populations along range boundaries, is necessary if we are to anticipate the continued viability of crucial species, communities, and ecosystems (Valladares *et al.* 2014; Merow *et al.* 2017). Equally, distinguishing how vital rate characteristics manifest under differing environmental regimes will help resolve the climate envelopes of different species and ecosystems, allowing for more accurate predictions of population persistence or collapse (Trisos *et al.* 2020). Climatic warming is facilitating the poleward expansion of coral populations into subtropical coastal ecosystems (Beger *et al.* 2014; Vergés *et al.* 2019). The dynamics of coral populations establishing within tropicalising environments offer valuable insights into the ability of coral communities for persisting within suboptimal habitats and adapting to future, more variable, climates (Camp *et al.* 2018). However, our lack of an appreciation for the demographic characteristics of coral populations and their abiotic drivers (Edmunds *et al.* 2014; Edmunds & Riegl 2020) inhibits our capacity for exploring these insights.

The transient dynamics of populations define their responses to disturbance, and ultimately their dynamics within variable environments (Hastings 2004; Stott *et* *al.* 2011; McDonald *et al.* 2016; Hastings *et al.* 2018). Transient demographic theory has advanced our understanding of invasive potential, allowing us to forecast the ability of species to establish populations outside their core range (Iles *et al.* 2016; Merow *et al.* 2017; Jelbert *et al.* 2019). We have illustrated here how the transient dynamics of coral populations coordinate their establishment at higher latitudes, mediating their response to enhanced seasonal variation. Equally, *Acropora* spp. assemblages in southern Japan display the demographic plasticity necessary for the continued exploitation of higher latitude environments. However, with this work we have only begun to gather evidence of the mechanisms supporting the redistribution of coral populations. It is crucial we continue evaluating how patterns in the transient dynamics of coral populations translate across various species, and over broader spatial scales. Without improving current knowledge regarding the dynamics of coral populations we will be unable to predict the persistence and future reassembly of coral communities and their associated reef taxa (Edmunds & Riegl 2020; Pisapia *et al.* 2020; Cant *et al.* 2021a).

4.7. References

Adjeroud, M., Kayal, M. & Penin, L. (2017). Importance of recruitment processes in the dynamics and resilience of coral reef assemblages. In: *Marine Animal Forests: The Ecology of Benthic Biodiversity Hotspots* (eds. Rossi, S., Bramanti, L., Gori, A. & Orejas, C.). Springer International Publishing, Cham, pp. 549–569.

Angert, A.L. (2009). The niche, limits to species' distributions, and spatiotemporal variation in demography across the elevation ranges of two monkeyflowers. *Proc. Natl. Acad. Sci.*, 106, 19693–19698.

Antão, L.H., Pöyry, J., Leinonen, R. & Roslin, T. (2020). Contrasting latitudinal patterns in diversity and stability in a high-latitude species-rich moth community. *Glob. Ecol. Biogeogr.*, 29, 896–907.

Archibald, S.B., Bossert, W.H., Greenwood, D.R. & Farrell, B.D. (2010). Seasonality, the latitudinal gradient of diversity, and Eocene insects. *Paleobiology*, 36, 374–398.

Barlow, J., França, F., Gardner, T.A., Hicks, C.C., Lennox, G.D., Berenguer, E., *et* *al.* (2018). The future of hyperdiverse tropical ecosystems. *Nature*, 559, 517–526.

Beger, M., Sommer, B., Harrison, P.L., Smith, S.D.A. & Pandolfi, J.M. (2014). Conserving potential coral reef refuges at high latitudes. *Divers. Distrib.*, 20, 1–13.

Beissinger, S.R. & Westphal, M.I. (1998). On the use of demographic models of population viability in endangered species management. *J. Wildl. Manage.*, 62, 821–841.

Bramanti, L., Iannelli, M., Fan, T.Y. & Edmunds, P.J. (2015). Using demographic models to project the effects of climate change on scleractinian corals: Pocillopora damicornis as a case study. *Coral Reefs*, 34, 505–515.

Bries, J.M., Debrot, A.O. & Meyer, D.L. (2004). Damage to the leeward reefs of Curaçao and Bonaire, Netherlands Antilles from a rare storm event: Hurricane Lenny, November 1999. *Coral Reefs*, 23, 297–307.

Cameron, K.A. & Harrison, P.L. (2020). Density of coral larvae can influence settlement, post-settlement colony abundance and coral cover in larval restoration. *Sci. Rep.*, 10, 1–11.

Camp, E.F., Schoepf, V., Mumby, P.J., Hardtke, L.A., Rodolfo-Metalpa, R., Smith, D.J., *et al.* (2018). The future of coral reefs subject to rapid climate change: Lessons from natural extreme environments. *Front. Mar. Sci.*, 5, 1–21.

Cant, J., Salguero-Gómez, R. & Beger, M. (2021a). Transient demographic approaches can drastically expand the toolbox of coral reef science. *bioRxiv*, 2021.04.08.438926.

Cant, J., Salguero-Gómez, R., Kim, S.W., Sims, C.A., Sommer, B., Brooks, M., *et al.* (2021b). The projected degradation of subtropical coral assemblages by recurrent thermal stress. *J. Anim. Ecol.*, 90, 233–247.

Capdevila, P., Stott, I., Beger, M. & Salguero-Gómez, R. (2020). Towards a comparative framework of demographic resilience. *Trends Ecol. Evol.*, 35, 776–786.

Caswell, H. (2001). *Matrix population models: Construction, analysis and* *interpretation*. 2nd Edition. Oxford University Press Inc.

Caswell, H. (2019). *Sensitivity Analysis: Matrix Methods in Demography and Ecology*. Springer, Cham.

Connell, J.H. (1997). Disturbance and recovery of coral assemblages. *Coral Reefs*, 16, 101–113.

Crone, E.E., Menges, E.S., Ellis, M.M., Bell, T., Bierzychudek, P., Ehrlén, J., *et al.* (2011). How do plant ecologists use matrix population models? *Ecol. Lett.*, 14, 1–8.

Darling, E.S., McClanahan, T.R., Maina, J., Gurney, G.G., Graham, N.A.J., Januchowski-Hartley, F., *et al.* (2019). Social–environmental drivers inform strategic management of coral reefs in the Anthropocene. *Nat. Ecol. Evol.*, 3, 1341–1350.

Davidson, J., Thompson, A., Logan, M. & Schaffelke, B. (2019). High spatio-temporal variability in Acroporidae settlement to inshore reefs of the Great Barrier Reef. *PLoS One*, 14, 1–22.

Denis, V., Mezaki, T., Tanaka, K., Kuo, C.Y., de Palmas, S., Keshavmurthy, S., *et al.* (2013). Coverage, diversity, and functionality of a high-latitude coral community (Tatsukushi, Shikoku Island, Japan). *PLoS One*, 8, 1–9.

Dietzel, A., Bode, M., Connolly, S.R. & Hughes, T.P. (2020). Long-term shifts in the colony size structure of coral populations along the Great Barrier Reef. *Proc. R. Soc. B Biol. Sci.*, 287, 1–9.

Doropoulos, C., Roff, G., Bozec, Y., Zupan, M., Werminghausen, J. & Mumby, P.J. (2016). Characterizing the ecological trade-offs throughout the early ontogeny of coral recruitment. *Ecol. Monogr.*, 86, 20–44.

Easterling, M.R., Ellner, S.P. & Dixon, P.M. (2000). Size-specific sensitivity: applying a new structured population model. *Ecology*, 81, 694–708.

Edmunds, P.J. (2020). Vital rates of small reef corals are associated with variation in climate. *Limnol. Oceanogr.*, 1–13.

Edmunds, P.J., Burgess, S.C., Putnam, H.M., Baskett, M.L., Bramanti, L., Fabina, N.S., *et al.* (2014). Evaluating the causal basis of ecological success within the scleractinia: an integral projection model approach. *Mar. Biol.*, 161, 2719–2734.

Edmunds, P.J. & Riegl, B. (2020). Urgent need for coral demography in a world where corals are disappearing. *Mar. Ecol. Prog. Ser.*, 635, 233–242.

Ellis, M.M. & Crone, E.E. (2013). The role of transient dynamics in stochastic population growth for nine perennial plants. *Ecology*, 94, 1681–1686.

Ellner, S.P. & Rees, M. (2006). Integral projection models for species with complex demography. *Am. Nat.*, 167, 410–428.

Ezard, T.H.G., Bullock, J.M., Dalgleish, H.J., Millon, A., Pelletier, F., Ozgul, A., *et al.* (2010). Matrix models for a changeable world: The importance of transient dynamics in population management. *J. Appl. Ecol.*, 47, 515–523.

Fine, P.V.A. (2015). Ecological and evolutionary drivers of geographic variation in species diversity. *Annu. Rev. Ecol. Evol. Syst.*, 46, 369–392.

Fukami, H., Budd, A.F., Paulay, G., Solé -Cava, A., Chen, C.A., Iwao, K., *et al.* (2004). Conventional taxonomy obscures deep divergence between Pacific and Atlantic corals. *Nature*, 427, 829–832.

Galipaud, M. & Kokko, H. (2020). Adaptation and plasticity in life-history theory: How to derive predictions. *Evol. Hum. Behav.*, 41, 493–501.

Gilmour, J., Speed, C.W. & Babcock, R. (2016). Coral reproduction in Western Australia. *PeerJ*, 1–43.

Hall, V.R. & Hughes, T.P. (1996). Reproductive strategies of modular organisms: Comparative studies of reef-building corals. *Ecology*, 77, 950–963.

Hastings, A. (2001). Transient dynamics and persistence of ecological systems. *Ecol. Lett.*, 4, 215–220.

Hastings, A. (2004). Transients: The key to long-term ecological understanding? *Trends Ecol. Evol.*, 19, 39–45.

Hastings, A., Abbott, K.C., Cuddington, K., Francis, T., Gellner, G., Lai, Y.C., *et al.* (2018). Transient phenomena in ecology. *Science*, 361, 1–9.

Healy, K., Ezard, T.H.G., Jones, O.R., Salguero-Gómez, R. & Buckley, Y.M. (2019). Animal life history is shaped by the pace of life and the distribution of age-specific mortality and reproduction. *Nat. Ecol. Evol.*, 3, 1217–1224.

Hillebrand, H. (2004). On the generality of the latitudinal diversity gradient. *Am. Nat.*, 163, 192–211.

Hillebrand, H., Blasius, B., Borer, E.T., Chase, J.M., Downing, J.A., Eriksson, B.K., *et al.* (2018). Biodiversity change is uncoupled from species richness trends: Consequences for conservation and monitoring. *J. Appl. Ecol.*, 55, 169–184.

Hodgson, D., McDonald, J.L. & Hosken, D.J. (2015). What do you mean, “resilient”? *Trends Ecol. Evol.*, 30, 503–506.

Hoegh-Guldberg, O., Poloczanska, E.S., Skirving, W. & Dove, S. (2017). Coral reef ecosystems under climate change and ocean acidification. *Front. Mar. Sci.*, 4, 1–20.

Hoshino, S., Esteban, M., Mikami, T., Takagi, H. & Shibayama, T. (2016). Estimation of increase in storm surge damage due to climate change and sea level rise in the Greater Tokyo area. *Nat. Hazards*, 80, 539–565.

Hughes, T.P., Baird, A.H., Dinsdale, E.A., Moltschaniwskyj, N.A., Pratchett, M.S., Tanner, J.E., *et al.* (2000). Supply-side ecology works both ways: The link between benthic adults, fecundity, and larval recruits. *Ecology*, 81, 2241–2249.

Hughes, T.P., Barnes, M.L., Bellwood, D.R., Cinner, J.E., Cumming, G.S., Jackson, J.B.C., *et al.* (2017). Coral reefs in the Anthropocene. *Nature*, 546, 82–90.

Hughes, T.P., Kerry, J.T., Baird, A.H., Connolly, S.R., Dietzel, A., Eakin, C.M., *et al.* (2018). Global warming transforms coral reef assemblages. *Nature*, 556, 492–496.

von Humboldt, A. (1808). *Ansichten der Natur: mit wissenschaftlichen Erläuterungen*. J. G. Cotta, Tübingen, Germany.

Iles, D.T., Salguero-Gómez, R., Adler, P.B. & Koons, D.N. (2016). Linking transient dynamics and life history to biological invasion success. *J. Ecol.*, 104, 399–408.

Janzen, D.H. (1967). Why mountain passes are higher in the tropics. *Am. Nat.*, 101, 233–249.

Jelbert, K., Buss, D., McDonald, J., Townley, S., Franco, M., Stott, I., *et al.* (2019). Demographic amplification is a predictor of invasiveness among plants. *Nat. Commun.*, 10, 1–6.

Keyfitz, N. (1968). *Introduction to the mathematics of population*. Addison-Wesley Publishing Co., Reading, Massachusetts, USA.

Kim, W.S., Sampayo, M.E., Sims A. C., Sommer, B., Gómez-Cabrera, M.C., Dalton, S.J., *et al.* (2019). Refugia under threat: Mass bleaching of coral assemblages in high-latitude eastern Australia. *Glob. Chang. Biol.*, 25, 3918–3931.

Kitagawa, E.M. (1955). Components of a difference between two rates. *J. Am. Stat. Assoc.*, 50, 1168–1194.

Kleypas, J.A., Mcmanusi, J.W. & Menez, L.A.B. (1999). Environmental limits to coral reef development: Where do we draw the line? *Am. Zool.*, 39, 146–15.

Koons, D.N., Iles, D.T., Schaub, M. & Caswell, H. (2016). A life-history perspective on the demographic drivers of structured population dynamics in changing environments. *Ecol. Lett.*, 19, 1023–1031.

Kroeker, K.E., Bell, L.E., Donham, E.M., Hoshijima, U., Lummis, S., Toy, J.A., *et al.* (2020). Ecological change in dynamic environments: Accounting for temporal environmental variability in studies of ocean change biology. *Glob. Chang. Biol.*, 26, 54–67.

Kumagai, N.H., Molinos, J.G., Yamano, H., Takao, S., Fujii, M. & Yamanaka, Y. (2018). Ocean currents and herbivory drive macroalgae-to-coral community shift under climate warming. *Proc. Natl. Acad. Sci.*, 115, 8990–8995.

Layton-Matthews, K., Grøtan, V., Hansen, B.B., Loonen, M.J.J.E., Fuglei, E. & Childs, D.Z. (2021). Environmental change reduces body condition, but not population growth, in a high-arctic herbivore. *Ecol. Lett.*, 24, 227–238.

Madin, J.S., Baird, A.H., Baskett, M.L., Connolly, S.R. & Dornelas, M.A. (2020). Partitioning colony size variation into growth and partial mortality. *Biol. Lett.*, 16, 1–5.

Madin, J.S. & Connolly, S.R. (2006). Ecological consequences of major hydrodynamic disturbances on coral reefs. *Nature*, 444, 477–480.

Maldonado-Chaparro, A.A., Blumstein, D.T., Armitage, K.B. & Childs, D.Z. (2018). Transient LTRE analysis reveals the demographic and trait-mediated processes that buffer population growth. *Ecol. Lett.*, 21, 1693–1703.

Mannion, P.D., Upchurch, P., Benson, R.B.J. & Goswami, A. (2014). The latitudinal biodiversity gradient through deep time. *Trends Ecol. Evol.*, 29, 42–50.

McDonald, J.L., Stott, I., Townley, S. & Hodgson, D.J. (2016). Transients drive the demographic dynamics of plant populations in variable environments. *J. Ecol.*, 104, 306–314.

Merow, C., Bois, S.T., Allen, J.M., Xie, Y. & Silander, J.A. (2017). Climate change both facilitates and inhibits invasive plant ranges in New England. *Proc. Natl. Acad. Sci.*, 114, 1–9.

Mori, N., Yasuda, T., Arikawa, T., Kataoka, T., Nakajo, S., Suzuki, K., *et al.* (2019). 2018 Typhoon Jebi post-event survey of coastal damage in the Kansai region, Japan. *Coast. Eng. J.*, 61, 278–294.

Muir, P., Wallace, C.., Done, T. & Aguirre, J.D. (2015). Limited scope for latitudinal extension of reef corals. *Science*, 348, 1135–1138.

Nakabayashi, A., Yamakita, T., Nakamura, T., Aizawa, H., Kitano, Y.F., Iguchi, A., *et al.* (2019). The potential role of temperate Japanese regions as refugia for the coral Acropora hyacinthus in the face of climate change. *Sci. Rep.*, 9, 1–12.

Nakamura, M., Kumagai, N.H., Sakai, K., Okaji, K., Ogasawara, K. & Mitarai, S. (2015). Spatial variability in recruitment of acroporid corals and predatory starfish along the Onna coast, Okinawa, Japan. *Mar. Ecol. Prog. Ser.*, 540, 1–12.

Nishihira, M. & Veron, J.E.N. (1995). *Hermatypic corals of Japan*. Kaiyusha, Tokyo, Japan.

Noreen, A.M.E., Harrison, P.L. & van Oppen, M.J.H. (2009). Genetic diversity and connectivity in a brooding reef coral at the limit of its distribution. *Proc. R. Soc. B Biol. Sci.*, 276, 3927–3935.

Nozawa, Y., Tokeshi, M. & Nojima, S. (2008). Structure and dynamics of a high-latitude scleractinian coral community in Amakusa, southwestern Japan. *Mar. Ecol. Prog. Ser.*, 358, 151–160.

Paniw, M., Ozgul, A. & Salguero-Gómez, R. (2018). Interactive life-history traits predict sensitivity of plants and animals to temporal autocorrelation. *Ecol. Lett.*, 21, 275–286.

Pearson, G.A., Lago-Leston, A. & Mota, C. (2009). Frayed at the edges: Selective pressure and adaptive response to abiotic stressors are mismatched in low diversity edge populations. *J. Ecol.*, 97, 450–462.

Pecl, G., Araujo, M.B., Bell, J.D., Blanchard, J. & Bonebrake, T.C. (2017). Biodiversity redistribution under climate change: Impacts on ecosystems and human well-being Publication Details. *Science*, 355, 1–9.

Pisapia, C., Burn, D. & Pratchett, M.S. (2019). Changes in the population and community structure of corals during recent disturbances (February 2016-October 2017) on Maldivian coral reefs. *Sci. Rep.*, 9, 1–12.

Pisapia, C., Edmunds, P.J., Moeller, H. V., Riegl, B.M., McWilliam, M., Wells, C.D., *et al.* (2020). Projected shifts in coral size structure in the Anthropocene. In: *Advances in Marine Biology*. Academic Press, pp. 31–60.

Poincaré, H. (1885). Sur l'équilibre d'une masse fluide animée d'un movement de rotation. *Acta Math.*, 7, 259–380.

Precoda, K., Baird, A.H., Madsen, A., Mizerek, T., Sommer, B., Su, S.N., *et al.* (2018). How does a widespread reef coral maintain a population in an isolated environment? *Mar. Ecol. Prog. Ser.*, 594, 85–94.

Price, N.N., Muko, S., Legendre, L., Steneck, R., Van Oppen, M.J.H., Albright, R., *et al.* (2019). Global biogeography of coral recruitment: Tropical decline and subtropical increase. *Mar. Ecol. Prog. Ser.*, 621, 1–17.

Purves, D.W. (2009). The demography of range boundaries versus range cores in eastern US tree species. *Proc. R. Soc. B Biol. Sci.*, 276, 1477–1484.

Randall, C.J. & Szmant, A.M. (2009). Elevated temperature reduces survivorship and settlement of the larvae of the Caribbean scleractinian coral, Favia fragum (Esper). *Coral Reefs*, 28, 537–545.

Richards, Z.T., Berry, O. & van Oppen, M.J.H. (2016). Cryptic genetic divergence within threatened species of Acropora coral from the Indian and Pacific Oceans. *Conserv. Genet.*, 17, 577–591.

Richards, Z.T. & Hobbs, J.P.A. (2015). Hybridisation on coral reefs and the conservation of evolutionary novelty. *Curr. Zool.*, 61, 132–145.

Riegl, B. & Purkis, S. (2015). Coral population dynamics across consecutive mass mortality events. *Glob. Chang. Biol.*, 21, 3995–4005.

Riegl, B.M., Bruckner, A.W., Rowlands, G.P., Purkis, S.J. & Renaud, P. (2012). Red Sea coral reef trajectories over 2 decades suggest increasing community homogenization and decline in coral size. *PLoS One*, 7, 1–7.

Roth, L., Muller, E.M. & Van Woesik, R. (2013). Tracking Acropora fragmentation and population structure through thermal-stress events. *Ecol. Modell.*, 263, 223–232.

Roth, M.S., Goericke, R. & Deheyn, D.D. (2012). Cold induces acute stress but heat is ultimately more deleterious for the reef-building coral Acropora yongei. *Sci. Rep.*, 2, 1–5.

Sagarin, R.D. & Gaines, S.D. (2002). The “abundant centre” distribution: to what extent is it a biogeographical rule? *Ecol. Lett.*, 5, 137–147.

Selwood, K.E., Mcgeoch, M.A. & Mac Nally, R. (2015). The effects of climate change and land-use change on demographic rates and population viability. *Biol. Rev.*, 90, 837–853.

Sexton, J.P., McIntyre, P.J., Angert, A.L. & Rice, K.J. (2009). Evolution and ecology of species range limits. *Annu. Rev. Ecol. Evol. Syst.*, 40, 415–436.

Shlesinger, T. & van Woesik, R. (2021). Different population trajectories of two reef-building corals with similar life-history traits. *J. Anim. Ecol.*, 90, 1379–1389.

Sommer, B., Beger, M., Harrison, P.L., Babcock, R.C. & Pandolfi, J.M. (2018). Differential response to abiotic stress controls species distributions at biogeographic transition zones. *Ecography*, 41, 478–490.

Sommer, B., Sampayo, E.M., Beger, M., Harrison, P.L., Babcock, R.C. & Pandolfi, J.M. (2017). Local and regional controls of phylogenetic structure at the high-latitude range limits of corals. *Proc. R. Soc. Biol. Sci. Ser. B*, 284, 1–13.

Stott, I., Hodgson, D.J. & Townley, S. (2012). Popdemo: An R package for population demography using projection matrix analysis. *Methods Ecol. Evol.*, 3, 797–802.

Stott, I., Townley, S. & Hodgson, D. (2011). A framework for studying transient dynamics of population projection matrix models. *Ecol. Lett.*, 14, 959–970.

Thomas, L., Kennington, W.J., Evans, R.D., Kendrick, G.A. & Stat, M. (2017). Restricted gene flow and local adaptation highlight the vulnerability of high-latitude reefs to rapid environmental change. *Glob. Chang. Biol.*, 23, 2197–2205.

Trisos, C.H., Merow, C. & Pigot, A.L. (2020). The projected timing of abrupt ecological disruption from climate change. *Nature*, 580, 496–501.

Valladares, F., Matesanz, S., Guilhaumon, F., Araújo, M.B., Balaguer, L., Benito-Garzón, M., *et al.* (2014). The effects of phenotypic plasticity and local adaptation on forecasts of species range shifts under climate change. *Ecol. Lett.*, 17, 1351–1364.

Vergés, A., Doropoulos, C., Malcolm, H.A., Skye, M., Garcia-Pizá, M., Marzinelli, E.M., *et al.* (2016). Long-term empirical evidence of ocean warming leading to tropicalization of fish communities, increased herbivory, and loss of kelp. *Proc. Natl. Acad. Sci.*, 113, 13791–13796.

Vergés, A., McCosker, E., Mayer-Pinto, M., Coleman, M.A., Wernberg, T., Ainsworth, T., *et al.* (2019). Tropicalisation of temperate reefs: Implications for ecosystem functions and management actions. *Funct. Ecol.*, 1–14.

Vergés, A., Steinberg, P.D., Hay, M.E., Poore, A.G.B., Campbell, A.H., Ballesteros, E., *et al.* (2014). The tropicalization of temperate marine ecosystems: climate-mediated changes in herbivory and community phase shifts. *Proc. R. Soc. B*, 281, 1–10.

Vermeij, M.J.A., Smith, J.E., Smith, C.M., Vega Thurber, R. & Sandin, S.A. (2009). Survival and settlement success of coral planulae: Independent and synergistic effects of macroalgae and microbes. *Oecologia*, 159, 325–336.

Veron, J.E.N., Stafford-Smith, M.G., Turak, E. & DeVantier, L.M. (2016). *Corals of the World*. Available at: http://www.coralsoftheworld.org/page/home/. Last accessed 12 November 2019.

Villellas, J., Morris, W.F. & García, M.B. (2013). Variation in stochastic demography between and within central and peripheral regions in a widespread short-lived herb. *Ecology*, 94, 1378–1388.

Vucetich, J.A. & Waite, T.A. (2003). Spatial patterns of demography and genetic processes across the species' range: Null hypotheses for landscape conservation genetics. *Conserv. Genet.*, 4, 639–645.

Williams, J.E. & Blois, J.L. (2018). Range shifts in response to past and future climate change: Can climate velocities and species' dispersal capabilities explain variation in mammalian range shifts? *J. Biogeogr.*, 45, 2175–2189.

Williams, J.L., Miller, T.E.X. & Ellner, S.P. (2012). Avoiding unintentional eviction from integral projection models. *Ecology*, 93, 2008–2014.

Willig, M.R., Kaufman, D.M. & Stevens, R.D. (2003). Latitudinal gradients of biodiversity: Pattern, process, scale, and synthesis. *Annu. Rev. Ecol. Evol. Syst.*, 34, 273–309.

Wilson, J. & Harrison, P. (2005). Post-settlement mortality and growth of newly settled reef corals in a subtropical environment. *Coral Reefs*, 24, 418–421.

Yamano, H., Sugihara, K., Watanabe, T., Shimamura, M. & Hyeong, K. (2012). Coral reefs at 34°N, Japan: Exploring the end of environmental gradients. *Geology*, 40, 835–838.

Zuidema, P.A., Jongejans, E., Chien, P.D., During, H.J. & Schieving, F. (2010). Integral projection models for trees: A new parameterization method and a validation of model output. *J. Ecol.*, 98, 345–355.

Chapter 4

Coral assemblages at higher latitudes favour short-term potential over long-term performance

James Cant[1], James D. Reimer[2,3], Brigitte Sommer[4], Katie Cook[1], Sun W. Kim[5], Carrie A. Sims[5], Takuma Mezaki[6], Cliodhna O'Flaherty[1], Maxine Brooks[1], Hamish A. Malcolm[7], John M. Pandolfi[5], Roberto Salguero-Gómez[8,9,10], Maria Beger[1,9]

1. School of Biology, Faculty of Biological Sciences, University of Leeds, Leeds, LS2 9JT United Kingdom.
2. Molecular Invertebrate Systematics and Ecology Laboratory, Graduate School of Engineering and Science, University of the Ryukyus, Nishihara, Okinawa, Japan.
3. Tropical Biosphere Research Centre, University of the Ryukyus, Nishihara, Okinawa, Japan.
4. School of Life and Environmental Science, University of Sydney, Camperdown, NSW 2006, Australia.
5. Australian Research Council Centre of Excellence for Coral Reef Studies, School of Biological Sciences, The University of Queensland, Brisbane, QLD 4072, Australia.
6. Kuroshio Biological Research Foundation, Nishidomari, Otsuki-cho, Kochi, Japan.
7. Solitary Islands Marine Park, Department of Primary Industries, Coffs Harbour, NSW 2450, Australia.
8. Department of Zoology, University of Oxford, Oxford, 11a Mansfield Rd, OX1 3SZ United Kingdom.
9. Centre for Biodiversity and Conservation Science, School of Biological Sciences, University of Queensland, Brisbane, QLD, 4072 Australia.
10. Max Planck Institute for Demographic Research, Konrad Zuße Straße 1, 18057 Rostock, Germany.

In preparation for Proceedings of the National Academy of Sciences and available as a preprint on BioRxiv at https://doi.org/10.1101/2021.09.29.462350.

Coral assemblages at higher latitudes favour short-term potential over long-term performance

5.1. Abstract

The current exposure of species assemblages to high environmental variability may grant them resilience to future increases in climatic variability. In globally threatened coral reef ecosystems, management seeks to protect resilient reefs within variable environments. Yet, our lack of understanding for the determinants of coral population performance within variable environments hinders forecasting the future reassembly of global coral communities. Here, using Integral Projection Models, we compare the short- (*i.e.*, transient) and long-term (*i.e.*, asymptotic) demographic characteristics of tropical and subtropical coral assemblages to evaluate how thermal variability influences the structural composition of coral communities over time. Exploring spatial variation across the dynamics of functionally different competitive, stress-tolerant, and weedy coral assemblages in Australia and Japan, we illustrate that coral populations trade-off long-term performance for transient potential in response to exposure to thermal variability. We illustrate how, by exploiting volatile short-term demographic strategies, coral assemblages can reduce their susceptibility towards environmental variation, thus enhancing their persistence within variable environments. However, we also reveal considerable variation across the vulnerability of competitive, stress-tolerant, and weedy coral assemblages towards future increases in thermal variability, with stress-tolerant and weedy corals possessing an enhanced capacity for elevating their transient potential in response to environmental variability. Accordingly, despite their current exposure to high thermal variability, future climatic shifts threaten the structural complexity of coral assemblages, derived mostly from competitive coral taxa within highly variable subtropical environments, emulating the degradation expected across global coral communities.

5.2. Introduction

Coral reefs worldwide are threatened by unprecedented climatic and anthropogenic disruption (Hughes *et al.* 2018, 2019). The conservation of coral reef ecosystems now relies on enhancing the resilience of coral communities, specifically their capacity to resist and recover from increased climatic variability (Kleypas *et al.* 2021; McLeod *et al.* 2021). Changes in environmental regimes provoke spatial shifts in the performance and distribution of populations, which ultimately upscale to the compositional reassembly of biological communities (Totland & Nyléhn 1998; Pecl *et al.* 2017). Exposure to increased variability is, however, expected to indirectly augment the capacity for populations to resist and recover from repeated disturbances (Boyd *et al.* 2016; Rivest *et al.* 2017). Yet, nuanced interactions between population characteristics and biophysical conditions ensure inconsistent responses towards climate shifts, even across populations within the same region (Parmesan & Yohe 2003; Chen *et al.* 2011). For instance, differential sensitivities to habitat change can accelerate or reverse expected poleward range shifts in response to climate warming (Chen *et al.* 2011). Thus, anticipating the future resilience of natural communities requires understanding the collective vulnerabilities of their constituent populations (Williams *et al.* 2008) and the determinants underpinning their resilience to increasing environmental variability (Vázquez *et al.* 2017; Iles *et al.* 2019). However, regional variations in the response of coral assemblages to climatic disturbances have generated misconceptions in our interpretation of the status of coral communities worldwide, with global population sizes of many species perhaps larger than previously anticipated (Dietzel *et al.* 2021). Only by linking the mechanisms underpinning heterospecific variation across the responses of populations to environmental variability can one predict the resilience of biological communities to increased climatic variability (Williams *et al.* 2008; Dawson *et al.* 2011; Foden *et al.* 2013). Evidently, to accurately forecast the ongoing reassembly of global coral communities we must improve our understanding for how environmental variability shapes coral population performance across community- and regional-scales (Rivest *et al.* 2017).

To explore the performance of populations exposed to recurrent disturbances within variable environments, one needs to consider their transient (*i.e.*, short-term) dynamics (Hastings 2004; Ezard *et al.* 2010; Hastings *et al.* 2018; Cant *et al.* 2021b). Yet, the asymptotic (*i.e.*, long-term) population growth rate (λ), a metric that describes temporal changes in population size at stationary equilibrium (Caswell 2001), is the predominant metric used to quantify population performance (Caswell 2001; Crone *et al.* 2011). In reality, though, natural populations are exposed to repeated disturbances that favour the persistence of transient conditions, preventing the emergence of stationary equilibria (Hastings 2001, 2004; Hastings *et al.* 2018). Within variable environments, repeated disturbances impose short-term changes upon the structure of populations that can elevate (*amplification*) or diminish (*attenuation*) their growth rates, resulting in population performance characteristics deviating from long-term expectations (Ezard *et al.* 2010; Stott *et al.* 2011). Quantifying how transient population performance deviates from long-term expectations (henceforth *transient potential*) is therefore crucial for predicting the success or failure of natural populations (Koons *et al.* 2005); an approach that remains neglected within coral research (Cant *et al.* 2021b).

Located at the intersection of tropical and temperate ecoregions, subtropical coral communities provide an opportunity for evaluating the abiotic determinants of coral population performance (Beger *et al.* 2014; Camp *et al.* 2018; Burt *et al.* 2020). Over recent decades, subtropical coral communities have undergone transformation with various coral taxa undergoing poleward range expansions in response to shifting thermal regimes (Precht & Aronson 2004; Yamano *et al.* 2011; Baird *et al.* 2012; Tuckett *et al.* 2017; Booth & Sears 2018). However, at higher latitudes, coral communities are exposed to enhanced seasonality and cooler winter temperatures, and thus experience greater abiotic variability relative to their tropical reef counterparts (Yamano *et al.* 2012; Sommer *et al.* 2014, 2017). Over time, the persistence of populations within stable environments logically diminishes their capacity for tolerating novel environmental states, thus reducing their resilience towards future climatic shifts (Boyd *et al.* 2016). Consequently, the endurance of subtropical coral communities within variable high-latitude environments is expected to enhance their abiotic resilience (Rivest *et al.* 2017). Indeed, as seen across other communities (McDonald *et al.* 2016), enhanced transient potential can elevate the performance of acroporid coral populations within variable subtropical environments (Cant *et al.* 2021a). Yet, without knowledge for how hetero- and conspecific coral populations utilise demographic strategies to mediate their performance in response to local environmental variability, we will be unable to forecast the impacts of increasing climatic variability on the composition of global coral communities.

In species rich ecosystems, evaluating the dynamics of communities requires a trait-based approach to condense vast quantities of demographic detail (Chalmandrier *et al.* 2021). Considering the diversity of coral reef ecosystems, exploring patterns across the demographic characteristics of cooccurring coral species presents a logistical challenge (Madin *et al.* 2016b). Yet, this is a challenge that can be navigated by pooling individuals based on shared trait characteristics. Morphological, physiological and phenological functional traits influence the fitness of individuals and thus determine the demographic characteristics of their populations (Violle *et al.* 2007), their responses to disturbances (Grime & Pierce 2012), and subsequently the assembly of biological communities (McGill *et al.* 2006; Cadotte *et al.* 2011; Falster *et al.* 2017). Indeed, functional trait characteristics impact upon the demographic properties of coral populations (e.g., colony growth and reproduction; Madin *et al.* [2012]; Álvarez-Noriega *et al.* [2016]), mediating their ability to respond to local abiotic patterns (Sommer *et al.* 2014). Given such strong links between coral traits and demographic performance, the categorisation of coral taxa into competitive, stress tolerant, generalist and weedy life history assemblages (*sensu* Darling *et al.* 2012) is used to evaluate broadscale patterns in coral community reassembly (Darling *et al.* 2013, 2019; Zinke *et al.* 2018). The trait-based assessment of coral community assembly can also offer greater insight into the wider implications of ongoing community shifts, thereby aiding the management of critical coral reef ecosystems (Darling *et al.* 2019).

Here, we investigate how the performance characteristics of coral populations map onto patterns of environmental variability across assemblages of competitive, stress-tolerant, and weedy coral taxa. Using Integral Projection Models (IPMs; Easterling *et al.* 2000), we quantify the association between different dimensions of thermal variability (monthly mean sea surface temperature [SST], monthly SST variance, and monthly SST frequency spectrum) and the transient potential and long-term performance characteristics of tropical and subtropical coral assemblages in southern Japan and eastern Australia (Fig. 5.1). Specifically, we anticipate that, in accordance with their exposure to elevated thermal variability, subtropical coral assemblages will possess greater transient potential in comparison to tropical

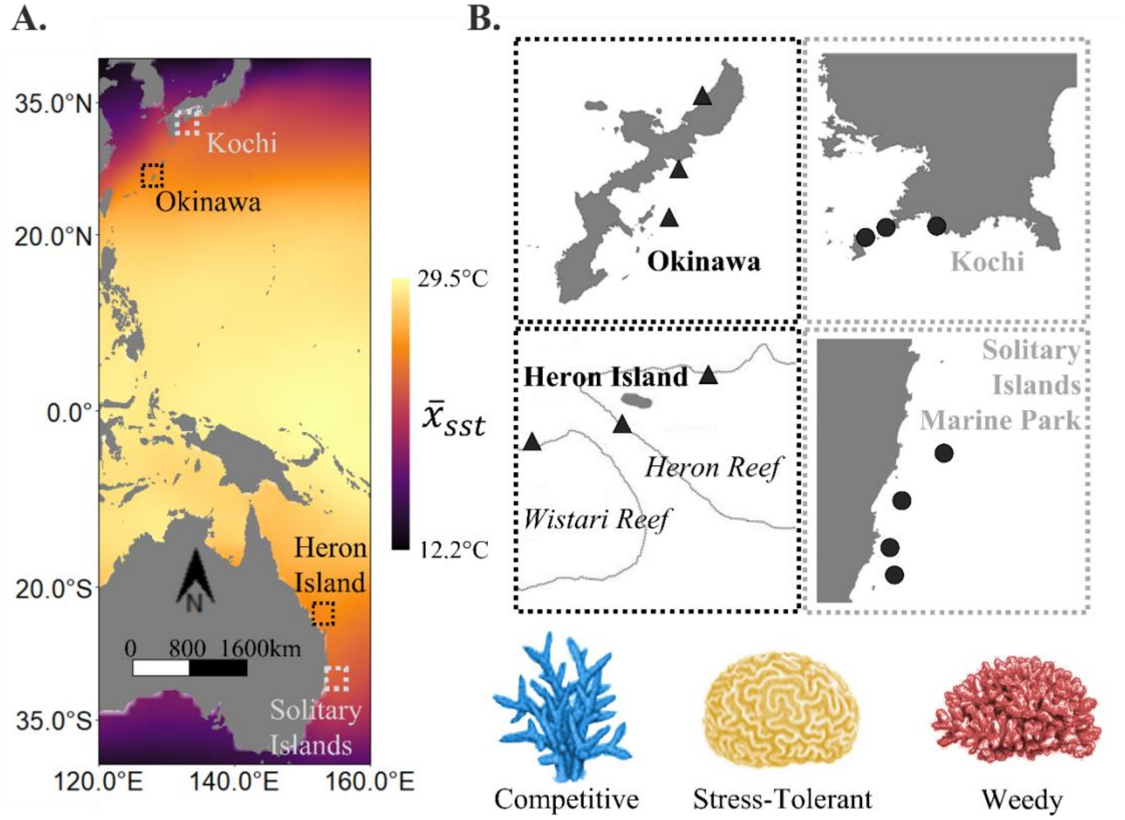

Figure 5.1. Using repeated annual surveys of tagged individual colonies, conducted between 2016 and 2019, we quantified the influence of environmental variability on the long-term performance and transient potential of tropical and subtropical coral populations in southern Japan and eastern Australia. **(A)** As climate shifts induce range expansions in many coral species worldwide, their populations are increasingly exposed to a gradient in thermal regimes, illustrated here by mean monthly sea surface temperatures ($\bar{x}_{sst}$; °C) recorded between 1950 and 2019 (Rayner *et al.* 2003). **(B)** To explore spatial patterns in the long-term performance and transient (*i.e.*, short-term) potential of coral populations exposed to varying thermal regimes, we constructed Integral Projection Models (IPMs) describing the dynamics of tropical and subtropical assemblages of competitive, stress-tolerant, and weedy coral taxa. To parameterise these models, between 2016 and 2019 we documented the survival, growth, fragmentation, and recruitment patterns of 3171 tagged individual colonies within the tropical reef communities (▲) of Okinawa (Japan) and Heron Island (Australia), and within the subtropical coral communities (●) of Kochi (Japan) and the Solitary Islands Marine Park (Australia).

conspecifics. We expect that this pattern will persist irrespective of functional strategy, corresponding with the need for subtropical coral populations to exploit periodically disturbed environments.

5.3. Methods

5.3.1. Modelling population dynamics

Integral Projection Models (IPMs) capture the influences of the state composition of individuals on the performance of populations over discrete time periods (t to $t+1$; Easterling *et al.* 2000). Here, to quantify the long-term performance characteristics and transient (short-term) potential of coral populations, we used IPMs describing patterns in colony survival (σ), transitions in size (growth and shrinkage, γ), fragmentation probability (κ), fecundity (φ), and recruitment (ϕ), each as function of colony size (z; visible horizontal surface area, cm^2). Specifically, our IPMs took the form

$$n[z', t+1] = \int_L^U (P_{Z'Z} + F_{Z'Z}\, n[z,t]\, \delta z) \tag{5.1}$$

$$P_{Z'Z} = (1 - \kappa_Z)\, \sigma_Z\, \gamma_{Z'Z} + (\kappa_Z\, \kappa b_Z\, \kappa_Z^0) \tag{5.2}$$

$$F_{Z'Z} = \varphi_Z\, \phi C_1 \tag{5.3}$$

with [L, U] representing the range of possible colony sizes; calculated as 10% above and below observed maximum and minimum colony sizes to avoid accidental eviction (Williams *et al.* 2012). Accordingly, the structure of a population at time $t+1$ ($n[z', t+1]$) is a product of its structure at time t ($n[z', t]$) subject to the survival (σ_Z) and transition of individual colonies from size z to size z' ($\gamma_{z'z}$); the probability of colony fragmentation (κ_Z) and the number (κb_Z) and size distribution of any colony remnants produced (κ_Z^0); and colony fecundity (φ_Z) combined with the probability of successful recruitment (ϕ) and the size distribution of surviving recruits (C_1).

5.3.2. Data Collection

We parameterised our IPMs using data collected during repeated annual surveys of 3171 tagged colonies within tropical and subtropical coral communities in southern Japan and eastern Australia, conducted between 2016 and 2019 (Fig. 5.1; Appendix 4.1). We tagged individual colonies using permanent plots arranged haphazardly throughout four focal coral communities (Australian subtropics [AS], Australian tropics [AT], Japanese subtropics [JS], Japanese tropics [JT]) and demarcated with numbered tags (Cant *et al.* 2021c, a). All tagged colonies were identified *in-situ* to the lowest possible taxonomic level (either genus or species). No samples were taken from tagged colonies, as although this would have allowed us to resolve species identity, we wanted to avoid any lasting interference with the processes of colony survival, growth, and fragmentation.

To facilitate comparing population characteristics observed across spatially distinct regions in Australia and Japan with varying degrees of species overlap (Veron *et al.* 2016), we grouped tagged colonies across each region into assemblages according to shared morphological functional traits (*sensu* Darling *et al.* 2012, 2013; Zinke *et al.* 2018). We categorised colonies as competitive, weedy, stress-tolerant or generalist following the genera classification specifications of Darling *et al.* (2012), with minor adaptions made based on local expertise (see Appendix 4.2 for a detailed list). In the event that genera represented species classified across different categories (19 cases) we randomly assigned individuals across the relevant categories in proportion with the number of species within each category known to occur in the area (*sensu* Zinke *et al.* 2018). Following the pooling of colonies according to shared morphological and ecological traits, we omitted all individuals defined as generalists from subsequent analyses due to their limited representation across our regional samples (n: AS = 22 colonies; AT = 31; JS = 17; JT = 65). Consequently, we constructed IPMs concerning the dynamics of 12 coral assemblages corresponding with competitive, stress-tolerant, and weedy coral taxa across four geographical locations (Fig. 5.1).

Photographs capturing the visible horizontal extent of tagged colonies were used to follow individuals over successive surveys and obtain longitudinal records of colony surface area (cm^2; transformed to a $\log_{10}$ scale) over time. Using generalised linear mixed models (GLMMs), we estimated size-specific patterns in colony survival (σ), transitions in size (γ), and fragmentation probability (κ) for each population Appendix 4.1). In each case, our GLMMs included random effects to account for any autocorrelation between observations and within-subject variability associated with our pooling of data recorded from individuals followed across multiple years, and at different sites. Colony survival (σ) reflected the continued presence of tagged individuals across survey intervals (t to $t+1$) and was modelled as a logistic function of colony surface area at time t. Colony size transitions (γ), representing both growth through colony extension, and shrinkage through partial mortality (Madin *et al.* 2020), were modelled using the polynomial relationship between initial colony surface area at time t and subsequent surface area at time $t+1$. Colony fragmentation probability (κ) was then modelled as a polynomial logistic function of colony size at time t. During our surveys, we recorded fragmentation in the event of observed colony breakage, recording the size (surface area, cm^2) of all remnants produced in each case. Subsequently, we also modelled the number (κb_z) and size (κ_Z^0) of remnant colonies produced during fragmentation as a function of colony size at time t, using Poisson and polynomial GLMMs, respectively.

Alongside our surveys of tagged individual colonies, we also monitored colony recruitment within our permanent coral plots. During each annual survey, we recorded the number and size of new colonies appearing within each plot. These recruitment counts enabled us to quantify annual and regional variability in recruit densities (Table S4.2), as well as estimate population-specific recruit size distributions (C_1; Appendix 4.1). However, prior to parameterising recruitment dynamics within our IPMs, we determined patterns in colony fecundity (φ). This approach was necessary because evaluating population performance requires an explicit consideration of fecundity to link the dynamics of existing individuals with the introduction of new, genetically distinct individuals (Caswell 2001). Using data relating colony size and larval output (larval density, cm^3) extracted from the Coral Trait Database (Hall & Hughes 1996; Madin *et al.* 2016a), we calculated colony fecundity (φ) as the polynomial relationship between colony size at t and expected larval output (Appendix 4.1). Next, to ensure our modelled recruitment dynamics accurately reflected our empirical observations we parameterised a recruit survival function (ϕ) within our IPMs. Here, recruit survival (ϕ) serves as a probability function converting expected larval output into a proportional contribution of observed recruit counts as a function of colony size; which we calculated by dividing total expected larval output in any given year by the corresponding annual recruitment count (Appendix 4.1, *sensu* Bramanti *et al.* 2015; Cant *et al.* 2021c).

5.3.3. Quantifying population characteristics

From our IPMs, we obtained estimates of long-term performance (asymptotic population growth, λ), generation time (T), and transient potential (damping ratio [ρ], maximal amplification [$\bar{\rho}_{max}$] & transient envelope [TE]) for each tropical and subtropical coral assemblage (Caswell 2001; Gaillard *et al.* 2005; Stott *et al.* 2010, 2011; Capdevila *et al.* 2020). Estimates of λ are typically used as a measure of long-term population viability (Crone *et al.* 2011), and reflect whether a population is expected to grow ($\lambda > 1$) or decline ($\lambda < 1$) when at stationary equilibrium (Caswell 2001). Generation time is a measure of population turnover, describing the time needed for individuals of a population to be replaced (Gaillard *et al.* 2005). Alternatively, the measures of transient potential describe the expected characteristics of populations following their displacement from stationary equilibrium due to disturbances. The damping ratio constitutes a measure of demographic recovery (Hodgson *et al.* 2015; Capdevila *et al.* 2020), describing the rate at which a population perturbed from its stationary equilibrium converges back to its asymptotic growth trajectory (Caswell 2001). Meanwhile, maximal amplification quantifies the greatest increase in population size following a disturbance, relative to its asymptotic growth trajectory (Stott *et al.* 2010, 2011). Finally, the transient envelope quantifies the magnitude by which the transient dynamics of a population deviates from its long-term trajectory (Capdevila *et al.* 2020).

To calculate the aforementioned demographic characteristics, we discretised our IPMs into large matrices. We attained these matrices by applying the ‘midpoint rule’ to integrate each IPM into a high-dimension matrix (200×200 cells), with the probability of transitioning from one cell to the next approximated at the cell midpoint and multiplied by the cell width (Zuidema *et al.* 2010). Estimates of λ were then identified as the dominant eigenvalue of each discretised matrix, whilst we estimated damping ratios as the ratio between the subdominant and dominant eigenvalues. With the *R* package *Rage* (Jones *et al.* 2021) we then calculated generation time using estimates of net reproductive rate (R_0) and λ obtained from each matrix,

$$T = \log(R_0) - \log(\lambda). \tag{5.4}$$

Next, we determined the transient envelope of each assemblage using their associated Kreiss bounds of amplification ($\overline{K_\lambda^*}$) and attenuation ($\underline{K_\lambda^*}$),

$$TE = \overline{K}_{\lambda}^{*} - \underline{K}_{\lambda}^{*}. \tag{5.5}$$

Respectively, the Kreiss bounds of amplification and attenuation reflect the largest and smallest expected long-term density of a population following the dissipation of transient conditions, relative to its asymptotic growth trajectory (Kreiss 1962; Townley *et al.* 2007; Townley & Hodgson 2008). We acknowledge here that this definition is more commonly applied to measures of population inertia (Stott *et al.* 2011), which are more typically used in estimating transient envelopes (Capdevila *et al.* 2020). However, Kreiss bound estimates have been demonstrated to align with corresponding estimates of population inertia and, unlike estimates of population inertia, are not sensitive to imprimitive population models (*i.e.*, non-negative models permitting transitions between all state classes, but with transitions between certain stages occurring only at periodic intervals; Caswell [2001]; Stott *et al.* [2011]); hence their selection here. We derived these Kreiss bounds, alongside estimates of maximal amplification, using their corresponding functions in the *R* package *popdemo* (Stott *et al.* 2012).

Across each demographic measure, we determined the variance in our assemblage-specific estimates through Jack-knife resampling. During resampling, we generated 1,000 IPM variants for each assemblage, each time using 95% of our original data sample without replacement, whilst permitting recruit survival probabilities (ϕ) to vary within observed limits. Finally, prior to their inclusion in further analyses, the jack-knifed distributions of the λ, generation time, transient envelope, and maximal amplification variables required transforming to ensure approximate normality. We omitted 26 variants for which $\lambda > 2$, as these presented unrealistic illustrations of population performance (*i.e.*, more than doubling population size every year), before applying a log transformation to the generation time variable and a power transformation (y^{x}) across the damping ratio ($y^{-2.0}$), transient envelope ($y^{-0.1}$) and maximal amplification variables ($y^{-0.5}$).

5.3.4. Evaluating spatial trends in population characteristics

To test for patterns in the spatial variation of long-term performance and transient potential across tropical and subtropical coral assemblages, we utilised partial least squares regression, ANOVA, and Type 2 linear regression. Initially, we applied a partial least squares regression to test whether trade-offs between the long-term performance characteristics and transient potential of coral assemblages align with their exposure to abiotic variability. Partial least squares regression quantifies the association between multiple predictor variables and one or more dependant variables (Carrascal *et al.* 2009). Subsequently, using this technique we simultaneously evaluated the relationships between mean estimates of λ, damping ratio, and transient envelope obtained for each assemblage, and their correlation with patterns in thermal conditions to provide an insight into the demographic trade-offs of coral assemblages and their mechanistic drivers.

To evaluate how abiotic variability mediates the trade-off between the short- and long-term performance characteristics of coral assemblages, within our partial least squares regression we quantified the abiotic conditions experienced by each coral assemblage using three measures of local sea surface temperature (SST) regimes: mean monthly SST ($\bar{x}_{sst}$), monthly SST variance (cv_{sst}), and monthly SST frequency spectrum (β_{sst}; Appendix 4.3). Focusing on the four geographical regions in which our focal coral assemblages were surveyed (GPS: AS = -30.3°, 153.1°; AT = -23.4°, 151.9°; JS = 32.8°, 132.6°; JT = 26.5°, 128.1°; Fig. 5.1), we extracted high resolution monthly SST readings (°C; overlaid on a 1° latitude-longitude grid) taken between January 1950 and December 2019, inclusive, from the HadISST dataset (Rayner *et al.* 2003). Arranging these SST records into 69-year timeseries for each location, we then calculated the mean ($\bar{x}_{sst}$) and coefficient of variance (cv_{sst}) for each timeseries. Next, we estimated the frequency spectrum of each time series. Spectral analysis is used to quantify the periodicity of recurrent variability within a timeseries, with higher frequencies associated with shorter-term fluctuations (Greenman & Benton 2005). The frequency spectrum of a time series is represented by its spectral exponent (β) and equal to the negative slope between its log spectral density and log frequency (Vasseur & Yodzis 2004), which we calculated using the package *stats* (*R* Core Team 2019). After testing these abiotic predictor variables for collinearity (Appendix 4.3), we performed our partial least square regression analyses using the *R* package *plsdepot* (Sanchez 2012).

Next, we assessed how patterns in the long-term performance, and capacity for coral assemblages to benefit from recurrent disturbance vary between tropical and subtropical regions, and how this variation manifests across coral taxa. Using a three-way ANOVA, we separately investigated variation in estimates of λ and maximal amplification across the three factors of country (Australia *vs*. Japan), ecoregion (tropical *vs*. subtropical), and assemblage classification (Competitive, Stress-Tolerant or Weedy). With maximal amplification estimates inverted during transformation, larger values subsequently reflect reduced amplification potential. For the purposes of clarity in this analysis, we will henceforth refer to this reversed scale as a *demographic stability index* (DSI), with lower values corresponding with enhanced amplification. Finally, we evaluated drivers of long- and short-term performance, by using Type 2 linear regression to separately evaluate the relationship between generation time (T) and estimates of λ and transient envelope (TE). Type 2 linear regression is an approach for quantifying the relationship between two non-independent variables, such that both variables include an element of error (Sokal & Rohlf 1995). Here, due to differences in the magnitude of the variance (σ^2) across our variables of generation time, λ, and transient envelope (σ^2: $T = 1.139$; $\lambda = 0.009$; $TE = 0.016$) we performed a Ranged Major Axis regression using the *R* package *lmodel2* (Legendre 2018).

5.4. Results and Discussion

Our analyses reveal a trade-off between long-term performance and transient potential across examined coral assemblages. We find that this trade-off corresponds with the exposure of coral populations to thermal variability along a gradient from warmer, more stable environments to cooler, more variable conditions (Fig. 5.2). Using partial least squares regression, we evaluate how patterns in the long-term performance, demographic recovery, and transient potential, of coral populations conform with their exposure to abiotic variability. We obtain estimates of long-term population performance (asymptotic population growth rate, λ), demographic recovery (damping ratio, ρ, *i.e.*, a relative measure of the time needed for a population to converge to a stable equilibrium; Caswell [2001]), and transient potential (transient envelope, *TE*, *i.e.*, the difference between maximum and minimum population size following disturbance; Stott *et al.* [2011]; Capdevila *et al.* [2020]) from IPMs depicting the dynamics of tropical and subtropical assemblages of competitive, stress-tolerant, and weedy coral taxa in Japan and Australia (Fig. 5.1; Appendix 4.1 & 4.2). Further, we quantify the exposure of these assemblages to thermal variability using three measures of local SST regimes: monthly mean SST ($\bar{x}_{sst}$), monthly SST variance (cv_{sst}), and monthly SST frequency spectrum (β_{sst}; Appendix 4.3).

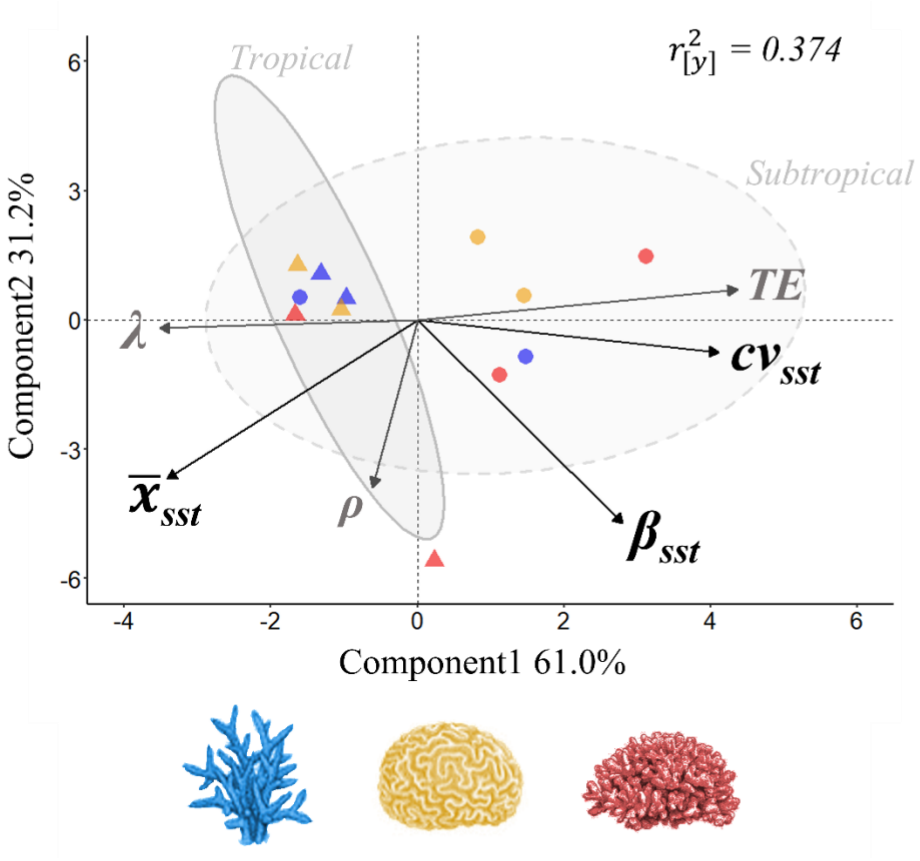

Figure 5.2. A trade-off exists between long-term performance and transient potential across our examined coral populations, corresponding with their relative exposure to thermal variability. Partial least squares regression **s**core plot illustrating the association between thermal conditions, and the long-term performance (λ) and transient potential (transient envelope [TE] & damping ratio [ρ]) of tropical (▲) and subtropical (●) populations of competitive (blue), stress-tolerant (yellow), and weedy (red) coral taxa. To quantify the thermal conditions experienced by each coral population, we used sea surface temperatures (SST) recorded between 1950 and 2019 to calculate regional estimates of mean monthly SST ($\bar{x}_{sst}$), monthly SST variance (cv_{sst}), and monthly SST frequency spectrum (β_{sst}). Component scores illustrate the relative degree of variance explained in the thermal predictor variables, whilst $r^2_{[y]}$ reflects the cumulative variance explained across the demographic characteristics. The shaded polygons reflect the clustering of tropical and subtropical populations, whilst the dotted lines delineate regions of association to facilitate the visualisation of patterns in correlation between the abiotic and demographic variables.

Notably, the coral assemblages exposed to more variable thermal conditions display enhanced transient potential. Our partial least squares regression explains 92.17% of the variance in the three measures of thermal exposure ($\bar{x}_{sst}$, cv_{sst}, and β_{sst}), whilst also capturing 37.43% of the variance in long-term performance (λ), demographic recovery (ρ), and transient potential (*TE*; Fig. 5.2, $r^2_{[y]}$). The first partial least squares regression component reflects a gradient in SST variability, capturing 60.97% of the variance in thermal conditions experienced by our examined coral assemblages. It is along this component that divergent patterns within estimates of λ and transient envelope (*TE*) are most obvious. Subsequently, estimates of transient envelope are positively correlated with the measures of thermal variability (cv_{sst}) and frequency spectrum (β_{sst}), whilst higher λ estimates associate with warmer mean monthly SSTs ($\bar{x}_{sst}$; Fig. 5.2). Meanwhile, damping ratio (ρ) estimates are aligned with the second partial least squares regression component describing secondary patterns in the mean SST ($\bar{x}_{sst}$) and frequency (β_{sst}) variables. Enhanced transient potential is thought to buffer the performance of populations in response to elevated abiotic variability, thereby underpinning their capacity to exploit more variable environments (Ellis & Crone 2013; McDonald *et al.* 2016). However, variation in how transient potential manifests across the assemblages of differing coral taxa, in response to increased thermal variability, suggests that exposure to abiotic variability does not assure resilience towards future climatic variability.

The trade-off between long-term performance and transient potential does not manifest consistently across the examined tropical and subtropical coral assemblages (Fig. 5.3A & Table 5.1), with inter-specific variation mediated instead by characteristics of population turnover (Fig. 5.3B & C). We explore inter-specific variation across estimates of long-term performance and population growth potential following a disturbance. Again, we quantify long-term performance using λ, whilst estimates of demographic stability index (DSI) calculated from our IPMs provide a measure of post-disturbance growth potential. A three-way ANOVA reveals significant interactions between the three factors of assemblage classification (Competitive, Stress-Tolerant or Weedy), ecoregion (tropical *vs*. subtropical), and country (Australia vs. Japan; ANOVA_{λ}: $F_{2,11562} = 5698.47$, $p < 0.001$; $\mathrm{ANOVA}_{\mathrm{DSI}}$: $F_{2,11581} = 589.8$, $p < 0.001$). Despite this, the tropical assemblages routinely possess higher estimates of λ relative to their corresponding subtropical counterparts (Tukey:

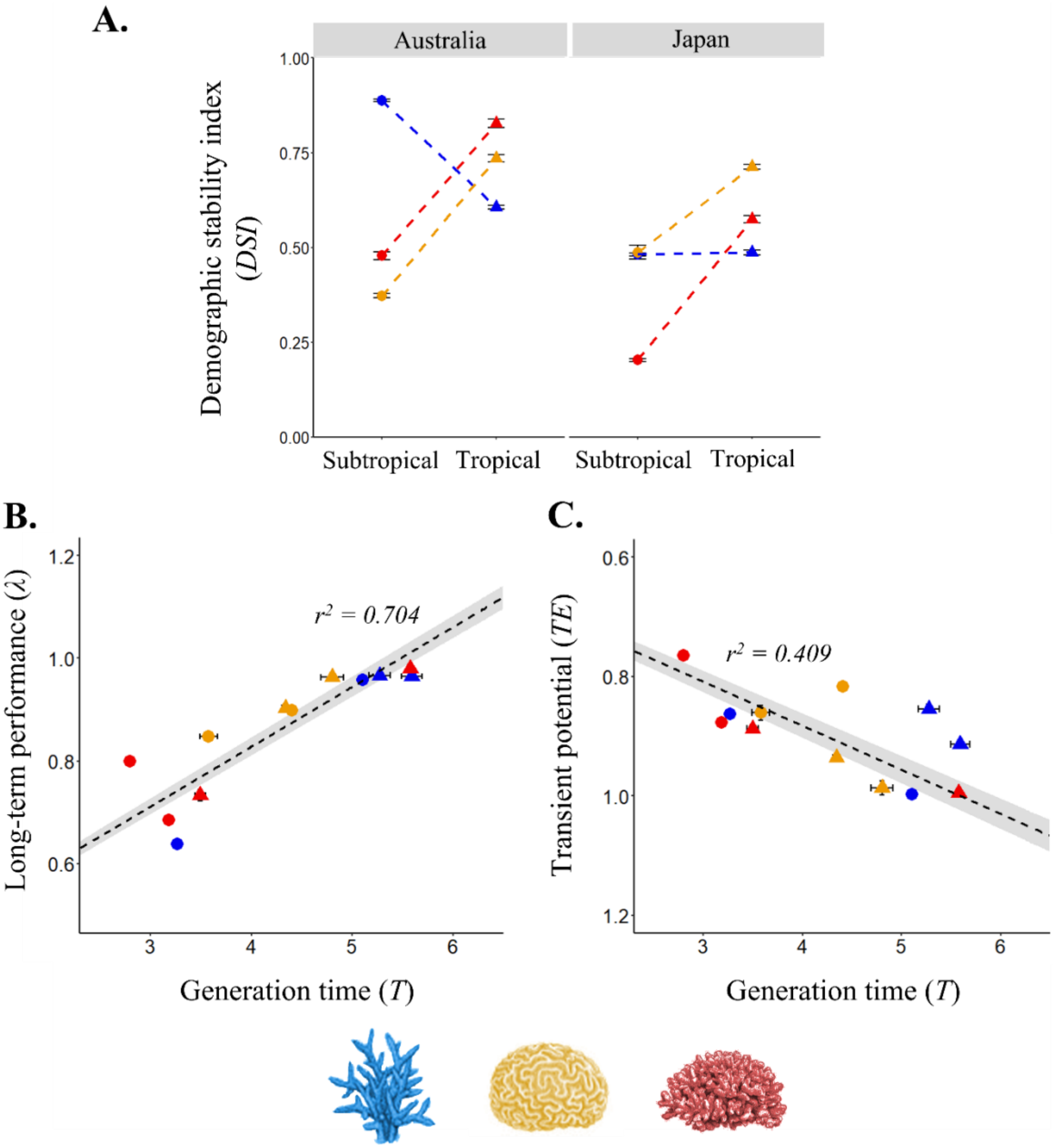

Figure 5.3. Inter-specific variation within the trade-off observed between long-term performance and transient potential across tropical and subtropical correlates with patterns in population turnover rate. **(A)** Interaction plot showcasing how estimates of demographic stability index (DSI) vary between associated tropical (▲) and subtropical (●) populations of competitive (blue), stress-tolerant (yellow), and weedy (red) coral taxa in Australia and Japan. We present DSI, as an inverse measure of maximal amplification ($\bar{\rho}_{max}$), describing the ability for populations to undergo elevated growth following disturbance. Thus, lower DSI estimates correspond with enhanced amplification capacity. We also applied Type 2 linear

regression to separately explore the association of population turnover characteristics with **(B)** long-term performance (asymptotic population growth rate; λ), and **(C)** transient potential (transient envelope, *TE*) across tropical and subtropical populations of competitive, stress-tolerant, and weedy coral taxa in Australia and Japan. We note here that transient envelope estimates were reversed during transformation to achieve normality, thus higher values reflected diminished transient potential. We have therefore displayed transient potential on a reversed scale to facilitate comparisons with patterns in long-term performance (λ). We used generation time (displayed here on the log scale) as a measure of population turnover rate, with higher estimates reflecting slower rates of population turnover. Across panels B and C r^2 values are provided as measure of model fit. Across all panels error is displayed using 95% CI.

$p < 0.001$ in all cases; Table 5.1). The one exception were weedy corals in Japan, where λ is highest in the subtropics ($\lambda_{[t]} = 0.760$ [95% CI: 0.750, 0. 770], $\lambda_{[s]} = 0.807$ [0.802, 0.812]; $p < 0.001$). Alternatively, the subtropical coral assemblages typically possess a greater capacity for amplifying population growth following a disturbance than the tropical assemblages (Fig. 5.3A). However, this pattern is not consistent across life history classes, with competitive assemblages exhibiting the opposite trend in Australia ($p < 0.001$), and no variation in *DSI* in Japan ($p = 0.999$).

The long-term performance and transient potential of the coral assemblages corresponds with patterns in their generation time (Fig. 5.3B & C). To further evaluate the drivers mediating coral population performance within variable environments we use Type 2 linear regression (Sokal & Rohlf 1995) to explore the relationship between estimates of generation time (*T*, *i.e.*, the time needed for individuals of a population to be replaced; Gaillard *et al.* [2005]), long-term performance (λ), and transient potential (*TE*) calculated from our IPMs. Generation time is a strong predictor of long-term population growth rate ($r^2 = 0.704$), with long-term performance increasing with generation time (Fig. 5.3B). Conversely, longer generation times are associated with reduced transient potential (Fig. 5.3C; $r^2 = 0.409$). Hence, our observed trade-off between long-term performance and transient potential, in response to thermal

Table 5.1. Population growth rates (λ) obtained from corresponding tropical and subtropical populations of competitive, stress-tolerant, and weedy coral taxa in Australia and Japan. Shading used to highlight the highest estimate of population growth across each tropical-subtropical pairing. Error displayed using 95% CI.

Country	Life-history group	Tropical	Subtropical
Australia	Competitive	0.983 [0.981, 0.984]	0.958 [0.957, 0.959]
	Stress-tolerant	0.983 [0.980, 0.985]	0.899 [0.898, 0.899]
	Weedy	0.981 [0.980, 0.982]	0.686 [0.684, 0.687]
Japan	Competitive	1.001 [0.999, 1.004]	0.640 [0.639, 0.641]
	Stress-tolerant	0.913 [0.909, 0.917]	0.885 [0.877, 0.894]
	Weedy	0.760 [0.750, 0.770]	0.807 [0.802, 0.812]

variability, manifests inconsistently across our examined tropical and subtropical coral assemblages, due to variation in their characteristics of population turnover.

5.4.1. Transient buffering in variable environments

Principally, a trade-off between long-term performance and transient potential implies that long-term performance does not predict the capacity for populations to endure repeated disturbances. Simultaneously, however, it also suggests that whilst enhanced transient potential may enable natural populations to persist within variable environments, it comes at a cost to their long-term performance. Historically, variability in population growth rate was thought to diminish individual fitness (Pfister 1998), thus hindering the persistence of populations (Lande 1993). This understanding formed the basis of the demographic buffering hypothesis, whereby populations can minimise the influence of environmental variability on their long-term performance by limiting temporal variability in crucial vital-rates (e.g. survival, development and reproduction; Morris & Doak 2004). Thus, variable environments were assumed to select for populations with the ability to buffer key vital rates, thereby reducing temporal variation in performance characteristics (Pfister 1998; Morris & Doak 2004; Hilde *et al.* 2020). More recently, however, enhanced transient potential has been presented as an adaptive mechanism evolving to allow populations to exploit variable environments (McDonald *et al.* 2016). Indeed, Ellis & Crone (2013) demonstrated how increased transient variability can buffer the effects of stochastic conditions on population growth rates, an effect that was increasingly evident in populations possessing lower λ estimates. It is not unexpected, therefore, that coral assemblages established within more variable environments, would possess enhanced transient potential (Fig. 5.2). Yet, if the vital rate schedules of these assemblages have indeed evolved specifically to maximise their short-term performance, this would carry an energetic cost to their long-term performance characteristics.

Our finding that transient potential is greatest in the assemblages displaying reduced long-term performance contrasts with previous work showing a positive association between population growth rates and transient potential (e.g. Morris *et al.* 2008; Gamelon *et al.* 2014). Faster population growth rates are assumed of populations characterised by faster individual development and high fecundity (Oli 2004). Consequently, these same populations are expected to exhibit greater variability in size following disturbances (Gamelon *et al.* 2014). However, whilst it is concerning that each of our surveyed assemblages are in, or close to, a state of long-term decline ($\lambda < 1$; Table 5.1), projected long-term performance is greatest in the tropical assemblages which also typically display lower amplificatory potential (Fig. 5.3A). Yet, these findings agree with evidence that transient potential is mediated by population turnover. Populations exhibiting longer generation times typically display reduced temporal variability in size corresponding with the fact that higher individual survival reduces the need to counteract disturbances (Morris *et al.* 2008); a pattern that we show to be evident in our examined coral assemblages (Fig. 5.3C). Accordingly, our observation that long-term performance is positively correlated with generation time in coral populations (Fig. 5.3B), perhaps presents a more intriguing result. Although, with the long- and short-term performance characteristics of coral assemblages corresponding with their relative exposure to thermal variability (Fig. 5.2), this finding further implies that trading off long-term performance for transient potential is an adaptive characteristic in coral populations.

5.4.2. Forecasting community reassembly

Here we show that stress-tolerant and weedy coral taxa possess greater transient potential, presenting a mechanism supporting their persistence at higher latitudes. Using a subset of the dataset present here, Cant *et al.* (2021a) recently demonstrated how short-term increases in population growth following disturbance could support the establishment of a subtropical coral assemblage of competitive *Acropora* spp. in southern Japan. However, the subtropical-tropical variation in the amplification capacity of competitive coral assemblages appears minimal in comparison to the variation we observe across the stress-tolerant and weedy assemblages in both Australia and Japan (Fig. 5.3A). Weedy corals comprise species that exhibit small colony sizes, fast growth rates, and internal fertilisation producing larvae that settle quickly after release (Knowlton 2001; Darling *et al.* 2012). Together, these strategies support faster population turnover, enabling weedy coral species to proliferate within highly disturbed environments (Adjeroud *et al.* 2018). Conversely, stress-tolerant corals display slower growth rates, longer life expectancies, high fecundity, and broadcast spawning strategies (Darling *et al.* 2012; Klepac & Barshis 2020). The larger, more robust, morphologies associated with stress-tolerant coral taxa maximise energy storage, promoting their persistence within challenging environments (van Woesik *et al.* 2012). Meanwhile, longer lifespans and elevated fecundity allow stress-tolerant corals to endure abiotic variation by taking advantage of sporadic improvements in local conditions (Darling *et al.* 2012). Consequently, our findings support existing projections that weedy and stress-tolerant coral taxa are likely to become increasingly prevalent throughout disturbed coral communities (Loya *et al.* 2001; Cant *et al.* 2021c). However, these projections herald the future loss of the structural complexity considered essential to the functioning of reef ecosystems (Graham & Nash 2013).

Importantly, our findings do not reflect the current reality for many coral assemblages within variable environments, suggesting that the composition of coral communities is not solely mediated by the interplay between transient dynamics and abiotic variability. Despite the lower amplificatory capacity we report in the subtropical competitive coral assemblages compared to across the other subtropical assemblages, competitive coral taxa such as *Acropora* spp. dominate many subtropical coral communities (Harriott *et al.* 1995; Nozawa *et al.* 2008; Sugihara *et al.* 2009). Utilising fast growth and broadcast spawning strategies, *Acropora* spp. colonies are capable of rapidly colonising available substrate, quickly outcompeting heterospecific colonies for both space and light (Darling *et al.* 2012). Whilst this competitive nature perhaps explains the enhanced amplificatory capacity of the tropical competitive assemblages relative to the tropical stress-tolerant and weedy assemblages (Fig. 5.3A), their sensitivity to environmental change means acroporid populations are regarded as early successional, dominating only within optimal environments and receding as reef ecosystems approach climax states (Ohba *et al.* 2008; Wilson *et al.* 2019). Within subtropical environments, however, coral community composition is strictly mediated by environmental pressures that filter the occurrence of species according to their trait characteristics (Sommer *et al.* 2014). As a result, subtropical coral assemblages typically consist of a subset of tropical species. The dominance of subtropical *Acropora* spp. populations, despite their reduced transient performance relative to other coral taxa, therefore, implies further evidence that competitive interactions greatly influence the performance of coral populations (Idjadi & Karlson 2007; Brito-Millán *et al.* 2019). Certainly, further investigation is needed to disentangle how the dynamics of coexistence between coral populations facilitate their persistence within variable environments.

5.5. Conclusions

Limitations in our understanding for the abiotic determinants driving the dynamics of coral populations inhibits our capacity to forecast their future performance and, therefore, manage global coral community reassembly (Edmunds *et al.* 2014; Edmunds 2020; Edmunds & Riegl 2020). Thus, to reveal the underlying determinants of coral population performance and enhance our capacity for predicting future condition of global coral communities, we explored patterns across characteristics of long-term performance, and transient potential in coral assemblages exposed to varying thermal variability regimes. We demonstrate how coral assemblages within variable environments exhibit demographic strategies associated with enhanced transient potential (Fig. 5.2). Although at a cost to their long-term performance, this transient buffering (*sensu* Ellis & Crone 2013) mediates the performance of coral assemblages within variable environments, thus supporting their existence along subtropical coastlines. However, the relationship that we observed between transient potential and thermal variability was not universal across coral taxa, nor did it manifest identically across different tropical-subtropical transition zones. Subtle patterns in the association between population dynamics and their climate drivers hinder predictions of the consequences of environmental change within biological communities (Coulson *et al.* 2011). Nevertheless, it is crucial that we continue to advance our understanding for how transient patterns within the dynamics of coral populations attune their performance within variable environments and will, therefore, determine their future responses to climatic change (Ellis & Crone 2013; Cant *et al.* 2021b).

5.6. References

Adjeroud, M., Kayal, M., Iborra-Cantonnet, C., Vercelloni, J., Bosserelle, P., Liao, V., *et al.* (2018). Recovery of coral assemblages despite acute and recurrent disturbances on a South Central Pacific reef. *Sci. Rep.*, 8.

Álvarez-Noriega, M., Baird, A.H., Dornelas, M., Madin, J.S., Cumbo, V.R. & Connolly, S.R. (2016). Fecundity and the demographic strategies of coral morphologies. *Ecol. Soc. Am.*, 97, 3485–3493.

Baird, A.H., Sommer, B. & Madin, J.S. (2012). Pole-ward range expansion of Acropora spp. along the east coast of Australia. *Coral Reefs*, 31, 1063.

Beger, M., Sommer, B., Harrison, P.L., Smith, S.D.A. & Pandolfi, J.M. (2014). Conserving potential coral reef refuges at high latitudes. *Divers. Distrib.*, 20, 1–13.

Booth, D.J. & Sears, J. (2018). Coral expansion in Sydney and associated coral-reef fishes. *Coral Reefs*, 37, 995.

Boyd, P.W., Cornwall, C.E., Davison, A., Doney, S.C., Fourquez, M., Hurd, C.L., *et al.* (2016). Biological responses to environmental heterogeneity under future ocean conditions. *Glob. Chang. Biol.*, 22, 2633–2650.

Bramanti, L., Iannelli, M., Fan, T.Y. & Edmunds, P.J. (2015). Using demographic models to project the effects of climate change on scleractinian corals: Pocillopora damicornis as a case study. *Coral Reefs*, 34, 505–515.

Brito-Millán, M., Werner, B.T., Sandin, S.A. & McNamara, D.E. (2019). Influence of aggregation on benthic coral reef spatio-temporal dynamics. *R. Soc. Open Sci.*, 6, 1–14.

Burt, J.A., Camp, E.F., Enochs, I.C., Johansen, J.L., Morgan, K.M., Riegl, B., *et al.* (2020). Insights from extreme coral reefs in a changing world. *Coral Reefs*, 39, 495–507.

Cadotte, M.W., Carscadden, K. & Mirotchnick, N. (2011). Beyond species: Functional diversity and the maintenance of ecological processes and services. *J. Appl. Ecol.*, 48, 1079–1087.

Camp, E.F., Schoepf, V., Mumby, P.J., Hardtke, L.A., Rodolfo-Metalpa, R., Smith, D.J., *et al.* (2018). The future of coral reefs subject to rapid climate change: Lessons from natural extreme environments. *Front. Mar. Sci.*, 5, 1–21.

Cant, J., Cook, K., Reimer, J.D., Mezaki, T., Nakamura, M., O'Flaherty, C., *et al.* (2021a). Transient amplification enhances the persistence of tropicalising coral populations in marginal high latitude environments. *BioRxiv*, 2021.04.23.441133.

Cant, J., Salguero-Gómez, R. & Beger, M. (2021b). Transient demographic approaches can drastically expand the toolbox of coral reef science. *bioRxiv*, 2021.04.08.438926.

Cant, J., Salguero-Gómez, R., Kim, S.W., Sims, C.A., Sommer, B., Brooks, M., *et al.* (2021c). The projected degradation of subtropical coral assemblages by recurrent thermal stress. *J. Anim. Ecol.*, 90, 233–247.

Capdevila, P., Stott, I., Beger, M. & Salguero-Gómez, R. (2020). Towards a comparative framework of demographic resilience. *Trends Ecol. Evol.*, 35, 776–786.

Carrascal, L.M., Galván, I. & Gordo, O. (2009). Partial least squares regression as an alternative to current regression methods used in ecology. *Oikos*, 118, 681–690.

Caswell, H. (2001). *Matrix population models: Construction, analysis and interpretation*. 2nd Edition. Oxford University Press Inc.

Chalmandrier, L., Hartig, F., Laughlin, D.C., Lischke, H., Pichler, M., Stouffer, D.B., *et al.* (2021). Linking functional traits and demography to model species-rich communities. *Nat. Commun.*, 12, 1–9.

Chen, I.C., Hill, J.K., Ohlemüller, R., Roy, D.B. & Thomas, C.D. (2011). Rapid range shifts of species associated with high levels of climate warming. *Science*, 333, 1024–1026.

Coulson, T., Macnulty, D.R., Stahler, D.R., VonHoldt, B., Wayne, R.K. & Smith, D.W. (2011). Modeling effects of environmental change on wolf population dynamics, trait evolution, and life history. *Science*, 334, 1275–1278.

Crone, E.E., Menges, E.S., Ellis, M.M., Bell, T., Bierzychudek, P., Ehrlén, J., *et al.* (2011). How do plant ecologists use matrix population models? *Ecol. Lett.*, 14, 1–8.

Darling, E.S., Alvarez-Filip, L., Oliver, T.A., Mcclanahan, T.R. & Côté, I.M. (2012). Evaluating life-history strategies of reef corals from species traits. *Ecol. Lett.*, 15, 1378–1386.

Darling, E.S., McClanahan, T.R. & Côté, I.M. (2013). Life histories predict coral community disassembly under multiple stressors. *Glob. Chang. Biol.*, 19, 1930–1940.

Darling, E.S., McClanahan, T.R., Maina, J., Gurney, G.G., Graham, N.A.J., Januchowski-Hartley, F., *et al.* (2019). Social–environmental drivers inform strategic management of coral reefs in the Anthropocene. *Nat. Ecol. Evol.*, 3, 1341–1350.

Dawson, T.P., Jackson, S.T., House, J.I., Prentice, I.C. & Mace, G.M. (2011). Beyond predictions: Biodiversity conservation in a changing climate. *Science*, 332, 53–58.

Dietzel, A., Bode, M., Connolly, S.R. & Hughes, T.P. (2021). The population sizes and global extinction risk of reef-building coral species at biogeographic scales. *Nat. Ecol. Evol.*, 5, 663–669.

Easterling, M.R., Ellner, S.P. & Dixon, P.M. (2000). Size-specific sensitivity: applying a new structured population model. *Ecology*, 81, 694–708.

Edmunds, P.J. (2020). Vital rates of small reef corals are associated with variation in climate. *Limnol. Oceanogr.*, 1–13.

Edmunds, P.J., Burgess, S.C., Putnam, H.M., Baskett, M.L., Bramanti, L., Fabina, N.S., *et al.* (2014). Evaluating the causal basis of ecological success within the scleractinia: an integral projection model approach. *Mar. Biol.*, 161, 2719–2734.

Edmunds, P.J. & Riegl, B. (2020). Urgent need for coral demography in a world where corals are disappearing. *Mar. Ecol. Prog. Ser.*, 635, 233–242.

Ellis, M.M. & Crone, E.E. (2013). The role of transient dynamics in stochastic population growth for nine perennial plants. *Ecology*, 94, 1681–1686.

Ezard, T.H.G., Bullock, J.M., Dalgleish, H.J., Millon, A., Pelletier, F., Ozgul, A., *et al.* (2010). Matrix models for a changeable world: The importance of transient dynamics in population management. *J. Appl. Ecol.*, 47, 515–523.

Falster, D.S., Brännström, Å., Westoby, M. & Dieckmann, U. (2017). Multitrait successional forest dynamics enable diverse competitive coexistence. *Proc. Natl. Acad. Sci. U. S. A.*, 114, E2719–E2728.

Foden, W.B., Butchart, S.H.M., Stuart, S.N., Vié, J.C., Akçakaya, H.R., Angulo, A., *et al.* (2013). Identifying the world's most climate change vulnerable species: A systematic trait-based assessment of all birds, amphibians and corals. *PLoS One*, 8.

Gaillard, J., Yoccoz, N.G., Lebreton, J., Bonenfant, C., Devillard, S., Loison, A., *et al.* (2005). Generation Time: A reliable metric to measure life-history variation among mammalian populations. *Am. Nat.*, 166, 119–123.

Gamelon, M., Gimenez, O., Baubet, E., Coulson, T., Tuljapurkar, S. & Gaillard, J.M. (2014). Influence of life-history tactics on transient dynamics: A comparative analysis across mammalian populations. *Am. Nat.*, 184, 673–683.

Graham, N.A.J. & Nash, K.L. (2013). The importance of structural complexity in coral reef ecosystems. *Coral Reefs*, 32, 315–326.

Greenman, J. V. & Benton, T.G. (2005). The frequency spectrum of structured discrete time population models : its properties and their ecological implications. *Oikos*, 110, 369–389.

Grime, J.P. & Pierce, S. (2012). *The evolutionary strategies that shape ecosystems*. John Wiley and Sons Ltd.

Hall, V.R. & Hughes, T.P. (1996). Reproductive strategies of modular organisms: Comparative studies of reef-building corals. *Ecology*, 77, 950–963.

Harriott, V.J., Harrison, P.L. & Banks, S.A. (1995). The coral communities of Lord

Howe Island. *Mar. Freshw. Res.*, 46, 457–465.

Hastings, A. (2001). Transient dynamics and persistence of ecological systems. *Ecol. Lett.*, 4, 215–220.

Hastings, A. (2004). Transients: The key to long-term ecological understanding? *Trends Ecol. Evol.*, 19, 39–45.

Hastings, A., Abbott, K.C., Cuddington, K., Francis, T., Gellner, G., Lai, Y.C., *et al.* (2018). Transient phenomena in ecology. *Science*, 361, 1–9.

Hilde, C.H., Gamelon, M., Sæther, B.E., Gaillard, J.M., Yoccoz, N.G. & Pélabon, C. (2020). The demographic buffering hypothesis: Evidence and challenges. *Trends Ecol. Evol.*, 35, 523–538.

Hodgson, D., McDonald, J.L. & Hosken, D.J. (2015). What do you mean, “resilient”? *Trends Ecol. Evol.*, 30, 503–506.

Hughes, T.P., Anderson, K.D., Connolly, S.R., Heron, S.F., Kerry, J.T., Lough, J.M., *et al.* (2018). Spatial and temporal patterns of mass bleaching of corals in the Anthropocene. *Science*, 359, 80–83.

Hughes, T.P., Kerry, J.T., Baird, A.H., Connolly, S.R., Chase, T.J., Dietzel, A., *et al.* (2019). Global warming impairs stock–recruitment dynamics of corals. *Nature*, 568, 387–390.

Idjadi, J.A. & Karlson, R.H. (2007). Spatial arrangement of competitors influences coexistence of reef-building corals. *Ecology*, 88, 2449–2454.

Iles, D.T., Rockwell, R.F. & Koons, D.N. (2019). Shifting vital rate correlations alter predicted population responses to increasingly variable environments. *Am. Nat.*, 193, E57–E64.

Jones, O.R., Barks, P., Stott, I., James, T.D., Levin, S., Petry, W.K., *et al.* (2021). Rcompadre and Rage - two R packages to facilitate the use of the COMPADRE and COMADRE databases and calculation of life history traits from matrix population models. *bioRxiv*, 2021.04.26.441330.

Klepac, C.N. & Barshis, D.J. (2020). Reduced thermal tolerance of massive coral species in a highly variable environment: Reduced heat tolerance of massive corals. *Proc. R. Soc. B Biol. Sci.*, 287, 19–21.

Kleypas, J., Allemand, D., Anthony, K., Baker, A.C., Beck, M.W., Hale, L.Z., *et al.* (2021). Designing a blueprint for coral reef survival. *Biol. Conserv.*, 257, 1–7.

Knowlton, N. (2001). The future of coral reefs. *Proc. Natl. Acad. Sci.*, 98, 5419–5425.

Koons, D.N., Grand, J.B., Zinner, B. & Rockwell, R.F. (2005). Transient population dynamics: Relations to life history and initial population state. *Ecol. Modell.*, 185, 283–297.

Kreiss, H.O. (1962). Über Die Stabilitätsdefinition Für Differenzengleichungen Die Partielle Differentialgleichungen Approximieren. *BIT*, 2, 153–181.

Lande, R. (1993). Risks of population extinction from demographic and environmental stochasticity and random catastrophes. *Am. Nat.*, 142, 911–927.

Legendre, P. (2018). lmodel2: Model II regression.

Loya, Y., Sakai, K., Yamazato, K., Nakano, Y., Sambali, H. & van Woesik, R. (2001). Coral bleaching: the winners and the losers. *Ecol. Lett.*, 4, 122–131.

Madin, J.S., Anderson, K.D., Andreasen, M.H., Bridge, T.C., Cairns, S.D., Connolly, S.R., *et al.* (2016a). The Coral Trait Database, a curated database of trait information for coral species from the global oceans. *Sci. Data*, 3, 1–21.

Madin, J.S., Baird, A.H., Baskett, M.L., Connolly, S.R. & Dornelas, M.A. (2020). Partitioning colony size variation into growth and partial mortality. *Biol. Lett.*, 16, 1–5.

Madin, J.S., Hoogenboom, M.O. & Connolly, S.R. (2012). Integrating physiological and biomechanical drivers of population growth over environmental gradients on coral reefs. *J. Exp. Biol.*, 215, 968–976.

Madin, J.S., Hoogenboom, M.O., Connolly, S.R., Darling, E.S., Falster, D.S., Huang, D., *et al.* (2016b). A trait-based approach to advance coral reef science. *Trends Ecol. Evol.*, 31, 419–428.

McDonald, J.L., Stott, I., Townley, S. & Hodgson, D.J. (2016). Transients drive the demographic dynamics of plant populations in variable environments. *J. Ecol.*, 104, 306–314.

McGill, B.J., Enquist, B.J., Weiher, E. & Westoby, M. (2006). Rebuilding community ecology from functional traits. *Trends Ecol. Evol.*, 21, 178–185.

McLeod, E., Shaver, E.C., Beger, M., Koss, J. & Grimsditch, G. (2021). Using resilience assessments to inform the management and conservation of coral reef ecosystems. *J. Environ. Manage.*, 277, 1–8.

Morris, W.F. & Doak, D.F. (2004). Buffering of life histories against environmental stochasticity: Accounting for a spurious correlation between the variabilities of vital rates and their contributions to fitness. *Am. Nat.*, 163, 579–590.

Morris, W.F., Pfister, C.A., Tuljapurkar, S., Haridas, C. V., Boggs, C.L., Boyce, M.S., *et al.* (2008). Longevity can buffer plant and animal populations against changing climatic variability. *Ecology*, 89, 19–25.

Nozawa, Y., Tokeshi, M. & Nojima, S. (2008). Structure and dynamics of a high-latitude scleractinian coral community in Amakusa, southwestern Japan. *Mar. Ecol. Prog. Ser.*, 358, 151–160.

Ohba, H., Hashimoto, K., Shimoike, K., Shibuno, T. & Fujioka, Y. (2008). Secondary succession of coral reef communities at Urasoko Bay , Ishigaki Island , the Ryukyus (southern Japan). In: *Proceedings of the 11th International Coral Reef Symposium*. pp. 321–325.

Oli, M.K. (2004). The fast-slow continuum and mammalian life-history patterns: An empirical evaluation. *Basic Appl. Ecol.*, 5, 449–463.

Parmesan, C. & Yohe, G. (2003). A globally coherent fingerprint of climate change. *Nature*, 421, 37–42.

Pecl, G., Araujo, M.B., Bell, J.D., Blanchard, J. & Bonebrake, T.C. (2017). Biodiversity redistribution under climate change: Impacts on ecosystems and human well-being Publication Details. *Science*, 355, 1–9.

Pfister, C.A. (1998). Patterns of variance in stage-structured populations: Evolutionary predictions and ecological implications. *Proc. Natl. Acad. Sci.*, 95, 213–218.

Precht, W.F. & Aronson, R.B. (2004). Climate flickers and range shifts of reef corals. *Front Ecol Env.*, 2, 307–314.

R Core Team. (2019). R: A language and environment for statistical computing.

Rayner, N.A., Parker, D.E., Horton, E.B., Folland, C.K., Alexander, L. V., Rowell, D.P., *et al.* (2003). Global analyses of sea surface temperature, sea ice, and night marine air temperature since the late nineteenth century. *J. Geophys. Res.*, 108, 1–37.

Rivest, E.B., Comeau, S. & Cornwall, C.E. (2017). The role of natural variability in shaping the response of coral reef organisms to climate change. *Curr. Clim. Chang. Reports*, 3, 271–281.

Sanchez, G. (2012). plsdepot: Partial least squares (PLS) data analysis methods.

Sokal, R.R. & Rohlf, F.J. (1995). *Biometry: The principles and practice of statistics in biological research*. 3rd Editio. W. H. Freeman & Co.

Sommer, B., Harrison, P.L., Beger, M. & Pandolfi, J.M. (2014). Trait-mediated environmental filtering drives assembly at biogeographic transition zones. *Ecology*, 95, 1000–1009.

Sommer, B., Sampayo, E.M., Beger, M., Harrison, P.L., Babcock, R.C. & Pandolfi, J.M. (2017). Local and regional controls of phylogenetic structure at the high-latitude range limits of corals. *Proc. R. Soc. Biol. Sci. Ser. B*, 284, 1–13.

Stott, I., Franco, M., Carslake, D., Townley, S. & Hodgson, D. (2010). Boom or bust? A comparative analysis of transient population dynamics in plants. *J. Ecol.*, 98, 302–311.

Stott, I., Hodgson, D.J. & Townley, S. (2012). Popdemo: An R package for population demography using projection matrix analysis. *Methods Ecol. Evol.*, 3, 797–802.

Stott, I., Townley, S. & Hodgson, D. (2011). A framework for studying transient dynamics of population projection matrix models. *Ecol. Lett.*, 14, 959–970.

Sugihara, K., Sonoda, N., Imafuku, T., Nagata, S., Ibusuki, T. & Yamano, H. (2009). Latitudinal changes in hermatypic coral communities from west Kyushu to Oki

Islands in Japan. *J. Japanese Coral Reef Soc.*, 11, 51–67.

Totland, Ø. & Nyléhn, J. (1998). Assessment of the effects of environmental change on the performance and density of Bistorta vivipara: The use of multivariate analysis and experimental manipulation. *J. Ecol.*, 86, 989–998.

Townley, S., Carslake, D., Kellie-Smith, O., Mccarthy, D. & Hodgson, D. (2007). Predicting transient amplification in perturbed ecological systems. *J. Appl. Ecol.*, 44.

Townley, S. & Hodgson, D.J. (2008). Erratum et addendum: Transient amplification and attenuation in stage-structured population dynamics. *J. Appl. Ecol.*, 45, 1836–1839.

Tuckett, C.A., de Bettignies, T., Fromont, J. & Wernberg, T. (2017). Expansion of corals on temperate reefs: Direct and indirect effects of marine heatwaves. *Coral Reefs*, 36, 947–956.

Vasseur, D.A. & Yodzis, P. (2004). The color of environmental noise. *Ecology*, 85, 1146–1152.

Vázquez, D.P., Gianoli, E., Morris, W.F. & Bozinovic, F. (2017). Ecological and evolutionary impacts of changing climatic variability. *Biol. Rev.*, 92, 22–42.

Veron, J.E.N., Stafford-Smith, M.G., Turak, E. & DeVantier, L.M. (2016). *Corals of the World*. Available at: http://www.coralsoftheworld.org/page/home/. Last accessed 12 November 2019.

Violle, C., Navas, M., Vile, D., Kazakou, E., Fortunel, C., Hummel, I., *et al.* (2007). Let the concept of trait be functional! *Oikos*, 116, 882–892.

Williams, J.L., Miller, T.E.X. & Ellner, S.P. (2012). Avoiding unintentional eviction from integral projection models. *Ecology*, 93, 2008–2014.

Williams, S.E., Shoo, L.P., Isaac, J.L., Hoffmann, A.A. & Langham, G. (2008). Towards an integrated framework for assessing the vulnerability of species to climate change. *PLoS Biol.*, 6.

Wilson, S.K., Robinson, J.P.W., Chong-Seng, K., Robinson, J. & Graham, N.A.J. (2019). Boom and bust of keystone structure on coral reefs. *Coral Reefs*, 38, 625–635.

van Woesik, R., Irikawa, A., Anzai, R. & Nakamura, T. (2012). Effects of coral colony morphologies on mass transfer and susceptibility to thermal stress. *Coral Reefs*, 31, 633–639.

Yamano, H., Sugihara, K. & Nomura, K. (2011). Rapid poleward range expansion of tropical reef corals in response to rising sea surface temperatures. *Geophys. Res. Lett.*, 38, 1–6.

Yamano, H., Sugihara, K., Watanabe, T., Shimamura, M. & Hyeong, K. (2012). Coral reefs at 34°N, Japan: Exploring the end of environmental gradients. *Geology*, 40, 835–838.

Zinke, J., Gilmour, J.P., Fisher, R., Puotinen, M., Maina, J., Darling, E., *et al.* (2018). Gradients of disturbance and environmental conditions shape coral community structure for south-eastern Indian Ocean reefs. *Divers. Distrib.*, 24, 605–620.

Zuidema, P.A., Jongejans, E., Chien, P.D., During, H.J. & Schieving, F. (2010). Integral projection models for trees: A new parameterization method and a validation of model output. *J. Ecol.*, 98, 345–355.

Discussion

Future climate change is expected to expose populations worldwide to increasingly variable environments (IPCC 2014). This increased exposure is expected to arise both directly through changes in local abiotic variability regimes (Coumou & Rahmstorf 2012; Thornton *et al.* 2014) and indirectly as species expand their distributions at higher latitudes and elevations (Pintor *et al.* 2015; Spence & Tingley 2020). Predicting the future condition of biological communities thus requires an understanding for how changing abiotic variability influences population viability and resilience (Vázquez *et al.* 2017; Bright Ross *et al.* 2020). Evaluating the future viability of natural populations typically involves a consideration of climatic vulnerability, specifically, how sensitive populations are likely to be to future climatic shifts (Williams *et al.* 2008; Dawson *et al.* 2011). Often, this vulnerability is inferred from a populations past experience of disturbance regimes, with prior exposure to disturbances expected to cultivate the ability for populations to endure further disturbance events (Boyd *et al.* 2016). However, I illustrate how, across a range of taxa, the recent exposure of populations to environmental stochasticity cannot alone predict their capacity to resist, recover from, or even benefit from, disturbances (Chapter 1). Populations within more variable environments are thought to possess enhanced resilience towards future climatic disturbance (Rivest *et al.* 2017; Hughes *et al.* 2019; Walker 2020). Instead, I show how the attributes of resilience exhibited by natural populations are more contingent on selection legacies placed on characteristics of long-term performance irrespective of recent environmental stochasticity (Chapter 1).

The decoupling of resilience potential and exposure to abiotic variability, has considerable implications across the management and conservation of natural ecosystems. Subtropical coral populations, located at the intersection of tropical and temperate ecoregions, are thought to offer insight into the vulnerabilities of coral populations to increasing climatic stress (Beger *et al.* 2014; Sommer *et al.* 2014; Camp *et al.* 2018; Burt *et al.* 2020); and have fostered notions of high-latitude climate refugia (Glynn 1996; Riegl & Piller 2003). Yet, limited knowledge of the biophysical determinants of coral population performance inhibits the accurate prediction of coral population viability (Edmunds *et al.* 2014; Edmunds & Riegl 2020; Shlesinger & van Woesik 2021). I demonstrate how, despite their exposure to broader thermal spectra relative to tropical coral taxa, projected increases in sea surface temperature will cripple the viability of many subtropical coral assemblages (Chapter 2). In fact, future thermal stress events will instigate losses of structural complexity within subtropical coral communities analogous to those expected throughout tropical reefs. Accordingly, the persistence of populations within more variable environments neither guarantees enhanced resilience to repeated disturbances, nor a reduced susceptibility to extreme stress events. However, with abiotic variability known to impact upon population performance (Lande *et al.* 2003), understanding the future condition of global biodiversity requires us to continue evaluating how environmental variability influences the dynamics of natural populations (Vázquez *et al.* 2017; Iles *et al.* 2019).

Variable environments expose populations to regular and repeated disturbances that induce short-term (*i.e.,* transient) fluctuations in their structural composition, causing deviations from long-term (*i.e.,* asymptotic) performance trajectories (henceforth transient potential; Hastings 2001, 2004; Hastings *et al.* 2018). Throughout this thesis I have primarily focused on quantifying the transient potential of populations to explore their responses to environmental variability. Enhanced transient potential is thought to buffer the performance of populations within highly variable environments (Ellis & Crone 2013). Indeed, prioritising the ability to undergo short-term increases in population growth (*i.e.,* transient amplification) over long-term population growth can elevate the performance of plant populations both within variable environments (McDonald *et al.* 2016), and outside of their native range (Jelbert *et al.* 2019). The same is also true of a subtropical *Acropora* spp. population in southern Japan, which displays an enhanced capacity for transient amplification, relative to a down-current tropical population (Chapter 3). Allowing their dynamics to fluctuate in response to external environmental factors enables populations to exploit periodic improvements in abiotic conditions and respond to cyclic resource availability (Morris *et al.* 2006; Koons *et al.* 2009). Thus, this finding provides an insight into the mechanisms supporting the establishment of subtropical coral assemblages.

Enhanced transient potential is also evident in subtropical populations across other coral taxa and again is associated with their exposure to increased thermal variability (Chapter 4). However, patterns within the variation in transient potential between tropical and subtropical coral populations are not consistent across all coral taxa. Stress-tolerant and Weedy coral taxa show the greatest capacity for elevating their transient potential in response to elevated thermal variability (Chapter 4); thereby forecasting the loss of morphologically complex competitive coral taxa (e.g., *Acropora*; Agudo-Adriani *et al.* 2016) as a consequence of increasing climatic variability. The subsequent loss of the structural complexity associated with these taxa carries considerable implications for the wider functioning of coral-associated ecosystems, particularly the loss of habitable space for many reef fish (Alvarez-Filip *et al.* 2009; Graham & Nash 2013). Regrettably, this bleak outlook reflects scenarios also expected in response to increasingly frequent abiotic extremes (Chapter 2; Loya *et al.* 2001; Alvarez-Filip *et al.* 2009), compounding the vulnerability of reef ecosystems to future climatic change. However, heterogeneity in the transient response of coral populations towards increased thermal variability does agree with the argument that exposure to environmental variability alone does not determine demographic resilience (Chapter 1). Accordingly, these findings also reinforce the difficulties associated with predicting the resilience of natural populations (Donohue *et al.* 2013, 2016; Kéfi *et al.* 2019).

6.1. Challenges in modelling coral population dynamics

Throughout my thesis, implementing long-term demographic assessments on coral populations entailed a host of challenges that require recognition when interpreting projected population trajectories and performance characteristics. Most notably, the planktonic larval phase within the complex lifecycle of many coral taxa provided the greatest challenge in evaluating the dynamics of coral populations. A challenge of particular relevance, given that I was quantifying the dynamics of subtropical coral assemblages whose persistence is mediated by the influence of boundary currents on the movements of coral larvae (Harriott & Banks 1995; Banks & Harriott 1996; Harriott 1999). To assess the characteristics and conditions of marine benthic invertebrate communities, it is necessary to understand the biophysical drivers influencing the dynamics of their planktonic larval phases (Eckman 1996; Adjeroud *et al.* 2017). Comparatively, reproduction is well studied across coral taxa (Harrison 2011). Subsequently, we have detailed knowledge of coral spawning patterns (Baird *et al.* 2021), the abiotic tolerances and longevity of coral larvae (Dixon *et al.* 2015; Bergman *et al.* 2018; Miller *et al.* 2020), and the biotic and abiotic drivers of larval settlement (Vermeij *et al.* 2009; Doropoulos *et al.* 2012; Hata *et al.* 2017; Price *et al.*

2019). However, two key areas of coral reproduction in which our understanding remains insufficient are size-specific patterns in colony fecundity (Álvarez-Noriega *et al.* 2016) and patterns in larval dispersal (van Oppen & Gates 2006; Underwood *et al.* 2009; Edmunds *et al.* 2018).

The Coral Trait Database is a compilation of coral life history trait data, containing over 100,000 entries across 158 traits from more than 1,500 coral species (Madin *et al.* 2016). Yet, across this database there exists only one instance of an assessment into fecundity (larval output) as a function of colony size pertaining to research by Hall & Hughes (1996) across multiple species at Lizard Island, on the Great Barrier Reef. Difficulties associated with the *in-situ* assessment of colony spawning limits our capacity for documenting individual fecundity over an extensive range of colonies (Gilmour *et al.* 2016). Although, I acknowledge here that Álvarez-Noriega *et al.* (2016) also present a more recent multi-species assessment into the relationship between colony size and fecundity, also conducted within the reef communities of Lizard Island. Subsequently, our understanding for how colony fecundity changes as a function of colony size, is restricted both taxonomically and spatially. Throughout this thesis, I navigated the challenge of including fecundity within demographic models by inferring size-specific relationships from those presented by Hall & Hughes (1996). This approach implies an explicit assumption of spatial consistencies in the fecundity patterns of coral taxa, yet is consistent with the work of Precoda *et al.* (2018) and Shlesinger & van Woesik (2021) both whom parameterised size-specific fecundity rates through the manipulation of earlier datasets. An alternative approach would have been to omit fecundity completely, and instead model recruitment patterns as a function of population density/coverage (*sensu* Madin *et al.* 2012; Edmunds *et al.* 2014; Kayal *et al.* 2018; Scavo Lord *et al.* 2020). However, this approach presents its own challenge, requiring prior knowledge of expected recruit densities given the composition of local populations, and an awareness of regional patterns in larval dispersal and/or retention.

Quantifying patterns in larval dispersal has long been regarded as crucial for managing and maintaining coral reef biodiversity and resilience (Cowen & Sponaugle 2009). Yet, our understanding of critical dispersal patterns remains insufficient, especially at the resolution necessary for their inclusion within assessments of coral population performance (Werner *et al.* 2007; Edmunds *et al.* 2018). Evaluating the viability of populations and their ability to track favourable abiotic conditions requires knowledge of how the dispersal of organisms influences population performance (Gaillard *et al.* 2010; Morales *et al.* 2010). Coral populations exist on a connectivity spectrum ranging from fully closed (*i.e.*, self-sustaining) to fully open (100% larval exchange with surrounding populations; Jones *et al.* 2009). Individual reef communities, therefore, often do not exist in isolation and instead are part of a metacommunity supported by the dispersal of larvae between reefs (Munday *et al.* 2009). This dispersal of larvae offers a pathway for the introduction of beneficial genes and traits across non-adjacent reef communities facilitating the adaptation of coral populations towards future climatic shifts (Matz *et al.* 2020; McManus *et al.* 2021). However, climate change is also expected to impact upon the dynamics of larval dispersal, affecting the pelagic duration (time spent in the water column) and behaviour of larvae across many coral species, potentially diminishing the connectivity, and thus the performance and resilience, of global reef populations (Munday *et al.* 2009). To fully comprehend the future viability of global coral communities it is, therefore, necessary that we resolve gaps in our understanding of reef connectivity (Edmunds *et al.* 2018), so that we might quantify eco-evolutionary patterns within the dynamics of coral communities.

6.2. Future advancements

Irrespective of their limitations, demographic approaches can offer an extensive insight into the future viability and functioning of coral communities, and the reef ecosystems they support (Edmunds & Riegl 2020; Pisapia *et al.* 2020). Therefore, demographic approaches are becoming increasingly popular for informing on the conservation of keystone coral species and communities (Bramanti *et al.* 2019). Yet, a further advantage of demographic models is their flexible mathematical frameworks, ensuring there is no limit to their complexity (Ellner & Rees 2006; Ellner *et al.* 2016). Provided there are adequate data, and that the questions and biological system justify increased sophistication (Getz *et al.* 2018), there is still considerable scope for answering increasingly complex questions regarding the dynamics of coral populations, their wider community interactions, and their future responses to climatic and anthropogenic disturbances.

Firstly, with future changes expected across regional climate regimes, the conservation of biological communities requires an ability to predict changes in species distributions following shifts in favourable environmental conditions (Chen *et al.* 2020). Species Distribution Models (SDMs) were initially developed to predict the potential redistribution of populations using observed correlations between species occurrences and environmental parameters (Guisan & Zimmermann 2000). However, this approach relies on the incorrect assumption that high environmental suitability guarantees high local abundance (Csergő *et al.* 2017; Merow *et al.* 2017; Weber *et al.* 2017). Instead, as already highlighted for coral populations, the distribution of natural populations is a consequence of the interaction between population dynamics, dispersal, and their abiotic drivers (García-Valdés *et al.* 2013; Chen *et al.* 2020). This understanding has since lead to the development of techniques such as Dynamic Range Models (DRMs), which combine environmental suitability, species occurrence data, dispersal kernels, and patterns in population dynamics, to predict future range shifts (Pagel & Schurr 2012). DRMs offer the opportunity to not only evaluate the reassembly and redistribution of coral communities, but to also quantify the extent to which this will influence the wider ecosystems, and ecosystem services they support.

Secondly, considering the diversity of coral reefs worldwide, managing the viability and reassembly of global coral communities, requires forecasting the simultaneous, and often related, responses of multiple co-occurring species and populations. Quantifying the mechanisms that promote the coexistence of multiple species has huge implications on our capacity to manage and conserve biological communities (Chu & Adler 2015). Competitive interactions between both con- and heterospecific individuals play a fundamental role in regulating the viability of populations (Collins *et al.* 1998), mediating the establishment of species within novel environments (Levine *et al.* 2004), and buffering the impacts of climatic change (Suttle *et al.* 2007; Gilman *et al.* 2010). Yet, approaches to quantify the influence of species coexistence on the wider dynamics of biological communities remain neglected (Barraquand & Gimenez 2019; Ellner *et al.* 2019). Evaluating the influence of species coexistence on the compositional structure of coral communities, and their capacity to endure future climate shifts is therefore an aspect of demographic research in need of development.

Although assessments into the impacts of coexistence on the dynamics of populations are scarce, previous research demonstrates pertinent methodologies for evaluating patterns of coexistence between coral species and populations. Adler *et al.* (2010) applied a spatially implicit Integral Projection Model (IPM) to explore patterns of coexistence within a grassland community. To achieve this, Adler *et al.* included measures of the size and distance to neighbouring individuals within their assessments of plant survival, growth, and reproduction. This approach allowed the authors to quantify how individual interactions influenced the dynamics of their focal populations. Similarly, Barraquand & Gimenez (2019) introduced a mathematical approach for Integrated Community Models (ICM), building on the existing framework of state-structured population models. Briefly, an ICM simultaneously captures the differing vital rates of co-occurring populations (*i.e.*, survival, growth, and reproduction) whilst weighting vital rates according to known interaction pressures. For instance, in their example Barraquand & Gimenez (2019) parameterised an ICM describing a predator-prey interaction such that prey reproduction and survival decreased with increasing predator density, whereas predator reproduction increases with increasing prey density. Whilst the interaction mechanisms within coral communities are more complex than this example, the setup of permanent plots used throughout my thesis facilitates following the distances between individuals over time. Accordingly, it would be possible to conduct both ongoing and retrospective analyses into coexistence within coral communities, exploring how interactions influence the dynamics of coral populations, and how the loss of individuals could release others from competitive restraints.

Finally, it would be worthwhile to explore whether transient demographic approaches can be used to predict the impacts of diminished recovery on the subsequent resilience of populations. Transient dynamics represent measures of recovery and resistance providing an opportunity for quantifying population resilience (Stott *et al.* 2011; Hodgson *et al.* 2015; Capdevila *et al.* 2020). However, due to the matrix framework used in evaluating transient dynamics, the transient properties of any given population are connected, such that their estimates of resistance and recovery are linked. Therefore, the current application of transient demographic theory in evaluating population resilience assumes that populations will be afforded space and/or time to elicit a recovery response. In reality the increasing frequency of climatic and anthropogenic disturbance events means this assumption is becoming increasingly unlikely (Seneviratne *et al.* 2014; Hughes *et al.* 2018; McDowell *et al.* 2018). Crucially, there is a precedent for manipulating population models to isolate key population characteristics, most notably the division of projection matrices by their dominant eigenvalues to differentiate their asymptotic and transient characteristics (Townley & Hodgson 2008; Stott *et al.* 2011). Thus, can projection matrices also be manipulated to diminish selected transient characteristics thereby simulating scenarios of limited recovery or resistance? If possible, such a framework would then provide valuable insights for the management of vulnerable ecosystems experiencing increasingly recurrent disturbances, therefore limiting their chances for recovery.

6.3. Conclusions

Throughout this thesis, I advocate for the improved use of demographic tools within the assessment of global coral populations. I argue particularly for the adoption of transient demographic theory, which provides a truer representation of populations within natural environments. Variation in the transient dynamics of populations cannot be solely attributed to differences in their exposures to abiotic variability. Yet, I have demonstrated how understanding the relative transient potential of coral populations will help us to accurately predict the future reassembly of global coral communities under scenarios of increasing climatic change. Without a greater commitment towards understanding the transient dynamics of coral populations we will be unable to forecast the future resilience, viability, and condition of global coral communities, thereby limiting our capacity to effectively conserve reef ecosystems worldwide.

6.4. References

Adjeroud, M., Kayal, M. & Penin, L. (2017). Importance of recruitment processes in the dynamics and resilience of coral reef assemblages. In: *Marine Animal Forests: The Ecology of Benthic Biodiversity Hotspots* (eds. Rossi, S., Bramanti, L., Gori, A. & Orejas, C.). Springer International Publishing, Cham, pp. 549–569.

Adler, P.B., Ellner, S.P. & Levine, J.M. (2010). Coexistence of perennial plants: An embarrassment of niches. *Ecol. Lett.*, 13, 1019–1029.

Agudo-Adriani, E.A., Cappelletto, J., Cavada-Blanco, F. & Croquer, A. (2016). Colony geometry and structural complexity of the endangered species Acropora cervicornis partly explains the structure of their associated fish assemblage. *PeerJ*, 4, 1–23.

Alvarez-Filip, L., Dulvy, N.K., Gill, J.A., Côté, I.M. & Watkinson, A.R. (2009). Flattening of Caribbean coral reefs: Region-wide declines in architectural complexity. *Proc. R. Soc. B Biol. Sci.*, 276, 3019–3025.

Álvarez-Noriega, M., Baird, A.H., Dornelas, M., Madin, J.S., Cumbo, V.R. & Connolly, S.R. (2016). Fecundity and the demographic strategies of coral morphologies. *Ecol. Soc. Am.*, 97, 3485–3493.

Baird, A.H., Guest, J.R., Edwards, A.J., Bauman, A.G., Bouwmeester, J., Mera, H., *et al.* (2021). An Indo-Pacific coral spawning database. *Sci. Data*, 8, 1–9.

Banks, S.A. & Harriott, V.J. (1996). Patterns of coral recruitment at the Gneering Shoals, southeast Queensland, Australia. *Coral Reefs*, 15, 225–230.

Barraquand, F. & Gimenez, O. (2019). Integrating multiple data sources to fit matrix population models for interacting species. *Ecol. Modell.*, 411, 1–25.

Beger, M., Sommer, B., Harrison, P.L., Smith, S.D.A. & Pandolfi, J.M. (2014). Conserving potential coral reef refuges at high latitudes. *Divers. Distrib.*, 20, 1–13.

Bergman, J.L., Harii, S., Kurihara, H. & Edmunds, P.J. (2018). Behavior of brooded coral larvae in response to elevated pCO2. *Front. Mar. Sci.*, 4, 1–11.

Boyd, P.W., Cornwall, C.E., Davison, A., Doney, S.C., Fourquez, M., Hurd, C.L., *et al.* (2016). Biological responses to environmental heterogeneity under future ocean conditions. *Glob. Chang. Biol.*, 22, 2633–2650.

Bramanti, L., Santangelo, G., Benedetti, M.C., Iannelli, M. & Guizien, K. (2019). Demography and conservation of deep corals: The study of population structure and dynamics. In: *Mediterranean Cold-Water Corals: Past, Present and Future: Understanding the Deep-Sea Realms of Coral* (eds. Orejas, C. & Jiménez, C.). Springer, pp. 423–434.

Bright Ross, J.G., Newman, C., Buesching, C.D. & Macdonald, D.W. (2020). What lies beneath? Population dynamics conceal pace-of-life and sex ratio variation, with implications for resilience to environmental change. *Glob. Chang. Biol.*, 26, 3307–3324.

Burt, J.A., Camp, E.F., Enochs, I.C., Johansen, J.L., Morgan, K.M., Riegl, B., *et al.* (2020). Insights from extreme coral reefs in a changing world. *Coral Reefs*, 39, 495–507.

Camp, E.F., Schoepf, V., Mumby, P.J., Hardtke, L.A., Rodolfo-Metalpa, R., Smith, D.J., *et al.* (2018). The future of coral reefs subject to rapid climate change: Lessons from natural extreme environments. *Front. Mar. Sci.*, 5, 1–21.

Capdevila, P., Stott, I., Beger, M. & Salguero-Gómez, R. (2020). Towards a comparative framework of demographic resilience. *Trends Ecol. Evol.*, 35, 776–786.

Chen, Y.H., Shertzer, K.W. & Viehman, T.S. (2020). Spatio-temporal dynamics of the threatened elkhorn coral Acropora palmata: Implications for conservation. *Divers. Distrib.*, 26, 1582–1597.

Chu, C. & Adler, P.B. (2015). Large niche differences emerge at the recruitment stage to stabilize grassland coexistence. *Ecol. Monogr.*, 85, 373–392.

Collins, S.L., Knapp, A.K., Briggs, J.M., Blair, J.M. & Steinauer, E.M. (1998). Modulation of diversity by grazing and mowing in native tallgrass prairie. *Science*, 280, 745–747.

Coumou, D. & Rahmstorf, S. (2012). A decade of weather extremes. *Nat. Clim. Chang.*, 2, 491–496.

Cowen, R.K. & Sponaugle, S. (2009). Larval dispersal and marine population connectivity. *Ann. Rev. Mar. Sci.*, 1, 443–466.

Csergő, A.M., Salguero-Gómez, R., Broennimann, O., Coutts, S.R., Guisan, A., Angert, A.L., *et al.* (2017). Less favourable climates constrain demographic strategies in plants. *Ecol. Lett.*, 20, 969–980.

Dawson, T.P., Jackson, S.T., House, J.I., Prentice, I.C. & Mace, G.M. (2011). Beyond predictions: Biodiversity conservation in a changing climate. *Science*, 332, 53–58.

Dixon, G.B., Davies, S.W., Aglyamova, G. V., Meyer, E., Bay, L.K. & Matz, M. V. (2015). Genomic determinants of coral heat tolerance across latitudes. *Science*, 348, 1460–1462.

Donohue, I., Hillebrand, H., Montoya, J.M., Petchey, O.L., Pimm, S.L., Fowler, M.S., *et al.* (2016). Navigating the complexity of ecological stability. *Ecol. Lett.*, 19, 1172–1185.

Donohue, I., Petchey, O.L., Montoya, J.M., Jackson, A.L., Mcnally, L., Viana, M., *et al.* (2013). On the dimensionality of ecological stability. *Ecol. Lett.*, 16, 421–429.

Doropoulos, C., Ward, S., Diaz-Pulido, G., Hoegh-Guldberg, O. & Mumby, P.J. (2012). Ocean acidification reduces coral recruitment by disrupting intimate larval-algal settlement interactions. *Ecol. Lett.*, 15, 338–346.

Eckman, J.E. (1996). Closing the larval loop: Linking larval ecology to the population dynamics of marine benthic invertebrates. *J. Exp. Mar. Bio. Ecol.*, 200, 207–237.

Edmunds, P.J., Burgess, S.C., Putnam, H.M., Baskett, M.L., Bramanti, L., Fabina, N.S., *et al.* (2014). Evaluating the causal basis of ecological success within the scleractinia: an integral projection model approach. *Mar. Biol.*, 161, 2719–2734.

Edmunds, P.J., McIlroy, S.E., Adjeroud, M., Ang, P., Bergman, J.L., Carpenter, R.C., *et al.* (2018). Critical information gaps impeding understanding of the role of larval connectivity among coral reef islands in an era of Global Change. *Front. Mar. Sci.*, 5, 1–16.

Edmunds, P.J. & Riegl, B. (2020). Urgent need for coral demography in a world where corals are disappearing. *Mar. Ecol. Prog. Ser.*, 635, 233–242.

Ellis, M.M. & Crone, E.E. (2013). The role of transient dynamics in stochastic population growth for nine perennial plants. *Ecology*, 94, 1681–1686.

Ellner, S.P., Childs, D.Z. & Rees, M. (2016). *Data-driven Modelling of Structured Populations*. Springer International Publishing, Switzerland.

Ellner, S.P. & Rees, M. (2006). Integral projection models for species with complex demography. *Am. Nat.*, 167, 410–428.

Ellner, S.P., Snyder, R.E., Adler, P.B. & Hooker, G. (2019). An expanded modern coexistence theory for empirical applications. *Ecol. Lett.*, 22, 3–18.

Gaillard, J.M., Hebblewhite, M., Loison, A., Fuller, M., Powell, R., Basille, M., *et al.* (2010). Habitat-performance relationships: Finding the right metric at a given spatial scale. *Philos. Trans. R. Soc. B Biol. Sci.*, 365, 2255–2265.

García-Valdés, R., Zavala, M.A., Araújo, M.B. & Purves, D.W. (2013). Chasing a moving target: Projecting climate change-induced shifts in non-equilibrial tree species distributions. *J. Ecol.*, 101, 441–453.

Getz, W.M., Marshall, C.R., Carlson, C.J., Giuggioli, L., Ryan, S.J., Romañach, S.S., *et al.* (2018). Making ecological models adequate. *Ecol. Lett.*, 21, 153–166.

Gilman, S.E., Urban, M.C., Tewksbury, J., Gilchrist, G.W. & Holt, R.D. (2010). A framework for community interactions under climate change. *Trends Ecol. Evol.*, 25, 325–331.

Gilmour, J., Speed, C.W. & Babcock, R. (2016). Coral reproduction in Western Australia. *PeerJ*, 1–43.

Glynn, P. (1996). Coral reef bleaching: facts, hypotheses and implications. *Glob. Chang. Biol.*, 2, 495–509.

Graham, N.A.J. & Nash, K.L. (2013). The importance of structural complexity in coral reef ecosystems. *Coral Reefs*, 32, 315–326.

Guisan, A. & Zimmermann, N.E. (2000). Predictive habitat distribution models in ecology. *Ecol. Modell.*, 135, 147–186.

Hall, V.R. & Hughes, T.P. (1996). Reproductive strategies of modular organisms: Comparative studies of reef-building corals. *Ecology*, 77, 950–963.

Harriott, V.J. (1999). Coral recruitment at a high latitude Pacific site: A comparison with Atlantic reefs. *Bull. Mar. Sci.*, 65, 881–891.

Harriott, V.J. & Banks, S.A. (1995). Recruitment of scleractinian corals in the Solitary Islands Marine Reserve, a high latitude coral-dominated community in

Eastern Australia. *Mar. Ecol. Prog. Ser.*, 123, 155–161.

Harrison, P.L. (2011). Sexual reproduction of scleractinian corals. In: *Coral Reefs: An Ecosystem in Transition* (eds. Dubinsky, Z. & Stambler, N.). New York, U.S.A, pp. 59–85.

Hastings, A. (2001). Transient dynamics and persistence of ecological systems. *Ecol. Lett.*, 4, 215–220.

Hastings, A. (2004). Transients: The key to long-term ecological understanding? *Trends Ecol. Evol.*, 19, 39–45.

Hastings, A., Abbott, K.C., Cuddington, K., Francis, T., Gellner, G., Lai, Y.C., *et al.* (2018). Transient phenomena in ecology. *Science*, 361, 1–9.

Hata, T., Madin, J.S., Cumbo, V.R., Denny, M., Figueiredo, J., Harii, S., *et al.* (2017). Coral larvae are poor swimmers and require fine-scale reef structure to settle. *Sci. Rep.*, 7, 1–9.

Hodgson, D., McDonald, J.L. & Hosken, D.J. (2015). What do you mean, “resilient”? *Trends Ecol. Evol.*, 30, 503–506.

Hughes, T.P., Anderson, K.D., Connolly, S.R., Heron, S.F., Kerry, J.T., Lough, J.M., *et al.* (2018). Spatial and temporal patterns of mass bleaching of corals in the Anthropocene. *Science*, 359, 80–83.

Hughes, T.P., Kerry, J.T., Connolly, S.R., Baird, A.H., Eakin, C.M., Heron, S.F., *et al.* (2019). Ecological memory modifies the cumulative impact of recurrent climate extremes. *Nat. Clim. Chang.*, 9, 40–43.

Iles, D.T., Rockwell, R.F. & Koons, D.N. (2019). Shifting vital rate correlations alter predicted population responses to increasingly variable environments. *Am. Nat.*, 193, E57–E64.

IPCC. (2014). *Climate Change 2014: Synthesis Report. Contribution of Working Groups I, II and III to the Fifth Assessment Report of the Intergovernmental Panel on Climate Change. [Core Writing Team, R.K. Pachauri and L.A. Meyer (eds.)]*. Geneva, Switzerland,.

Jelbert, K., Buss, D., McDonald, J., Townley, S., Franco, M., Stott, I., *et al.* (2019).

Demographic amplification is a predictor of invasiveness among plants. *Nat. Commun.*, 10, 1–6.

Jones, G.P., Almany, G.R., Russ, G.R., Sale, P.F., Steneck, R.S., Van Oppen, M.J.H., *et al.* (2009). Larval retention and connectivity among populations of corals and reef fishes: History, advances and challenges. *Coral Reefs*, 28, 307–325.

Kayal, M., Lenihan, H.S., Brooks, A.J., Holbrook, S.J., Schmitt, R.J. & Kendall, B.E. (2018). Predicting coral community recovery using multi-species population dynamics models. *Ecol. Lett.*, 22, 605–615.

Kéfi, S., Domínguez-García, V., Donohue, I., Fontaine, C., Thébault, E. & Dakos, V. (2019). Advancing our understanding of ecological stability. *Ecol. Lett.*, 22, 1349–1356.

Koons, D.N., Pavard, S., Baudisch, A. & Jessica, C. (2009). Is life-history buffering or lability adaptive in stochastic environments? *Oikos*, 118, 972–980.

Lande, R., Engen, S. & Sther, B.E. (2003). *Stochastic population dynamics in ecology and conservation*. Oxford University Press, Oxford.

Levine, J.M., Adler, P.B. & Yelenik, S.G. (2004). A meta-analysis of biotic resistance to exotic plant invasions. *Ecol. Lett.*, 7, 975–989.

Loya, Y., Sakai, K., Yamazato, K., Nakano, Y., Sambali, H. & van Woesik, R. (2001). Coral bleaching: the winners and the losers. *Ecol. Lett.*, 4, 122–131.

Madin, J.S., Anderson, K.D., Andreasen, M.H., Bridge, T.C., Cairns, S.D., Connolly, S.R., *et al.* (2016). The Coral Trait Database, a curated database of trait information for coral species from the global oceans. *Sci. Data*, 3, 1–21.

Madin, J.S., Hughes, T.P. & Connolly, S.R. (2012). Calcification, Storm Damage and Population Resilience of Tabular Corals under Climate Change. *PLoS One*, 7, 1–10.

Matz, M. V., Treml, E.A. & Haller, B.C. (2020). Estimating the potential for coral adaptation to global warming across the Indo-West Pacific. *Glob. Chang. Biol.*, 26, 3473–3481.

McDonald, J.L., Stott, I., Townley, S. & Hodgson, D.J. (2016). Transients drive the demographic dynamics of plant populations in variable environments. *J. Ecol.*, 104, 306–314.

McDowell, N.G., Michaletz, S.T., Bennett, K.E., Solander, K.C., Xu, C., Maxwell, R.M., *et al.* (2018). Predicting chronic climate-driven disturbances and their mitigation. *Trends Ecol. Evol.*, 33, 15–27.

McManus, L.C., Forrest, D.L., Tekwa, E.W., Schindler, D.E., Colton, M.A., Webster, M.M., *et al.* (2021). Evolution and connectivity influence the persistence and recovery of coral reefs under climate change in the Caribbean, Southwest Pacific, and Coral Triangle. *Glob. Chang. Biol.*, 1–15.

Merow, C., Wilson, A.M. & Jetz, W. (2017). Integrating occurrence data and expert maps for improved species range predictions. *Glob. Ecol. Biogeogr.*, 26, 243–258.

Miller, M.W., Bright, A.J., Pausch, R.E. & Williams, D.E. (2020). Larval longevity and competency patterns of Caribbean reef-building corals. *PeerJ*, 8, 1–16.

Morales, J.M., Moorcroft, P.R., Matthiopoulos, J., Frair, J.L., Kie, J.G., Powell, R.A., *et al.* (2010). Building the bridge between animal movement and population dynamics. *Philos. Trans. R. Soc. B Biol. Sci.*, 365, 2289–2301.

Morris, W.F., Tuljapurkar, S., Haridas, C. V., Menges, E.S., Horvitz, C.C. & Pfister, C.A. (2006). Sensitivity of the population growth rate to demographic variability within and between phases of the disturbance cycle. *Ecol. Lett.*, 9, 1331–1341.

Munday, P.L., Leis, J.M., Lough, J.M., Paris, C.B., Kingsford, M.J., Berumen, M.L., *et al.* (2009). Climate change and coral reef connectivity. *Coral Reefs*, 28, 379–395.

van Oppen, M.J.H. & Gates, R.D. (2006). Conservation genetics and the resilience of reef-building corals. *Mol. Ecol.*, 15, 3863–3883.

Pagel, J. & Schurr, F.M. (2012). Forecasting species ranges by statistical estimation of ecological niches and spatial population dynamics. *Glob. Ecol. Biogeogr.*, 21, 293–304.

Pintor, A.F. V., Schwarzkopf, L. & Krockenberger, A.K. (2015). Rapoport's rule: Do climatic variability gradients shape range extent? *Ecol. Monogr.*, 85, 643–659.

Pisapia, C., Edmunds, P.J., Moeller, H. V., Riegl, B.M., McWilliam, M., Wells, C.D., *et al.* (2020). Projected shifts in coral size structure in the Anthropocene. In: *Advances in Marine Biology*. Academic Press, pp. 31–60.

Precoda, K., Baird, A.H., Madsen, A., Mizerek, T., Sommer, B., Su, S.N., *et al.* (2018). How does a widespread reef coral maintain a population in an isolated environment? *Mar. Ecol. Prog. Ser.*, 594, 85–94.

Price, N.N., Muko, S., Legendre, L., Steneck, R., Van Oppen, M.J.H., Albright, R., *et al.* (2019). Global biogeography of coral recruitment: Tropical decline and subtropical increase. *Mar. Ecol. Prog. Ser.*, 621, 1–17.

Riegl, B. & Piller, W.E. (2003). Possible refugia for reefs in times of environmental stress. *Int. J. Earth Sci.*, 92, 520–531.

Rivest, E.B., Comeau, S. & Cornwall, C.E. (2017). The role of natural variability in shaping the response of coral reef organisms to climate change. *Curr. Clim. Chang. Reports*, 3, 271–281.

Scavo Lord, K., Lesneski, K.C., Bengtsson, Z.A., Kuhn, K.M., Madin, J., Cheung, B., *et al.* (2020). Multi-Year viability of a reef coral population living on mangrove roots suggests an important role for mangroves in the broader habitat mosaic of corals. *Front. Mar. Sci.*, 7, 1–16.

Seneviratne, S.I., Donat, M.G., Mueller, B. & Alexander, L. V. (2014). No pause in the increase of hot temperature extremes. *Nat. Clim. Chang.*, 4, 161–163.

Shlesinger, T. & van Woesik, R. (2021). Different population trajectories of two reef-building corals with similar life-history traits. *J. Anim. Ecol.*, 90, 1379–1389.

Sommer, B., Harrison, P.L., Beger, M. & Pandolfi, J.M. (2014). Trait-mediated environmental filtering drives assembly at biogeographic transition zones. *Ecology*, 95, 1000–1009.

Spence, A.R. & Tingley, M.W. (2020). The challenge of novel abiotic conditions for species undergoing climate-induced range shifts. *Ecography*, 43, 1571–1590.

Stott, I., Townley, S. & Hodgson, D. (2011). A framework for studying transient dynamics of population projection matrix models. *Ecol. Lett.*, 14, 959–970.

Suttle, K.B., Thomsen, M.A. & Power, M.E. (2007). Species interactions reverse grassland responses to changing climate. *Science*, 315, 640–642.

Thornton, P.K., Ericksen, P.J., Herrero, M. & Challinor, A.J. (2014). Climate variability and vulnerability to climate change: A review. *Glob. Chang. Biol.*, 20, 3313–3328.

Townley, S. & Hodgson, D.J. (2008). Erratum et addendum: Transient amplification and attenuation in stage-structured population dynamics. *J. Appl. Ecol.*, 45, 1836–1839.

Underwood, J.N., Smith, L.D., Van Oppen, M.J.H. & Gilmour, J.P. (2009). Ecologically relevant dispersal of corals on isolated reefs: Implications for managing resilience. *Ecol. Appl.*, 19, 18–29.

Vázquez, D.P., Gianoli, E., Morris, W.F. & Bozinovic, F. (2017). Ecological and evolutionary impacts of changing climatic variability. *Biol. Rev.*, 92, 22–42.

Vermeij, M.J.A., Smith, J.E., Smith, C.M., Vega Thurber, R. & Sandin, S.A. (2009). Survival and settlement success of coral planulae: Independent and synergistic effects of macroalgae and microbes. *Oecologia*, 159, 325–336.

Walker, B.H. (2020). Resilience: what it is and is not. *Ecol. Soc.*, 25, 1–3.

Weber, M.M., Stevens, R.D., Diniz-Filho, J.A.F. & Grelle, C.E. V. (2017). Is there a correlation between abundance and environmental suitability derived from ecological niche modelling? A meta-analysis. *Ecography*, 40, 817–828.

Werner, F.E., Cowen, R.K. & Paris, C.B. (2007). Coupled biological and physical models: Present capabilities and necessary developments for future studies of population connectivity. *Oceanography*, 20, 54–69.

Williams, S.E., Shoo, L.P., Isaac, J.L., Hoffmann, A.A. & Langham, G. (2008). Towards an integrated framework for assessing the vulnerability of species to climate change. *PLoS Biol.*, 6.

Appendix

Supplementary material 1

Evolutionary processes, not environmental drivers, determine demographic resilience

1.1. Species List

Table S1.1. The list of six algae (Light blue), 113 animal (Orange), and 441 plant (Dark Blue) species extracted from the COMPADRE & COMADRE databases during this study. Each species is listed along with their corresponding realm classification (Terrestrial, Freshwater or Marine), the number of population replicates extracted initially, and the number of population replicates retained in our final refined sample.

	Species	Realm	Extracted	Retained
🟦	*Ascophyllum nodosum*	Marine	1	1
🟦	*Cystoseira zosteroides*	Marine	4	
🟦	*Gracilaria gracilis*	Marine	8	8
🟦	*Laminaria digitata*	Marine	1	1
🟦	*Macrocystis pyrifera*	Marine	1	
🟦	*Pterygophora californica*	Marine	6	
🟨	*Alces alces*	Terrestrial	15	8
🟨	*Alouatta seniculus*	Terrestrial	4	
🟨	*Amazona vittata*	Terrestrial	1	1
🟨	*Ambloplites rupestris*	Aquatic	3	
🟨	*Ammocrypta pellucida*	Aquatic	1	1
🟨	*Amphimedon compressa*	Marine	2	
🟨	*Anser anser*	Terrestrial	1	
🟨	*Anthropoides paradiseus*	Terrestrial	11	
🟨	*Astroblepus ubidiai*	Aquatic	6	4
🟨	*Bostrychia hagedash*	Terrestrial	1	1
🟨	*Brachyteles hypoxanthus*	Terrestrial	25	25
🟨	*Buteo solitarius*	Terrestrial	4	4
🟨	*Calidris temminckii*	Terrestrial	2	
🟨	*Callorhinus ursinus*	Marine	1	
🟨	*Callospermophilus lateralis*	Terrestrial	18	7
🟨	*Calyptorhynchus lathami*	Terrestrial	2	
🟨	*Canis lupus*	Terrestrial	1	1
🟨	*Capra ibex*	Terrestrial	4	
🟨	*Cardisoma guanhumi*	Terrestrial	3	3

Cebus capucinus	Terrestrial	22	22
Cercopithecus mitis	Terrestrial	28	28
Certhia americana	Terrestrial	1	
Cervus elaphus	Terrestrial	3	
Chelodina expansa	Aquatic	2	2
Chelydra serpentina	Aquatic	1	1
Chen caerulescens	Terrestrial	6	
Chrysemys picta	Aquatic	3	1
Cicindela ohlone	Terrestrial	14	5
Colias alexandra	Terrestrial	5	
Connochaetes taurinus	Terrestrial	2	
Cottus bairdi	Aquatic	3	
Crocodylus johnsoni	Aquatic	4	2
Crocodylus niloticus	Aquatic	2	
Cryptophis nigrescens	Terrestrial	1	1
Dasypus novemcinctus	Terrestrial	3	3
Diadema antillarum	Marine	4	
Dipodomys spectabilis	terrestrial	2	1
Eidolon helvum	Terrestrial	1	
Elephas maximus	Terrestrial	1	
Emydura macquarii	Aquatic	2	2
Epidalea calamita	Aquatic	1	
Epinephelus morio	Marine	1	
Etheostoma flabellare	Aquatic	3	
Eumetopias jubatus	Marine	1	
Falco peregrinus	Terrestrial	13	
Fulmarus glacialis	Terrestrial	1	1
Giraffa camelopardalis	Terrestrial	4	4
Gorilla beringei	Terrestrial	41	41
Haliaeetus albicilla	Terrestrial	2	
Homo sapiens	Terrestrial	26	
Hoplocephalus bungaroides	Terrestrial	1	1
Hystrix refossa	Terrestrial	1	
Kinosternon subrubrum	Aquatic	3	3
Kobus ellipsiprymnus defassa	Terrestrial	2	
Lagopus muta	Terrestrial	1	1
Larus heermanni	Terrestrial	2	
Leptonychotes weddellii	Marine	21	
Macaca mulatta	Terrestrial	12	12
Malaclemys terrapin	Aquatic	1	1
Marmota flaviventris	Terrestrial	2	2
Montastraea annularis	Marine	13	
Nipponia nippon	Terrestrial	1	
Nocomis leptocephalus	Aquatic	3	
Nuttallia obscurata	Marine	2	1
Odocoileus virginianus	Terrestrial	14	13

Oncorhynchus tshawytscha	Marine	5	
Onychogalea fraenata	Terrestrial	1	1
Ovis aries	Terrestrial	6	
Ovis canadensis	Terrestrial	8	
Ovis canadensis sierrae	Terrestrial	14	6
Pan troglodytes schweinfurthii	Terrestrial	45	45
Panthera pardus	Terrestrial	1	1
Papio cynocephalus	Terrestrial	37	37
Paramuricea clavata	Marine	11	10
Phoca vitulina	Marine	1	
Phoebastria immutabilis	Terrestrial	1	1
Phrynosoma cornutum	Terrestrial	2	2
Plexaura sp.	Marine	4	
Pocillopora damicornis	Marine	1	
Podocnemis expansa	Aquatic	1	1
Presbytis thomasi	Terrestrial	1	
Propithecus edwardsi	Terrestrial	2	2
Propithecus verreauxi	Terrestrial	24	24
Rangifer tarandus platyrhynchus	Terrestrial	1	
Rutilus rutilus	Aquatic	1	1
Saguinus fuscicollis	Terrestrial	4	
Saguinus imperator	Terrestrial	3	
Sceloporus grammicus	Terrestrial	8	8
Sceloporus mucronatus mucronatus	Terrestrial	1	1
Scolytus ventralis	Terrestrial	5	5
Spermophilus dauricus	Terrestrial	1	1
Sterna hirundo	Terrestrial	8	
Sternotherus odoratus	Aquatic	2	
Sternula antillarum browni	Terrestrial	1	
Strix occidentalis occidentalis	Terrestrial	12	11
Sus scrofa scrofa	Terrestrial	1	
Tamias striatus	Terrestrial	11	
Tamiasciurus hudsonicus	Terrestrial	1	1
Thalassarche melanophris	Terrestrial	1	
Umbonium costatum	Marine	8	8
Urocitellus armatus	Terrestrial	1	1
Urocitellus beldingi	Terrestrial	1	
Urocyon littoralis	Terrestrial	2	2
Ursus americanus	Terrestrial	4	4
Ursus arctos horribilis	Terrestrial	1	
Ursus maritimus	Terrestrial	5	5
Vipera aspis	Terrestrial	1	1
Xenosaurus grandis	Terrestrial	4	4
Xenosaurus platyceps	Terrestrial	6	6
Xestospongia muta	Marine	5	2
Zalophus californianus	Marine	9	7

🟨	*Zoarces viviparus*	Marine	4	1
	Zootoca vivipara	Terrestrial	1	
🟦	*Abies balsamea*	Terrestrial	2	
	Abies concolor	Terrestrial	12	11
	Abies homolepis	Terrestrial	1	
	Abies magnifica	Terrestrial	11	9
	Abies sachalinensis	Terrestrial	3	2
	Acacia aneura	Terrestrial	1	
	Acacia victoriae	Terrestrial	1	
	Acer palmatum	Terrestrial	2	2
	Acer pictum	Terrestrial	2	2
	Acer rufinerve	Terrestrial	2	2
	Acer saccharum	Terrestrial	6	6
	Achnatherum calamagrostis	Terrestrial	3	3
	Actaea cordifolia	Terrestrial	5	3
	Actaea elata	Terrestrial	4	2
	Actaea spicata	Terrestrial	12	12
	Adenocarpus gibbsianus	Terrestrial	13	2
	Aesculus turbinata	Terrestrial	3	
	Agave marmorata	Terrestrial	2	
	Agave potatorum	Terrestrial	2	
	Agave vivipara	Terrestrial	2	
	Agrimonia eupatoria	Terrestrial	10	6
	Agropyron cristatum	Terrestrial	2	
	Ailanthus altissima	Terrestrial	1	1
	Alliaria petiolata	Terrestrial	38	
	Allium monanthum	Terrestrial	2	1
	Allium vineale	Terrestrial	2	
	Alnus rubra	Terrestrial	6	5
	Ambrosia deltoidea	Terrestrial	1	1
	Anarrhinum fruticosum	Terrestrial	5	3
	Andira aubletii	Terrestrial	1	1
	Andropogon gerardii	Terrestrial	20	9
	Androsace vitaliana	Terrestrial	2	2
	Anemone patens	Terrestrial	1	1
	Anthericum liliago	Terrestrial	6	
	Anthericum ramosum	Terrestrial	11	
	Anthyllis vulneraria	Terrestrial	36	23
	Anthyllis vulneraria alpicola	Terrestrial	4	
	Antirrhinum lopesianum	Terrestrial	3	2
	Antirrhinum subbaeticum	Terrestrial	2	2
	Aquilaria crassna	Terrestrial	1	1
	Aquilegia chrysantha	Terrestrial	1	1
	Aquilegia sp.	Terrestrial	1	
	Araucaria cunninghamii	Terrestrial	4	4
	Araucaria muelleri	Terrestrial	4	4

Arctophila fulva	Terrestrial	3	
Arenaria grandiflora	Terrestrial	5	3
Arisaema serratum	Terrestrial	1	1
Arisaema triphyllum	Terrestrial	4	
Armeria maritima	Terrestrial	1	1
Armeria merinoi	Terrestrial	10	4
Arnica angustifolia	Terrestrial	1	
Artemisia genipi	Terrestrial	4	4
Asclepias meadii	Terrestrial	2	2
Aspasia principissa	Terrestrial	1	1
Asplenium adulterinum	Terrestrial	18	
Asplenium cuneifolium	Terrestrial	12	12
Asplenium scolopendrium	Terrestrial	6	6
Aster amellus	Terrestrial	27	
Aster pyrenaeus	Terrestrial	5	
Astragalus alopecurus	Terrestrial	15	6
Astragalus bibullatus	Terrestrial	4	4
Astragalus cremnophylax	Terrestrial	2	
Astragalus michauxii	Terrestrial	1	1
Astragalus scaphoides	Terrestrial	115	101
Astragalus tremolsianus	Terrestrial	5	3
Astragalus tyghensis	Terrestrial	45	36
Astrocaryum mexicanum	Terrestrial	7	5
Astrophytum asterias	Terrestrial	8	7
Astrophytum capricorne	Terrestrial	3	3
Astrophytum ornatum	Terrestrial	3	3
Atriplex acanthocarpa	Terrestrial	3	2
Atriplex canescens	Terrestrial	3	3
Aurinia saxatilis subsp. Saxatilis	Terrestrial	6	
Avicennia germinans	Terrestrial	1	1
Balsamorhiza sagittata	Terrestrial	5	
Banksia ericifolia	Terrestrial	1	1
Bertholletia excelsa	Terrestrial	2	2
Betula pubescens pumila	Terrestrial	3	
Boechera fecunda	Terrestrial	14	13
Borassus aethiopum	Terrestrial	4	4
Bothriochloa insculpta	Terrestrial	4	
Bouteloua rigidiseta	Terrestrial	3	
Brassica insularis	Terrestrial	36	31
Brosimum alicastrum	Terrestrial	1	
Bursera glabrifolia	Terrestrial	3	1
Calamagrostis canescens	Terrestrial	1	
Calamus nambariensis	Terrestrial	1	
Calamus rhabdocladus	Terrestrial	1	
Calocedrus decurrens	Terrestrial	6	6
Calochortus albus	Terrestrial	2	2

Calochortus lyallii	Terrestrial	44	44
Calochortus obispoensis	Terrestrial	2	1
Calochortus pulchellus	Terrestrial	2	1
Calochortus tiburonensis	Terrestrial	2	2
Camellia japonica	Terrestrial	2	1
Carduus nutans	Terrestrial	5	4
Carex bigelowii	Terrestrial	1	
Carex humilis	Terrestrial	8	
Carlina vulgaris	Terrestrial	8	3
Carnegiea gigantea	Terrestrial	1	1
Castanea dentata	Terrestrial	24	23
Catopsis compacta	Terrestrial	3	3
Catopsis sessiliflora	Terrestrial	2	1
Cecropia obtusifolia	Terrestrial	3	3
Cedrela odorata	Terrestrial	15	
Centaurea horrida	Terrestrial	3	3
Centaurea jacea	Terrestrial	4	
Cephalocereus senilis	Terrestrial	1	
Chamaecrista lineata	terrestrial	12	11
Chamaedorea radicalis	Terrestrial	8	7
Cheirolophus metlesicsii	Terrestrial	5	2
Cherleria obtusiloba	Terrestrial	1	1
Chlorocardium rodiei	Terrestrial	1	1
Cirsium acaule	Terrestrial	2	2
Cirsium dissectum	Terrestrial	13	
Cirsium palustre	Terrestrial	3	
Cirsium pannonicum	Terrestrial	1	1
Cirsium perplexans	Terrestrial	2	2
Cirsium pitcheri	Terrestrial	142	87
Cirsium vulgare	Terrestrial	3	
Cleistesiopsis bifaria	Terrestrial	7	
Cleistesiopsis divaricata	Terrestrial	5	
Clidemia hirta	Terrestrial	6	4
Coccothrinax readii	Terrestrial	1	1
Coespeletia spicata	Terrestrial	1	1
Coespeletia timotensis	Terrestrial	1	1
Conradina glabra	Terrestrial	4	3
Coprinopsis cinerea	Terrestrial	2	2
Corallorhiza trifida	Terrestrial	5	4
Cornus florida	Terrestrial	1	1
Cucurbita pepo	Terrestrial	3	3
Cynoglossum officinale	Terrestrial	1	
Cypripedium calceolus	Terrestrial	30	
Cypripedium fasciculatum	Terrestrial	24	23
Cypripedium lentiginosum	Terrestrial	1	
Cyrtandra dentata	Terrestrial	20	20

Cytisus scoparius	Terrestrial	20	18
Dactylorhiza lapponica	Terrestrial	4	2
Daemonorops poilanei	Terrestrial	1	
Danthonia sericea	Terrestrial	10	8
Daphne rodriguezii	Terrestrial	41	
Dendropanax trifidus	Terrestrial	1	
Dicentra canadensis	Terrestrial	9	
Dicerandra frutescens	Terrestrial	59	40
Dicorynia guianensis	Terrestrial	1	1
Dicymbe altsonii	Terrestrial	1	1
Digitaria eriantha	Terrestrial	4	
Dioon caputoi	Terrestrial	3	3
Dioon edule	Terrestrial	3	
Dioon merolae	Terrestrial	8	3
Dioon sonorense	Terrestrial	1	1
Dioon spinulosum	Terrestrial	2	2
Dioscorea chouardii	Terrestrial	1	1
Dipsacus fullonum	Terrestrial	2	
Disporum sessile	Terrestrial	2	1
Disporum smilacinum	Terrestrial	2	1
Dracocephalum austriacum	Terrestrial	36	28
Duguetia neglecta	Terrestrial	1	1
Echeveria longissima	Terrestrial	1	
Echinacea angustifolia	Terrestrial	8	8
Echinocactus platyacanthus	Terrestrial	12	12
Echinospartum ibericum	Terrestrial	5	1
Encephalartos cycadifolius	Terrestrial	1	1
Encephalartos villosus	Terrestrial	1	1
Entandrophragma cylindricum	Terrestrial	1	1
Eperua falcata	Terrestrial	1	1
Epilobium latifolium	Terrestrial	2	
Epipactis atrorubens	Terrestrial	11	3
Eremophila forrestii	Terrestrial	9	9
Eremophila maitlandii	Terrestrial	12	10
Eriogonum longifolium	Terrestrial	16	16
Eritrichium caucasicum	Terrestrial	4	2
Erodium paularense	Terrestrial	10	10
Erophila verna	Terrestrial	1	
Erycina crista-galli	Terrestrial	2	2
Eryngium alpinum	Terrestrial	9	8
Eryngium cuneifolium	Terrestrial	48	38
Eryngium maritimum	Terrestrial	2	2
Erythranthe cardinalis	Terrestrial	12	10
Erythranthe lewisii	Terrestrial	12	8
Erythronium japonicum	Terrestrial	2	2
Escobaria robbinsorum	Terrestrial	12	9

Escontria chiotilla	Terrestrial	2	2
Eupatorium perfoliatum	Terrestrial	3	
Eupatorium resinosum	Terrestrial	3	
Euphorbia fontqueriana	Terrestrial	5	4
Euterpe edulis	Terrestrial	3	3
Euterpe precatoria	Terrestrial	4	4
Fagus crenata	Terrestrial	1	
Fagus grandifolia	Terrestrial	3	3
Festuca eskia	Terrestrial	2	
Frasera speciosa	Terrestrial	34	
Fritillaria biflora	Terrestrial	2	
Fuscospora fusca	terrestrial	6	6
Gardenia actinocarpa	Terrestrial	4	2
Gentiana pneumonanthe	Terrestrial	4	2
Gentianella campestris	Terrestrial	1	
Geonoma deversa	Terrestrial	4	
Geonoma macrostachys	Terrestrial	1	1
Geonoma pohliana	Terrestrial	2	2
Geonoma schottiana	Terrestrial	4	2
Geranium sylvaticum	Terrestrial	3	3
Geum reptans	Terrestrial	4	
Geum rivale	Terrestrial	6	3
Goeppertia ovandensis	Terrestrial	16	3
Grias peruviana	Terrestrial	1	1
Guaiacum sanctum	Terrestrial	4	2
Guarianthe aurantiaca	Terrestrial	3	3
Guettarda viburnoides	Terrestrial	3	3
Helenium virginicum	Terrestrial	1	1
Helianthemum juliae	Terrestrial	9	7
Helianthemum polygonoides	Terrestrial	5	5
Helianthemum teneriffae	Terrestrial	5	3
Helianthus divaricatus	Terrestrial	8	
Heliconia acuminata	Terrestrial	9	9
Heteropogon contortus	Terrestrial	4	3
Heteropsis flexuosa	Terrestrial	2	
Heteropsis macrophylla	Terrestrial	2	
Heteropsis oblongifolia	Terrestrial	2	
Hilaria mutica	Terrestrial	4	4
Himantoglossum hircinum	Terrestrial	1	1
Himatanthus drasticus	Terrestrial	8	8
Horkelia congesta	Terrestrial	6	
Hudsonia montana	Terrestrial	1	
Hydrastis canadensis	Terrestrial	29	
Hylocomium splendens	Terrestrial	12	
Hypericum cumulicola	Terrestrial	66	35
Hypochaeris radicata	Terrestrial	2	

Iriartea deltoidea	Terrestrial	5	5
Isatis tinctoria	Terrestrial	1	
Jacobaea vulgaris	Terrestrial	3	
Jacquiniella leucomelana	Terrestrial	3	
Jacquiniella teretifolia	Terrestrial	3	
Juniperus procera	Terrestrial	1	1
Jurinea fontqueri	Terrestrial	5	3
Khaya senegalensis	Terrestrial	12	11
Knautia arvensis	Terrestrial	1	
Kosteletzkya pentacarpos	Terrestrial	8	7
Lantana camara	Terrestrial	10	
Laserpitium longiradium	Terrestrial	5	3
Lathyrus vernus	Terrestrial	32	17
Lechea cernua	Terrestrial	8	8
Lechea deckertii	Terrestrial	8	7
Leontodon saxatilis	Terrestrial	4	4
Lepidium davisii	Terrestrial	22	4
Leptocoryphium lanatum	Terrestrial	1	
Lespedeza juncea sericea	Terrestrial	2	
Lespedeza juncea sericea	Terrestrial	1	
Lespedeza virginica	Terrestrial	1	
Liatris scariosa	Terrestrial	15	7
Ligularia sibirica	Terrestrial	33	6
Limonium carolinianum	Terrestrial	1	1
Limonium erectum	Terrestrial	5	5
Limonium malacitanum	Terrestrial	5	2
Linum catharticum	Terrestrial	1	
Lomatium bradshawii	Terrestrial	9	9
Lomatium cookii	Terrestrial	10	9
Lonicera maackii	Terrestrial	2	2
Lophophora diffusa	Terrestrial	2	2
Lotus arinagensis	Terrestrial	6	
Lupinus tidestromii	Terrestrial	9	9
Lycaste aromatica	Terrestrial	3	
Machaerium cuspidatum	Terrestrial	3	
Magnolia macrophylla	Terrestrial	3	3
Mammillaria crucigera	Terrestrial	2	2
Mammillaria dixanthocentron	Terrestrial	1	1
Mammillaria gaumeri	Terrestrial	24	
Mammillaria hernandezii	Terrestrial	6	5
Mammillaria huitzilopochtli	Terrestrial	5	5
Mammillaria magnimamma	Terrestrial	4	4
Mammillaria napina	Terrestrial	3	2
Mammillaria pectinifera	Terrestrial	1	1
Mammillaria solisioides	Terrestrial	3	3
Mammillaria supertexta	Terrestrial	1	1

Manilkara zapota	Terrestrial	2	2
Mauritia flexuosa	Terrestrial	1	1
Melaleuca viridiflora	Terrestrial	3	
Melocactus bahiensis	Terrestrial	2	2
Melocactus ernestii	Terrestrial	4	4
Miconia albicans	Terrestrial	1	1
Miconia prasina	Terrestrial	8	
Microberlinia bisulcata	Terrestrial	1	1
Mimulus guttatus	Terrestrial	22	
Molinia caerulea	Terrestrial	12	6
Myrsine guianensis	Terrestrial	1	
Nardostachys jatamansi	Terrestrial	1	1
Neobuxbaumia macrocephala	Terrestrial	7	7
Neobuxbaumia mezcalaensis	Terrestrial	6	6
Neobuxbaumia polylopha	Terrestrial	2	2
Neobuxbaumia tetetzo	Terrestrial	6	6
Neotinea ustulata	Terrestrial	5	5
Oenothera deltoides	Terrestrial	16	16
Olearia flocktoniae	Terrestrial	8	
Oncidium poikilostalix	Terrestrial	2	2
Opuntia macrocentra	Terrestrial	2	
Opuntia macrorhiza	Terrestrial	27	6
Opuntia microdasys	Terrestrial	4	
Opuntia rastrera	Terrestrial	14	9
Orchis purpurea	Terrestrial	36	28
Oreocarya flava	Terrestrial	3	3
Oxalis acetosella	Terrestrial	6	
Oxandra asbeckii	Terrestrial	1	1
Oxytropis jabalambrensis	Terrestrial	4	2
Pachycereus pecten-aboriginum	Terrestrial	3	3
Paeonia officinalis	Terrestrial	15	
Paliurus ramosissimus	Terrestrial	2	
Panax quinquefolius	Terrestrial	2	1
Parkinsonia aculeata	Terrestrial	1	1
Parolinia glabriuscula	Terrestrial	5	4
Paronychia pulvinata	Terrestrial	1	1
Pediomelum esculentum	Terrestrial	8	6
Pentaclethra macroloba	Terrestrial	1	1
Periandra mediterranea	Terrestrial	1	1
Persoonia bargoensis	Terrestrial	4	3
Persoonia glaucescens	Terrestrial	3	3
Petrophile pulchella	Terrestrial	1	1
Phyllanthus emblica	Terrestrial	8	6
Phyllanthus indofischeri	Terrestrial	3	3
Picea glehnii	Terrestrial	1	
Picea jezoensis	Terrestrial	1	

Pilosella floribunda	Terrestrial	1	
Pinguicula alpina	Terrestrial	1	1
Pinguicula villosa	Terrestrial	1	1
Pinguicula vulgaris	Terrestrial	1	
Pinus jeffreyi	Terrestrial	1	
Pinus lambertiana	Terrestrial	6	6
Pinus maximartinezii	Terrestrial	1	1
Pinus nigra	Terrestrial	3	1
Pinus ponderosa	Terrestrial	1	1
Pinus strobus	Terrestrial	9	9
Pityopsis aspera	Terrestrial	2	1
Plantago coronopus	Terrestrial	35	29
Plantago lanceolata	Terrestrial	3	
Platanthera hookeri	Terrestrial	4	
Poa alpina	Terrestrial	6	
Polemonium van-bruntiae	Terrestrial	9	
Polygonum basiramium	Terrestrial	8	2
Potentilla anserina	Terrestrial	3	
Potentilla recta	Terrestrial	1	
Primula elatior	Terrestrial	21	13
Primula farinosa	Terrestrial	16	7
Primula veris	Terrestrial	4	1
Primula vulgaris	Terrestrial	44	37
Prioria copaifera	Terrestrial	2	2
Prosartes lanuginosa	Terrestrial	4	4
Prosopis glandulosa	Terrestrial	4	4
Prosopis laevigata	Terrestrial	2	2
Prunus africana	Terrestrial	2	2
Prunus serotina	Terrestrial	3	2
Pseudomitrocereus fulviceps	Terrestrial	1	1
Pseudophoenix sargentii	Terrestrial	7	7
Pterocarpus angolensis	Terrestrial	1	1
Pterocereus gaumeri	Terrestrial	4	4
Ptychosperma macarthurii	Terrestrial	1	1
Purshia subintegra	Terrestrial	14	8
Pyrrocoma radiata	Terrestrial	85	65
Quercus mongolica	Terrestrial	1	1
Quercus rugosa	Terrestrial	1	1
Ramonda myconi	Terrestrial	15	13
Ranunculus acris	Terrestrial	2	
Ranunculus peltatus	Terrestrial	5	3
Rhizophora mangle	Terrestrial	1	1
Rhododendron maximum	Terrestrial	3	1
Rhododendron ponticum	Terrestrial	20	4
Rhopalostylis sapida	Terrestrial	2	2
Rhus aromatica	Terrestrial	8	

	Rhus copallinum	Terrestrial	3	
	Rosa multiflora	Terrestrial	1	
	Rosmarinus tomentosus	Terrestrial	12	
	Roupala montana	Terrestrial	1	
	Rourea induta	Terrestrial	2	
	Rubus praecox	Terrestrial	3	
	Rubus saxatilis	Terrestrial	6	
	Rubus ursinus	Terrestrial	3	
	Rumex rupestris	Terrestrial	5	4
	Ruppia maritima	Terrestrial	3	
	Sabal minor	Terrestrial	3	2
	Salix arctica	Terrestrial	7	
	Santolina melidensis	Terrestrial	5	3
	Saponaria bellidifolia	Terrestrial	14	5
	Sarcocapnos baetica	Terrestrial	2	1
	Sarcocapnos pulcherrima	Terrestrial	4	2
	Sarracenia purpurea	Terrestrial	3	3
	Saussurea medusa	Terrestrial	4	
	Saxifraga aizoides	Terrestrial	4	3
	Saxifraga cotyledon	Terrestrial	8	
	Scaphium macropodum	Terrestrial	6	6
	Scorzonera hispanica	Terrestrial	1	1
	Serapias cordigera	Terrestrial	39	24
	Shorea leprosula	Terrestrial	3	3
	Silene acaulis	Terrestrial	25	13
	Silene ciliata	Terrestrial	7	5
	Silene douglasii	Terrestrial	3	3
	Silene spaldingii	Terrestrial	12	
	Solidago fistulosa	Terrestrial	3	1
	Sonchus pustulatus	Terrestrial	1	1
	Spartina alterniflora	Terrestrial	1	
	Spathoglottis plicata	Terrestrial	3	3
	Stenocereus eruca	Terrestrial	15	3
	Stryphnodendron microstachyum	Terrestrial	1	1
	Succisa pratensis	Terrestrial	12	9
	Swallenia alexandrae	Terrestrial	1	1
	Swietenia macrophylla	Terrestrial	1	1
	Syngonanthus nitens	Terrestrial	15	
	Syzygium jambos	Terrestrial	1	1
	Taraxacum campylodes	Terrestrial	1	
	Taraxacum erythrospermum	Terrestrial	2	
	Tetraberlinia bifoliolata	Terrestrial	1	1
	Tetraneuris herbacea	Terrestrial	3	
	Thrinax radiata	Terrestrial	3	3
	Thymus vulgaris	Terrestrial	4	1
	Tillandsia brachycaulos	Terrestrial	3	

Tillandsia deppeana	Terrestrial	2	2
Tillandsia juncea	Terrestrial	2	1
Tillandsia macdougallii	Terrestrial	5	5
Tillandsia multicaulis	Terrestrial	2	2
Tillandsia punctulata	Terrestrial	2	2
Tillandsia violacea	Terrestrial	3	3
Tolumnia variegata	Terrestrial	1	
Tragopogon pratensis	Terrestrial	1	
Triadica sebifera	terrestrial	12	12
Trillium camschatcense	Terrestrial	1	1
Trillium grandiflorum	Terrestrial	46	41
Trillium ovatum	Terrestrial	23	2
Trillium persistens	Terrestrial	12	12
Trollius laxus	Terrestrial	11	10
Tsuga canadensis	Terrestrial	4	4
Vella pseudocytisus	Terrestrial	9	24
Vella pseudocytisus paui	Terrestrial	20	
Verbascum fontqueri	Terrestrial	6	4
Verbascum thapsus	Terrestrial	1	
Verticordia staminosa	Terrestrial	4	
Vincetoxicum rossicum	Terrestrial	20	
Viola elatior	Terrestrial	2	2
Viola pumila	Terrestrial	2	2
Viola sagittata	Terrestrial	1	1
Vriesea sanguinolenta	Terrestrial	4	4
Vulpicida pinastri	Terrestrial	6	6
Zamia amblyphyllidia	Terrestrial	2	
Zamia inermis	Terrestrial	1	1
Zea diploperennis	Terrestrial	4	3
	Total	**3890**	**2242**

1.2. Geographical distribution of sampled populations

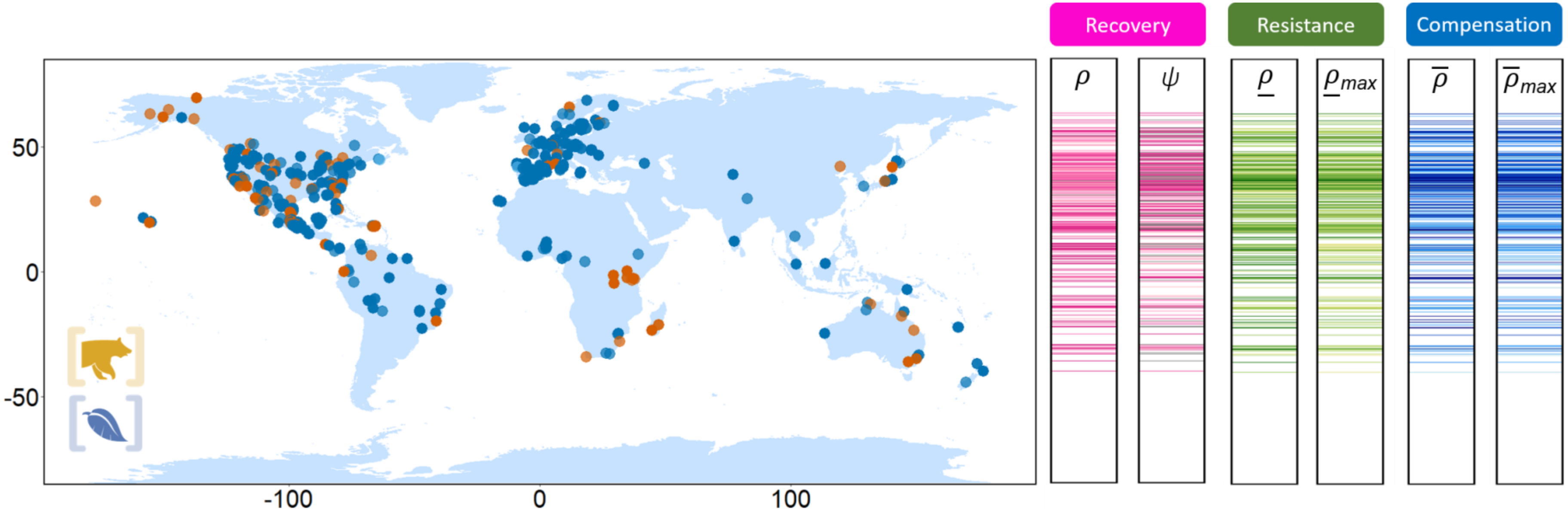

Figure S1.1. The global distribution of the 2,242 populations considered in this study. Using metrics of transient dynamics estimated using Matrix Population Models (MPMs) extracted from the global COMPADRE (Blue, plants) and COMADRE (Orange, animals) databases we explored selection pressures placed on the demographic attributes of *recovery* (damping ratio [ρ] and period of oscillation [ψ]), *resistance* (first-step attenuation [$\underline{\rho}$] and maximal attenuation [$\underline{\rho}_{max}$]) and *compensation* (reactivity [$\bar{\rho}$] and maximal amplification [$\bar{\rho}_{max}$]). The coloured strips illustrate latitudinal patterns in the transient estimates obtained across our population sample with darker shades representing higher latitudinal means.

1.3. Data cleaning

Table S1.2. The relative effect of data cleaning on our demographic and environmental variables. Descriptive summary showing the number of outlying values omitted, the transformation format used to achieve normality, and the total number of populations missing estimates for each our demographic and environmental variables. Total number of populations is 2242 across all variables.

Variable	**Omissions**	**Transformation**	**Missing***
DAMPING RATIO (ρ)	29	$1/y^{1.1}$	29
Survival	112	*NA*	112
Progression	112	*NA*	112
Retrogression	114	*NA*	114
Reproduction	112	*NA*	112
PERIOD OF OSCILLATION (ψ)	33	$1/y^{0.4}$	799
Survival	71	*NA*	837
Progression	71	*NA*	837
Retrogression	71	*NA*	837
Reproduction	68	*NA*	834
REACTIVITY ($\bar{\rho}$)	55	$1/y^{0.6}$	55
Survival	112	$log(\lvert y_{max}\rvert - y)$	113
Progression	60	$log(\lvert y_{max}\rvert - y)$	60
Retrogression	69	$log(y + \lvert y_{min}\rvert)$	69
Reproduction	81	$log(\lvert y_{max}\rvert - y)$	81
ATTENUATION ($\underline{\rho}$)	0	$y^{0.7}$	0
Survival	44	*NA*	45
Progression	60	$log(\lvert y_{max}\rvert - y)$	60
Retrogression	41	*NA*	41
Reproduction	54	$log(\lvert y_{max}\rvert - y)$	54
MAXIMAL AMPLIFICATION ($\bar{\rho}_{max}$)	55	$1/y^{0.5}$	55
Survival	112	*NA*	113

Progression	68	$log(\lvert y_{max}\rvert - y)$	68
Retrogression	112	*NA*	112
Reproduction	103	$log(\lvert y_{max}\rvert - y)$	103
MAXIMAL ATTENUATION ($\underline{\rho}_{max}$)	0	$y^{0.4}$	0
Survival	62	*NA*	63
Progression	87	$log(\lvert y_{max}\rvert - y)$	87
Retrogression	63	$log(y + \lvert y_{min}\rvert)$	63
Reproduction	89	*NA*	89
FREQUENCY SPECTRUM (Temperature, β_T)	7	*NA*	70
AUTOCORRELATION (Temperature, a_T)	37	*NA*	100
THERMAL RANGE (m)	1	*NA*	307
FREQUENCY SPECTRUM (Precipitation, β_P)	0	*NA*	63
AUTOCORRELATION (Precipitation, a_P)	0	*NA*	84

**includes omitted values*

1.4. Constructing population-level phylogenetic trees

A phylogenetic tree was constructed to ensure all our analyses accounted for covariance between closely related species. The scientific names of all unique species within our subset of Matrix Population Models (MPMs) extracted from the COMPADRE (Salguero-Gómez *et al.* 2015) and COMADRE databases (Salguero-Gómez *et al.* 2016), were cross-checked and taxonomically updated using the R package '*taxize*' (Chamberlain & Szocs 2013; Chamberlain *et al.* 2020). Next, we used the R package '*rotl*' (Michonneau *et al.* 2016), to extract phylogenetic data for each species from the Open tree of Life (OTL; Hinchliff *et al.* 2015). With this phylogenetic data, we constructed separate subtrees for brown/red algae, plants, and animal entities at the species level. Next we fused the three subtrees using the *bind.tree* tool from the '*phytools'* package (Revell 2012). Whilst binding our subtrees, we combined the algae and plant subtrees first before then adding the animal subtree with marine sponges (*Demospongiae*) set as the outgroup.

We refined the structure of our species-level phylogenetic tree, specifically ensuring the tree was rooted and free of polytomies using the *is.rooted* and *multi2di* tools from the '*ape*' package (Paradis & Schliep 2018). Branch lengths were calculated using the Grafen method (Grafen 1989) assuming a Brownian motion mode of trait evolution, whereby the variance between species' characteristics is directly proportional to time since divergence (Revell *et al.* 2008). The phylogenetic tree was then time-calibrated using the *chronos* function and checked to confirm ultrametricity, with any duplicated node labels renamed. Lastly, to accommodate intra-specific spatial variation in vital rates, we expanded this phylogenetic tree to include population-level information for the 257 species where data was available for more than one population (Fig. S1.2). For these repeated species, a number of artificial branches equal to the number of replicates, were bound to the corresponding species' tip of the original phylogenetic tree. This process was carried out using the *bind.tip* function, with each of these artificial branches assigned an equal length of infinitesimally small value (*i.e.*, 0.0000001). Next, we re-forced the tree into an ultrametric structure. The branch lengths for our taxonomic tree were then used in all further analyses to ensure our findings accounted for ancestral relationships (Revell 2010).

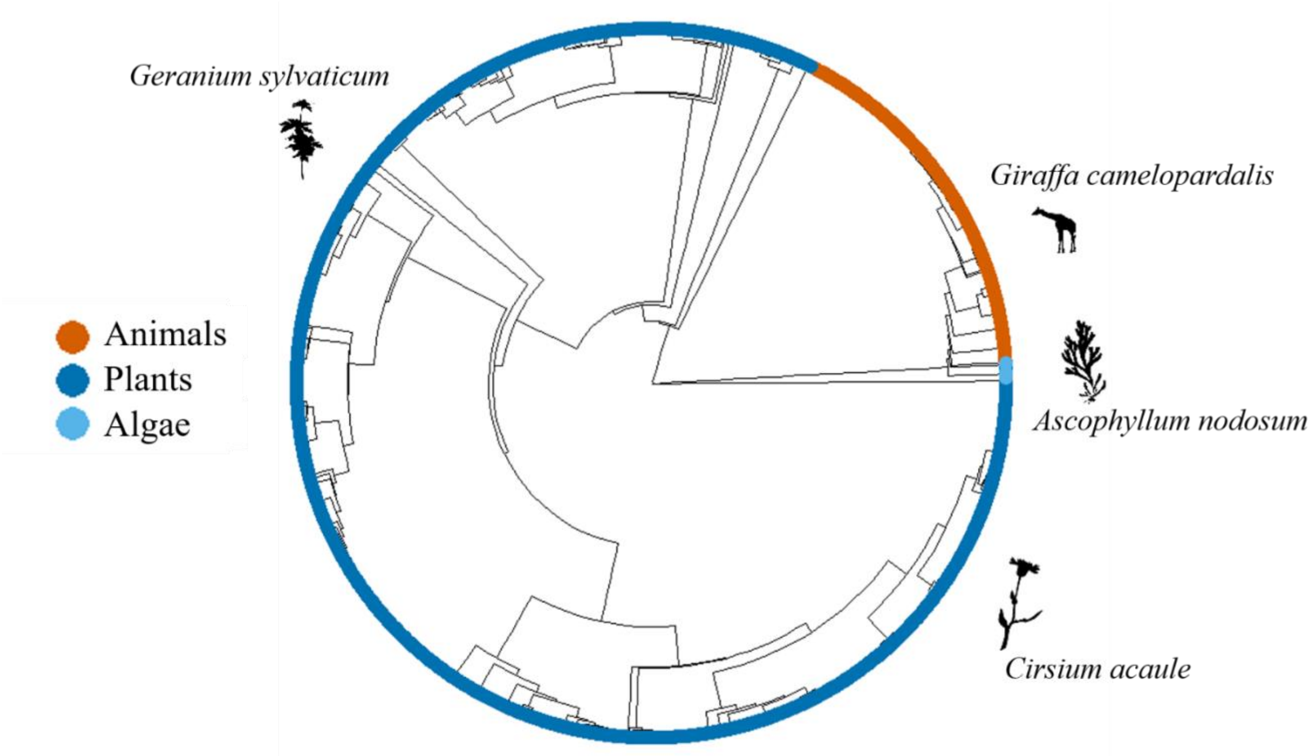

Figure S1.2. Population-level phylogenetic tree displaying the relatedness of the 61 [37] animals, 305 [219] plants, and 3 [1] red/brown algae species used in this comparative assessment. All our analyses have accounted for the phylogenetic signal between species. However, we have also allowed for the existence of multiple population entries for a number of species (shown above in square brackets), whilst assuming no within species trait variation.

1.5. Quantifying exposure to environmental stochasticity

We quantified the level of abiotic variability to which each population has been exposed, to examine the role of environmental stochasticity in shaping the resilience characteristics of *compensation*, *resistance*, and *recovery* across our 369 species. Using the GPS location information supplied with each extracted MPM from the COMPADRE & COMADRE databases, we linked each natural population to their corresponding abiotic environments.

To determine environmental stochasticity, we focused on maximum, and minimum monthly temperature (°C), and mean monthly precipitation records (kg m^{-2}). These abiotic variables were selected as they are universally important across all ecoregions, with the exception of many marine environments that are not directly affected by precipitation. Accordingly, we excluded MPMs associated with marine populations for this portion of our analysis (29 populations from 6 animal species, and 10 populations from 3 algal species). For our remaining 2184 terrestrial and 19 freshwater populations, we sourced high resolution (1 km^2) monthly temperature and precipitation records from the CHELSA climate database (Karger *et al.* 2017). For each population, we extracted maximum, and minimum temperature readings, and mean precipitation records for a timeframe equal to the period during which the population was surveyed plus an additional 50 years prior to survey onset, to account for the effects of environmental legacy (Cavender-Bares *et al.* 2016). Within our sample there was a total of 2 freshwater and 277 terrestrial populations for which no environmental data could be sourced. Subsequently, these 279 populations (12.7%) were excluded from our analyses into the role of environmental variance in shaping resilience attributes.

We used five metrics to quantify the extent of environmental variance imposed on each population: thermal autocorrelation (a_T), thermal range (m), thermal frequency spectrum (β_T), precipitation autocorrelation (a_P), and precipitation frequency spectrum (β_P). Extracted abiotic variables were arranged into time series depicting the 50+ year abiotic regimes to which each population was exposed. We then estimated the temporal autocorrelation of each temperature (a_T) and precipitation (a_P) time series, using the '*colorednoise*' package (Pilowsky 2019). Next, we calculated the frequency spectrum of each time series. This metric is often referred to as the colour of environmental variation, and represented by a red to blue colour scale, with blue describing higher frequency variation and red variation dominated by low frequencies (Ruokolainen *et al.* 2009). The frequency spectrum of a time series is expressed by its spectral exponent (β), which is calculated as the negative slope coefficient of the linear regression between the log spectral density and log frequency of the time series (Vasseur & Yodzis 2004). The spectral exponent of the temperature (β_T) and precipitation (β_P) regimes to which each population was exposed were calculated using the *spectrum* command from the '*stats*' package (*R* Core Team 2019). Finally, thermal range (m) was estimated as the mean difference between maximum and minimum monthly temperatures throughout a time series, providing a measure of the magnitude of any abiotic variation. Finally, prior to further analyses, outliers outside of the 95% confidence intervals were discarded for each of the aforementioned metrics of environmental variability (Table S1.2), and each variable was checked for normality.

A Principal Components analysis (PCA) was used to explore the interrelationships between our five abiotic variables (Fig. S1.3), whilst we also evaluated for collinearity using variance-inflation factors (VIF). VIF reflects the degree to which, in a regression model, estimates of coefficients for any given variable are inflated by collinearity, with values of between 1 and 10 representing low collinearity (Mansfield & Helms 1982; Schroeder 1990). VIF values were estimated using the *multicol* function from the '*fuzzySim*' package (Barbosa 2015). In our PCA the majority of the variation across our abiotic variables could be explained using the just the first two principal components (Proportional variance: PC1 0.43; PC2 0.28; PC3 0.16, PC4 0.08, PC5 0.05; Fig. S3). Here the first two principal components describe a gradient between the autocorrelation (a_T & a_P) and frequency spectrum (β_T & β_P) characteristics of abiotic environments (Table S1.3), reflecting a transition from red coloured environments characterised by positive autocorrelation (future abiotic conditions are conditional and similar to current conditions) and low frequency oscillations (seasonality), towards blue coloured environments with higher frequency oscillations, and negative temporal autocorrelation (i.e. future conditions contrast with current conditions). This trend corresponds with conditions expected of natural environments, as terrestrial environments are typically characterised by red coloured variation with marine environments considered even less variable (Vasseur & Yodzis

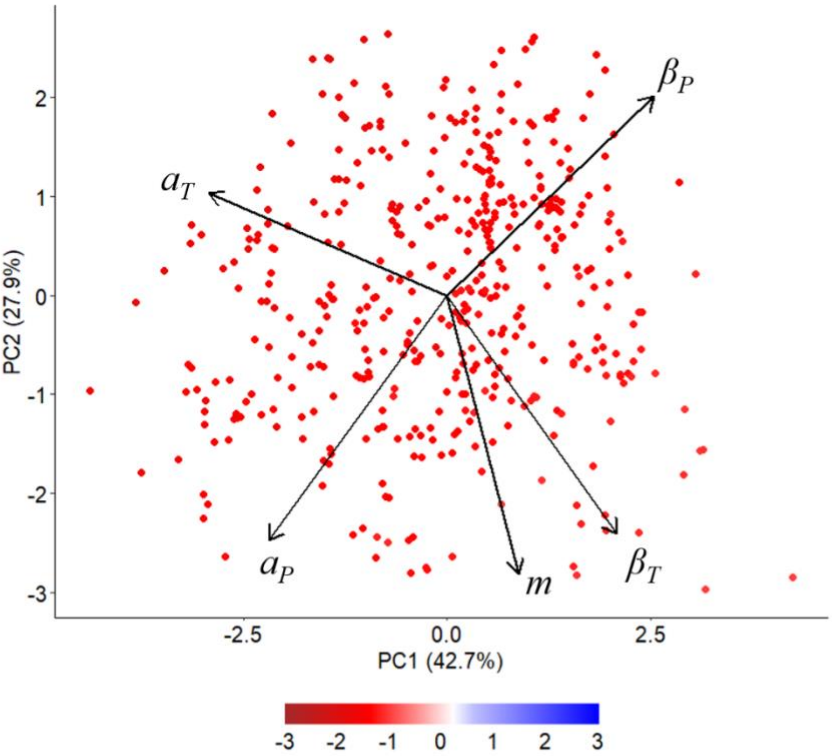

Figure S1.3. Variation in the exposure of populations to environmental stochasticity corresponded with gradients in the autocorrelation and frequency spectrum characteristics of local abiotic regimes. Principal component analysis (PCA) of the five metrics used to quantify exposure to environmental stochasticity: thermal autocorrelation (a_T), thermal range (m), thermal frequency spectrum (β_T), precipitation autocorrelation (a_P), and precipitation frequency spectrum (β_P) illustrating the degree of collinearity between the different variables. Colour scale depicts the gradient of environmental noise corresponding with transitions from red coloured environments characterised by positive autocorrelation and low frequency oscillations, towards blue coloured environments with higher frequency oscillations, and negative temporal autocorrelation. The colour of each environment was defined based on its associated thermal frequency exponent (β_T) to demonstrate how abiotic variance regimes align with our five selected metrics.

2004; Gilljam *et al.* 2019); hence the lack of blue coloured environments within our PCA (Fig. S1.3). However, with VIF confirming there was no collinearity among our five abiotic variables (VIF: β_T = 1.85; a_T = 2.12; m = 1.17; β_P = 1.83; a_P = 1.93), all variables were retained in further analyses.

Table S1.3. Patterns within temperature and precipitation regimes characterised the relative exposure of populations to environmental stochasticity. Principal component loadings of the five measures of environmental stochasticity, thermal autocorrelation (a_T), thermal range (m), thermal frequency spectrum (β_T), precipitation autocorrelation (a_P), and precipitation frequency spectrum (β_P) showing the relative influence of each abiotic variable across each principal component.

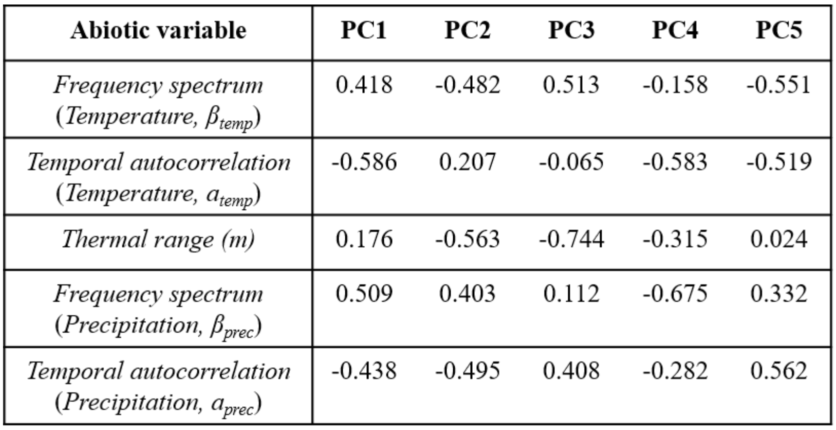

Abiotic variable	**PC1**	**PC2**	**PC3**	**PC4**	**PC5**
Frequency spectrum (Temperature, β_{temp}*)*	0.418	-0.482	0.513	-0.158	-0.551
Temporal autocorrelation (Temperature, a_{temp}*)*	-0.586	0.207	-0.065	-0.583	-0.519
Thermal range (m)	0.176	-0.563	-0.744	-0.315	0.024
Frequency spectrum (Precipitation, β_{prec}*)*	0.509	0.403	0.112	-0.675	0.332
Temporal autocorrelation (Precipitation, a_{prec}*)*	-0.438	-0.495	0.408	-0.282	0.562

1.6. Phylogenetically weighted Partial Least Squares

The code provided below was used to carry out phylogenetically corrected Partial Least Squares regression analysis (pPLS). This function is an adaptation arising from the open source code provided by Adams & Felice (2014), and a modification of the *phyl.pca* function from the '*phytools*' package (Revell 2009, 2012).

```
# This function simultaneously carries out carries out two partial
squares regression analyses to investigate the selection pressures
on transient dynamics and the correlation between environmental
measures and the transient properties of populations.

Phylo.PLS <-function(BlockY, BlockX1, BlockX2, tree, marine.list){
      # this function takes three variable sets and the associated
      phylogenetic tree.
      # BlockY is a vector/matrix of numerical values describing a
      transient property measured from various populations (i.e.,
      Damping ratio, Period of Oscillation, Reactivity, Maximal
      Amplification, First-step Attenuation, Maximal Attenuation)
      # BlockX1 is a matrix describing the population specific
      sensitivities of the transient parameter (BlockY) to each of
      the vital rates Survival, Progression, Retrogression and
      Reproduction.
      # BlockX2 is a matrix describing the environmental variability
      to which each population is exposed. This variable set will
      consist of five abiotic variables: Thermal variance frequency,
      thermal autocorrelation, thermal range (variance magnitude,
      precipitation variance frequency, and precipitation
      autocorrelation.
      # BlockY and BlockX2 will be used in the analysis of
      Hypothesis 1: Investigating the role played by the intensity
      and frequency of environmental variability in defining a
      population's resilience characteristics, with exposure to
      broader scales of abiotic variance selecting for enhanced
      resistance/resonance potential, whereas environments
      characterised by higher frequency variation would promote
      recovery capacities.
      # BlockY and BlockX1 will be used in the analysis of
      Hypothesis 2: Evaluating whether the attributes of resilience
      align with the fast-slow continuum of life history strategies,
      with the expectation that a trade-off exists between recovery
      and stability (resistance or resonance), with stability
      increased by greater investments in survival, and recovery
      correlating with reproductive investment.
      # The function uses the phylogenetic tree to ensure each
      analysis is weighted by phylogenetic covariance.
      # The marine.list is then a list of species (in the same
      format as the row names of the Block matrices) that are
      marine. This list will be used to remove marine populations
      from the analysis of hypothesis 1 (As there is no
      environmental data for these populations.

  # 1. Function loads required packages
  library(ape) # phylogenetic functions
  library(phytools) # phylogenetic functions
  library(pls) # partial least squares analysis

  # 2. Confirm that the input phylogenetic tree is of class 'phylo'
```

```
  if (class(tree) != "phylo"){
    stop("phy must be of class 'phylo.")}

  # 3. Count the number of taxa and create a vector of the species
names:
  # Block 1
  num.taxa.Y<-nrow(BlockY)
  namesY<-rownames(BlockY)
  if (is.null(namesY)){ # a little break if R cannot find species
names
    stop("No specimen names in BlockY.")}
  # Block 2
  num.taxa.X1<-nrow(BlockX1)
  namesX1<-rownames(BlockX1)
  if (is.null(namesX1)){
    stop("No specimen names in Block X1.")} #confirms species names
in block 2
  # Block 3
  num.taxa.X2<-nrow(BlockX2)
  namesX2<-rownames(BlockX2)
  if (is.null(namesX2)){
    stop("No specimen names in Block X2.")} #confirms species names
in block 3

  # 4. Confirm species lists match between the phylo tree and
between each variable block.
  # first do the dimensions (species numbers) match.
  if (length(match(tree$tip.label, namesY)) != num.taxa.Y &&
length(tree$tip.label) < num.taxa.Y){ #confirm that there are equal
numbers of taxa in the tree and the dataset
    stop("Tree is missing some taxa present in the data matrix") }
  if (length(match(tree$tip.label, namesY)) != num.taxa.Y &&
num.taxa.Y < length(tree$tip.label)){ #confirm that there are equal
numbers of taxa in the tree and the dataset
    stop("Tree contains some taxa not present in present in the data
matrix") }
  if (length(BlockY[which(is.na(BlockY)),]) != 0) {
    stop("Transient data contains missing values. Estimate these
first.")  } #no missing values are allowed
  if (length(BlockY[which(is.na(BlockX1)),]) != 0) {
    stop("Sensitivity matrix contains missing values. Estimate these
first.") }
  if (length(BlockX2[which(is.na(BlockX2))]) != 0) {
    cat("Environmental data matrix contains missing values.") }

  # This section checks that the species IDs match between the
blocks and the phylo tree.
  if (is.null(namesY) == FALSE && is.null(namesX1) == FALSE &&
is.null(namesX2) == FALSE) {
      mtch.A <- namesY[is.na(match(namesY, namesX1))]
    if (length(mtch.A) > 0) {
      stop("Specimen names in data sets are not the same.")}
#confirms that the species names match in both blocks of data
      mtch.B <- namesX1[is.na(match(namesX1, namesX2))]
    if (length(mtch.B) > 0) {
      stop("Taxa labels on tree and taxa matrix are not the same.")}
#confirms that the species names match in the data and the phylogeny
      mtch.C <- namesX2[is.na(match(namesY, namesX2))]
    if (length(mtch.C) > 0) {
        stop("Taxa labels on tree and taxa matrix are not the
same.")}
```

```
  }

  # 5. Format variable blocks ready for use in the PPLS analysis
ensuring they are in correct matrix format.
  # and then brings variables together that require phylogenetic
correction
  # Block Y
  BlockY <- as.matrix(BlockY) #transient variable
  # Block X1
  BlockX1 <- as.matrix(BlockX1) # vital rate sensitivties
  #demographic info - Transient metrics and sensitivities (requires
phylogenetic adjustment).
  demog.data <- cbind(BlockY, BlockX1)
  # Block X2
  enviro.data <- as.matrix(BlockX2) # environmental variance
variables

  # 6. Create phylogenetic covariance matrix - this allows for the
weighting in the pls analysis below.
  # this will be the same matrix regardless of which hypothesis is
being worked on
  C <- vcv.phylo(tree, anc.nodes = FALSE) # finds the phylogenetic
variance-covariance matrix for the input phylogeny (this function
will assume a Brownian motion correlation)
  Nspec <- nrow(C) # calculate the number of species in the vcv
matrix
  # The covariance matrix C is used to compute other phylogenetic
metrics using the tree and specific dataset, again this is done
assuming a brownian motion distribution (denoted by lambda = 1)
  temp <- phyl.vcv(demog.data, C, lambda = 1.0)
  C <- temp$C # this output is the same as the vcv.phylo function
but is just code to ensure all further workings are singing to the
same tune.
  a <- t(temp$alpha) #estimation of phylogenetic mean - the
character values at the root of the phylogeny (estimate the common
ancestral trait values)

  # 7. Transform data to adjust for phylogenetic relationship
  C <- C[rownames(demog.data),rownames(demog.data)] #sorts the VCV
matrix to be in the same order as the data matrix requiring
adjustment
  eigC <- eigen(C) # eigenanalysis of covariance matrix
  one <- matrix(1, nrow = Nspec, ncol = 1)  #generates a vector of
1's with length = number of taxa in phylo tree
  D.mat <- solve(eigC$vectors %*% diag(sqrt(eigC$values)) %*%
t(eigC$vectors)) #transformation matrix D
  Phy.data <- D.mat %*% (demog.data - one %*% a) # this is the
phylogenetically transformed data (equation 4 in the manuscript
listed as Reference 1 above)
  # Split the demographic data for use below
  transientY <- as.matrix(Phy.data[,1:dim(BlockY)[2]]) #
phylogenetically adjusted transient estimate
  SensX <- Phy.data[,(dim(BlockY)[2]+1):dim(Phy.data)[2]] #
phylogenetically adjusted vital rate sensitivities

  # In hypothesis 2 the analysis is only interested in terrestrial
populations. Here the provided list of marine species will be used
to remove these populations.
  # from the second part of the analysis.
  rownames(transientY) <- rownames(BlockY)
```

```
  transientY2 <- transientY[!(rownames(transientY) %in%
marine.list)]
  enviro.data <- enviro.data[!(rownames(enviro.data) %in%
marine.list),]

  ##### Hypothesis 1 #####
  # Using vital rate sensitivities to test for selection pressures
or trade-offs between metrics of the transient properties of natural
populations.

  # 8a. Carryout PLS analysis.
  # Run the analyses
  # There is no need to include weighting factors here as phylogeny
has already been adjusted for
  # estimate the correlation between Y and each X variable (Y =
transient variable, X = Vital rate sensitivity matrix)
  cor1 <- cor(transientY, SensX)
  # run the PLS (using an unweighted format)
  pls.H1 <- plsr(transientY~SensX, scale = TRUE, centre = TRUE)
  #########################

  ##### Hypothesis 2 ######
  # First bring together the relevant matrix blocks to remove
incomplete cases (within the environmental variables)
  blocks.combined <- cbind(transientY2, enviro.data)
  blocks.combined <-
blocks.combined[complete.cases(blocks.combined),]
  # and then split back into their two original matrix blocks
  transientY2 <- as.matrix(blocks.combined[,1:dim(BlockY)[2]])
  enviro.data <-
blocks.combined[,(dim(BlockY)[2]+1):dim(blocks.combined)[2]]

  # Run the analyses
  # Testing for correlations between measures of environmental
variability and the transient properties of natural populations
  # estimate the correlation between Y and each X variable (Y =
transient variable, X = Environmental variables matrix)
  cor2 <- cor(transientY2, enviro.data)
  # 8b. Carry out second PLS analysis
  pls.H2 <- plsr(transientY2 ~ enviro.data, scale = TRUE, centre =
TRUE)

  # N.B. For this analysis replacing transientY2 with SensX (after
subsetting) could also work for investigating how vital rate
sensitivities correlate with environmental variability.
  # This would provide an alternative angle for investigating the
role of the environment in constraining resilience charactersitics.
  #########################

  # A quick peice of indexing to subset the transient variable to
match the data used in the second pls analysis
  BlockY <- BlockY[which(rownames(BlockY) %in%
rownames(transientY2)),]

  # 9.Return keyout outputs
  return(list("Vital Rate Correlation" = cor1, "Hypothesis 1 pls" =
pls.H1,
              "Environmental variance correlation" = cor2,
"Hypothesis 2 pls" = pls.H2,
              "Transient variable" = BlockY))}
```

1.7. Phylogenetically imputed Partial Least Squares Regression analyses

We initially carried out all pPLS analyses using only complete entries, omitting all populations missing estimates for any one variable, scaling and mean centring all predictor and response variables in each case. Across our dataset, no variable was missing from more than 6% of populations, except for the five variables describing the period of oscillation and its vital rate sensitivities, which were missing in 35-38% of populations (Table S1.2). To maximise our sample size (*n*) across each regression analysis, we omitted populations with incomplete entries separately across subsets of our data relating to each transient metric (n_{ρ} = 1969; n_{ψ} = 1263; $n_{\bar{\rho}}$ = 2055; $n_{\bar{\rho}max}$ = 2017; $n_{\underline{\rho}}$ = 2044; $n_{\underline{\rho}max}$ = 1988). However, we also repeated each analysis, with missing entries across the demographic variables estimated using phylogenetic imputation. To impute missing values we first calculated the phylogenetic signal (Pagel's λ [Pagel 1999]) of each transient and sensitivity variable using the *phylosig* function from the '*phytools*' package (Revell 2012). Pagel's λ exists on the scale 0 < λ > 1, with 0 indicating traits have evolved independently of phylogeny, and 1 representing a high phylogenetic signal. Next, for all variables exhibiting a strong phylogenetic signal (Pagel's $\lambda \geq 0.65$) any missing entries were imputed assuming a Brownian motion evolutionary model using the *phylopars* function of the '*Rphylopars*' package (Goolsby *et al.* 2017).

Here we present the outputs of our regression analyses involving this imputed data as further evidence for any emerging patterns in the relationships between the transient dynamics of populations, their exposure to gradients in environmental stochasticity (Fig. S1.4), and their vital-rate sensitivities (Fig. S1.5). Our analysis using this imputed data displays congruent patterns to those reported using only complete entries. Indeed, our observations of limited association between gradients in environmental stochasticity and patterns in the transient dynamics of populations are maintained within the imputed data (Fig. S1.4; r^2 < 0.002), whereas the predictive capacity of our imputed vital rate sensitivity variables remains almost identical to those originally reported (r^2; Fig S1.5). We note here that whilst each transient metric relating to the resilience attributes of compensation and resistance, and their vital rate sensitivities all displayed a strong phylogenetic signal (Pagel's λ > 0.94; *see results*), this was not the case for our measures of demographic recovery. Both the transient metrics of damping ratio and period of oscillation displayed strong phylogenetic signal

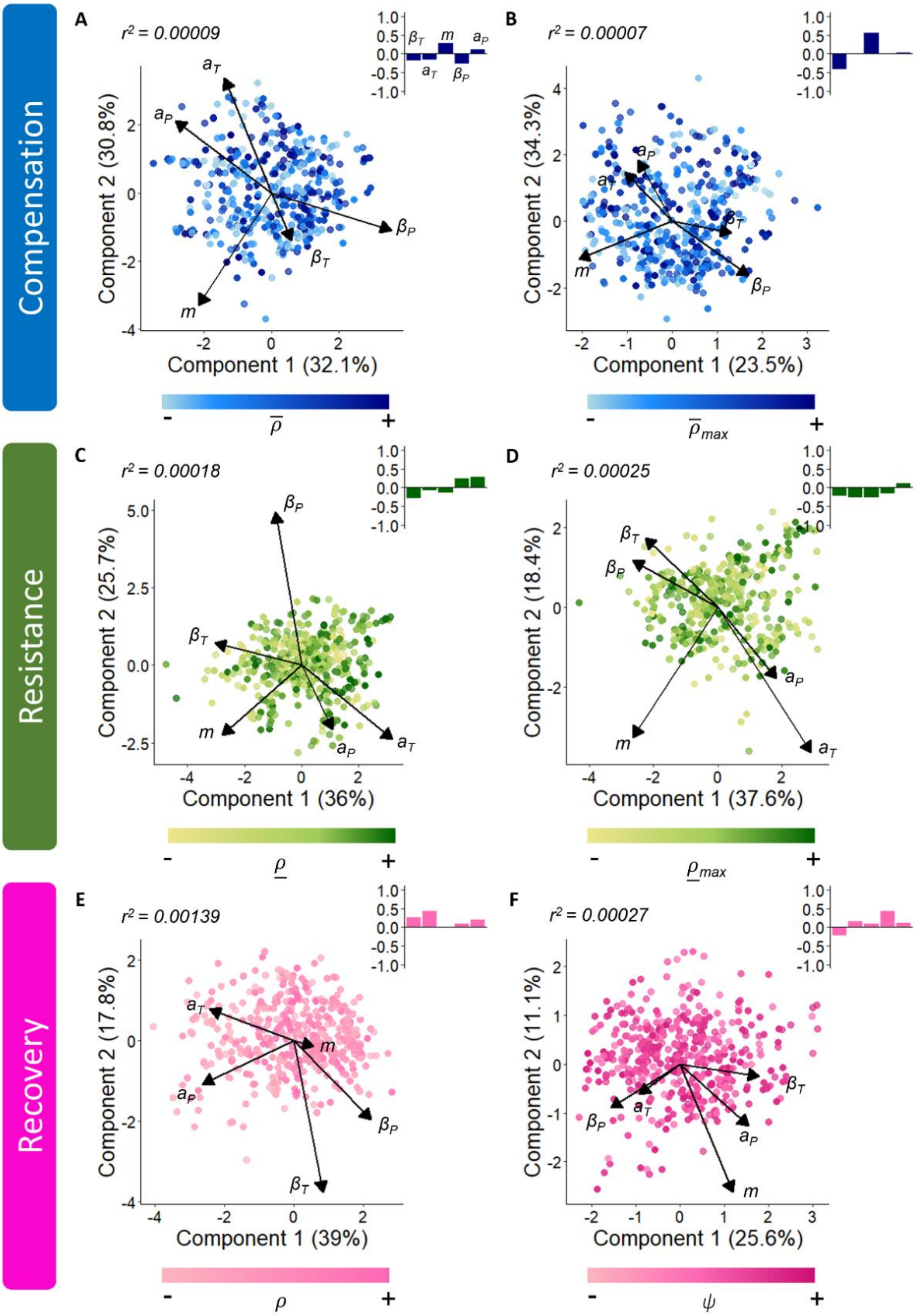
Compensation
A
$r^2 = 0.00009$
β_T a_T m β_P a_P
Component 1 (32.1%)
Component 2 (30.8%)
$\overline{\rho}$
B
$r^2 = 0.00007$
Component 1 (23.5%)
Component 2 (34.3%)
$\overline{\rho}_{max}$
Resistance
C
$r^2 = 0.00018$
Component 1 (36%)
Component 2 (25.7%)
$\underline{\rho}$
D
$r^2 = 0.00025$
Component 1 (37.6%)
Component 2 (18.4%)
$\underline{\rho}_{max}$
Recovery
E
$r^2 = 0.00139$
Component 1 (39%)
Component 2 (17.8%)
ρ
F
$r^2 = 0.00027$
Component 1 (25.6%)
Component 2 (11.1%)
ψ
-
+

Figure S1.4. The limited association between patterns across the demographic resilience attributes of compensation (blue), resistance (green), and recovery (pink) and the relative exposure of populations to environmental stochasticity is insensitive to phylogenetic imputation. Scores and loadings from a phylogenetically-weighted Partial Least Squares regression analysis exploring the correlation between patterns in the variation of the six transient metrics of **(A)** reactivity ($\overline{\rho}$), **(B)** maximal amplification ($\overline{\rho}_{max}$), **(C)** first-step attenuation ($\underline{\rho}$), **(D)** maximal attenuation ($\underline{\rho}_{max}$), **(E)** damping ratio (ρ), and **(F)** period of oscillation (ψ), and our five measures of environmental stochasticity, temperature frequency spectrum (β_T), temperature autocorrelation (a_T), thermal range/magnitude (m), precipitation frequency spectrum (β_P), and precipitation autocorrelation (a_P) using a dataset with missing entries estimated through phylogenetic imputation. Colour gradation reflects the relative magnitude of each transient metric estimated for each population, with darker shades indicating higher estimates. Associated bar plots are the standardised regression coefficients (b) highlighting the relative weighting of each abiotic variable in the overall capacity of each model to explain variation within each transient metric (r^2).

(Pagel's λ: $\rho = 0.996$; $\psi = 0.992$), but their vital rate sensitivities did not (*see results*). Subsequently, we were only able to examine patterns in the demographic selection pressures of recovery using complete entries.

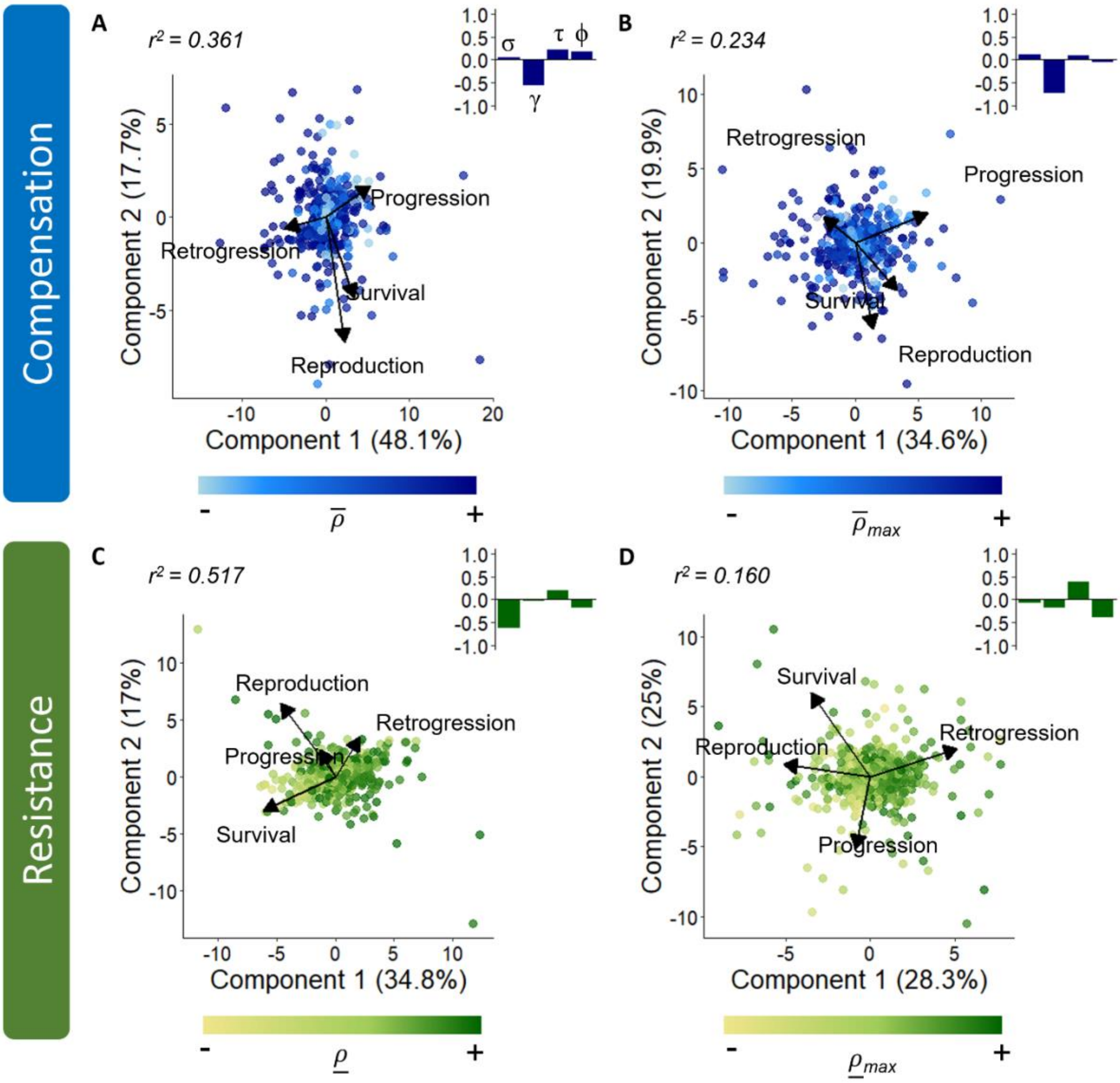

Figure S1.5. Patterns within the vital rate sensitivities of the resilience attributes of compensation (blue) and resistance (green) are insensitive to phylogenetic imputation. Scores and loadings from Partial Least Squares regression analysis of the sensitivity patterns of the four metrics of transient dynamics **(A)** reactivity, **(B)** maximal amplification, **(C)** first-step attenuation, and **(D)** maximal attenuation, with regards to the vital rates of survival (σ), progression (γ), retrogression (τ), and reproduction (ϕ) using a dataset with missing demographic entries phylogenetically imputed. Note that the transient metrics of damping ratio and period of oscillation have been excluded from this analysis due to a limited phylogenetic signal within the vital rate sensitivity variables of these two metrics. Colour gradation represents the magnitude of each transient metric recorded across each population, with darker shades indicating higher estimates. Associated bar plots are the standardised regression coefficients (*b*) highlighting the relative weighting of each vital rate in the overall capacity of each model to explain variation within each transient metric (r^2).

1.8. Accounting for population longevity

We quantified the exposure of each population, within our sample, to environmental stochasticity using local temperature and precipitation records collected during the 50 years prior to the collection of any demographic data. However, the significance of any abiotic patterns experienced by each population during this 50-year window is likely contingent on their longevity. Across a 50-year period long-lived species, with generations spanning multiple decades, will experience fewer generations than shorter-lived species thereby diminishing the observable impact of any selection pressures on their trait characteristics (Robert *et al.* 2004). Thus, it was necessary we ensured that our capacity for exploring the selection pressures exerted by environmental stochasticity on the resilience attributes of natural populations was not inhibited by the inclusion of long-lived species.

To evaluate the influence of population longevity on our observations we repeated our phylogenetically weighted Partial Least Squares analyses evaluating the relationship between environmental stochasticity and the transient dynamics of populations using only short-lived species (Fig. S1.6). Each population was categorised as long- or short-lived according to its mean life expectancy (η_e), which we estimated from its associated MPM using the R package '*IPMpack*' (Metcalf *et al.* 2013). We then repeated our pPLS analyses using only populations for which $\eta_e \leq 10$ years (n = 1606 populations). This threshold was selected to maximise the number of generations experienced by populations during our 50-year abiotic time series, whilst maintaining a suitable sample size for our analyses. Overall, whilst omitting longer-lived species did improve the predictive capacity our abiotic variables by an order of magnitude, the association between gradients in environmental variation and the resilience attributes of populations still remained negligible ($r^2 < 0.001$; Fig. S1.6). Indeed, the absolute magnitude of the Pearson's coefficients ($|r|$) obtained when exploring the correlation between our measures of environmental stochasticity and transient dynamics all reflected a limited correlation between our abiotic and demographic variables ($|r| < 0.03$; Table S1.4).

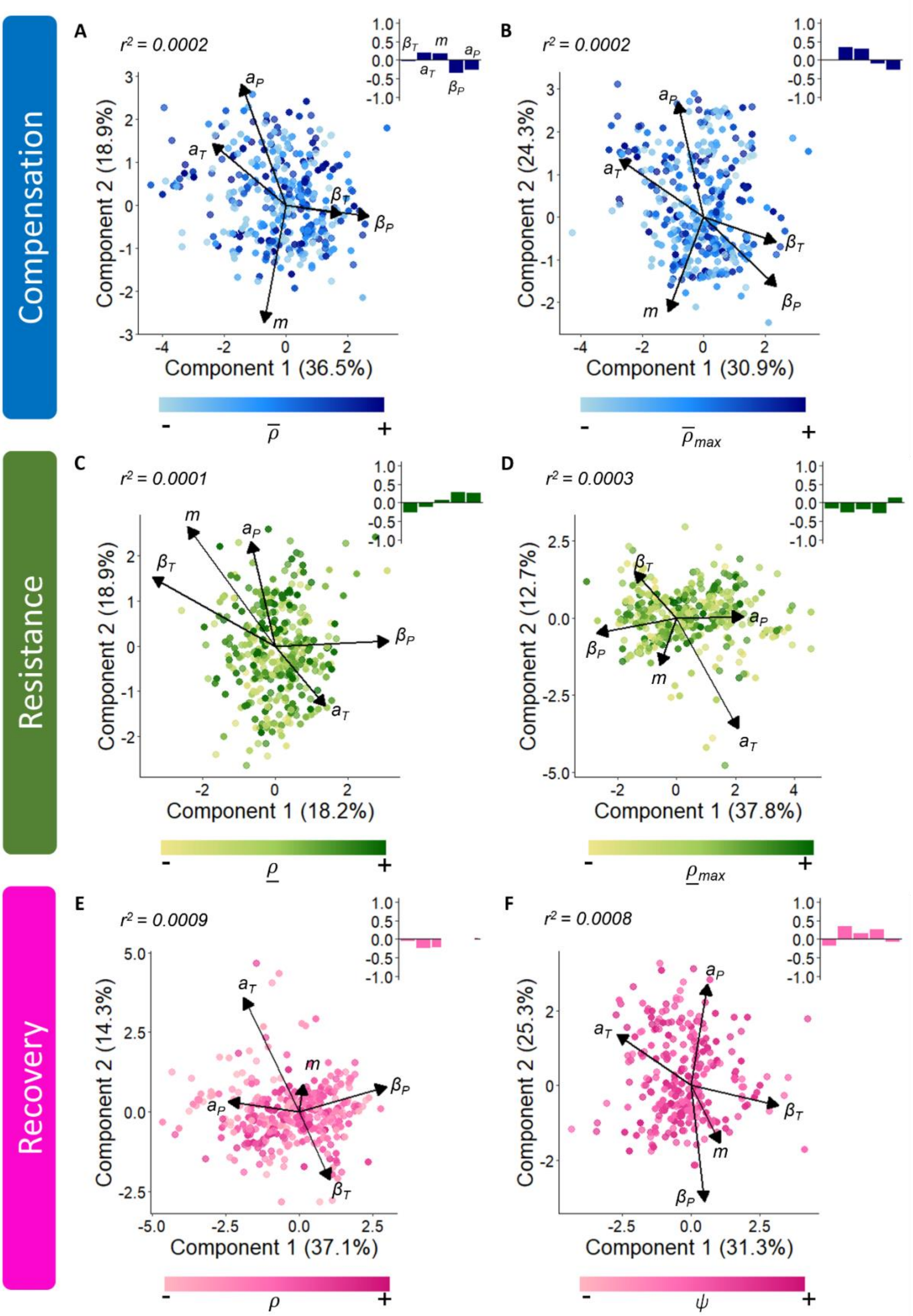
Compensation
Resistance
Recovery
A
$r^2 = 0.0002$
Component 2 (18.9%)
Component 1 (36.5%)
a_P
a_T
β_T
β_P
m
β_T m a_P
a_T β_P
1.0 0.5 0.0 -0.5 -1.0
$\bar{\rho}$
- +
B
$r^2 = 0.0002$
Component 2 (24.3%)
Component 1 (30.9%)
a_P
a_T
β_T
β_P
m
$\bar{\rho}_{max}$
C
$r^2 = 0.0001$
Component 2 (18.9%)
Component 1 (18.2%)
m
a_P
β_T
β_P
a_T
$\underline{\rho}$
D
$r^2 = 0.0003$
Component 2 (12.7%)
Component 1 (37.8%)
β_T
a_P
β_P
m
a_T
$\underline{\rho}_{max}$
E
$r^2 = 0.0009$
Component 2 (14.3%)
Component 1 (37.1%)
a_T
m
β_P
a_P
β_T
ρ
F
$r^2 = 0.0008$
Component 2 (25.3%)
Component 1 (31.3%)
a_P
a_T
β_T
m
β_P
ψ

Figure S1.6. The limited correlation between patterns across the demographic resilience attributes of compensation (blue), resistance (green), and recovery (pink) and the relative exposure of populations to environmental stochasticity is evident across short-lived populations. Scores and loadings from a phylogenetically-weighted Partial Least Squares regression analysis exploring the correlation between patterns in the variation of the six transient metrics of **(A)** reactivity ($\overline{\rho}$), **(B)** maximal amplification ($\overline{\rho}_{max}$), **(C)** first-step attenuation ($\underline{\rho}$), **(D)** maximal attenuation ($\underline{\rho}_{max}$), **(E)** damping ratio (ρ), and **(F)** period of oscillation (ψ), and our five measures of environmental stochasticity: temperature frequency spectrum (β_T), temperature autocorrelation (a_T), thermal range/magnitude (m), precipitation frequency spectrum (β_P), and precipitation autocorrelation (a_P). Populations were selected for the analysis on the basis that they possess life expectancies of ≤ 10 years. Colour gradation reflects the relative magnitude of each transient metric estimated for each population, with darker shades indicating higher estimates. Associated bar plots are the standardised regression coefficients (b) highlighting the relative weighting of each abiotic variable in the overall capacity of each model to explain variation within each transient metric (r^2).

Table S1.4. Patterns across the resilience attributes of compensation (blue), resistance (green), and recovery (pink) of short-lived populations do not correlate with their relative exposure to environmental stochasticity. Using a phylogenetically-corrected Pearson's test of correlation, we explored the correlation between the transient metrics of damping ratio (ρ), period of oscillation (ψ), reactivity ($\overline{\rho}$), maximal amplification ($\overline{\rho}_{max}$), first-timestep attenuation ($\underline{\rho}$), and maximal attenuation ($\underline{\rho}_{max}$), and each of our five measures of environmental stochasticity: temperature frequency spectrum (β_T), temperature autocorrelation (a_T), thermal range (m), precipitation frequency spectrum (β_P), and precipitation autocorrelation (a_P). Populations were selected for the analysis on the basis that they possessed life expectancies of ≤ 10 years.

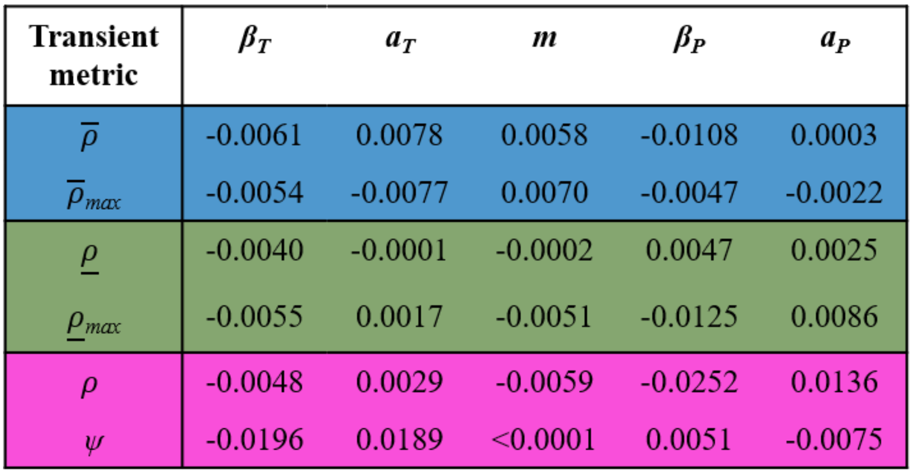

Transient metric	β_T	a_T	m	β_P	a_P
$\overline{\rho}$	-0.0061	0.0078	0.0058	-0.0108	0.0003
$\overline{\rho}_{max}$	-0.0054	-0.0077	0.0070	-0.0047	-0.0022
$\underline{\rho}$	-0.0040	-0.0001	-0.0002	0.0047	0.0025
$\underline{\rho}_{max}$	-0.0055	0.0017	-0.0051	-0.0125	0.0086
ρ	-0.0048	0.0029	-0.0059	-0.0252	0.0136
ψ	-0.0196	0.0189	<0.0001	0.0051	-0.0075

1.9. References

Adams, D.C. & Felice, R.N. (2014). Assessing trait covariation and morphological integration on phylogenies using evolutionary covariance matrices. *PLoS One*, 9.

Barbosa, A.M. (2015). fuzzySim: Applying fuzzy logic to binary similarity indices in ecology. *Methods Ecol. Evol.*, 6, 853–858.

Cavender-Bares, J., Ackerly, D.D., Hobbie, S.E. & Townsend, P.A. (2016). Evolutionary legacy effects on ecosystems: Biogeographic origins, plant traits, and implications for management in the era of global change. *Annu. Rev. Ecol. Evol. Syst.*, 47, 433–462.

Chamberlain, S. & Szocs, E. (2013). taxize - taxonomic search and retrieval in R.

Chamberlain, S., Szoecs, E., Foster, Z., Arendsee, Z., Boettiger, C., Ram, K., *et al.* (2020). taxize: Taxonomic information from around the web.

Gilljam, D., Knape, J., Lindén, A., Mugabo, M., Sait, S.M. & Fowler, M.S. (2019). The colour of environmental fluctuations associated with terrestrial animal population dynamics. *Glob. Ecol. Biogeogr.*, 28, 118–130.

Goolsby, E.W., Bruggeman, J. & Ané, C. (2017). Rphylopars: fast multivariate phylogenetic comparative methods for missing data and within-species variation. *Methods Ecol. Evol.*, 8, 22–27.

Grafen, A. (1989). The phylogenetic regression. *Philos. Trans. R. Soc. London. Ser. B. Biol. Sci.*, 326, 119–157.

Hinchliff, C.E., Smith, S.A., Allman, J.F., Burleigh, J.G., Chaudhary, R., Coghill, L.M., *et al.* (2015). Synthesis of phylogeny and taxonomy into a comprehensive tree of life. *Proc. Natl. Acad. Sci.*, 112, 12764–12769.

Karger, D.N., Conrad, O., Böhner, J., Kawohl, T., Kreft, H., Soria-Auza, R.W., *et al.* (2017). Climatologies at high resolution for the earth's land surface areas. *Sci. Data*, 4, 1–20.

Mansfield, E.R. & Helms, B.P. (1982). Detecting multicollinearity. *Am. Stat.*, 36, 158–160.

Metcalf, C.J.E., McMahon, S.M., Salguero-Gómez, R. & Jongejans, E. (2013). IPMpack: An R package for integral projection models. *Methods Ecol. Evol.*, 4, 195–200.

Michonneau, F., Brown, J. & Winter, D. (2016). rotl: An R package to interact with the Open Tree of Life data. *Methods Ecol. Evol.*, 7, 1–17.

Pagel, M. (1999). Inferring the historical patterns of biological evolution. *Nature*, 401, 877–884.

Paradis, E. & Schliep, K. (2018). ape 5.0: an environment for modern phylogenetics and evolutionary analyses in R. *Bioinformatics*, 35.

Pilowsky, J. (2019). colorednoise: Simulate temporally autocorrelated populations.

R Core Team. (2019). R: A language and environment for statistical computing.

Revell, L.J. (2009). Size-correction and principal components for interspecific comparative studies. *Evolution*, 63, 3258–3268.

Revell, L.J. (2010). Phylogenetic signal and linear regression on species data. *Methods Ecol. Evol.*, 1, 319–329.

Revell, L.J. (2012). phytools: An R package for phylogenetic comparative biology (and other things). *Methods Ecol. Evol.*, 3, 217–223.

Revell, L.J., Harmon, L.J. & Collar, D.C. (2008). Phylogenetic signal, evolutionary process, and rate. *Syst. Biol.*, 57, 591–601.

Robert, A., Sarrazin, F., Couvet, D. & Legendre, S. (2004). Releasing adults versus young in reintroductions: Interactions between demography and genetics. *Conserv. Biol.*, 18, 1078–1087.

Ruokolainen, L., Lindén, A., Kaitala, V. & Fowler, M.S. (2009). Ecological and evolutionary dynamics under coloured environmental variation. *Trends Ecol. Evol.*, 24, 555–563.

Salguero-Gómez, R., Jones, O.R., Archer, C.R., Bein, C., de Buhr, H., Farack, C., *et al.* (2016). COMADRE: A global data base of animal demography. *J. Anim. Ecol.*, 85, 371–384.

Salguero-Gómez, R., Jones, O.R., Archer, C.R., Buckley, Y.M., Che-Castaldo, J., Caswell, H., *et al.* (2015). The COMPADRE Plant Matrix Database: An open online repository for plant demography. *J. Ecol.*, 103, 202–218.

Schroeder, M.A. (1990). Diagnosing and dealing with multicollinearity. *West. J. Nurs. Res.*, 12, 175–187.

Vasseur, D.A. & Yodzis, P. (2004). The color of environmental noise. *Ecology*, 85, 1146–1152.

Supplementary material 2

The projected degradation of subtropical coral assemblages by recurrent thermal stress

2.1. Details of plot set up within the Solitary Islands Marine Park.

Table S2.1. Number of plots set up and lost during each census

	Census									
	Apr 2016	**Oct 2016**			**Aug 2017**			**Aug 2018**		
Site (GPS)	Set up	Lost	Set up	Surveyed*	Lost	Set up	Surveyed*	Lost	Set up	Surveyed*
N Solitaries (-29.9294°, 153.3915°; Offshore)	9	1	0	8	3	0	5	1	2	6
S Solitaries (-30.2052°, 153.2671°; Offshore)	8	0	0	8	0	0	8	0	1	9
NW Solitaries (-30.0178°, 153.2714°; Inshore)	9	2	0	7	1	4	10	0	0	10
SW Solitaries (-30.1607°, 153.2272°; Inshore)	5	4	0	1	1	8	8	0	0	8
Black Rock (-30.9492°, 153.0765°; Inshore)	0	0	0	0	0	4	4	1	0	3
Total	**31**			**24**			**35**			**36**

*includes both replacement plots and plots remaining from previous census.

2.2. Correcting for the mismatch in annual survey schedule.

Prior to use in analysis, all size data recorded for colonies surveyed in April 2016 needed ‘advancing’ by 4 months. This adjustment was required due to a mismatch in the survey schedule which meant there was an inconsistency in the census intervals between April 2016 – August 2017 (16 months) and August 2017 – August/September 2018 (~12 months). To correct for this mismatch, observed colony sizes recorded during the April 2016, October 2016 and August 2017 surveys were arranged as a time series, showing the change in size for each tagged colony over the 6- and 16-month time intervals (Fig. S2.1). A regression analysis was then used to quantify the relationship between the length of growth period (6 or 16 months) and change in colony size. Carrying out the analysis in this way provided us with an estimate of the mean monthly change in colony size across our tagged sample, whilst accounting for varying growth conditions between April – October 2016 and October 2016 – August 2017. We used our monthly growth formula to then adjust colony sizes measured in April 2016, advancing them by four months to estimate the size of each tagged coral in August 2016. Subsequently, all further analyses represented annual intervals.

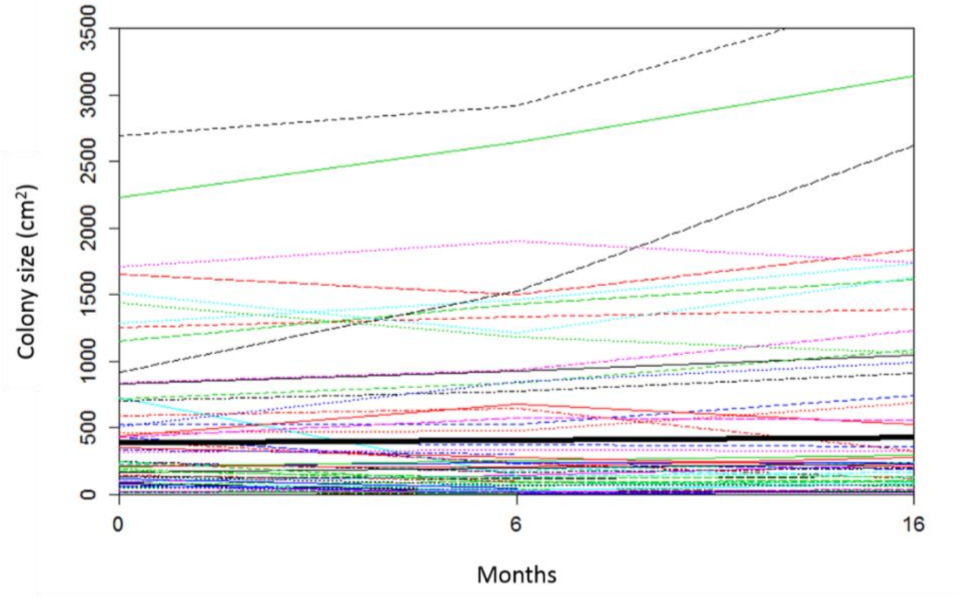

Figure S2.1. Temporal change in the size of each tagged colony from month 0 (April 2016) to month 16 (August 2016). Solid black line represents the estimated mean growth trend from which the mean monthly growth increment was estimated.

2.3. Estimation of coral colony fecundity.

To estimate the fecundity of our tagged colonies, data comparing colony size (cm^2) with colony fecundity (combined density of eggs & testes/mm^3) were extracted from the Coral Trait Database (Madin *et al.* 2016). These data were originally collected for different coral species at Lizard Island, on the Great Barrier Reef (-14.665°, 145.465°; Hall & Hughes 1996). We divided these data into morphological groups comparable with the divisions used in our main study, which resulted in three distinct groups: (i) *Acropora* (composed of *A. gemmifera*, *A. hyacinthus*, *A. millepora*, and *A. nana*), (ii) small-massive/encrusting types (*Goniastrea retiformis*), and (iii) small *Pocilloporids* (*Stylophora pistillata*). The relationship between colony size and fecundity was then determined for each of these three coral groups using non-linear least squared regression (Fig. S2.2). The resulting model coefficients were extracted and used to predict the fecundity of our tagged colonies, with the exact coefficients used determined by the specific genus/morphological classification of our tagged corals.

Estimating the fecundity of our tagged colonies in this way involves two key assumptions. Firstly, we assume phylogenetic conservatism, whereby the reproductive biology of coral taxa remains fixed regardless of tropical or subtropical locality. Baird *et al*. (2009) showed this to be a reasonable assumption, demonstrating that reproductive biology and colony sexuality is highly systemic, and remains largely consistent within monophyletic clades, families, and genera. Equally, we are assuming that despite the different timings of our work and that of Hall & Hughes (1996), it is still sufficient for us to implement their estimated size specific colony fecundity relationships within our demographic models. To account for the temporal mismatch, and the contrasting subtropical-tropical localities of our studies, we incorporated a recruit settlement factor (ψ) into our analyses (see *Estimating vital rates*). This factor was estimated as the ratio between the number of recruits observed during our surveys, and the total larval output expected given our observed colony size distributions and the colony size-fecundity relationships reported by Hall & Hughes (1996). Subsequently, the use of size-specific fecundity relationships merely allowed us to link the demographics of mature colonies and the recruitment of new individuals, with estimates of ψ ensuring that predicted recruitment rates were weighted to reflect observed trends.

Finally, the *Turbinaria* group was the only group without an analogous fecundity model. In this case, the *Acropora* fecundity model was used because *Turbinaria* spp. exhibits similar reproductive strategies to *Acropora* spp. within the Pacific region (Richmond & Hunter 1990). As Hall & Hughes (1996) define fecundity as a measure of the combined density of eggs and testes, we halved predicted colony fecundity in order to obtain instead a measure of expected larval output as a function of size.

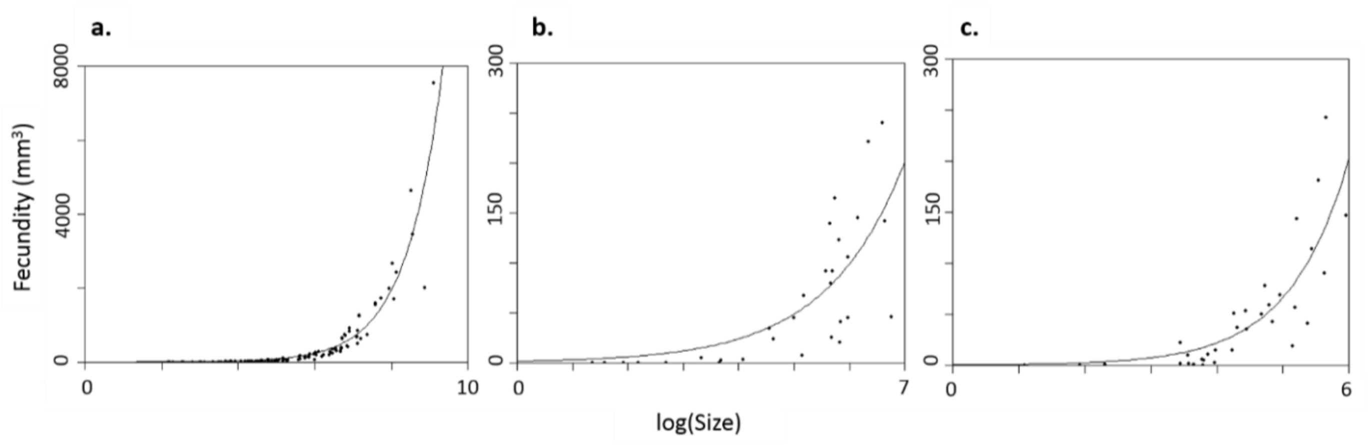

Figure S2.2. Fecundity as a function of colony size estimated using data from Hall & Hughes (1996) for **(a)** *Acropora* **(b)** small-massive/encrusting types and **(c)** small *pocilloporids*.

2.4. Defining the break point between continuous and discrete size classes and estimating vital rates.

Constructing a two-stage IPM

All IPMs used in this study followed a two-stage model format, each combining a discrete and continuous stage. This approach was chosen due to the fact that our sites comprised only few very large colonies (*Acropora*: n = 3, *Turbinaria*: n = 10, *Pocillopora*: n = 16, Encrusting: n = 18). Ultimately, this meant that accurately portraying the dynamics of very large colonies as a continuous function of size, whilst also comparing between bleaching and non-bleaching, was not possible. This constraint was particularly true when modelling the growth dynamics of larger colonies, with their growth on a continuous scale reflecting mathematical artefacts of the regression model rather than following biological expectations (Fig. S2.3). Instead, using a two-stage IPM format allowed for a continuous stage to capture the dynamics of both small and intermediately sized corals, with corals larger than a predetermined size promoted to a discrete size class. However, this approach required the estimation of a threshold size between the continuous and discrete stages.

We defined the threshold size as the point of intersection between the bleaching and non-bleaching growth vital-rate models. Growth was modelled as the relationship between size at time *t* and size at time *t+1* using generalised linear regression, with time included as a fixed effect allowing for the comparison between bleaching and non-bleaching periods. The exact shape of the model was allowed to follow either linear or non-linear forms with visual checks and AIC scores used to determine the most parsimonious model. The *curve_intersect* function from the R package '*reconPlots*' (Heiss 2019) was then used to identify the point at which the regression lines for the bleaching and non-bleaching growth models intersected. The value of size at time *t* corresponding with this point of intersection was retained as the threshold size (Fig. S3). Only in the case of *Pocillopora aliciae* did the growth vital rates during stress and non-stress not intersect. Here, the threshold size was taken as the point at which the data points themselves began to come together.

Model sensitivity to the positioning of the continuous to discrete class size threshold was also tested. For each coral group we constructed a string of size threshold values (typically ranging 0.5 units either side of the actual values used). In

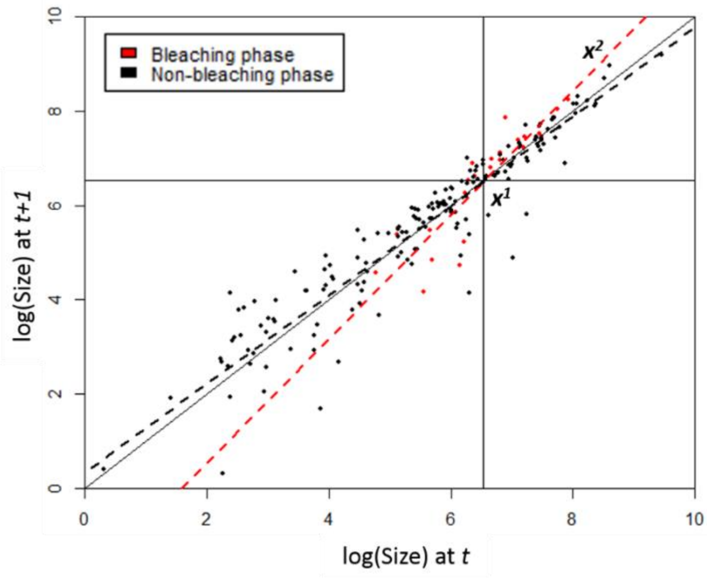

Figure S2.3. Growth vital rate as a function of size showing the intersect point (***x*^1^**) between the bleaching and non-bleaching growth trends (dashed lines), and how the lack of data for very large colonies results in a biologically unrealistic growth trend (x^2). The diagonal solid line represents neither growth nor shrinkage, and the vertical and horizontal lines show how the threshold size can be used to construct a two stage IPM.

sequence we then worked through each threshold value constructing IPMs for both stress and non-stress phases using the corresponding vital rates. From these models we extracted values of population growth rate (λ) to evaluate how the relative value of the size threshold impacted on measures of viability (Fig. S2.4). We also calculated the overall sensitivity of each model ($S_{threshold}$) using equation S2.1, where Δx is the difference between the maximum and minimum size threshold used in each case.

$$S_{threshold} = \frac{\Delta\lambda}{\Delta x} \qquad \text{(S2.1)}$$

Estimating vital rates

Aside from growth, we also determined the relationship between the vital rates of survival and fragmentation probability (Fig. S2.5). Given the low density of our coral plots (Fig. S2.6) all vital rates were modelled assuming density independence. Colony survival and fragmentation were evaluated using logistic regression including time as

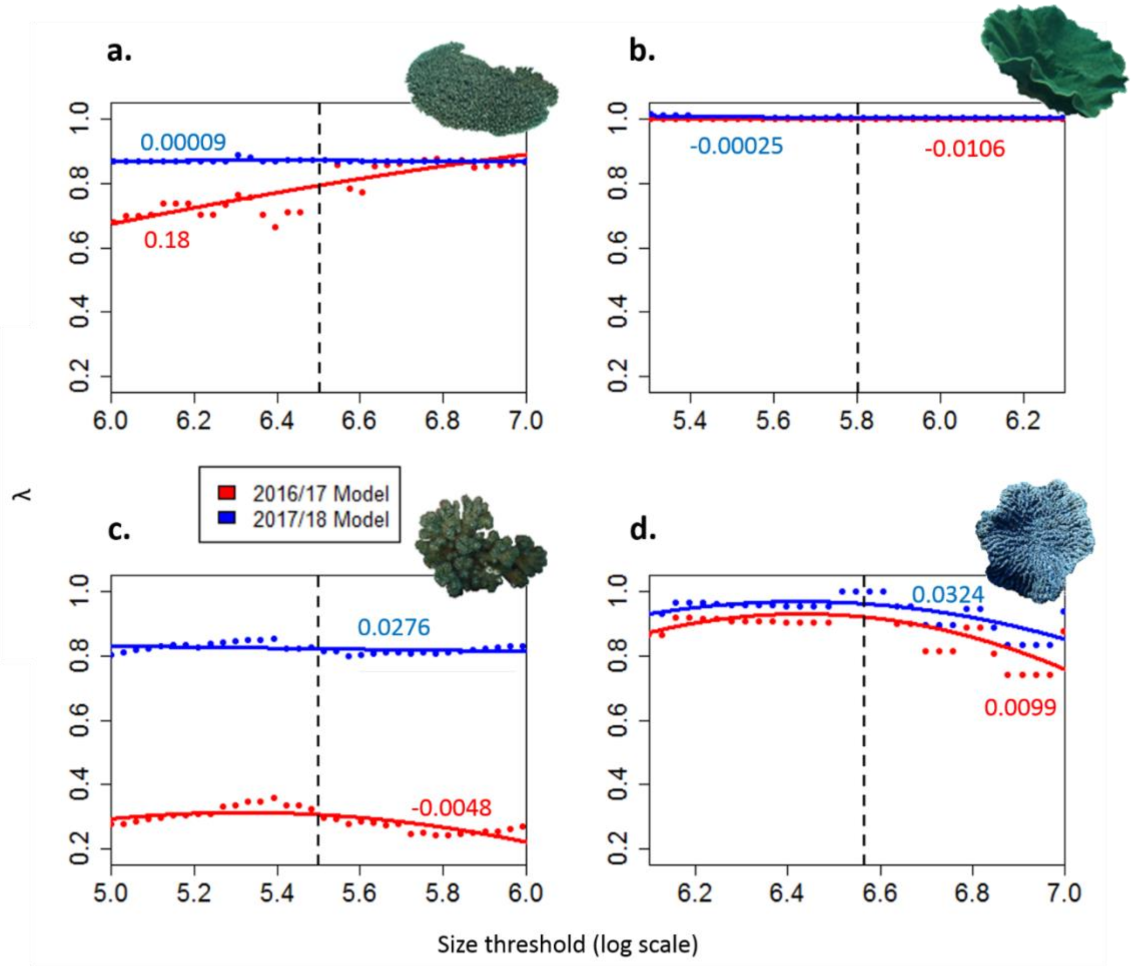

Figure S2.4. Model sensitivity to the positioning of the continuous to discrete size threshold for each coral group **(a)** *Acropora* spp., **(b)** *Turbinaria* spp., **(c)** *Pocillopora aliciae*, and **(d)** Encrusting corals. Sensitivity was evaluated as the change in λ with respect to the change in size threshold value and was determined for models corresponding with both stress (red) and non-stress periods (blue). Horizontal dashed lines indicate the size threshold value actually used for each coral group. Overall sensitivity values are also included on each panel.

a fixed effect and allowing the models to follow any shape with visual checks and AIC scores used to ensure the best models were retained. We then determined the number of fragments produced as a function of size using generalised linear models set to a Poisson distribution, with the relationship between mean fragment size and parent colony size calculated using linear regression. The only exception to this was the

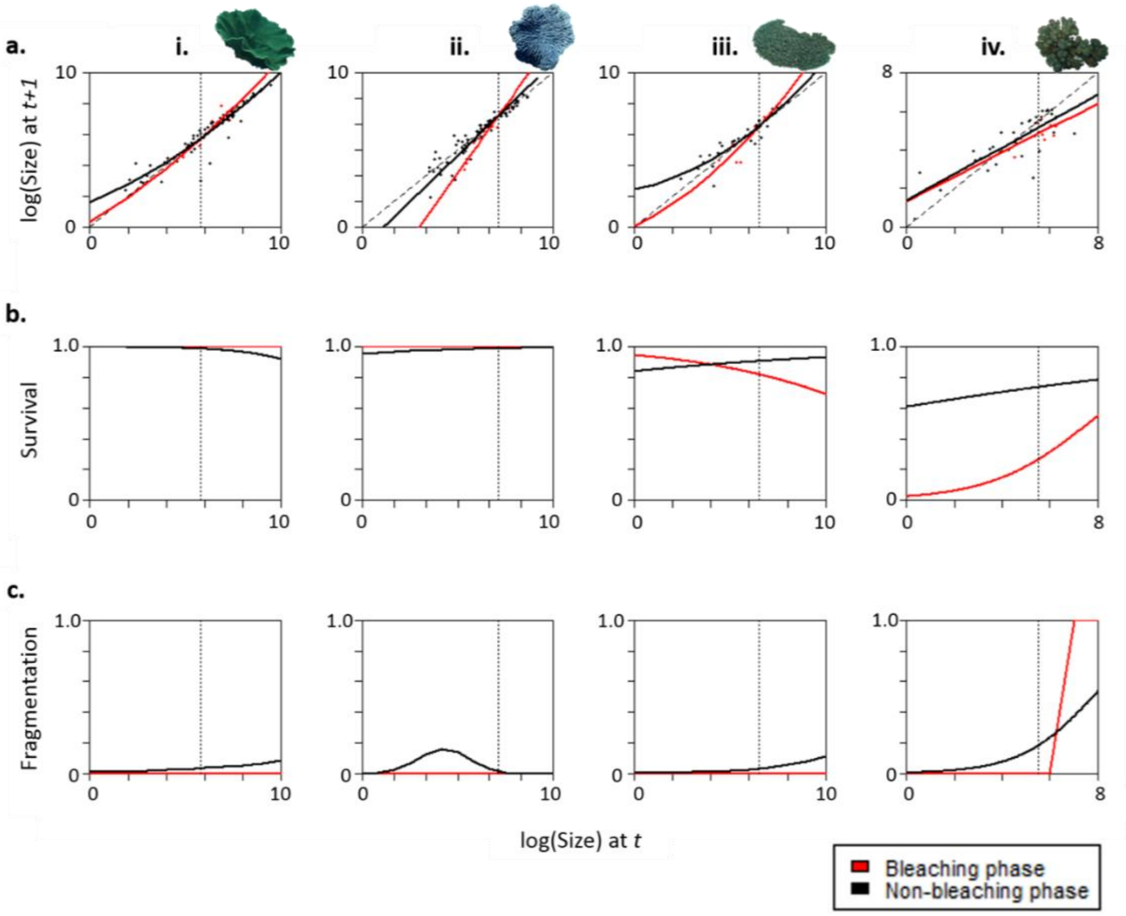

Figure S2.5. (a) Growth, **(b)** survival and **(c)** fragmentation vital rates as a function of size at time *t*, and how they vary between bleaching and non-bleaching periods for the different morphological groups: **(i)** *Turbinaria* spp. **(ii)** Encrusting **(iii)** *Acropora* spp. and **(iv)** *Pocillopora aliciae*. Diagonal dashed lines on growth panels indicate null growth, and the vertical dotted lines on all panels reflect the location of the population's threshold size between its continuous and discrete size classes.

tabular *Acropora* group, for which only one fragmentation event was observed. In this case, the ratio of fragment size to parent colony size was used to provide a measure of the size relationship. In all cases the variation in colony growth and fragment size were also allowed to vary with initial colony size. We achieved this by modelling both the growth model and fragment size model residuals against initial colony size using a general linear model set to a gamma distribution to ensure variance could not fall below zero.

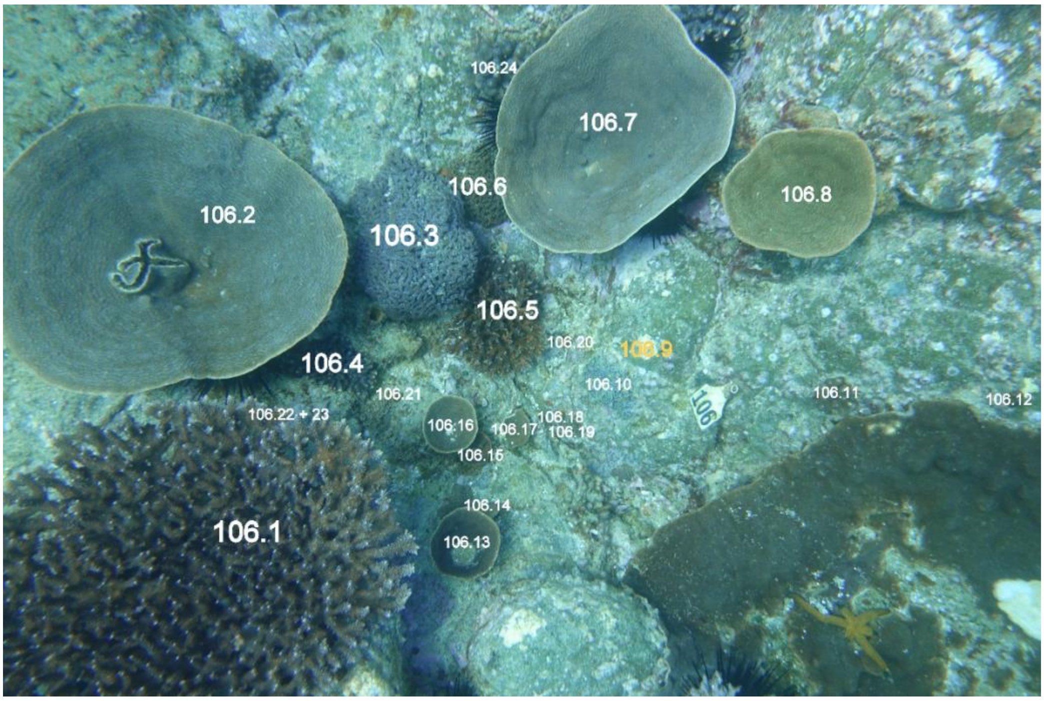

Figure S2.6. Coral plot 106 located at South-West Solitary Island showing the characteristic low density of coral assemblages within the Solitary Islands Marine Park. Annotated colonies represent tagged individuals, with yellow text referencing the location of colonies lost through mortality.

All vital-rate regressions were initially calculated using the full available size range for each model. When constructing the two-stage IPMs, these vital-rates where then only applied to corals smaller than the threshold size and used to predict the rates for the mean colony size within the discrete class; this ensured that the artificially defined size threshold between the continuous and discrete classes did not have any bearing on the calculated vital-rates for colonies within the continuous size class.

Larval output was calculated as a function of colony size using a non-linear least squares regression, allowing for an exponential increase in output with increasing colony size. However, to ensure our models accounted for the fact that marine populations can exist in an open state (Yau *et al.* 2014), and that larval output had been estimated using data sourced from tropical populations, we also calculated a settlement success factor (ψ). The use of this factor insured that our models allowed for the fact that not all larvae produced will re-seed into the local population and ensured that modelled recruitment dynamics were restricted by the abundance of observed subtropical recruits. We calculated the settlement success factor as the ratio between the number of observed recruits and the total expected larval output of the population (Table S2.2).

Finally, we also calculated the size distribution of recruits. Recruit size was modelled independently of parent colony size, due to the challenges associated with determining the parental lineage of observed recruits. The exact shape of the recruit size distributions varied between models, but primarily corresponded to either a normal or skewed normal distribution. Skewed normal distributions were estimated using the *selm* function in the ‘sn’ package (Azzalini 2018).

Table S2.2. Total number of recruits observed and corresponding larval settlement success estimates (all sites combined)

	Bleached period		Non-bleached period	
Population	**Recruits**	**Settlement ratio**	**Recruits**	**Settlement ratio**
Acropora spp.	1	0.00064	2	0.00033
Pocillopora aliciae	0	0	24	0.01491
Turbinaria spp.	3	0.00076	12	0.00092
Encrusting	0	0	7	0.00177

2.5. Climate simulations for the Solitary Islands region.

To investigate the impacts of future recurrent thermal stress within the Solitary Islands Marine Park (SIMP), we first needed to estimate the future stress regimes projected for the region. To ensure that our assessments were comparable to other regional and global bleaching assessments, we simulated the trends in thermal stress predicted under the four different RCP pathways (IPCC 2014). To do so, we extracted simulated daily sea surface temperatures (SST) for the Solitary Islands region (-30.2052°, 153.2671°) from three CMIP5 climate models; HadGEM2 – ES, IPSL-CM5A-LR and CCSM4. The data extracted, from each climate model, covered the time period 2018 to 2100 under each of the four RCP pathways (2.6, 4.5, 6.0 and 8.5). All data were sourced from the CEDA Archive (http://data.ceda.ac.uk/badc/cmip5/data/cmip5/output1).

From this simulated SST data, we first determined weekly mean SSTs for the time period 2018-2100 under each pathway. Weekly thermal hotspots, defined as periods during which projected weekly mean SSTs exceed the region's mean monthly maximum (MMM), were then calculated. The MMM is the localised mean monthly maximum temperature for the timeframe 1985-1995 and was estimated using daily temperature records from the NOAA Coral Reef Watch CoralTemp database (https://coralreefwatch.noaa.gov/product/5km/index_5km_sst.php).

Using the weekly thermal hotspots, we estimated the future thermal stress regimes expected for the Solitary Islands region by calculating degree heating weeks (DHW). DHWs are calculated as running summations of every 12 weekly hotspots. Typically, hotspots are only used in estimating DHWs if they exceed a 1°C threshold (Liu *et al.* 2003). However, removal of this 1°C threshold better correlates with the bleaching trends observed in subtropical corals (van Hooidonk & Huber 2009; Kim *et al.* 2019). Thus, in this study, all thermal hotspots were used in determining DHWs. Next, using a binary format we determined whether sufficient thermal stress for bleaching was projected to occur in any given year between 2018 and 2100 based on whether the simulated DHWs exceeded a threshold of 4 DHW during that year. This step provided the recurrent thermal stress regimes expected in the SIMP under each of the four RCP pathways (Fig. S2.7).

Finally, we compared the different recurrent thermal stress regimes projected by each RCP scenario. This step was carried out using a binomial regression to initially estimate future annual bleaching probabilities for the Solitary Islands region, and test for differences between the temporal bleaching frequencies projected under the different RCP pathways.

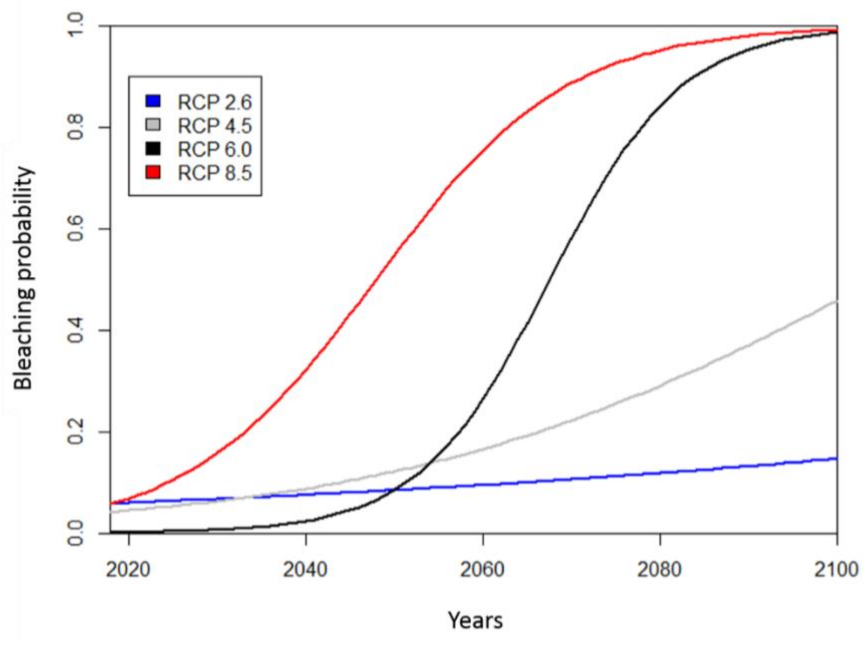

Figure S2.7. Temporal trends in the probability of bleaching within the Solitary Islands Marine Park, under the four different RCP scenarios.

2.6. References

Azzalini, A. (2018). The R package ‘sn’: the Skew-Normal and related distributions such as the Skew-t.

Baird, A.H., Guest, J.R. & Willis, B.L. (2009). Systematic and biogeographical patterns in the reproductive biology of scleractinian corals. *Annu. Rev. Ecol. Evol. Syst.*, 40, 551–571.

Hall, V.R. & Hughes, T.P. (1996). Reproductive strategies of modular organisms: Comparative studies of reef-building corals. *Ecology*, 77, 950–963.

Heiss, A. (2019). reconPlots: plot economics graphs with R.

van Hooidonk, R. & Huber, M. (2009). Quantifying the quality of coral bleaching predictions. *Coral Reefs*, 28, 579–587.

IPCC. (2014). *Climate Change 2014: Synthesis Report. Contribution of Working Groups I, II and III to the Fifth Assessment Report of the Intergovernmental Panel on Climate Change. [Core Writing Team, R.K. Pachauri and L.A. Meyer (eds.)]*. Geneva, Switzerland,.

Kim, W.S., Sampayo, M.E., Sims A. C., Sommer, B., Gómez-Cabrera, M.C., Dalton, S.J., *et al.* (2019). Refugia under threat: Mass bleaching of coral assemblages in high-latitude eastern Australia. *Glob. Chang. Biol.*, 25, 3918–3931.

Liu, G., Strong, A. & Skirving, W. (2003). Remote Sensing of Sea Surface Temperatures During 2002 Barrier Reef Coral Bleaching. *Eos*, 84, 137–144.

Madin, J.S., Anderson, K.D., Andreasen, M.H., Bridge, T.C., Cairns, S.D., Connolly, S.R., *et al.* (2016). The Coral Trait Database, a curated database of trait information for coral species from the global oceans. *Sci. Data*, 3, 1–21.

Richmond, R. & Hunter, C. (1990). Reproduction and recruitment of corals: comparisons among the Caribbean, the Tropical Pacific, and the Red Sea. *Mar. Ecol. Prog. Ser.*, 60, 185–203.

Yau, A.J., Lenihan, H.S. & Kendall, B.E. (2014). Fishery management priorities vary with self-recruitment in sedentary marine populations. *Ecol. Appl.*, 24,

1490–1504.

Supplementary material 3

Transient amplification enhances the persistence of tropicalising coral assemblages in marginal high-latitude environments

3.1. Quantifying the variation between the patterns of colony survival, growth, and fragmentation within tropical and subtropical environments.

To explore the influence of environmental variability on the transient dynamics of coral populations, we constructed Integral Projection Models (IPMs; Easterling *et al.* 2000) describing the respective dynamics of *Acropora* spp. assemblages from a tropical and subtropical environment. We parameterised our IPMs through an annual census of *Acropora* spp. colonies conducted in southern Japan between 2017 – 2019 (Fig. 1). In September 2017, we tagged *Acropora* individuals within the tropical reef communities of Okinawa at Hentona (26.75˚, 128.18˚), Oura Bay (26.54˚, 128.08˚), and Miyagi Channel (26.35˚, 127.99˚), using permanently marked plots (n = 32 plots, 2.4 ± 0.19 [SD] colonies/plot). Permanent plots were also set up within the subtropical communities of Kochi, Shikoku, to tag *Acropora* colonies at Okinoshima (32.75˚, 132.55˚), Kashiwajima (32.77˚, 132.62˚), and Nishidomari (32.78˚, E 132.73˚; n = 35 plots, 6.2 ± 0.25 colonies/plot). We assembled these permanent plots by fixing numbered tags into bare reef substrate, with each plot consisting of a tag and the surrounding coral colonies within a $2m^2$ area. Photographs, with scale bars included for reference, were used to capture the visible horizontal extent of all *Acropora* colonies within each plot. We estimated the horizontal surface area (cm^2) of tagged colonies using ImageJ (Schneider *et al.* 2012), before log-transforming colony sizes prior to further analyses to normalise the size distribution and improve the resolution of smaller colonies.

Colony survival

Repeated surveys of tagged colonies in August 2018, and August 2019, allowed us to quantify size-specific patterns in colony survival. Colony survival was recorded in the field as the presence or absence of tagged colonies during successive surveys and modelled as a function of colony size at time *t* using a logistic regression (Fig. S3.1). When modelling this relationship, we included the fixed effect of region (tropical or subtropical) allowing us to compare survival patterns across our tropical and subtropical assemblages. To parameterise patterns in colony survival, we used colony data pooled across years to ensure greater statistical power within our analyses. Our regression models for this vital rate therefore included colony identity as a random variable to account for repeated measures of individual colonies. We also initially included survey site location as a random effect to account for any nesting within our data, although this resulted in a singular fit, due to insufficient data to support the subsequent complexity of the model. Thus, we excluded the random effect of site to prevent overfitting within our model allowing us to best explore trends within the data. Overall, the probability of survival increased with colony size in both assemblages, although this trend was more pronounced within the subtropical assemblage (Fig. S3.1).

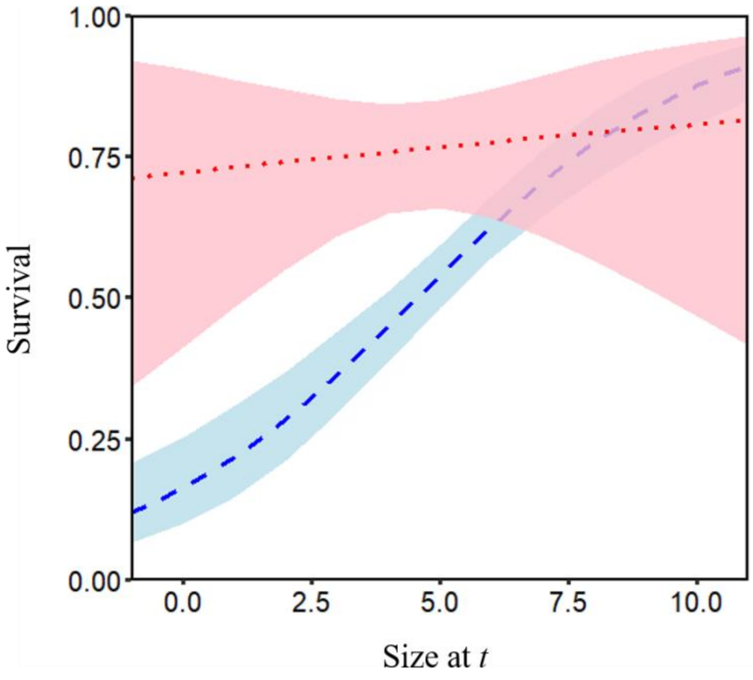

Figure S3.1. Size specific patterns in the survival probabilities of *Acropora* spp. colonies within a tropical (Red) and subtropical (Blue) setting. Size at *t* reflects colony area (cm^2) on the log scale. Shaded regions represent 95% Confidence Intervals.

Colony size distributions & changes in colony size

Revisiting tagged *Acropora* colonies in both Okinawa and Kochi allowed us to explore temporal trends in the size distributions of the tropical and subtropical assemblages (Fig. S3.2). We observed that between 2017 and 2019, both assemblages displayed declines in the dominance of larger individuals, and that in any given year, mean colony size was largest in the subtropics (Table S3.1). However, trends in the skewness of each assemblage's annual size distribution indicated transitions toward greater righthand skew, reflecting an increase in the density of smaller colonies; a trend that was particularly true for the subtropical assemblage during 2019 (Table S3.1).

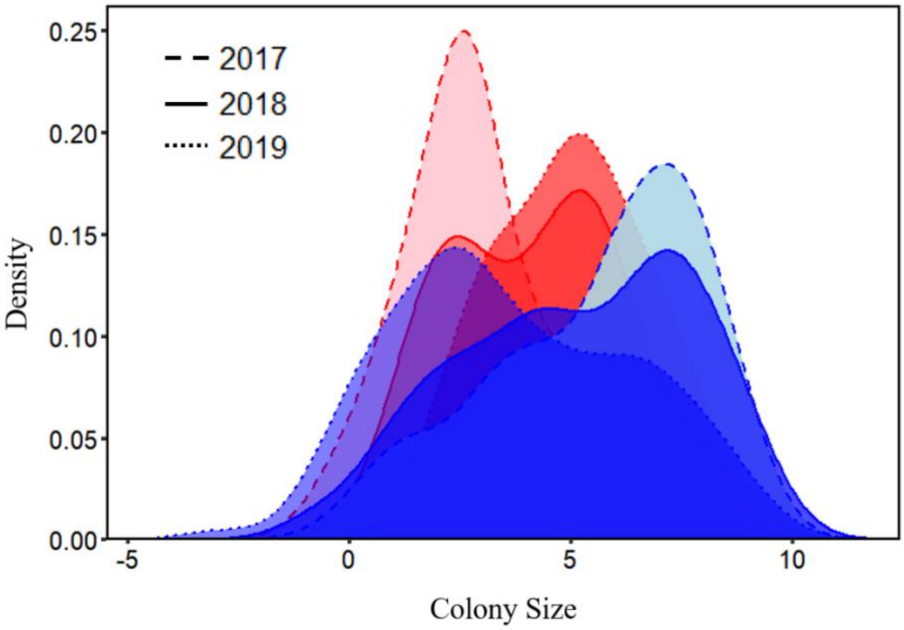

Figure S3.2. Temporal trends in the size distributions of tagged tropical (Red) and subtropical (Blue) *Acropora* spp. assemblages recorded during annual surveys between 2017 and 2019.

Table S3.1. Temporal trends in mean colony size and skew in the size distributions of tagged tropical and subtropical *Acropora* spp. assemblages recorded during annual surveys between 2017 and 2019. Error reported as 95% CI.

	Subtropical		**Tropical**	
Census	MEAN	SKEW	MEAN	SKEW
2017	5.62 [5.27, 5.96]	-0.63	5.00 [4.39, 5.62]	0.05
2018	5.14 [4.77, 5.52]	-0.30	4.27 [3.67, 4.88]	0.19
2019	3.69 [3.35, 4.04]	0.18	2.99 [2.56, 3.42]	0.48

We also quantified size-specific transitions in colony size using the difference between colony surface areas recorded during successive annual surveys. Patterns in colony size transitions were calculated using linear regression and reflected the relationship between colony size at time *t* and size at time *t+1.* As with our models of colony survival, we modelled colony growth with region included as a fixed effect, and colony identity included as a random variable, but excluded site as a random effect to avoid overfitting our models. Again, data regarding the annual size transitions of tagged colonies was pooled across years to enhance the resolution of our analyses. We found that patterns in the size transitions of colonies were largely consistent across both the tropical and subtropical assemblages, with enhanced positive growth reported in smaller colonies and stasis in larger colonies (Fig. S3.3). We also separately modelled the relationship between the variance in colony size at time *t+1* and colony size at time *t*. This relationship was determined by modelling the residuals from our colony growth model above, as a function of colony size at time *t*. For this relationship we assumed a gamma distribution, allowing for a non-linear pattern whilst preventing negative variance. For clarity, we did compare this gamma model with a linear regression format, however, model AIC scores confirmed our assumption of a gamma distribution to be appropriate (AIC: linear = 572.6; gamma = 326.5).

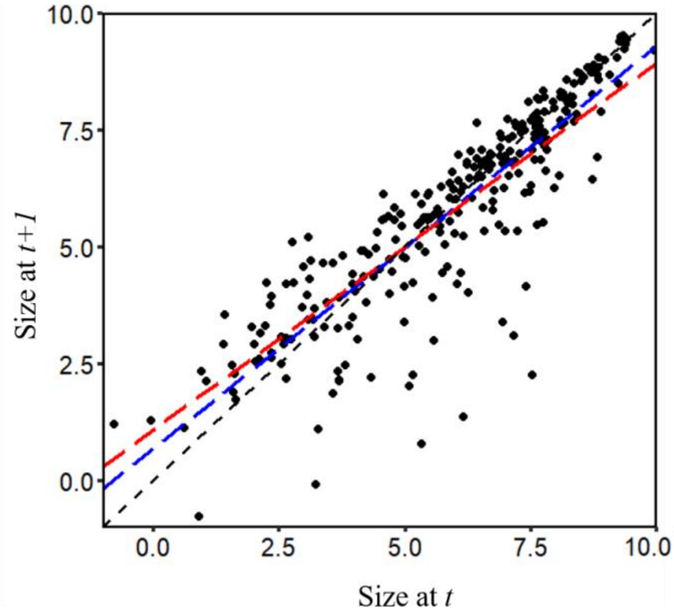

Figure S3.3. Size specific patterns in the size transitions of *Acropora* spp. colonies within a tropical (Red) and subtropical (Blue) setting. 1:1 diagonal line represents no change in size between times *t* and *t+1*.

Colony fragmentation

Through the demographic census of tagged colonies, we also estimated size-specific patterns in the probability of colony fragmentation. During each survey, we reported if tagged colonies had fragmented following observed evidence of colony breakage, but only in the event that colony remnants remained visible within our plots in order to distinguish between fragmentation and partial mortality. We modelled the probability of colony fragmentation during the interval *t* to *t+1* as a function of colony size at *t* using a logistic regression. However, due to the low frequency of annual fragmentation events (number of events reported, n_i^{κ}) within our tropical assemblage during both 2018 ($n_{tropical}^{\kappa}$ = 1, $n_{subtropical}^{\kappa}$ = 15, n_{total}^{κ} = 16), and 2019 ($n_{tropical}^{\kappa}$ = 5, $n_{subtropical}^{\kappa}$ = 14, n_{total}^{κ} = 19), we explored patterns in the probability of fragmentation using data pooled from both the tropical and subtropical assemblage (Fig. S3.4A). We modelled the vital rate of fragmentation without the random effect

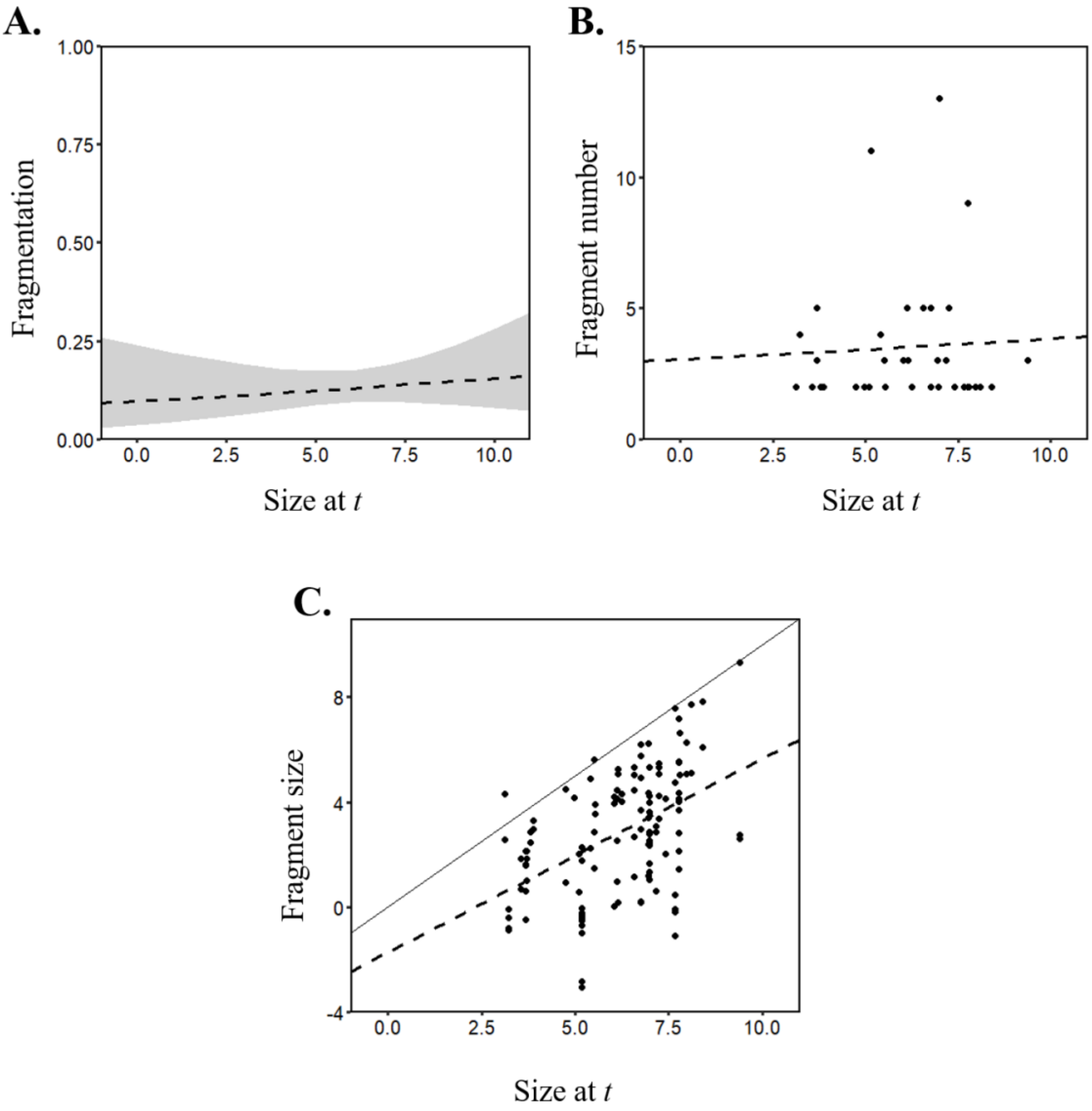

Figure S3.4. Size specific patterns in (**A**) the probability of fragmentation, (**B**) the number of fragments produced, and (**C**) the size of subsequent fragments, observed in tagged *Acropora* spp. colonies within southern Japan. Solid line in panel C represents the initial size of colonies prior to fragmentation.

of colony identity since fragmentation did not occur repeatedly enough across individuals to support the inclusion of this random variable. To ensure our approach of pooling data across populations did not prevent us from suitably capturing the differing prevalence of fragmentation within the dynamics of our tropical and subtropical assemblage, fragmentation patterns across our models were subsequently weighted according to the relative proportion of annual events recorded in our tropical and subtropical plots ($n_i^\kappa / n_{total}^\kappa$). Finally, alongside each reported fragmentation event, the quantity and size (surface area, cm^2) of all colony fragments produced were also recorded with, in each case, the largest fragment retaining the original colony's identity. We subsequently used these data to estimate patterns in both fragment production and fragment size at time $t+1$, as a function of initial colony size at time t, using linear regression (Fig. S3.4B & C).

3.2. Evaluating patterns of recruitment within tropical and subtropical coral assemblages.

Across our IPMs recruitment was represented using the three vital rates of colony fecundity (f_n), the probability of larval settlement (ψ), and the subsequent probability of recruit survival ($\digamma$). We did not directly measure colony fecundity using the tagged colonies. Instead we sourced data on the size-specific fecundity (larval volume, cm^3) of *Acropora* colonies on the Great Barrier Reef from the Coral Trait Database (Hall & Hughes 1996; Madin *et al.* 2016). These data describe an exponential increase in the larval output of *Acropora* colonies with increasing colony size, and subsequently, using non-linear least squares regression, we applied this relationship to estimate the expected larval output of each tagged colony, given their size in each year. Crucially, quantifying fecundity in this way assumes that the reproductive output of *Acropora* spp. remains fixed across varying environments, although this assumption has been illustrated to be reasonable in the absence of thermal stress (Howells *et al.* 2016). We have also addressed this assumption within our demographic models through the inclusion of the larval settlement and recruit survival parameters (see below) which constrained recruitment patterns within our models according to empirical observations made within the tagged populations. Equally, our use of the larval settlement parameter also served to translate colony fecundity estimates from measures of larval volume into expected counts of settling larvae within tropical and subtropical environments.

Alternatively, we estimated the parameters of larval settlement probability (ψ) and recruit survival probability ($\digamma$), for the tropical and subtropical assemblages, using larval counts made during prior settlement tile surveys conducted in both Okinawa (Nakamura *et al.* 2015) and Kochi (Nakamura, *unpublished data*). Between 2011 and 2013 settlement plate sets were deployed annually at seven sites along the Onna coastline of Okinawa (Fig. 1A), to quantify spatial and temporal variation in the number of settling *Acropora* larvae (see Nakamura *et al.* [2015] for further details). Each plate set consisted of two 10×10cm cement tiles fastened one above the other separated by a 2cm gap. Following pre-conditioning each plate set was deployed on the reef over a two-month period coinciding with local *Acropora* spawning events. Upon retrieval, across each tile set, only the upper and lower surfaces of the top tile and the upper surface of the lower tile were observed for coral spat, with the lower surface of the lowest tile having been used to secure both tiles to the reef. Subsequently, each plate set reflected a settlement area of 300 cm^2. A similar method was applied in Kochi, at Kashiwajima and Nishidomari during 2016–18 (Fig. 1A), providing a comparison between the annual rates of larvae settlement for *Acropora* spp. in both a tropical and subtropical setting. Again, plate sets consisting of two 10x10 cm cement tiles were deployed at Kashiwajima and Nishidomari. However, a key difference on this occasion was that upon retrieval of the plate sets both surfaces of both tiles were observed for coral spat. Thus, for these subtropical counts, each plate set reflected a settlement area of 400 cm^2.

We used these settlement counts to estimate the mean number of settling larvae per plate set which we subsequently scaled up to reflect larval settlement per unit area at the spatial scale of our plots (~2 m^2; Table S3.2). Dividing the total estimated larval outputs for our tagged tropical and subtropical *Acropora* colonies during each annual interval (2017-18 & 2018-19), by the corresponding regional average count of larval settlement per unit area, we were then able to determine ratios translating colony fecundity into the expected number of settling larvae (ψ; *sensu* Bramanti *et al.* 2015) within tropical and subtropical environments (Table S3.2). Next, we used our scaled estimates of larval density, and empirical counts of new *Acropora* colonies appearing within our tagged plots each year, to quantify ratios describing the annual post-settlement survival probability within both tropical and subtropical settings (*ϯ*; Table S3.2).

We acknowledge here that our approach to implement scaled settlement tile counts in estimating recruitment parameters entails two important considerations. Firstly, coral larvae predominantly settle close to the edge of settlement tiles resulting in a potential underestimation of larval settlement per unit area when scaling any counts (Price *et al.* 2019). Secondly, coral larvae are selective with settlement surfaces (Norström *et al.* 2007; Arnold *et al.* 2010) and identify suitable locations through a complex series of biotic cues (Price 2010). Accordingly, the area of substrate represented by our tagged plots may not be equivalent to the area of available effective substrate for larval settlement, leading to overestimates when scaling tile counts. Despite these pitfalls, scaling tile counts to more representative dimensions remains a common technique within recruitment assessments (Price *et al.* 2019), and with both these features opposing each other with regards to their impact on our capacity to accurately model regional recruitment patterns, we did not explicitly account for them within our parameter estimation.

Table S3.2. Temporal trends in larval settlement, and recruit survival within *Acropora* spp. assemblages in Okinawa and Kochi. Scaled larval densities were estimated by extrapolating mean settlement tile counts to reflect the spatial coverage of our tagged plots (~2 m^2). The scaled larval densities were then combined with estimates of total colony fecundity and empirical recruit counts from 2017-18 and 2018-19, to determine annual estimates of larval settlement probability (ψ) and recruit survival probability (f). Error displayed as 95% CI.

	Scaled larval density (larvae $plot^{-1}$)		Larval settlement probability (ψ)	Recruit density (Recruit $plot^{-1}$)	Recruit survival probability (f)
OKINAWA	1175.26 [1135.87, 1214.65]	2017-18	0.2143 [0.2071, 0.2215]	10	0.0085 [0.0082, 0.0088]
		2018-19	0.2997 [0.2896, 0.3097]	28	0.0238 [0.0231, 0.0247]
KOCHI	31.11 [22.96, 39.26]	2017-18	0.0004 [0.0003, 0.0005]	20	0.6429 [0.5094, 0.8710]
		2018-19	0.0005 [0.0004, 0.0006]	63	2.0250 [1.6047, 2.7436]

Finally, during plot surveys in 2018 and 2019 we recorded the size (cm^2) of new colonies appearing within the plots to provide a measure of recruit size (C_1) and how this varies between tropical and subtropical assemblages (Fig. S3.5). Due to the difficulties associated with identifying the parental lineage of new recruits, recruit size was modelled independently of parent colony size using linear regression. This approach is consistent with evidence that the complex dynamics of larval settlement and survival are coordinated by local biotic and abiotic constraints (Vermeij *et al.* 2009; Doropoulos *et al.* 2016), and therefore independent from parental characteristics. Initially, we modelled recruit size with ecoregion (subtropical *vs.* tropical) and survey year, included as fixed effects. However, this approach demonstrated no significant difference between the recruit size distributions of the tropical and subtropical assemblages, and little within-population variation between years (Fig. S3.5; GLM: $F_{3,117} = 1.09$, $p = 0.36$). We subsequently dropped the term of survey year from our model of recruit size but retained ecoregion as a fixed effect as AIC scores confirmed this to be the most appropriate model fit (AIC: no terms = 383.8; ecoregion only = 383.2, ecoregion * year = 386.5).

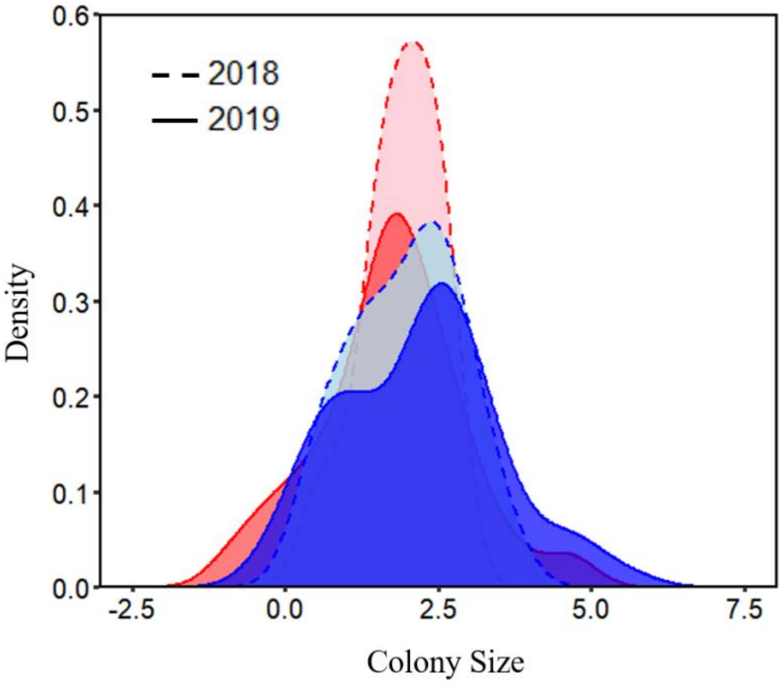

Figure S3.5. Temporal trends in the size distributions of surviving recruit cohorts observed within tropical (Red) and subtropical (Blue) *Acropora* assemblages during 2018 and 2019.

3.3. Exploring latitudinal trends in the traits of Acropora spp. assemblages.

We have demonstrated that there exists a latitudinal trade-off between the long-term persistence and short-term exploitation potential in *Acropora* spp. assemblages. In the subtropics the *Acropora* spp. assemblage displays a greater capacity for demographic compensation following disturbances, whereas in the tropics the assemblage instead exhibits more stable asymptotic growth rates (λ). We admit, however, that any interpretations of our results need to be approached with a degree of caution. Due to unresolved coral taxonomies and the prevalence of numerous cryptic species, it is difficult to identify *Acropora* spp. individuals to the species level in the field (Fukami *et al.* 2004; Richards & Hobbs 2015; Richards *et al.* 2016). Thus, we conducted all our analyses at the genus level. Yet without explicit data regarding the species compositions of our tagged tropical and subtropical *Acropora* spp. assemblages it would be inappropriate for us to ignore the fact that our reported demographic trends may simply coincide with latitudinal shifts in species configurations, rather than any demographic plasticity. Subsequently, it was necessary to disentangle the potential role shifts in species compositions, and therefore shifts in species traits between tropical and subtropical environments, play in mediating the demographic variation we observed.

Using the Coral Trait database (Madin *et al.* 2016) we extracted trait values for a series of numerical and categorical traits for *Acropora* species known to occur within the coral communities of Okinawa and/or Kochi (Table S3.3). As expected, species richness was highest in the tropics with 73 different species of *Acropora* reported in Okinawa. Alternatively, just 26 species have been recorded within the *Acropora* spp. assemblages of Kochi, of which only four are not found in Okinawa (Table S3.3). To explore variation in the characteristics between these *Acropora* spp. communities in southern Japan, we focused on seven numerical traits relating to calcification rate (µm cm^{-2} h^{-1}), corallite width (maximum and minimum; mm), depth (maximum, minimum, and mean; m), and colony growth rate (mm year^{-1}), alongside the three categorical traits of growth form, water clarity preference, and wave exposure preference. A single value for each trait was extracted to describe the characteristics of each *Acropora* species. For any species for which multiple estimates had been reported for any given trait we retained the mean (numerical traits), or modal trait value (categorical traits).

We used the extracted trait values to quantify how the characteristics of *Acropora* spp. assemblages vary between tropical and subtropical environments (Table S3.4; Fig. S3.6). T-tests confirmed that there exists no significant variation between the distributions of any of the selected numerical traits between the tropical and subtropical assemblages (Table S3.4). Equally, the proportional arrangements of the selected categorical traits remain similar across the assemblages from the two regions (Fig. S3.6). An exception to this trend is that there is a change in the composition of colony growth forms between the two regions. In the tropics there is a greater prevalence of arborescent morphologies (Fig. S3.6C). However, in the subtropics there is a shift towards increased exploitation of tabular growth forms (Fig. S3.6C), consistent with the need for *Acropora* spp. individuals to maximise their ability to compete for access to photosynthetic radiation, which is more limited at higher latitudes (Muir *et al.* 2015; Zawada *et al.* 2019).

Overall, the trait characteristics of *Acropora* species associated with tropical and subtropical environments appears fixed across both regions; providing evidence that our reported trade-off between demographic compensation and demographic stability is not a consequence of a shift in the species composition of tropical and subtropical *Acropora* spp. assemblages in southern Japan. Moreover, given that there is considerable overlap between the species configurations of the *Acropora* spp. assemblages of Okinawa and Kochi we can be more confident that our findings do indeed present evidence of demographic plasticity associated with the need for coral populations in subtropical environments to enhance their viability despite increased environmental variability.

Table S3.3. List of *Acropora* species reported to occur within the coral communities of Okinawa and/or Kochi (Nishihira & Veron 1995; Veron *et al.* 2016). Colour to the left of each species reflects its recorded distribution: Okinawa only (Red), both Okinawa & Kochi (Orange), and Kochi only (Blue).

🟥	*A. abrolhosensis*
🟥	*A. abrotanoides*
🟥	*A. aculeus*
🟥	*A. acuminata*
🟥	*A. akajimensis*
🟥	*A. austera*
🟥	*A. awi*
🟥	*A. brueggemanni*
🟥	*A. carduus*
🟥	*A. cerealis*
🟥	*A. clathrata*
🟥	*A. cytherea*
🟥	*A. danai*
🟥	*A. digitifera*
🟥	*A. echinata*
🟥	*A. efflorescens*
🟥	*A. exquisita*
🟥	*A. formosa*
🟥	*A. gemmifera*
🟥	*A. grandis*
🟥	*A. granulosa*
🟥	*A. horrida*
🟥	*A. humilis*
🟥	*A. inermis*
🟥	*A. irregularis*
🟥	*A. kirstyae*
🟥	*A. longicyathus*
🟥	*A. microclados*
🟥	*A. microphthalma*
🟥	*A. millepora*
🟥	*A. monticulosa*
🟥	*A. nana*
🟥	*A. nobilis*
🟥	*A. palifera*
🟥	*A. paniculata*
🟥	*A. parilis*
🟥	*A. pichoni*
🟥	*A. pulchra*
🟥	*A. robusta*
🟥	*A. rosaria*
🟥	*A. sarmentosa*
🟥	*A. secale*
🟥	*A. sekiseiensis*
🟥	*A. selago*
🟥	*A. subglabra*
🟥	*A. tenella*
🟥	*A. tenuis*
🟥	*A. valenciennesi*
🟥	*A. vaughani*
🟥	*A. wallaceae*
🟥	*A. yongei*
🟧	*A. anthocercis*
🟧	*A. aspera*
🟧	*A. copiosa*
🟧	*A. cuneata*
🟧	*A. dendrum*
🟧	*A. divaricata*
🟧	*A. florida*
🟧	*A. hyacinthus*
🟧	*A. insignis*
🟧	*A. latistella*
🟧	*A. listeri*
🟧	*A. loripes*
🟧	*A. nasuta*
🟧	*A. samoensis*
🟧	*A. solitaryensis*
🟧	*A. striata*
🟧	*A. subulata*
🟧	*A. teres*
🟧	*A. tumida*
🟧	*A. valida*
🟧	*A. verweyi*
🟧	*A. willisae*
🟦	*A. glauca*
🟦	*A. japonica*
🟦	*A. pruinosa*
🟦	*A. stoddarti*

Table S3.4. Comparison of the numerical trait characteristics of tropical and subtropical *Acropora* spp. assemblages from Okinawa and Kochi, respectively. T-tests were used to evaluate for any statistical significance in the trait distributions from the two regions. Error reported as ±SD.

Trait		Okinawa	Kochi	Test statistic
CALCIFICATION RATE (μm cm^{-2} h^{-1})		1.26 ± 1.18	1.35 ± 1.31	$p = 0.90$
CORALLITTE WIDTH (mm)	Max	1.20 ± 0.29	1.24 ± 0.26	$p = 0.64$
	Min	0.62 ± 0.20	0.69 ± 0.25	$p = 0.30$
DEPTH (m)	Max	25.08 ± 9.57	22.59 ± 8.32	$p = 0.26$
	Mean	14.82 ± 6.53	12.82 ± 4.75	$p = 0.14$
	Min	4.56 ± 4.75	3.04 ± 2.38	$p = 0.06$
GROWTH RATE (mm year^{-1})		50.50 ± 44.96	35.62 ± 21.86	$p = 0.28$

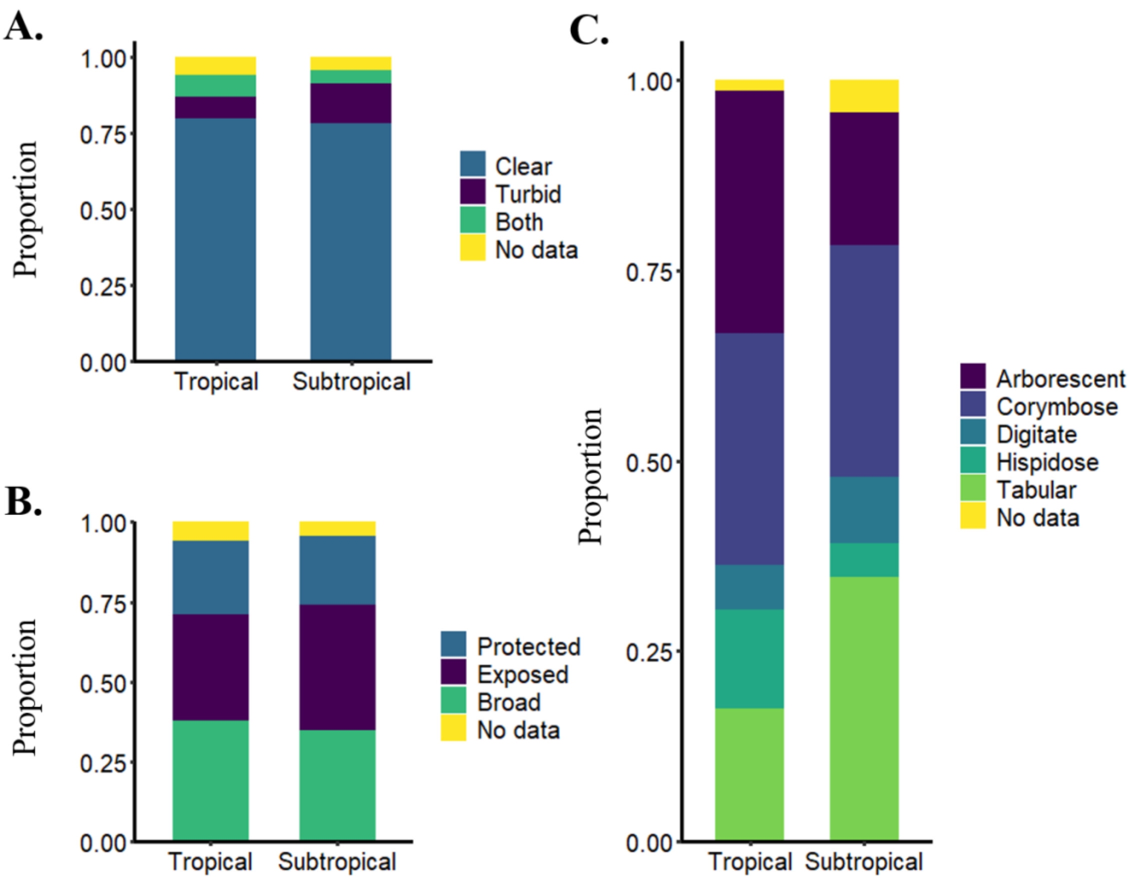

Figure S3.6. Patterns in the categorical traits of **(A)** water clarity preference, **(B)** wave exposure preference and **(C)** growth form within the respective tropical and subtropical *Acropora* spp. assemblages of Okinawa and Kochi. Proportions show the number of species exhibiting each trait relative to the number of species present in each region (Tropics, n = 73; Subtropics, n = 26).

3.4. References

Arnold, S.N., Steneck, R.S. & Mumby, P.J. (2010). Running the gauntlet: Inhibitory effects of algal turfs on the processes of coral recruitment. *Mar. Ecol. Prog. Ser.*, 414, 91–105.

Bramanti, L., Iannelli, M., Fan, T.Y. & Edmunds, P.J. (2015). Using demographic models to project the effects of climate change on scleractinian corals: Pocillopora damicornis as a case study. *Coral Reefs*, 34, 505–515.

Doropoulos, C., Roff, G., Bozec, Y., Zupan, M., Werminghausen, J. & Mumby, P.J. (2016). Characterizing the ecological trade-offs throughout the early ontogeny of coral recruitment. *Ecol. Monogr.*, 86, 20–44.

Easterling, M.R., Ellner, S.P. & Dixon, P.M. (2000). Size-specific sensitivity: applying a new structured population model. *Ecology*, 81, 694–708.

Fukami, H., Budd, A.F., Paulay, G., Solé -Cava, A., Chen, C.A., Iwao, K., *et al.* (2004). Conventional taxonomy obscures deep divergence between Pacific and Atlantic corals. *Nature*, 427, 829–832.

Hall, V.R. & Hughes, T.P. (1996). Reproductive strategies of modular organisms: Comparative studies of reef-building corals. *Ecology*, 77, 950–963.

Howells, E.J., Ketchum, R.N., Bauman, A.G., Mustafa, Y., Watkins, K.D. & Burt, J.A. (2016). Species-specific trends in the reproductive output of corals across environmental gradients and bleaching histories. *Mar. Pollut. Bull.*, 105, 532–539.

Madin, J.S., Anderson, K.D., Andreasen, M.H., Bridge, T.C., Cairns, S.D., Connolly, S.R., *et al.* (2016). The Coral Trait Database, a curated database of trait information for coral species from the global oceans. *Sci. Data*, 3, 1–21.

Muir, P., Wallace, C.., Done, T. & Aguirre, J.D. (2015). Limited scope for latitudinal extension of reef corals. *Science*, 348, 1135–1138.

Nakamura, M., Kumagai, N.H., Sakai, K., Okaji, K., Ogasawara, K. & Mitarai, S. (2015). Spatial variability in recruitment of acroporid corals and predatory starfish along the Onna coast, Okinawa, Japan. *Mar. Ecol. Prog. Ser.*, 540, 1–

12.

Nishihira, M. & Veron, J.E.N. (1995). *Hermatypic corals of Japan*. Kaiyusha, Tokyo, Japan.

Norström, A. V., Lokrantz, J., Nyström, M. & Yap, H.T. (2007). Influence of dead coral substrate morphology on patterns of juvenile coral distribution. *Mar. Biol.*, 150, 1145–1152.

Price, N. (2010). Habitat selection, facilitation, and biotic settlement cues affect distribution and performance of coral recruits in French Polynesia. *Oecologia*, 163, 747–758.

Price, N.N., Muko, S., Legendre, L., Steneck, R., Van Oppen, M.J.H., Albright, R., *et al.* (2019). Global biogeography of coral recruitment: Tropical decline and subtropical increase. *Mar. Ecol. Prog. Ser.*, 621, 1–17.

Richards, Z.T., Berry, O. & van Oppen, M.J.H. (2016). Cryptic genetic divergence within threatened species of Acropora coral from the Indian and Pacific Oceans. *Conserv. Genet.*, 17, 577–591.

Richards, Z.T. & Hobbs, J.P.A. (2015). Hybridisation on coral reefs and the conservation of evolutionary novelty. *Curr. Zool.*, 61, 132–145.

Schneider, C.A., Rasband, W.S. & Eliceiri, K.W. (2012). NIH Image to ImageJ: 25 years of image analysis. *Nat. Methods*, 9, 671–675.

Vermeij, M.J.A., Smith, J.E., Smith, C.M., Vega Thurber, R. & Sandin, S.A. (2009). Survival and settlement success of coral planulae: Independent and synergistic effects of macroalgae and microbes. *Oecologia*, 159, 325–336.

Veron, J.E.N., Stafford-Smith, M.G., Turak, E. & DeVantier, L.M. (2016). *Corals of the World*. Available at: http://www.coralsoftheworld.org/page/home/. Last accessed 12 November 2019.

Zawada, K.J.A., Madin, J.S., Baird, A.H., Bridge, T.C.L. & Dornelas, M. (2019). Morphological traits can track coral reef responses to the Anthropocene. *Funct. Ecol.*, 33, 962–975.

Supplementary material 4

Coral assemblages at higher latitudes favour short-term potential over long-term performance

4.1. Estimating population-specific vital rates

Through the setup of permanent plots, we tagged colonies of competitive, stress-tolerant, and weedy coral taxa (*see below*) within the tropical and subtropical coral communities of southern Japan and eastern Australia. Across these four regional coral communities (Australian subtropics [AS], Australian tropics [AT], Japanese subtropics [JS] and Japanese tropics [JT]), permanent plots were assembled by fixing numbered tags into bare reef substrate, with each plot then consisting of a numbered tag and its surrounding coral colonies within a 2m^2 area (Cant *et al.* 2021a, b). In 2016, plots were positioned throughout the subtropical Solitary Islands Marine Park (SIMP) region, Australia, at North Solitary Island (-29.93°, 153.39°), Northwest Solitary Island (-30.02°, 153.27°), South Solitary Island (-30.21°, 153.27°), Southwest Solitary Island (-30.16°, 153.23°) and Black Rock (Southwest Rocks; -30.95°, 153.08°). In 2017, further plots were then assembled in Japan, across three sites within the tropical reef communities of Okinawa (OKI; Oura Bay [26.54°, 128.08°], Hentona [26.75°, 128.18°], and Miyagi Channel [26.35°, 127.99°]) and at three sites within the subtropical communities of Kochi, Shikoku (KHI; Okinoshima [32.75°, 132.55°], Kashiwajima [32.77°, 132.62°], and Nishidomari [32.78°, 132.73°]). Finally, in 2018 plots were also arranged at three sites within the tropical reef community of Heron Island, Australia (HI; Libby’s Lair [-23.43°, 151.93°], Coral Gardens [-23.45°, 151.91°] and Wistari Reef [-23.46°, 151.87°]).

Following plot set up, annual repeated surveys of all tagged colonies, up to and including 2019, then allowed us to estimate size-specific patterns in colony survival, size transitions (growth & shrinkage; Madin *et al.* [2020]), fragmentation, and recruitment. Photographs, with a scale bar included for reference, were used to capture the visible horizontal extent of each tagged colony over successive surveys. With these photographs we produced longitudinal records of horizontal surface area (cm^2) measurements for each colony using ImageJ (Schneider *et al.* 2012). All colony size estimates were then log-transformed to ensure a normal distribution and enhance the resolution of smaller colonies. Next, to mitigate inconsistencies in the number of census intervals across our sites in Australia and Japan we pooled data across both years and sites for each of the three life-history categories (competitive, stress-tolerant, and weedy) at the four focal geographical locations (AS, AT, JS, and JT; Table S4.1). Using generalised linear mixed models (GLMMs) we then calculated size-specific patterns in colony survival, transitions in size, fragmentation probability, fecundity, and recruitment for each assemblage.

Table S4.1. Pooled number of colonies used to evaluate size-specific patterns in colony survival, transitions in size, fragmentation, and recruitment for each regional competitive, stress-tolerant, and weedy coral assemblage in Australia and Japan.

Life-history group	**Country**	**Tropical**	**Subtropical**
Competitive	Australia	207	217
	Japan	103	446
Stress-tolerant	Australia	162	329
	Japan	646	274
Weedy	Australia	93	290
	Japan	147	257

Survival

Colony survival represented the continued presence of tagged individuals across successive surveys. Using a binomial GLMM, we modelled the probability of colony survival as a function of colony size at time *t*, with the variables of life-history classification, country (Australia *vs.* Japan), and ecoregion (tropical *vs.* subtropical) included as fixed effects (Fig. S4.1). We also included the random effects of colony identify and survey location to address any within-subject-variability and autocorrelation arising from our pooling of data across multiple years and sites.

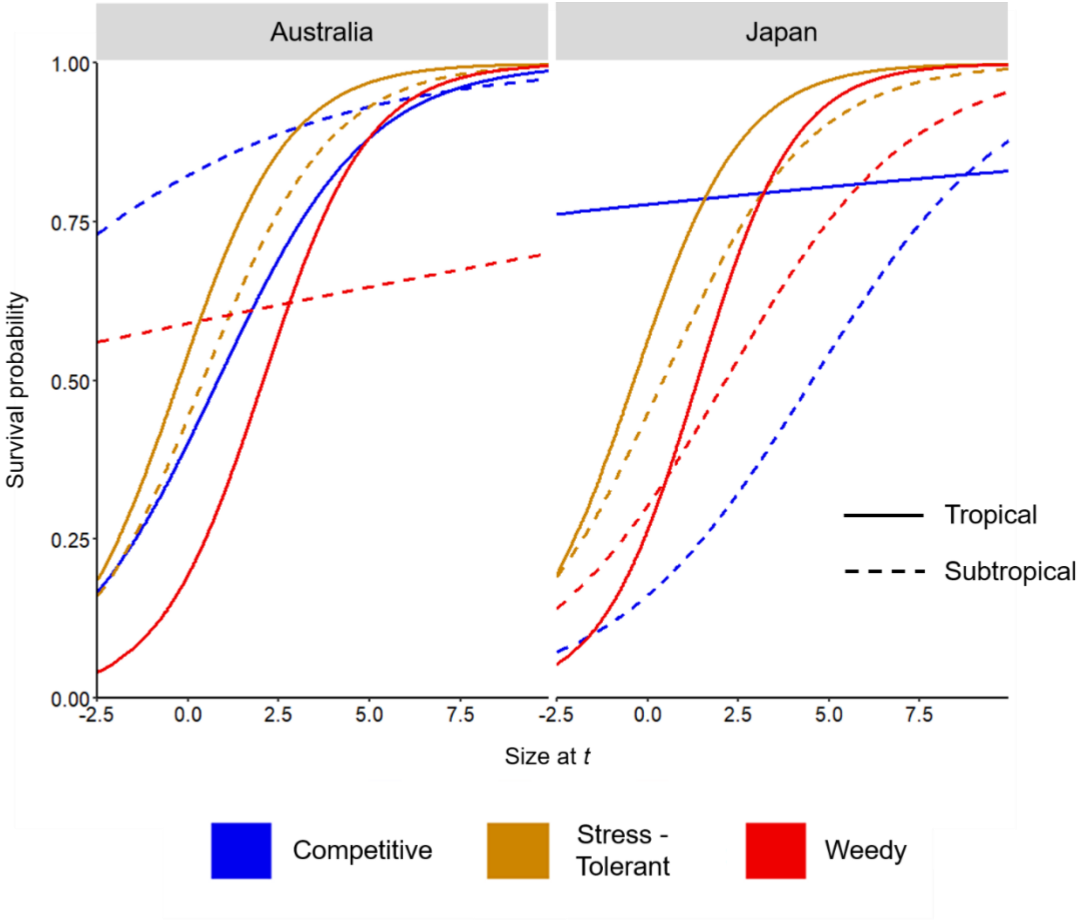

Figure S4.1. Colony survival probability as a function of colony size, showing the regional and interspecific variation in colony survival across assemblages of competitive, stress-tolerant, and weedy coral taxa in Australia and Japan.

<u>Size transitions</u>

Colony size transitions reflected the change in colony surface areas recorded across successive surveys, which we modelled as colony size at *t+1* as a function of colony size at *t* using a polynomial GLMM (Fig. S4.2). As with survival we modelled colony size transitions with the variables of life-history classification, country, and ecoregion included as fixed effects, and the variables of colony identity and survey location included as random effects.

Separately we also modelled the relationship between the variance in colony size at time *t+1* and colony size at time *t*. We determined this relationship by modelling the residuals from our initial colony size transition model as a function of colony size at time *t*, using a gamma GLMM to allow for a non-linear pattern whilst preventing negative variance. AIC scores confirmed the validity of this approach over an equivalent linear format (AIC: linear = 2413.5; gamma = 334.1). Again, we included life-history classification, country, and ecoregion as fixed effects, alongside the random effects of colony identify and site location.

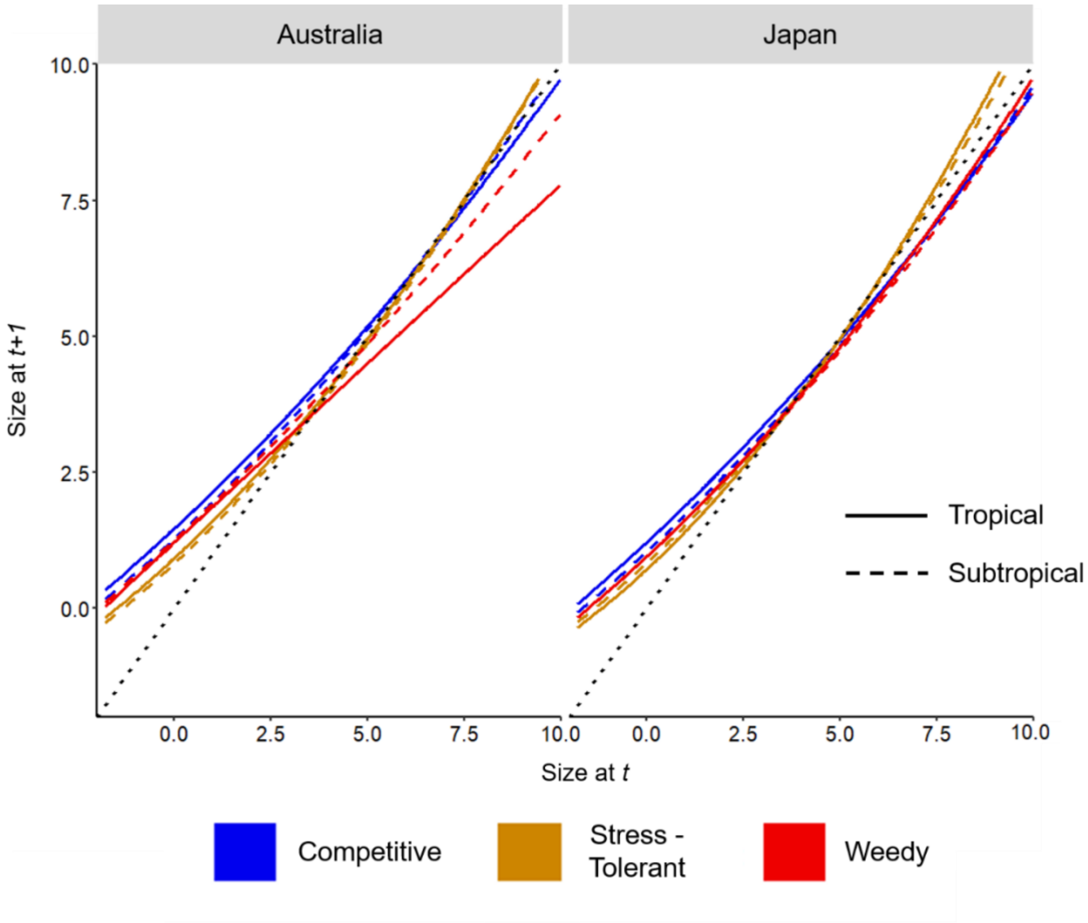

Figure S4.2. Colony size at time *t+1* as a function of colony size at time *t*, showing the regional and interspecific variation in size transition patterns across assemblages of competitive, stress-tolerant, and weedy coral taxa in Australia and Japan. 1:1 diagonal line (dotted) represents no change in size between times *t* and *t+1*.

Fragmentation

We recorded colony fragmentation in the event of observed colony breakage, recording the size (surface area, cm^2) of all remnants produced in each case. Using a polynomial binomial GLMM, we then modelled colony fragmentation probability as

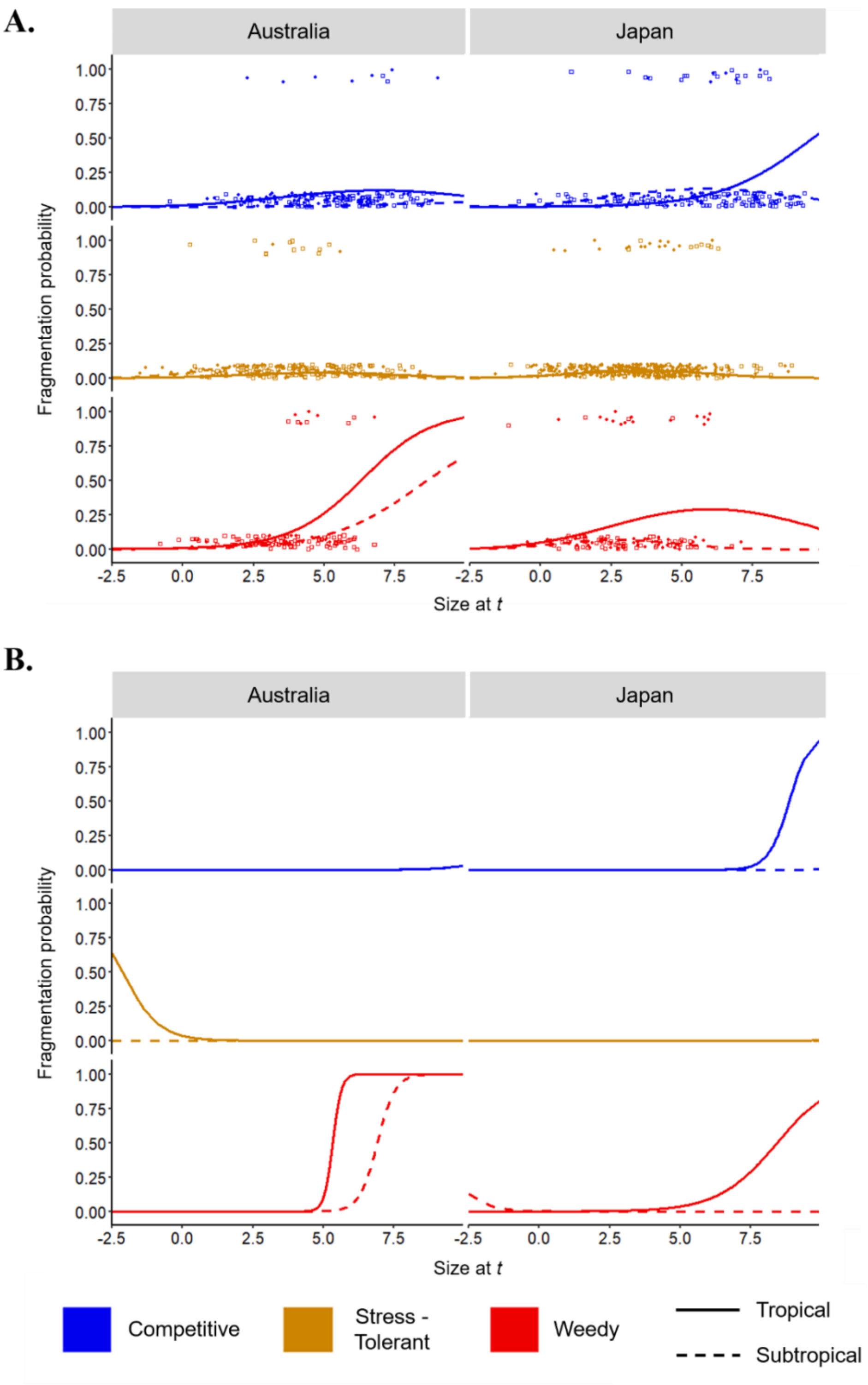

Figure S4.3. Comparison between size-specific patterns in fragmentation probability modelled as the **(A)** polynomial binomial function of colony size at time *t*, and as the **(B)** binomial function of colony size at time *t*, showing the regional and interspecific variation across assemblages of competitive, stress-tolerant, and weedy coral taxa in

Australia and Japan. Data points shown on panel A to help visualise the improved representation of observed fragmentation patterns presented by the polynomial binomial model.

a function of colony size at time *t* (Fig. S4.3A). Initially, we performed this analysis using only a binomial GLMM (Fig. S4.3B). However, despite AIC scores indicating this binomial model was the most accurate (AIC: binomial = 1167.1; polynomial binomial = 1245.1), the polynomial binomial format offered an improved representation of visual patterns within our fragmentation data (Fig. S4.3). As was the case across the other vital-rates, we included life-history classification, country, ecoregion, colony identity, and site location as fixed and random effects.

We also modelled the number and size of colony fragments produced during fragmentation events. With our observations of the number of fragments produced by fragmenting colonies representing count data, we modelled the number of fragments produced as a function of fragmenting colony size at time *t* using a poisson GLMM (Fig. S4.4A). Meanwhile, we modelled fragment size as a function of fragmenting colony size at time *t*, using a polynomial GLMM (Fig. S4.4B), which provided a more representative fit than an equivalent linear format (AIC: linear = 2243.5; polynomial = 2239.1). Finally, using a gamma GLMM we also modelled the variance in fragment sizes as a function of fragmenting colony size at time *t* (AIC: linear = 1578.0; gamma = 1440.1). Across each of our models exploring size-specific patterns in the number and size of any fragments produced during fragmentation events we only included life-history classification and country as fixed effects variables. There was insufficient replication in our data for us to include the fixed effect of ecoregion and the random effects of either survey location or colony identity. Subsequently, it was necessary for our analyses to assume that size-specific patterns in the number and size of fragments produced during fragmentation events is consistent across tropical and subtropical conspecifics.

Recruitment

During the repeated surveys of our permanent coral plots, we recorded the number and size of new colonies appearing within each plot. Using these recruit counts we quantified annual and regional variation in the recruit densities of competitive, stress-

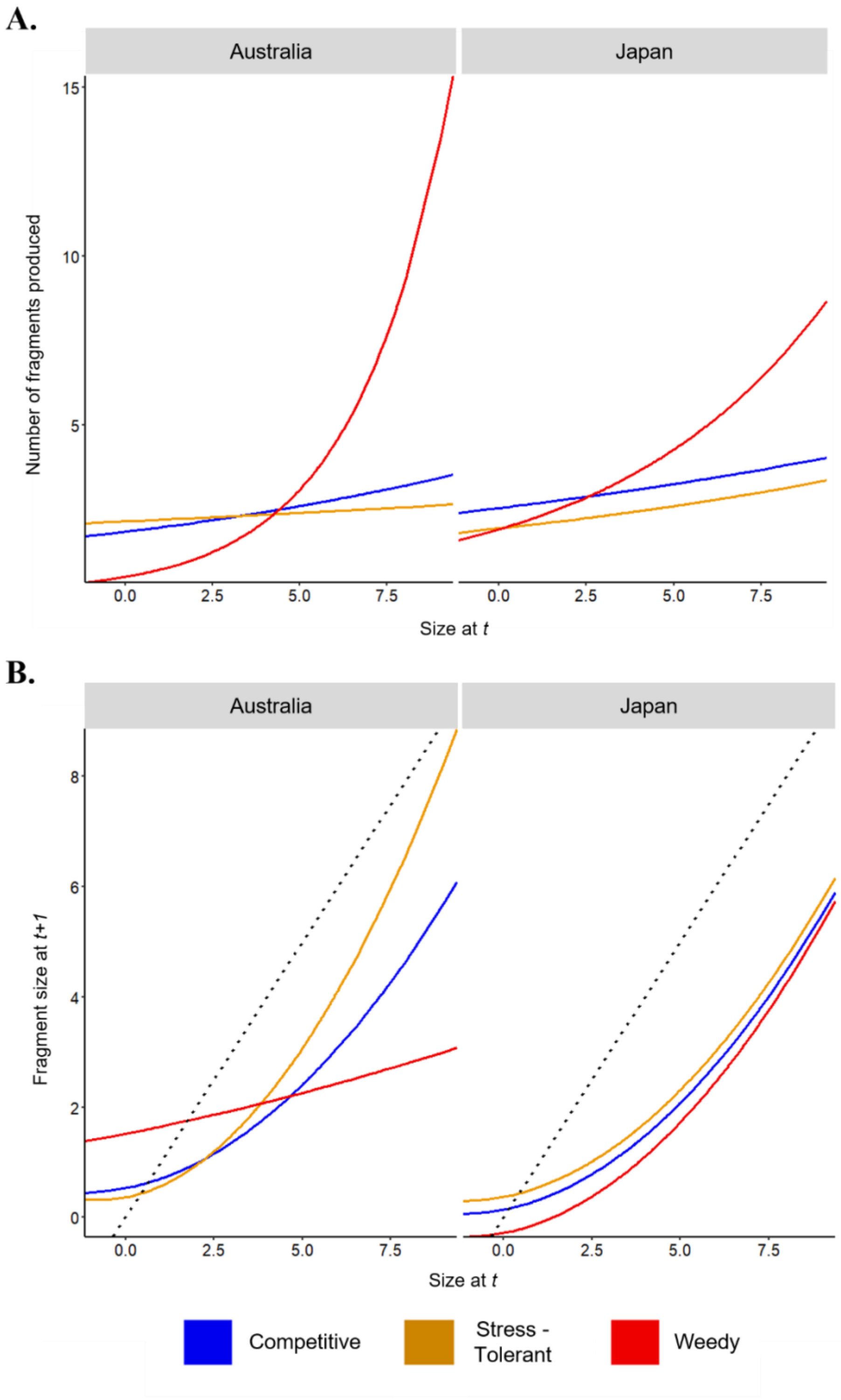

Figure S4.4. (A) Number and (B) size of fragments produced as a function of fragmenting colony size at time *t*, showing the regional and interspecific variation across assemblages of competitive, stress-tolerant, and weedy coral taxa in Australia and Japan. 1:1 diagonal line (dotted) on panel B represents the production of fragments of equal size to parent colony.

tolerant, and weedy coral populations (Table S4.2). We also used the size of observed recruits to estimate assemblage-specific recruit size distributions (Fig. S4.5). With the parental lineage of new recruits unknown, we modelled recruit size at time *t+1* independent to colony sizes at time *t* using a linear regression, extracting the mean recruit size and standard deviation for each assemblage. Initially, we included life-history classification, country, and ecoregion as fixed effects within this recruit size model allowing us to quantify both inter-assemblage and regional variation in the size of new recruits (Fig. S4.5). However, the majority of the variation between each population's recruit size distribution was solely generated by their life-history group classification (ANOVA. $F_{2,1108} = 48.8$, $p < 0.001$), with the country and ecoregion variables providing only a small contribution (ANOVA. Country: $F_{1,1108} = 6.4$, $p = 0.01$; Ecoregion: $F_{1,1108} = 0.007$, $p = 0.932$; Fig. S4.5). Subsequently, to maximise our sample size for estimating recruit size parameters we subsequently dropped both the ecoregion and country terms from the model.

Table S4.2. Densities of new colonies of competitive, stress-tolerant, and weedy coral taxa observed during the repeated surveys of our permanent coral plots in 2017, 2018, and 2019.

Country	Ecoregion	Population classification	2017	2018	2019
Australia	Tropical	Competitive	-	-	80
		Stress-Tolerant	-	-	83
		Weedy	-	-	59
	Subtropical	Competitive	4	16	33
		Stress-Tolerant	1	31	74
		Weedy	6	52	80
Japan	Tropical	Competitive	-	12	31
		Stress-Tolerant	-	108	188
		Weedy	-	10	12
	Subtropical	Competitive	-	34	73
		Stress-Tolerant	-	21	26
		Weedy	-	42	44

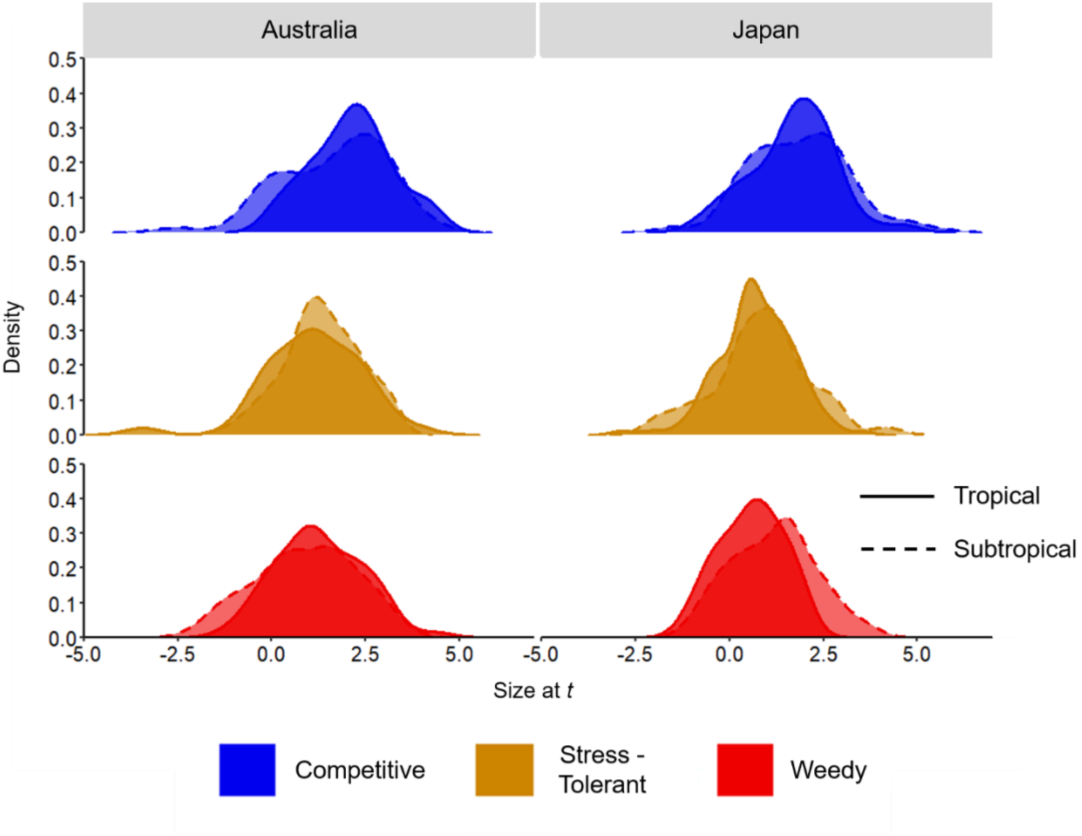

Figure S4.5. Regional and interspecific variation in the recruit size densities of competitive, stress-tolerant, and weedy coral assemblages in Australia and Japan.

Fecundity

Due to the logistical challenges associated with insitu measurements of colony fecundity (Gilmour *et al.* 2016), we did not empirically record the fecundity of our tagged colonies. Instead, we modelled size-specific patterns in colony fecundity using a relationship linking colony size and larval output (larval volume, mm^3) recorded in the coral communities at Lizard Island, on the Great Barrier Reef (Hall & Hughes 1996). Firstly, we categorised the coral species surveyed by Hall & Hughes (1996) as competitive, stress-tolerant, or weedy according to their shared life-history characteristics (*sensu* Darling *et al.* 2012). Using a polynomial GLMM we subsequently quantified a relationship between colony size and larval output for competitive, stress-tolerant, and weedy coral taxa (Fig. S4.6).

We acknowledge here that our approach to modelling fecundity does imply an assumption that all larvae produced by an assemblage will reseed back into that same assemblage; an assumption that is inappropriate for coral populations which typically exist as open populations with larvae capable of dispersing away from their source populations (Graham *et al.* 2008; Yau *et al.* 2014). We corrected this assumption by parameterising a recruit survival function (ϕ) into our IPMs. This recruit survival function serves to convert estimates of larval output from a measure of volume into the proportional contribution of colonies towards observed recruit densities, as a function of their size. Thus, although we have modelled fecundity using data from a distinctly different community, our use of the recruit survival function ensures that recruitment patterns within our IPMs were determined by empirical counts made within our focal communities and made no assumptions regarding the initial source of new recruits. Our IPMs were therefore not sensitive to changes in colony fecundity, and our inclusion of this vital rate merely allowed us to close the loop between the dynamics of existing colonies and the dynamics of recruitment in order to quantify measures of long-term population performance and transient potential. We estimated the recruit survival function as the ratio between the total expected larval output of a population in any given year and the corresponding annual recruitment count for that population (*sensu* Bramanti *et al.* 2015; Cant *et al.* 2021b).

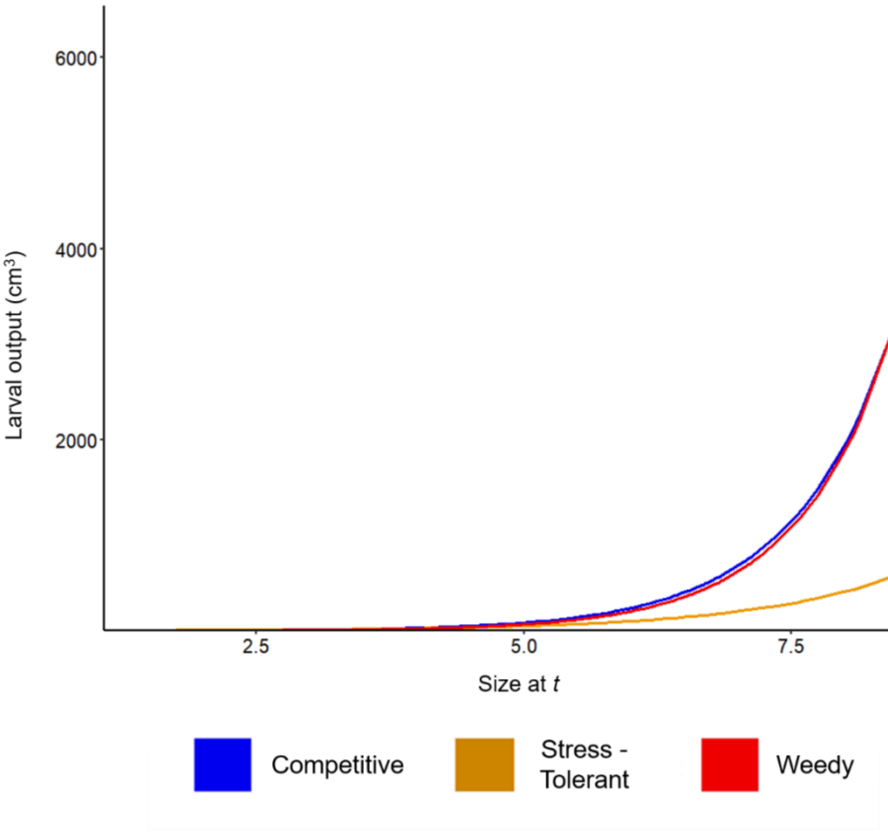

Figure S4.6. Size-specific patterns in larval output (cm^3) estimated for competitive, stress-tolerant, and weedy coral populations using data obtained from coral communities on Lizard Island, on the northern Great Barrier Reef (Hall & Hughes 1996).

4.2. Classifying tagged corals according to shared morphological and ecological trait characteristics

Table S4.3. Table of coral genus and species to which our tagged colonies were identified, alongside the proportion of each taxonomic rank assigned to each of the four assemblage classifications: Competitive, Generalist, Stress-tolerant, and Weedy. Greyscale used to differentiate between colonies tagged in subtropical Australia, tropical Australia, subtropical Japan, and tropical Japan.

Coral genus/species		**Competitive**	**Generalist**	**Stress tolerant**	**Weedy**	**Unassigned**	**Citation**
Acanthastrea	*echinata*			1.00			2,3
Acanthastrea				1.00			2,3
Acropora	*anthoceris*	1.00					2,3
Acropora	*cytherea*	1.00					1,2
Acropora	*glauca*	1.00					1,2
Acropora	*hyacinthus*	1.00					1
Acropora	*loripes*	1.00					1,2
Acropora	*solitaryensis*	1.00					1,2
Acropora		1.00					1,2
Acropora	*valida*	1.00					1,2
Astrea	*curta*			1.00			1
Cyphastrea				1.00			1,6
Dipsastraea	*speciosa*			1.00			2,3
Dipsastraea				1.00			2,3
Goniopora	*djiboutiensis*			1.00			2,3
Goniopora	*lobata*			1.00			2,3
Goniopora	*norfolkensis*			1.00			2,3
Micromussa	*amakusensis*			1.00			4

Micromussa	*lordhowensis*			1.00			2,3
Micromussa				1.00			4
Montipora		0.43	0.14	0.43			1,2,6
Montipora	*venosa*			1.00			1
Paragoniastrea	*australiensis*			1.00			1
Plesiastrea				1.00			2
Pocillopora	*aliciae*				1.00		5
Pocillopora	*damicornis*				1.00		1
Porites	*heronensis*			1.00			2,3
Porites	*murrayensis*			1.00			2,3
Porites	*stephensoni*			1.00			2,3
Porites (Encrusting & Massive)				1.00			2,3
Stylophora	*pistillata*				1.00		1
Stylophora					1.00		1,2
Turbinaria	*frondens*		1.00				1
Turbinaria	*mesenterina*	1.00					1
Turbinaria	*patula*		1.00				1,3,6
Turbinaria	*radicalis*			1.00			1,3,6
Acanthastrea				1.00			2,3
Acropora		1.00					1,2,3
Astrea	*curta*			1.00			2,3,7
Astreopora				1.00			1,2,3
Cyphastrea				1.00			1,2,3,6

	Dipsastraea				1.00			2,3
	Echinophyllia				1.00			1,2,3
	Echinopora			1.00				1,2,3,6
	Favites				1.00			2,3
	Fungia				1.00			2,3
	Galaxea				1.00			2,3
	Goniastrea				0.86	0.14		1,2,3,6
	Goniopora				1.00			2,3
	Hydnophora		0.33	0.33	0.33			1,2,3,6
	Isopora			1.00				3
	Leptastrea				0.60	0.40		1,2,3,6
	Leptoria				1.00			1,2,3
	Lobophyllia				1.00			1,2,3
	Merulina			1.00				1,2,3,6
	Montipora		0.31	0.24	0.45			1,2,6
	Mycedium			1.00				3
	Oulophyllia				1.00			3
	Pavona	*varians*			1.00			1,2
	Platygyra				1.00			1,2,3
	Pocillopora	*damicornis*				1.00		1
	Pocillopora		0.60			0.40		1,2,3,6,9
	Porites (Branching)					1.00		2,3
	Porites (Encrusting & Massive)				1.00			2,3
	Psammacora			0.80		0.20		1,2,3,6,8
	Seriatopora					1.00		1,2,3

Stylophora	*pistillata*				1.00		1,2,3
Stylophora					1.00		1,2,3
Symphyllia				1.00			3
Turbinaria	*frondens*		1.00				1
Turbinaria	*heronensis*		1.00				3,6
Turbinaria	*peltata*		1.00				3,6
Turbinaria		0.14	0.71	0.14			1,2,3
Acanthastrea				1.00			2,3
Acropora		1.00					1,2,3
Astrea	*curta*			1.00			2,3,7
Astrea				1.00			2,3,7
Coscinarea	*columna*			1.00			2,3
Cyphastrea				1.00			1,2,3,6
Dipsastrea				1.00			2,3
Euphyllia						1.00	6
Favites				1.00			1,2,3
Goniastrea				0.86	0.14		1,2,6
Leptastrea					1.00		1,2,6
Leptoseris				1.00			3
Lithophyllon						1.00	6
Lobophyllia				1.00			1,2,3
Micromussa				1.00			2,3,6
Montipora	*millepora*			1.00			1
Montipora		0.31	0.38	0.31			1,2,6
Pavona	*descussata*		1.00				1
Pavona			0.60	0.40			2,3,6
Pectinia						1.00	3

▓	*Platygyra*				1.00			1,2,3
	Plesiastrea				1.00			1,2,3
	Pocillopora	*damicornis*				1.00		1
	Pocillopora		0.67			0.33		1,2,6
	Porites (Encrusting & Massive)				1.00			2,3
	Psammocora			1.00				1,2,3,6,8
	Stylocoeniella						1.00	6
	Stylophora	*pistillata*				1.00		1,2,3
	Stylophora					1.00		1,2,3
	Tubastraea						1.00	6
░	*Acanthastrea*				1.00			2,3
	Acropora	*humilus*	1.00					1
	Acropora		1.00					1,2
	Astrea	*annuligera*			1.00			2,3,7
	Astrea	*curta*			1.00			2,3,7
	Astrea				1.00			2,3,7
	Astreopora				1.00			2,3
	Caulastrea				1.00			1,6
	Cyphastrea				1.00			1,6
	Diploastrea	*heliopora*			1.00			1
	Dipsastraea	*pallida*			1.00			1
	Dipsastraea				1.00			2,3
	Echinophyllia				1.00			2,3
	Echinopora			1.00				1,6
	Favites				1.00			2,3
	Galaxea	*fascicularis*			1.00			2

	Galaxea				1.00			2,3
	Goniastrea				0.86	0.14		1,2,6
	Hydnophora		0.25	0.25	0.50			1,2,6
	Leptastrea				0.60	0.40		1,2,6
	Leptoria				1.00			2,3
	Lithophyllon						1.00	6
	Lithophyllon	*undulatum*					1.00	6
	Lobophyllia				1.00			2,3
	Merulina			1.00				3
	Montastrea				1.00			2,3
	Montipora	*foliosa*			1.00			2
	Montipora		0.32	0.35	0.32			1,2,6
	Oxypora	*lacera*			1.00			1,2,3,6
	Pachyseris			1.00				1,3
	Pectinia						1.00	3,6,7
	Platygyra				1.00			2,3
	Plesiastrea				1.00			2
	Pocillopora	*damicornis*				1.00		1
	Pocillopora		0.67			0.33		1,2,6
	Porites (Branching)					1.00		2,3
	Porites (Encrusting & Massive)				1.00			2,3
	Psammocora	*nierstraszi*		1.00				2,3,6
	Psammocora			0.67		0.33		2,3,6
	Symphyllia				1.00			3
	Turbinaria	*irregularis*			1.00			6

	Turbinaria	0.17	0.67	0.17			1,2,3,6

Citation codes: 1. Darling *et al.* (2012), 2. Darling *et al.* (2013), 3. Zinke *et al.* (2018), 4. Ng *et al.* (2019), 5. Schmidt-Roach *et al.* (2013), 6. Veron *et al.* (2016), 7. Huang *et al.* (2014), 8. Benzoni *et al.* (2010), 9. Schmidt-Roach *et al.* (2014).

4.3. Quantifying exposure to thermal variability

To evaluate how the long-term performance characteristics and transient potential of coral assemblages correspond with gradients in their exposure to thermal variability we calculated four measures describing the local sea surface temperature (SST) regimes experienced by each population prior to, and during, our survey period. Specifically, we focused on the four measures of mean monthly SST ($\bar{x}_{sst}$), monthly SST variance (cv_{sst}), monthly SST autocorrelation (a_{sst}), and monthly SST frequency spectrum (β_{sst}). Using the NOAA Coastwatch ERDDAP data server (https://coastwatch.pfeg.noaa.gov/erddap/index.html) we sourced high resolution SST records (°C; overlaid on a 1° latitude-longitude grid), from the Met Office Hadley Centre climate dataset (HadISST; Rayner *et al.* 2003). From this dataset we then extracted monthly SST readings taken between January 1950 and December 2019, inclusive, at each of the four geographical regions in which our focal coral assemblages were surveyed (see Supplementary S1; GPS: SIMP = -30.3°, 153.1°; HI = -23.4°, 151.9°; KHI = 32.8°, 132.6°; OKI = 26.5°, 128.1°).

Arranging extracted monthly SST records into 69-year timeseries for each location, we then calculated the mean ($\bar{x}_{sst}$), variance (cv_{sst}), autocorrelation (a_{sst}), and frequency spectrum (β_{sst}) for each timeseries (Table S4.4). We quantified the variance of each time series using its coefficient of variation which we estimated using the corresponding function in the *raster* package (Hijmans 2020). We then estimated the autocorrelation of each time series using the *autocorrelation* function from the *colorednoise* package (Pilowsky 2019). Measures of autocorrelation describe the correlation between successive elements within a series, such that positive autocorrelation reflects the condition whereby the properties of any element are closely related to those preceding it (Sokal & Oden 1978). Next, we estimated the frequency spectrum of each time series. The frequency spectrum of a timeseries reflects the periodicity of any recurrent variability across the series, with higher frequencies associated with shorter-term fluctuations (Greenman & Benton 2005). The frequency spectrum of a time series is equal to its spectral exponent (β), and calculated as the negative slope between the log spectral density and log frequency of the time series (Vasseur & Yodzis 2004). We calculated the frequency spectra of each of our SST time-series using the *spectrum* function from the *stats* R package (*R* Core Team 2019).

Table S4.4. The sea surface temperature (SST) regimes experienced by coral assemblages in tropical and subtropical regions of Australia and Japan, quantified using measures of mean monthly SST ($\bar{x}_{sst}$), monthly SST variance (cv_{sst}), monthly SST autocorrelation (a_{sst}), and monthly SST frequency spectrum (β_{sst}). Measures estimated from 69-year SST timeseries obtained from the Met Office Hadley Centre climate dataset (Rayner *et al.* 2003).

Location	$\bar{x}_{sst}$	cv_{sst}	a_{sst}	β_{sst}
Solitary Islands *(-30.3°, 153.1°)*	22.77	9.00	0.86	-1.04
Heron Island *(-23.4°, 151.9°)*	24.72	9.28	0.86	-1.13
Kochi *(32.8°, 132.6°)*	22.14	17.10	0.86	-0.94
Okinawa *(26.5°, 128.1°)*	25.13	11.37	0.85	-0.90

Finally, prior to conducting partial least squares analyses into the association between the long-term performance and transient potential of coral assemblages with patterns in thermal conditions it was necessary for us to evaluate for collinearity across our abiotic variables. We tested for collinearity using the measure of tolerance which describes an inverse measure of the correlation between multivariate predictor variables with estimates of <0.1 evidence of collinearity (Fox 1991). We calculated measures of tolerance for our abiotic variables using the function *multicol* from the *fuzzySim* package (Barbosa 2015). Our test for multicollinearity, when we included all four SST variables, returned tolerance estimates of ~0 highlighting a strong correlation between one or more of the variables. Subsequently, we explored collinearity across each triple-wise combination of our four abiotic variables and determined that the triple-wise combination of the variables of mean monthly SST, monthly SST variance, and monthly SST frequency spectrum exhibited the least collinearity (Table S4.5). Accordingly, we omitted the variable of monthly SST autocorrelation (a_{sst}) from further analyses.

Table S4.5. Tolerance estimates obtained for each of the sea surface temperature (SST) measures of mean monthly SST ($\bar{x}_{sst}$), monthly SST variance (cv_{sst}), monthly SST autocorrelation (a_{sst}), and monthly SST frequency spectrum (β_{sst}) across each triple-wise combination possible with the four abiotic variables.

Combination	$\bar{x}_{sst}$	cv_{sst}	a_{sst}	β_{sst}
1	0.12	-	0.03	0.04
2	-	0.58	0.22	0.17
3	0.26	0.26	0.31	-
4	0.61	0.39	-	0.55

4.4. References

Barbosa, A.M. (2015). fuzzySim: Applying fuzzy logic to binary similarity indices in ecology. *Methods Ecol. Evol.*, 6, 853–858.

Benzoni, F., Stefani, F., Pichon, M. & Galli, P. (2010). The name game: Morpho-molecular species boundaries in the genus Psammocora (Cnidaria, Scleractinia). *Zool. J. Linn. Soc.*, 160, 421–456.

Bramanti, L., Iannelli, M., Fan, T.Y. & Edmunds, P.J. (2015). Using demographic models to project the effects of climate change on scleractinian corals: Pocillopora damicornis as a case study. *Coral Reefs*, 34, 505–515.

Cant, J., Cook, K., Reimer, J.D., Mezaki, T., Nakamura, M., O'Flaherty, C., *et al.* (2021a). Transient amplification enhances the persistence of tropicalising coral populations in marginal high latitude environments. *BioRxiv*, 2021.04.23.441133.

Cant, J., Salguero-Gómez, R., Kim, S.W., Sims, C.A., Sommer, B., Brooks, M., *et al.* (2021b). The projected degradation of subtropical coral assemblages by recurrent thermal stress. *J. Anim. Ecol.*, 90, 233–247.

Darling, E.S., Alvarez-Filip, L., Oliver, T.A., Mcclanahan, T.R. & Côté, I.M. (2012). Evaluating life-history strategies of reef corals from species traits. *Ecol. Lett.*, 15, 1378–1386.

Darling, E.S., McClanahan, T.R. & Côté, I.M. (2013). Life histories predict coral community disassembly under multiple stressors. *Glob. Chang. Biol.*, 19, 1930–1940.

Fox, J. (1991). *Regression diagnostics: An introduction*. Sage Publications, Newbury Park.

Gilmour, J., Speed, C.W. & Babcock, R. (2016). Coral reproduction in Western Australia. *PeerJ*, 1–43.

Graham, E.M., Baird, A.H. & Connolly, S.R. (2008). Survival dynamics of scleractinian coral larvae and implications for dispersal. *Coral Reefs*, 27, 529–539.

Greenman, J. V. & Benton, T.G. (2005). The frequency spectrum of structured discrete time population models : its properties and their ecological implications. *Oikos*, 110, 369–389.

Hall, V.R. & Hughes, T.P. (1996). Reproductive strategies of modular organisms: Comparative studies of reef-building corals. *Ecology*, 77, 950–963.

Hijmans, R.J. (2020). raster: Geographic data analysis and modeling.

Huang, D., Benzoni, F., Fukami, H., Knowlton, N., Smith, N.D. & Budd, A.F. (2014). Taxonomic classification of the reef coral families Merulinidae, Montastraeidae, and Diploastraeidae (Cnidaria: Anthozoa: Scleractinia). *Zool. J. Linn. Soc.*, 171, 277–355.

Madin, J.S., Baird, A.H., Baskett, M.L., Connolly, S.R. & Dornelas, M.A. (2020). Partitioning colony size variation into growth and partial mortality. *Biol. Lett.*, 16, 1–5.

Ng, C.S.L., Jain, S.S., Nguyen, N.T.H., Sam, S.Q., Kikuzawa, Y.P., Chou, L.M., *et al.* (2019). New genus and species record of reef coral Micromussa amakusensis in the southern South China Sea. *Mar. Biodivers. Rec.*, 12.

Pilowsky, J. (2019). colorednoise: Simulate temporally autocorrelated populations.

R Core Team. (2019). R: A language and environment for statistical computing.

Rayner, N.A., Parker, D.E., Horton, E.B., Folland, C.K., Alexander, L. V., Rowell, D.P., *et al.* (2003). Global analyses of sea surface temperature, sea ice, and night marine air temperature since the late nineteenth century. *J. Geophys. Res.*, 108, 1–37.

Schmidt-Roach, S., Miller, K.J. & Andreakis, N. (2013). Pocillopora aliciae: A new species of scleractinian coral (Scleractinia, Pocilloporidae) from subtropical Eastern Australia. *Zootaxa*, 3626, 576–582.

Schmidt-Roach, S., Miller, K.J., Lundgren, P. & Andreakis, N. (2014). With eyes wide open: A revision of species within and closely related to the Pocillopora damicornis species complex (Scleractinia; Pocilloporidae) using morphology and genetics. *Zool. J. Linn. Soc.*, 170, 1–33.

Schneider, C.A., Rasband, W.S. & Eliceiri, K.W. (2012). NIH Image to ImageJ: 25 years of image analysis. *Nat. Methods*, 9, 671–675.

Sokal, R.R. & Oden, N.L. (1978). Spatial autocorrelation in biology: 1. Methodology. *Biol. J. Linn. Soc.*, 10, 199–228.

Vasseur, D.A. & Yodzis, P. (2004). The color of environmental noise. *Ecology*, 85, 1146–1152.

Veron, J.E.N., Stafford-Smith, M.G., Turak, E. & DeVantier, L.M. (2016). *Corals of the World*. Available at: http://www.coralsoftheworld.org/page/home/. Last accessed 12 November 2019.

Yau, A.J., Lenihan, H.S. & Kendall, B.E. (2014). Fishery management priorities vary with self-recruitment in sedentary marine populations. *Ecol. Appl.*, 24, 1490–1504.

Zinke, J., Gilmour, J.P., Fisher, R., Puotinen, M., Maina, J., Darling, E., *et al.* (2018). Gradients of disturbance and environmental conditions shape coral community structure for south-eastern Indian Ocean reefs. *Divers. Distrib.*, 24, 605–620.